Analysis of copy number variation and disease mechanisms underlying Parkinson's disease

Celia van der Merwe

Dissertation presented for the degree of Doctor of Philosophy
(Human Genetics) in the Faculty of Medicine and Health Sciences
at Stellenbosch University

Supervisor: Assoc. Prof. Soraya Bardien

Co-supervisor: Dr. Ben Loos

March 2016

i

DECLARATION

By submitting this dissertation electronically, I declare that the entirety of the work contained therein is my own, original work, that I am the sole author thereof (save to the extent explicitly otherwise stated), that reproduction and publication thereof by Stellenbosch University will not infringe any third party rights and that I have not previously in its entirety or in part submitted it for obtaining any qualification.

Signature…………………………………………Date………………………………………

ABSTRACT

Parkinson's disease (PD) is a neurodegenerative movement disorder characterized by the loss of dopaminergic neurons in the substantia nigra of the midbrain. Although the aetiology of PD is still not fully understood, it is thought to involve a combination of environmental and genetic factors. To date, a number of PD-causing genes have been found. The *PINK1* gene is of particular interest for this study, and mutations in this gene result in autosomal recessive inheritance of early onset PD. PINK1 plays a vital role in mitochondrial quality control and homeostasis, and in its absence it is thought to result in an accumulation of dysfunctional mitochondria in neurons, culminating in neuronal cell death. Whilst pharmacological and surgical interventions are available for PD, the current options exhibit adverse side effects with long term treatment. There is a great need to develop new treatments with i. less side effects and ii. that can simultaneously target the multiple pathways associated with this disorder. One molecule is curcumin, the core component of the curry spice turmeric, which is well known for its antioxidant and anti-inflammatory properties and has already been studied for its possible neuroprotective role in Alzheimer's disease.

The aim of the present study was to create a cellular model of PD by decreasing the expression of PINK1 in SH-SY5Y neuroblastoma cells. Thereafter, we aimed to test the protective effects of curcumin on this model in the presence and absence of a known stressor, paraquat. This study also aimed to detect possible copy number variation (CNV) in *PINK1* (and other PD-causing genes) in a cohort of South African patients with PD, in order to obtain patient-derived fibroblasts to verify the results obtained from the original cellular model.

PINK1 was knocked down using siRNA (Qiagen, USA) in SH-SY5Y neuroblastoma cells, and the knock down was verified by quantitative real time PCR (qRTPCR) and western blotting. Thereafter, *PINK1* siRNA cells and control cells were separated into four treatment groups: i. untreated, ii. treated with 25µM paraquat for 24hours, iii. pre-treated with 2µM curcumin for 1hour then treated with 25µM paraquat for 24hours, or iv. treated with 2µM curcumin for 1hour, and various parameters of cellular and mitochondrial function were measured. Cell viability was measured by an MTT assay. Western blot analysis was performed using cleaved PARP and full-length caspase 3 markers to detect levels of apoptosis, and LC3-II and p62 markers to detect autophagic flux. Mitochondrial respiration experiments were completed on the Seahorse XF Analyser using the Mito Stress Test Kit and the Glycolysis Stress Test. Flow cytometry was utilised to measure mitochondrial membrane potential (MMP) using the JC-1 fluorochrome, and mitochondrial network was analysed by fluorescent microscopy. For CNV detection, MLPA was performed on 210 South African PD patients and putative mutations were verified by qRTPCR on the Lightcycler 96.

PINK1 was successfully knocked down at a gene and protein expression level. The *PINK1* siRNA cells exhibited a significant decrease in cell viability (p=0.0036), and an increase in apoptosis (p=0.0144). A decrease in PINK1 expression also resulted in significantly decreased MMP (p=0.0008), mitochondrial respiration (p=0.0015), ATP production (p=0.002) and glycolytic capacity (p=0.0445). No significant changes were observed in the connectivity of the mitochondrial network, but autophagic flux was significantly increased in the *PINK1* siRNA cells, as detected by increased LC3-II levels (p=0.0152).

As expected, paraquat-treated cells exhibited decreased cell viability, increased apoptosis, decreased MMP, autophagic flux, and a more fragmented mitochondrial network. Paraquat treatment therefore successfully acted as a stressor on the cells. Curcumin pre-treatment followed by paraquat treatment rescued cell viability in control cells (p=0.003), and significantly decreased apoptosis in *PINK1* siRNA cells (p=0.0018). Curcumin protected mitochondrial dysfunction in *PINK1* siRNA cells by increasing MMP (p=0.0472) and maximal respiration (p=0.0014), as well as significantly increasing MMP (p=0.0307) and maximal respiration (p=0.032) in control cells. Additionally, curcumin treatment resulted in increased autophagic flux (p=0.0017) in stressed control cells. These results highlight a protective effect of curcumin against paraquat and against the damaging effects on the mitochondria in cells with decreased PINK1 expression.

Lastly, MLPA analysis did not reveal any *PINK1* CNV mutations in a total of 210 South African PD patients, and fibroblasts were therefore not obtained. A number of false positive mutations were identified that were not verified by qRTPCR. A common polymorphism M192L resulting in a false positive *PARK2* exon 5 deletion was found in a number of patients, all of whom were of Black or Mixed Ancestry ethnic groups. One patient was shown to harbour a heterozygous deletion in *PARK2* exon 4.

In conclusion, *PINK1* siRNA-mediated knock down in SH-SY5Y neuroblastoma cells can be used as a model of PD to study aspects of mitochondrial dysfunction. Furthermore, curcumin should be considered as a possible therapeutic target for PD, as it exhibits protective effects against paraquat at a mitochondrial level. Given the low toxicity of curcumin, and the fact that it is already part of a dietary regimen in most populations worldwide, further studies on elucidating its biochemical and cellular properties are therefore warranted. The use of natural compounds such as curcumin as therapeutic agents is currently a topical and fast-growing area of research, and holds much promise for clinical application in various diseases including neurodegenerative disorders such as Alzheimer's disease and PD.

OPSOMMING

Parkinson se siekte (PD) is 'n neurodegeneratiewe beweging versteuring wat gekenmerk word deur die verlies van dopaminergiese neurone in die brein. Hoewel die etiologie van PD nog nie ten volle verstaan is nie, is daar denke dat dit 'n kombinasie van die omgewing en genetiese faktore behels. Tot dus ver is daar nog net 'n aantal gene wat PD-veroorsaak gevind. Die *PINK1* geen is van besondere belang vir hierdie studie, en mutasies in dié geen veroorsaak outosomale resessiewe oorerwing van vroeë aanvang PD. PINK1 speel 'n belangrike rol in die mitochondriale gehaltebeheer en homeostase, en in sy afwesigheid is dit gedink om te lei tot 'n opeenhoping van disfunksionele mitochondria in die neurone, wat kulmineer in neuronale sel dood. Terwyl farmakologiese en chirurgiese ingrepe beskikbaar is vir PD, die huidige opsies wys duidelike newe-effekte met lang termyn behandeling. Daar is 'n groot behoefte om nuwe behandelings te ontwikkel met i. minder newe-effekte en ii. wat gelyktydig die verskeie paaie wat verband hou met hierdie versteuring kan teiken. Een molekule is curcumin, die hoof komponent van die kerrie spesery borrie, wat wel bekend is vir, sy anti-oksidant en anti-inflammatoriese eienskappe, en is reeds bestudeer vir sy moontlike beskermende rol in Alzheimer's se siekte.

Die doel van hierdie projek is om 'n sellulêre model van PD te skep deur die vermindering van die uitdrukking van *PINK1* in SH-SY5Y neuroblastoom selle. Ons daarop gemik om die beskermende effek van curcumin te toets in die teenwoordigheid en afwesigheid van 'n bekende stressor, parakwat in ons model. 'n Additionele doelwit is om moontlike kopiegetal variasie (CNV) in die *PINK1* gene (en ander PD veroorsaakende gene) op te tel in 'n groep van die Suid-Afrikaanse pasiënte met PD. Die doel van hierdie was om pasiënt-afgeleibare fibroblaste te kry om die resultate te verifieer vanuit die oorspronklike model.

SH-SY5Y neuroblastoom selle was gekweek, en *PINK1* is platgeslaan deur gebruik te maak van siRNA en HiPerfect Transfectie Reagens (Qiagen, VSA). Klop van PINK1 is bevestig deur kwantitatiewe real time PCR (qRTPCR) en westelike klad. Daarna, *PINK1* siRNA selle en beheer selle was óf i. nie behandel nie, ii. behandel met 25 um paraquat vir 24 uur per dag, iii. vooraf behandel met 2μM curcumin vir 1 uur dan behandel met 25 um paraquat vir 24 uur per dag, of iv. behandel met 2μM curcumin vir 1 uur, en verskeie parameters van sellulêre en mitochondriale funksie is gemeet. Lewensvatbaarheid van die selle is gemeet deur 'n MTT toets. Westerne klad analise is uitgevoer met behulp van gekleefde PARP en vollengte caspase 3 merkers om die vlakke van apoptose te meet, en LC3-II en p62 merkers was gebruik om autophagic vloed op te spoor. Mitochondriale respirasie eksperimente is voltooi op die Seahorse XF Analyser met behulp van die Mito Stres Test Kit en die Glikolise Stres Toets. Vloeisitometrie is gebruik om mitochondriale membraan potensiaal (MMP) te meet met behulp van die JC-1 fluorochrome en die mitochondriale netwerk is geanaliseer deur fluorescent mikroskopie. Vir CNV opsporing, was MLPA uitgevoer op 210 Suid-Afrikaanse PD pasiënte en vermeende mutasies is bevestig deur qRTPCR op die Lightcycler 96.

PINK1 is suksesvol platgeslaan op 'n geen en proteïen uitdrukking vlak. Die *PINK1* siRNA selle betoon 'n beduidende afname in lewensvatbaarheid sel (p = 0.0036), en 'n toename in apoptose (p=0.0144). 'n

Afname in PINK1 uitdrukking het ook daartoe gelei na 'n beduidende vermindering in MMP (p=0.0008), mitochondriale respirasie (p=0.0015), ATP produksie (p=0.002) en glikolitiese kapasiteit (p=0.0445). Geen beduidende veranderinge is waargeneem in die verbinding van die mitochondriale netwerk nie, maar autophagic vloed het aansienlik toegeneem in die *PINK1* siRNA selle, soos waargeneem deur verhoogde vlakke in LC3-II (p=0.0152).

Soos verwag betoon, paraquat behandelde selle 'n afname in sel lewensvatbaarheid, verhoogde apoptose, afname in MMP, autophagic vloed, en 'n meer gefragmenteerde mitochondriale netwerk. Parakwat behandeling het dus suksesvol opgetree as 'n stressor op die selle. Curcumin vooraf-behandeling gevolg deur paraquat behandeling het sel lewensvatbaarheid gered in beheer selle (p=0.003), en aansienlik verminderde apoptose in *PINK1* siRNA selle (p=0.0018) betoon. Curcumin beskerm mitochondriale disfunksie deur die verhoging van MMP (p=0.0472, p=0.0307) en maksimale respirasie (p=0.0014, p=0.032) in beide *PINK1* siRNA en beheer selle. Additioneel, het curcumin behandeling gelei tot 'n verhoogde autophagic vloed (p=0.0017) in onderdrukte beheer selle. Hierdie resultate beklemtoon die beskermende effek van curcumin teen parakwat en teen die skadelike resultaat op die mitochondria in die selle met verlaagde PINK1 uitdrukking.

Laastens, MLPA ontleding het nie *PINK1* CNV mutasies openbaar in 'n totaal van 210 Suid-Afrikaanse PD pasiënte, en fibroblaste is dus nie verkry nie. 'n Aantal vals positiewe mutasies is geïdentifiseer wat nie geverifieer is deur qRTPCR. 'n Algemene polimorfisme M192L is in 'n aantal pasiënte gevind wat in 'n vals positiewe *PARK2* ekson 5 eliminasie ontaard, waarvan almal swart of gemengde afkoms etiese groepe is. Een pasiënt het getoon dat 'n heterosigotiese eliminasie in *PARK2* ekson 4 bevind is.

Ten slotte, *PINK1* siRNA-gemedieerde wat platgeslaan is in SH-SY5Y neuroblastoom selle kan gebruik word as 'n model van PD om aspekte van mitochondriale disfunksie te bestudeer. Verder moet curcumin beskou word as 'n moontlike terapeutiese teiken vir PD, omdat dit beskermende effekte teen parakwat op 'n mitochondriale vlak vertoon. Gegewe die lae toksisiteit van curcumin en die feit dat dit reeds 'n deel vorm van die dieët in meeste populasie groepe wêreldwyd, is verdere studies op die biochemiese en sellulêre eienskappe daarvan benodig. Die gebruik van natuurlike komposisies, soos curcumin as 'n terapeutiese middel is tans 'n relevante en vinnig groeiende area van navorsing en toon baie belofte vir kliniese toepassing in verskeie siektes soos Alzheimer's siekte en PD.

TABLE OF CONTENTS

Page

ACKNOWLEDGEMENTS

Firstly, I would like to acknowledge my supervisor, Professor Soraya Bardien, for her support throughout this study. Through her guidance and leadership, I have learnt how to work as an independent researcher. This project would not have been possible without it, thank you Soraya.

I would also like to thank my co-supervisor Dr. Ben Loos for his passion and excitement about this work. You provided me with motivation when I needed it most!

Thank you to Stellenbosch University and the Department of Biomedical Sciences for the use of their facilities. For project and bursary funding, I thank the NRF, MRC and Harry Crossley Foundation.

Thank you to Prof Francois van der Westhuizen and Ms Hayley van Dyk from North West University for hosting me and helping with the mitochondrial respiration experiments and data analysis.

To my co-workers in the MAGIC lab, thank you for helping me in all aspects of my research project. In particular, I would like to acknowledge Dr. Craig Kinnear for always being willing to help with any problem and every question I had. And to B, thanks for an awesome 5 years as my cubicle neighbour!

I want to thank Miko, my fiancé, for everything that you have done for me. I am so glad that we are doing life together, and without your unwavering faith in my abilities I know I would not have been able to achieve this. Thank you for pushing me to accomplish my goals, and for always encouraging my ambitions. I can't wait for the next phase in our life.

To my family and friends - Mom, Dad, Ez, Mila, Pete, Uncle Mark, Liesl - thank you for your love and patience, and for providing me with the strongest foundation upon which to grow. Dad, I dedicate this achievement to you. Words cannot express my gratitude, but I hope this gesture might.

Thank you Jesus for your guiding light in my life.

LIST OF ABBREVIATIONS

2-DG: 2-deoxy-glucose

6-OHDA: 6-hydroxydopamine

AAD: aromatic L-amino acid decarboxylase

AAO: age at onset

Aβ: amyloid-β

AD: Alzheimer's disease

ADP: adenosine diphosphate

AGVP: African Genome Variation Project

AIDS: acquired immunodeficiency disease

ALP: Autophagy-Lysosome Pathway

ANOVA: Analysis of Variance

AR: autosomal recessive

ATP: adenosine triphosphate

AV: autophagic vacuole

BafA1: Bafilomycin A1

BBB: Blood-brain barrier

BSA: bovine serum albumin

CCCP: Carbonyl cyanide 3-chlorophenylhydrazone

CMA: chaperone-mediated autophagy

CNV: copy number variation

Curc: Curcumin

DBS: Deep Brain Stimulation

DMEM: Dulbecco's Modified Eagle Medium

DMSO: Dimethyl sulfoxide

DNAJC: DNAJ- Homolog Subfamily C

e': electron

ECAR: Extracellular Acidification Rate

EIF4G1: eukaryotic translation initiation factor 4G1

EOPD: early onset Parkinson's disease

ETC: electron transport chain

$FADH_2$: reduced flavin adenine dinucleotide

FBOX7: F-box only protein 7

FBS: Fetal Bovine Serum

FCCP: Trifluorocarbonylcyanide phenylhydrazone

FITC: Fluorescein isothiocyanate

GBA: glucocerebrosidase

gDNA: genomic DNA

H^+: proton

HBB: β-globulin

HKG: house keeping gene

IMM: inner mitochondrial membrane

IMS: inter membrane space

iPSCs: induced pluripotent stem cells

JC-1: 5,5',6,6' tetrachloro – 1,1,3,3' tetraethylbenzimidazol-carbocyanine iodide

JNK: Jun N-terminal kinase

LB: Lewy body

LC3-II: microtubule-associated protein 1 light chain 3

LOPD: late onset Parkinson's disease

LRRK2: leucine-rich repeat kinase 2

MAO-B: monamine-oxidase B

MAPT: microtubule-associated protein tau

MEFs: mouse embryonic fibroblasts

mins: minutes

MLPA: Multiplex Ligation-dependent Probe Amplification

MMP: mitochondrial membrane potential

MOMP: Mitochondrial Outer Membrane Permeabilisation

MPP^+: 1-methyl-4-pyridinium

MPTP: 1-methyl-4-phenyl-1,2,3,6-tetrahydropyridine

MQC: mitochondrial quality control

mTOR: mammalian target of rapamycin

MTT: 3-(4,5-dimethylthiazol-2-yl)-2,5-diphenyltetrazolium bromide

NADH: reduced nicotinamide adenine dinucleotide

NGS: Next Generation Sequencing

OCR: Oxygen Consumption Rate

OMM: outer mitochondrial membrane

P70S6K: p70 ribosomal protein S6 kinase

PARP: Poly ADP-ribose

PBS: Phosphate-buffered saline

PCD: Programmed cell death

PCR: polymerase chain reaction

PD: Parkinson's disease

PE: phosphatidylethanolamine

PE: Phycoerythrin

Pi: inorganic phosphate

PINK1: PTEN-induced putative kinase 1

PN: peroxynitrite

PQ: paraquat, 1,1'-4,4'-bypyridium dichloride

PTP: permeability transition pore

qPCR: quantitative PCR

qRTPCR: quantitative real time PCR

ROS: reactive oxygen species

RPH: relative peak height

siRNA: small interfering RNA

SNc: substantia nigra pars compacta

SNCA: α-synuclein

SNP: single nucleotide polymorphism

TBST: Tris Buffered Saline with Tween 20

UCHL1: ubiquitin carboxyterminal hydrolase 1

UPS: Ubiquitin Proteasome System

VPS35: vacuolar protein sorting 35

WES: Whole Exome Sequencing

LIST OF FIGURES

Page

Page

Chapter 3

Page

Chapter 4

LIST OF TABLES

Chapter 1: Introduction

2

Page

1.1.   Background

Parkinson's disease (PD) is a neurodegenerative disorder that is characterised by the degeneration of the neuromelanin-containing dopaminergic neurons of the substantia nigra pars compacta (SNc). PD was first discovered almost two centuries ago in 1817 by Dr. James Parkinson. In his 'Essay on Shaking Palsy' (Parkinson, 2002), Parkinson described the disease as a movement disorder, with symptoms including resting tremor, abnormal posture and gait, and diminished muscle strength. Today, PD is recognised by four cardinal motor symptoms – bradykinesia (slowness of movement), rigidity, resting tremor and postural instability (Figure 1.1). Furthermore, patients suffering from PD also present with neuropsychiatric and non-motor symptoms including loss of smell, constipation, depression, sleep disorders, cognitive impairment, dementia and psychosis (Chaudhuri et al., 2006).
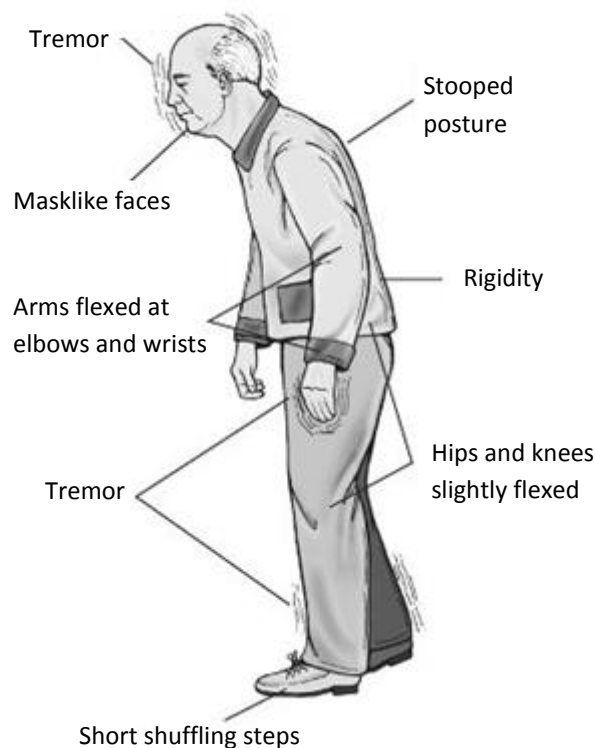
Figure 1.1. Illustration indicating the motor symptoms of Parkinson's disease. Taken from http://tajpharma.com/parkinson-disease-diseasesindex-taj-pharmaceuticals.htm

PD is rare in individuals under the age of 50, and increases with increasing age thereafter. A study analysing global incidence rates observed an overall incidence of 12.3 per 100 000, and 44.0 per 100 000 specifically for individuals over the age of 50 (Van den Eeden et al., 2003). A recent meta-analysis of 47 studies found that PD prevalence also increased with age, with 40.5 in 100 000 in 40-49 year olds compared to 1086.5 in 100 000 in 70-79 year olds (Pringsheim et al., 2014). It has also been found that there is increased mortality in PD patients compared to controls, and survival is reduced by approximately 5% every year of follow up (Macleod et al., 2014).

1.2.   Neuropathology of PD

Dopaminergic neurons, found in the SNc, are responsible for the production of the hormone dopamine. Dopamine is involved in several pathways in the brain, including reward-motivated behaviour and motor control, and can also act as a chemical messenger for the release of other hormones. Furthermore, dopamine-producing neurons also produce melanin, causing these neurons to be pigmented. PD is pathologically characterised by the loss of 70 – 80% of the dopaminergic neurons which results in depigmentation of the SNc (Figure 1.2A, B). This neuronal loss causes a substantial decrease in dopamine production, thus leading to the movement disturbances seen in PD patients.

A second pathological characteristic of PD, and referred to as the pathological hallmark of this disease, is the presence of proteinaceous deposits known as Lewy bodies (LBs) in the SNc and several other regions of the brain (Figure 1.2C,D). LBs are cytoplasmic protein inclusions composed predominantly of alpha-synuclein, neurofilament proteins and ubiquitin (Spillantini et al., 1997). It is hypothesized that the formation of LBs occurs prior to PD diagnosis in the dorsal motor nucleus, and progressively moves through the brainstem into the SNc and towards the cerebral cortex (Braak et al., 2003). Post mortem studies indicate that the extent of LB pathology correlates with the severity of the symptoms (Luk and Lee, 2014).
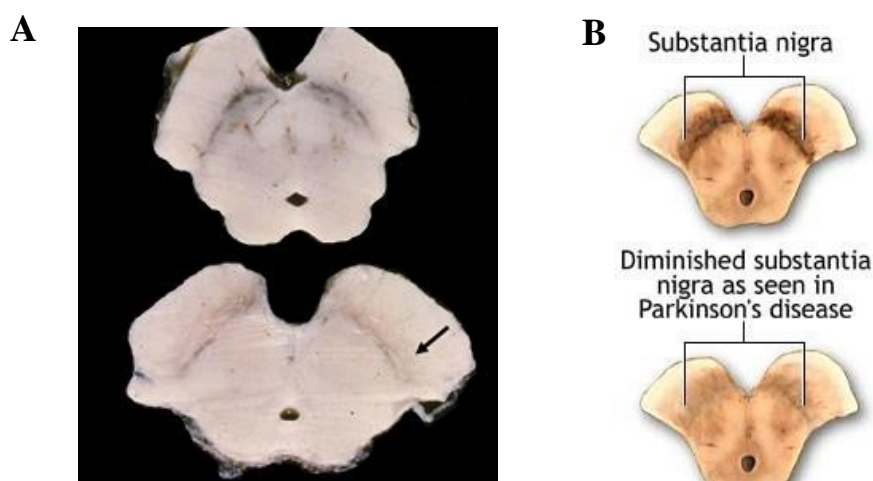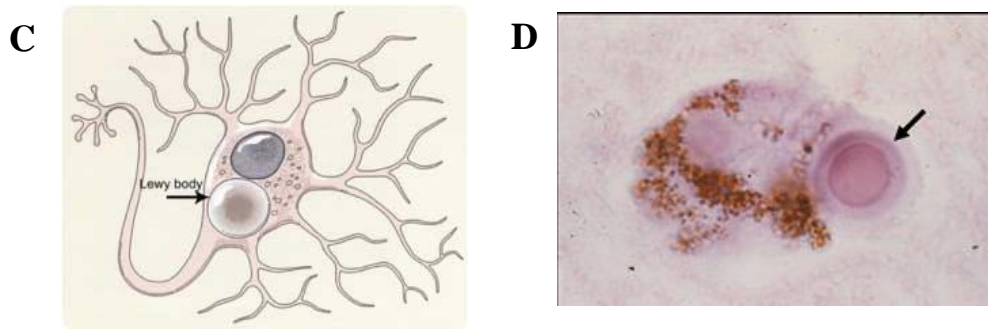
Figure 1.2. The pathology of the substantia nigra in Parkinson's disease. A, B. Cross-section images of the midbrain indicating the pigmented substantia nigra and dopamine-producing neurons of healthy individuals (top), compared to the loss of pigmentation on the substantia nigra in PD patients (bottom). C, D. Animation (C) and histological staining (D) images indicating the presence of a Lewy body. Adapted from http://belairecare.com

1.3. Age at onset

The age at onset (AAO) in PD patients is categorised into three sub-groups - juvenile onset PD, early onset PD (EOPD) and late onset PD (LOPD). Juvenile onset PD (AAO <20 years) is uncommon, and is caused by rare mutations in the genes that cause PD (Section 1.4.2). EOPD (≤40-50 years) is also relatively rare with predominantly genetic causative factors. Patients with an AAO over the age of 50 fall into the LOPD category, and this is thought to be caused by a combination of genetic and environmental factors. PD is an age-related disorder, and it has been found that an increase in age is one of the strongest risk factors.

1.4. Causes of PD

PD was traditionally considered to be a sporadic disease caused by environmental factors such as lifestyle and aging. However, the past eighteen years have been successful in proving the role of genetic factors in the cause of this condition. A positive family history is associated with a higher risk of PD and the aetiology of this disorder, although not fully understood, is considered to involve an interaction between genetic and environmental factors (Sherer et al., 2002).

1.4.1. Environmental causes

The search into environmental causes of PD began after an incident in 1982 where heroin users in California presented with cases of acute parkinsonism (Langston, 1985). Dr. J.W. Langston identified that the cause of these severe symptoms was the presence of the toxic agent 1-methyl-4-phenyl-1,2,3,6-tetrahydropyridine (MPTP) in the heroin. This discovery led to the development of animal models using MPTP, which displayed features of parkinsonism and led to selective degeneration of the dopaminergic neurons (Langston, 1985; Miller and DeLong, 1987).

MPTP is able to cross the blood-brain barrier (BBB), where it is converted to its metabolite 1-methyl-4-pyridinium (MPP^+) via monoamine-oxidase B (MAO-B). MPP^+ acts at the electron transport chain (ETC) as a mitochondrial complex I inhibitor, resulting in the disruption of oxidative phosphorylation, decreased ATP and increased reactive oxygen species (ROS) production, and ultimately cell death. This initial model of PD via the inhibition of complex I led researchers to search for agents with similar toxicological profiles (Goldman, 2014).

1.4.1.1. Pesticides

A meta-analysis determining environmental risk factors found that 11 out of 14 previous studies showed a positive association between pesticide exposure and PD (Priyadarshi et al., 2001). A second meta-analysis including 46 previous studies observed a risk ratio for PD of 1.6 for ever (versus never) for the variable pesticide exposure (van der Mark et al., 2011). It is therefore generally accepted that exposure to pesticides results in an increased risk of disease onset. Two such pesticides are rotenone and paraquat (1,1'-4,4'-bypyridium dichloride). Rotenone has been used as an alternative to MPTP in animal models as it also inhibits mitochondrial complex I, causing mitochondrial dysfunction (Alam and Schmidt, 2002; Sherer et al., 2003; Wrangel et al., 2015). It has been reported that autophagic dysfunction may contribute to neurodegeneration (Section 1.5.2; Dehay et al., 2010; Tan et al., 2014; Zhang et al., 2011), and rotenone has recently been shown to inhibit autophagic flux and induce lysosomal dysfunction in *in vitro* and *in vivo* models (Mader et al., 2012; Wu et al., 2015; Xilouri et al., 2013).

Paraquat

Much interest has been placed on paraquat, and in using paraquat to model PD, because its chemical structure closely resembles that of MPP^+ (Figure 1.3; Goldman, 2014). Paraquat is one of the most widely used nonselective dipyridyl pesticides worldwide, and several studies have associated paraquat

use with an increased risk of PD (Hertzman et al., 1990; Kamel et al., 2007; Liou et al., 1997; Tanner et al., 2011). Paraquat induces parkinsonian features in animal models through the generation of ROS, which results in increased lipid peroxidation, decreased antioxidant levels, and impaired mitochondrial function (Costello et al., 2009; McCormack et al., 2002). Like rotenone, paraquat also selectively kills dopaminergic neurons. It is thought that the reason for this selectivity is the fact that SNc neurons have an increased sensitivity to oxidative stress.

Evidence of the effect of paraquat on complex I has been conflicting. Some studies report that paraquat does not inhibit the mitochondrial complex I of the ETC (Mohammadi-Bardbori and Ghazi-Khansari, 2008; Richardson et al., 2005), whereas other studies report that superoxide production by paraquat may be due to its effect on complex I (Fukushima et al., 2002). It has also been suggested that paraquat causes inhibition of complexes III and IV (Fukushima et al., 1995). In spite of this, paraquat mitochondrial toxicity appears to be caused by its acceptance of electrons from the complexes of the mitochondrial ETC, which then rapidly react with molecular oxygen to form free radicals such as the superoxide anion (Mohammadi-Bardbori and Ghazi-Khansari, 2008).
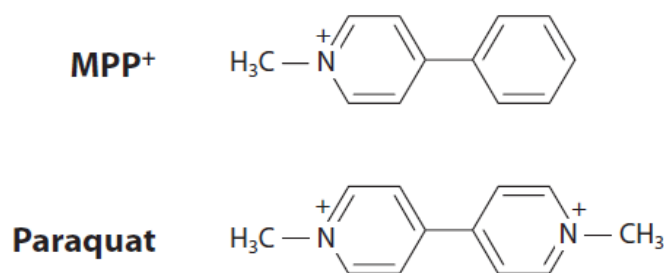
Figure 1.3. Structural similarity of MPP+ to paraquat. Taken from Goldman, 2014.

1.4.1.2.   Other environmental causes of PD

Although pesticide use is one of the highest environmental risk factors for PD, there are several secondary factors that have shown a positive association for increased risk of PD (Priyadarshi et al., 2001). Well-water can easily become contaminated with pesticides, volatile organic compounds and other chemicals, and drinking of this water could increase the risk of onset of disease. Furthermore, farming is also known to be a risk factor of PD, as this may result in direct contact with large quantities of pesticides through inhalation or absorption by the skin. It is due to both these reasons that rural living is also a risk factor (Priyadarshi et al., 2001), as well-water drinking and farming occur more frequently in rural areas. All of these factors are closely linked and interrelated to pesticide use, which may be the

reason why they are all positively associated with an increased risk of PD. Disease onset has also been linked to exposure to heavy metals such as iron, lead, manganese and mercury as well as head injury (Huang et al., 2006; Yamin et al., 2003; Jafari et al., 2013; Wirdefeldt et al., 2011), and studies suggest a dose-response relationship whereby the greater the number of head injuries, the greater the associated risk (Gao et al., 2015).

1.4.2.   Genetic causes

Insights into phenotypic variation and disease susceptibility can be made through the study of genetic variation between individuals. Such variation includes single nucleotide polymorphisms (SNPs), various repetitive elements such as short tandem repeats involving short DNA sequences, small (<1kb) insertion/ deletion polymorphisms, and genomic structural alterations known as copy number variation (CNV, Feuk et al., 2006). Of the known PD-causing genes, five are linked to autosomal dominant forms of the disease (*SNCA, LRRK2, VPS35, eIF4G1, CHCHD2*), and four with autosomal recessive inheritance (*parkin, PINK1, DJ-1, ATP13A2*). A summary of the PD-associated loci and genes can be found in Table 1.1.

1.4.2.1.   Autosomal dominant genes

The first known PD-causing gene, *SNCA*, was discovered in 1997 in a large Italian family that had a missense A53T mutation (Polymeropoulos et al., 1997). Since then, point mutations and whole-gene multiplications (duplications and triplications) of *SNCA* have been found in PD families worldwide (Ibáñez et al., 2004; Krüger et al., 2000; Singleton et al., 2003). Mutations of *SNCA* lead to missense variations and pathogenic overexpression of the encoded protein, α-synuclein (Corti et al., 2011), which is a major component of LBs, the pathological hallmark of PD (Tu et al., 1998). Since then, several other genes have been implicated in autosomal dominant inheritance of PD. *LRRK2*, for example, is responsible for the most common cause of autosomal dominant PD due to the G2019S mutation in exon 41 (Ozelius et al., 2006; Paisán-Ruíz et al., 2005). *VPS35* was recently discovered to be a PD-causing gene by two separate studies both using the Next Generation Sequencing (NGS) approach, more specifically Whole Exome Sequencing (WES, Vilariño-Güell et al., 2011; Zimprich et al., 2011). The

Table 1.1. Summary of Parkinson's disease-associated loci and genes

Gene	Locus	Inheritance	Mutations	Protein	Protein function
Juvenile & Early Onset					
Parkin	PARK2	Recessive	Point mutations; exonic rearrangements	Parkin	Cell signalling; protein degradation and clearance
PINK1	PARK6	Recessive	Point mutations; rare, large deletions	PTEN putative induced kinase	Unknown; possible role in mitochondrial protection during oxidative stress
DJ-1	PARK7	Recessive	Point mutations; large deletions	Oncogene DJ-1	Unknown; possible role in cellular protection against oxidative stress
ATP13A2	PARK9	Recessive	Point mutations	P5 subfamily of ATPases	Unknown; cellular cation homeostasis and maintenance of neuronal integrity
Late Onset					
VPS35	PARK17	Dominant	Point mutations	Vacuolar sorting protein 35	Transport of proteins from endosomes to trans-Golgi network
LRRK2	PARK8	Dominant	Point mutations	Leucine rich repeat kinase 2	Cellular and protein interactions and cell signalling
SNCA	PARK1/4	Dominant	Point mutations; gene duplications and triplications	Alpha synuclein	Synaptic vesicle recycling, compartmentalization of neurotransmitters
eIF4G1	PARK18	Dominant	Point mutations	Eukaryotic translation initiation factor 4 gamma 1	mRNA cap recognition, ATP dependent unwinding of 5' terminal secondary structure; recruitment of mRNA to ribosome
CHCHD2	-	Dominant	Point mutations	Coiled-coil-helix-coiled-coil-helix domain containing 2	Unknown; possible role in maintaining activity of oxidative phosphorylation
Genes associated with PD					
GBA	-	-	Point mutations	Glucocerebrosidase	Glucosidase is a lysosomal hydrolysing glucosylceramide, the penultimate intermediate in degradation of complex glycolipids
MAPT	-	-	Two distinct haplotypes can be associated with PD (H1 and H2)	Microtubule Associated Protein Tau	Promotion of microtubule assembly and stability
DNAJC	-	-	Point mutations	DNAJ- Homolog Subfamily C	Transport of target proteins from ER to the cell surface
FBOX7	PARK15	Recessive	Point mutations	F-box only protein 7	Substrate recognition component of a SKP1-CUL1 F-box protein E3 ubiquitin ligase complex
UCHL1	PARK5	Dominant	Point mutations	Ubiquitin Carboxyl-Terminal Esterase L1	A thiol protease that hydrolyses a peptide bond at the C-terminal glycine of ubiquitin
PLA2G6	PARK14	Recessive	Point mutations	Phospholipase A2, Group VI	Catalyses the release of fatty acids from phospholipids.

Adapted from Trinh and Farrer, 2013. Abbreviations: *GBA*, glucocerebrosidase; *LRRK2*, leucine-rich repeat kinase 2; *VPS35*, vacuolar protein sorting 35; *EIF4G1* = eukaryotic translation initiation factor 4G1; *PINK1* = PTEN-induced kinase 1; *SNCA* = α synuclein; *UCHL1* = ubiquitin carboxyterminal hydrolase 1; *MAPT* = microtubule-associated protein tau; *FBOX7* = F-box only protein 7; *DNAJC* = DNAJ- Homolog Subfamily C

D620N mutation was confirmed to be disease-causing in familial PD cases with dominant inheritance (Bonifati, 2014). Lastly, the *eIF4G1* gene mutation was first discovered in a large French family through a genome-wide linkage approach (Chartier-Harlin et al., 2011). The missense R1205H and A502V mutations are the only two mutations found to date (Chartier-Harlin et al., 2011; Lesage et al., 2012), and there are suggestions that mutations in this gene do not cause PD, but are rather rare benign variants as they are more frequent in controls than in cases (Nichols et al., 2015).

1.4.2.2.   Autosomal recessive genes

Parkin mutations are the most common cause of autosomal recessive early onset PD (Lücking et al., 2000), and such mutations result in a loss-of-function of the parkin protein. Functionally, parkin acts as an E3 ubiquitin ligase, and works in conjunction with E1 ubiquitin activating enzymes and E2 ubiquitin conjugating enzymes of the ubiquitin proteasome system (UPS, Section 1.5.1). Parkin is also selectively recruited to the outer mitochondrial membrane (OMM) where it is a key player in mitochondrial quality control (MQC, Kuroda et al., 2006; Narendra et al., 2008). After *parkin*, *PINK1* (PTEN-induced putative kinase 1) mutations, either homozygous or compound heterozygous, account for 1-8% of early onset cases (Nuytemans et al., 2010), and are the second most common cause of autosomal recessive PD. The PINK1 protein is comprised of a mitochondrial targeting domain, resulting in its localization to the mitochondrial membrane (Gandhi et al., 2009). PINK1 plays a pivotal role in MQC together with parkin, and this will be discussed in greater detail in Section 1.7. Mutations in the *DJ-1* and *ATP13A2* genes are rare causes of early onset autosomal recessive PD. There is speculation that DJ-1 may play a role in the PINK1/parkin pathway, but studies have been inconclusive to date (as reviewed in Van der Merwe et al., 2015).

1.4.2.3.   Copy Number Variation in PD

Originally, CNV was defined as a segment of DNA that is 1kb or larger and is present at a variable copy number in comparison with a reference genome (Feuk et al., 2006). More recently, however, CNV describes any structural variation, including smaller events less than 1kb in size such as exonic rearrangements (Alkan et al., 2011). Classes of CNV include insertions, deletions, multiplications (duplications/ triplications), inversions and translocations (Figure 1.4). The discovery and genotyping of structural variation has been central to understanding disease associations, and altered expression

levels of CNV genes may be responsible for observed phenotypic variability, disease susceptibility and complex behavioural traits (Toft and Ross, 2010). In PD, CNV accounts for a number of pathogenic mutations, and has been observed in *SNCA, parkin, PINK1* and *DJ-1*.
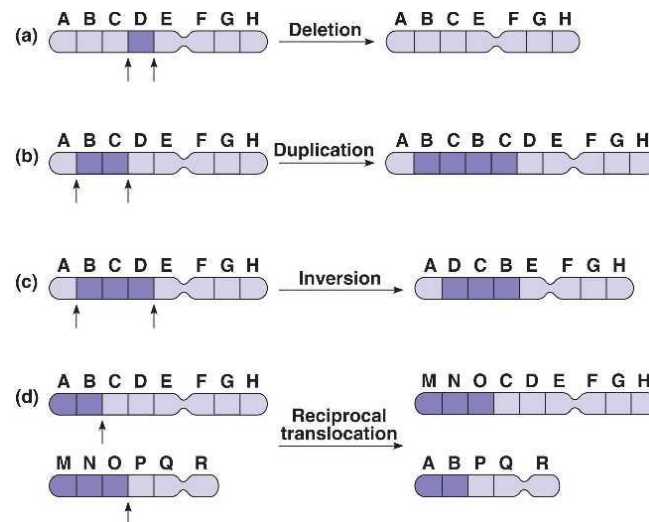
Figure 1.4. Illustration of different forms of chromosomal copy number variation including a) deletion, b) duplication, c) inversion and d) reciprocal translocation. Taken from http://bio1151.nicerweb.com/Locked/media/ch15/chromosome_mutations.html

The most widely used method for CNV detection in PD is Multiplex Ligation-dependent Probe Amplification (MLPA), a gene dosage technique that enables the detection of smaller deletions or insertions (i.e. a single gene or part of a gene/exon). This approach is PCR-based, and allows for simultaneous analysis of multiple genomic regions. Probes for the exons of the gene of interest are hybridised to patient and control DNA. After ligation and amplification, the resulting products are then analysed by capillary electrophoresis. Comparison of the peak patterns of the patient to that of the control allows for the observation of aberrant copy numbers. MLPA has been particularly successful in the detection of disease-causing exonic rearrangements in PD patients (Cazeneuve et al., 2009; Kay et al., 2010; Keyser et al., 2009; Moura et al., 2012). However, despite the success of this technique in CNV detection in PD, a major limitation is the resulting false positives that may occur due to the presence of SNPs in the region of the probe sequences. One such example of this phenomenon is due to the presence of a polymorphism (c,A574C, p.Met192Leu) in the annealing site of the probe for *parkin* exon 5 (Keyser et al., 2009; Yonova-Doing et al., 2012). This results in incorrect ligation of the probe

to the sample, and reduced PCR amplification. To correct for this, quantitative real time PCR (qRTPCR) is necessary to verify MLPA results.

The first evidence of genomic variation in PD was the discovery of genomic duplications and triplications of the entire *SNCA* locus (Ibáñez et al., 2004; Singleton et al., 2003). In *parkin*, the majority of CNV observed in PD patients are large exonic deletions, although exonic duplications and triplications have also been found to a lesser degree. Despite the large amount of CNV observed in *parkin*, CNVs in other autosomal recessive forms of PD such as *PINK1* and *DJ-1* are far less frequent. To date, a deletion of exons 4 – 8 in *PINK1* has been observed in a Sudanese family (Cazeneuve et al., 2009), an exon 6 – 8 deletion in a Japanese family (Li et al., 2005) and a whole gene deletion in an Italian patient (Marongiu et al., 2007). A large study performed on 51 Iranian families with inherited PD found two families with homozygous *PINK1* exon 4 and exon 5 deletions respectively. To date, no CNVs have been observed in *LRRK2, EIF4G1, VPS35* and *ATP13A2*.

1.5.   Mechanisms implicated in PD

To date, the pathogenic mechanisms of PD have not yet been fully established. However, growing evidence suggests that the specific neuronal cell death of the SNc neurons occurs by way of multiple apoptotic processes, including oxidative stress and mitochondrial dysfunction, proteolytic stress and the UPS, and dysfunction of the autophagic pathway. This section will focus on each of these aspects in greater detail to further elucidate and understand the underlying mechanisms that may be involved in PD pathogenesis.

1.5.1.   The Ubiquitin Proteasome System

The UPS is both a general and precise means for the disposal and removal of unwanted proteins in the cell that are either mutant, misfolded, damaged, terminally modified, or over-accumulated (Lehman, 2009). Interestingly, a common feature of neurodegenerative diseases such as PD, AD, prion diseases, tauopathies, motor neuron disease, spinocerebellar ataxia and amyotrophic lateral sclerosis is the accumulation, aggregation and deposition of abnormal proteins in the brain of patients with these disorders (Ciechanover and Brundin, 2003; Taylor et al., 2002). The resulting accumulation of damaged

and unwanted proteins leads to the formation of insoluble aggregates that are deposited in disease-specific inclusions (Taylor et al., 2002). For example, LBs are the result of a build-up of proteins in neuronal cells of PD patients. These observations led to the hypothesis that dysfunction in the UPS may be the primary cause, or one of the causes, of many of these neurological diseases.

The UPS is managed by three enzymes – namely an E1 ubiquitin-activating enzyme, E2 ubiquitin-conjugating enzymes, and E3 ubiquitin-ligating enzymes, of which parkin is an example. Initially, E1 activates ubiquitin in an ATP-dependent manner. Thereafter, E2 transfers the activated ubiquitin to the unwanted protein substrate that has been bound to E3, which subsequently attaches the ubiquitin to the protein. Additional activated ubiquitin molecules are added to the previous ubiquitin to form a polyubiquitin chain that acts as a label or tag on the unwanted protein. The protein is then recognised by the 26S proteasome, which unfolds and breaks down the complex into peptides and ubiquitin monomers to be recycled and reused (Figure 1.5).
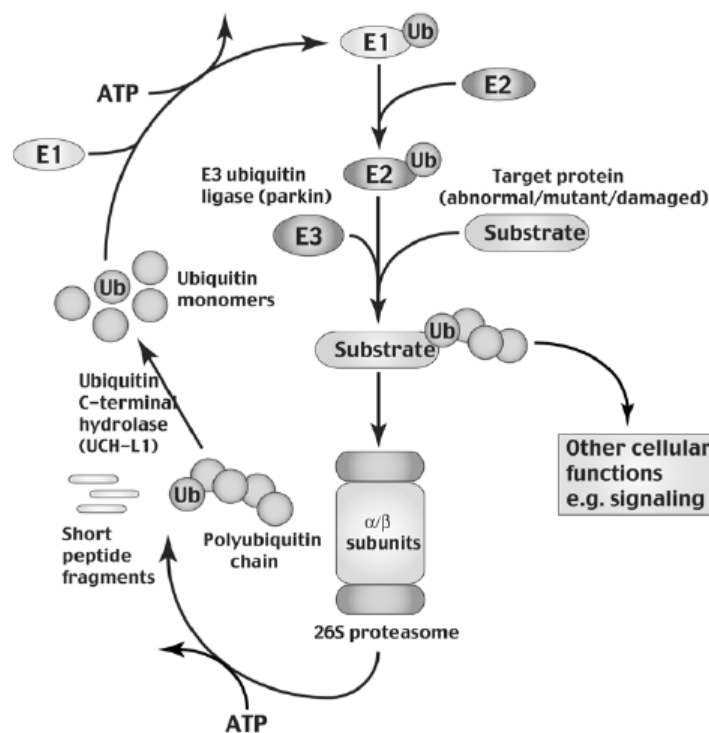
Figure 1.5. The Ubiquitin Proteasome System. Governed by the three enzymes - E1 ubiquitin-activating enzymes, E2 ubiquitin-conjugating enzymes and E3 ubiquitin-ligating enzymes, the UPS is responsible for the removal of damaged proteins from the cell via the 26S proteasome. Taken from Moore et al., 2003.

Dysfunction of the UPS is thought to be a mechanism of PD pathogenesis in both familial and sporadic PD, providing a link between sporadic and familial forms of the disorder (Moore et al., 2003). In sporadic cases, the structure and function of the 26S proteasome is altered in patients compared to controls, resulting in poor removal of unwanted proteins from the cell (Olanow and McNaught, 2006; McNaught et al., 2003). Alternatively, dysfunction of the UPS in familial PD is governed by mutations in either the *parkin* or the *SNCA* genes. Mutations in *SNCA* leads to a build-up of the α-synuclein protein, resulting in increased α-synuclein-positive aggregates. Multiplications (duplications and triplications) of the gene cause a three or four fold production of α-synuclein, and missense mutations increase the potential for the protein to misfold and aggregate (Olanow and McNaught, 2006). Interestingly, an accumulation of α-synuclein can also induce proteasomal damage, which can create a 'domino-effect' of increased α-synuclein and inability of the UPS to remove them due to the damaged proteasome caused by the α-synuclein (Snyder et al., 2003).

Mutations in *parkin* result in the loss-of-function of the parkin protein or a decrease in parkin enzyme activity, which cause substrates linked to parkin to accumulate in the cell. This has been shown to occur in the brains of PD patients and in *parkin* knockout mice (Ko et al., 2006, Ko et al., 2005). Studies in *Drosophila* and cell models of PD have revealed that accumulation of the parkin substrate Pael-R results in cell death, which is prevented by presence of parkin (Imai et al., 2003, Imai et al., 2000; Takahashi and Imai, 2003). Similarly, another substrate of parkin, FAF1, also accrues and results in cell death in SH-SY5Y cells, but this is abolished when parkin is present (Sul et al., 2013). Therefore an absence of functional parkin as a result of a mutation may cause the accumulation of unwanted and damaged proteins, thus resulting in cell death and ultimately disease onset.

1.5.2.   The Autophagy-Lysosome Pathway

Autophagy is defined as the global process by which intracellular components are degraded by lysosomes (Dehay et al., 2010). Cell survival is essentially only possible if there is a healthy balance between the formation and degradation of cellular proteins. Such degradation is carried out in partnership by two pathways – the afore-mentioned UPS, and the Autophagy-Lysosome Pathway (ALP). Autophagy can be separated into three processes, namely Chaperone Mediated Autophagy (CMA), microautophagy, and macroautophagy. CMA involves the selective targeting of cytosolic proteins to the lysosomal lumen for degradation. Microautophagy occurs when the lysosomal membrane invaginates and pinches off small vesicles of cytoplasm for digestion. Lastly,

macroautophagy (henceforth known as autophagy) is the large-scale degradation of cytoplasmic constituents, and will be the primary focus in this section.

Whilst the UPS is involved in highly selective degradation of short-lived intracellular and plasma membrane proteins, and misfolded/damaged proteins, autophagy encompasses the removal of long-lived stable proteins, large membrane proteins, and protein complexes that are too large to fit though the 26S proteasome. Furthermore, autophagy is the only process responsible for the degradation of aged or dysfunctional organelles. Various signalling pathways can either activate or inhibit autophagy, including the mTOR pathway, the Insulin/Akt pathway and the AMP kinase pathway (Chu, 2010). Known stresses that induce autophagy include nutrient and growth factor deprivation, and the presence of protein aggregates and damaged organelles (Nixon, 2006).

Initiated by these stresses, a double-sided isolation membrane will form around the damaged proteins or organelles and fuse to form an autophagosome (Figure 1.6). Once fully formed, the autophagosome then fuses with the lysosome, a cytoplasmic membrane-enclosed vacuole that contains a wide variety of hydrolytic enzymes, to form the autolysosome (also known as the autophagolysosome). Collectively, autophagosomes and autolysosomes can be referred to as autophagic vacuoles (AVs). At the formation of the autolysosome, the contents of the AV are degraded by the hydrolytic enzymes and recycled to provide amino acids and energy (Figure 1.6).
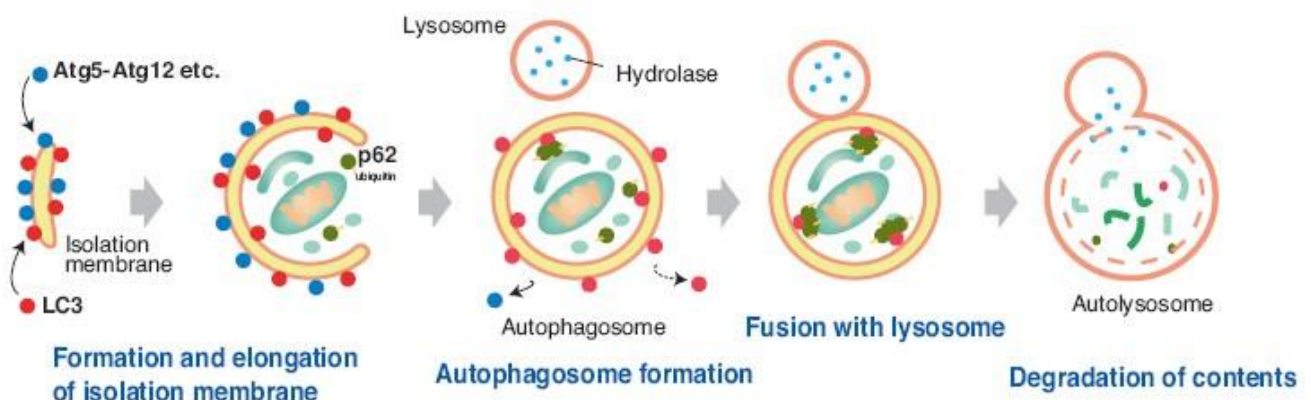
Figure 1.6. The Autophagy-Lysosome pathway. This illustration indicates the removal of cellular waste via the formation of an autophagosome and an autolysosome through the actions of Atg gene products Atg5-Atg12, LC3 and p62. Taken from www.bio-med.com.

In order to test the cells for autophagy, markers such as LC3-II (microtubule-associated protein 1 light chain 3) and p62 (SQSTM1/sequestosome) are used. Upon induction of autophagy, LC3-I is conjugated to phosphatidylethanolamine (PE) to generate LC3-II (Barth et al., 2010). The PE group then promotes integration of LC3-II into lipid membranes at the phagophore and autophagosomes, and LC3-II is subsequently degraded once the autolysosome is formed (Figure 1.6). The amount of LC3-II present in the sample correlates with the amount of autophagosome present in the sample (Mizushima, 2007).

The detection of an increased level of LC3-II or p62 is not always indicative of autophagy induction, but could also be representative of reduced autophagosome turnover and a blockade in autophagosome maturation (Zhang et al., 2013). Therefore, in order to distinguish between the two, autophagic flux needs to be measured. Autophagic flux is defined as the rate at which intracellular material is transported via the autophagic pathway to the lysosomes, and is measured by the difference in the amount of LC3-II/p62 before and after the addition of lysosomal inhibitors such as Bafilomycin A1 (BafA1). These inhibitors prevent the degradation of LC3-II by the lysosome, by preventing the fusion of the autophagosome with the lysosome. Therefore, if LC3-II and p62 is increased after the addition of BafA1, then there is an efficient autophagic flux. However if LC3-II remains at the same level after BafA1 treatment this is indicative of a defect in the process prior to lysosomal degradation.

An increase in autophagic flux indicates an increase in the rate of autophagy and clearance of damaged organelles and proteins, whereas a lower flux suggests a slower clearance rate, and therefore possible accumulation of these unwanted organelles and proteins in the cell. There is some ambiguity when using p62 as a measure for autophagic flux, because p62 is regulated at transcriptional and post-translational levels. Therefore if an autophagic inducer such as BafA1 activates p62 transcription, the increased autophagic flux may not be sufficient to clear intracellular p62. Therefore this measure of autophagy needs to be taken into consideration, and it is recommended to measure both LC3-II and p62 when determining autophagic flux (Puissant et al., 2012).

1.5.2.1.   Autophagy and PD pathogenesis

Despite its role in cell survival, autophagy has been implicated in various other processes including programmed cell death (PCD) and neurodegenerative disorders (Scott et al., 2007). Dysfunction can occur at various stages of the autophagic pathway, resulting in failure to protect the cell from damaged

and toxic proteins and organelles. For example, failure of autophagosome formation, failure of autophagosome fusion with the lysosome or deficiency of hydrolytic enzymes in the lysosome can all result in accumulation of dysfunctional substrates. Interestingly, an early study revealed an increase in the number of AVs and related structures of autophagy in the neurons of the substantia nigra from PD patients (Anglade et al., 1997). Cell models of PD induced by the addition of MPP$^+$ and rotenone also found increased AV presence compared to controls (Chu et al., 2007; Dagda et al., 2008; Zhu et al., 2007). Furthermore, several mouse models have shown that inhibition of the autophagy-related genes Atg5 and Atg7 leads to the formation of ubiquitinated cellular inclusions and neuronal cell loss (Hara et al., 2006; Komatsu et al., 2006). These studies confidently implicate autophagy in neurodegeneration and PD pathogenesis. Mitochondrial autophagy, or mitophagy, is a form of autophagy selective for degradation of mitochondria, and will be discussed in Section 1.7.

1.5.2.2.   Programmed Cell Death

PCD is described as the regulated death of a cell in any form, mediated by an intracellular program. Apoptosis, or Type I PCD, is characterised by the condensation of chromatin, nuclear fragmentation, cell shrinkage, and plasma membrane blebbing (the formation of protrusions in the membrane). Two pathways are known to be responsible for apoptosis – the extrinsic, or death receptor pathway, and the intrinsic, or mitochondrial pathway (Figure 1.7). Both pathways are controlled by caspases, which are either 'initiator' caspases (-2, -8, -9, -10) that start the apoptotic cascade, or 'effector' caspases (-3, -6, -7) that disassemble the cell. Briefly explained, death signals such as cellular stress, ROS and DNA damage result in the release of mitochondrial inter membrane space proteins conducive to Mitochondrial Outer Membrane Permeabilisation (MOMP), which is regulated by the Bcl family of proteins. MOMP causes the release of cytochrome c, which together with APAF-1 and pro-caspase 9 forms the apoptosome complex in the cytoplasm. This complex activates (cleaves) caspase 9 which in turn activates the effector caspases 3 and 7. The cascade accumulates in the activation (cleavage) of PARP (Poly ADP-ribose) which then results in dismantling of cellular structures and death. The extrinsic pathway is also initiated by death signals that activate death receptors at the plasma membrane. This results in the recruitment and activation of pro-caspases 8 and 10 which in turn activate the effector caspases.

Cleaved PARP is generally used as a marker of apoptosis in immunoblotting procedures. An increase in the levels of cleaved PARP is indicative of an increase in apoptosis. Any other caspase can be used

to further verify these results, but caspase 3 is predominantly used. Cleaved caspase 3 works in a similar manner to cleaved PARP, whereby when increased it signifies an increase in apoptosis. However, full-length caspase 3 is reduced when it is cleaved into its active form, and therefore increased levels of full-length caspase 3 indicate a decrease in apoptosis.
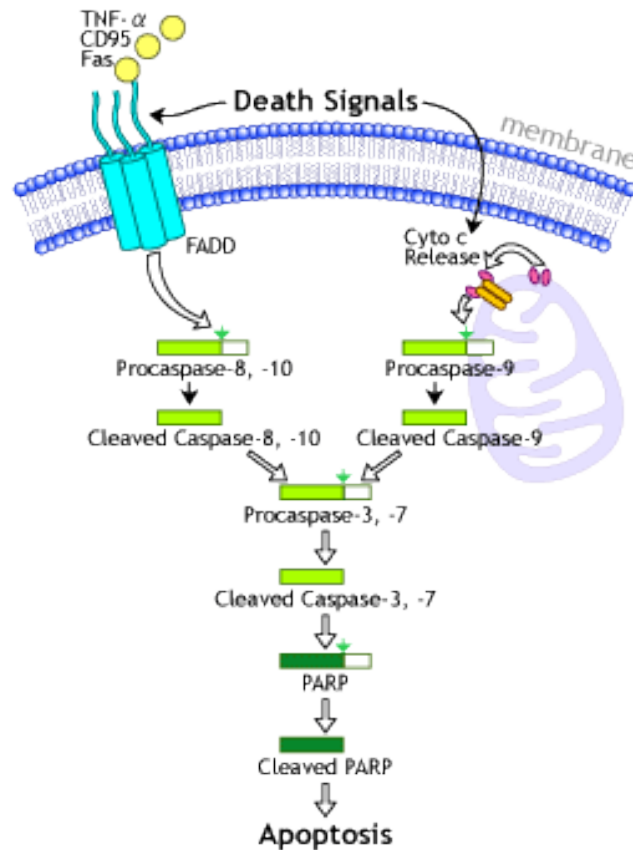
Figure 1.7. Summary of apoptotic cell death. The extrinsic (death receptor) pathway is initiated at the plasma membrane, and the intrinsic (mitochondrial) pathway at the outer mitochondrial membrane. Both pathways result in the cleavage and activation of PARP from the caspase cascade which activates apoptosis. Adapted from www.mdpi.com

In comparison to apoptotic cell death, autophagic cell death (also known as Type II PCD) is fast becoming a point of interest in neurodegenerative diseases. Neurons destined for elimination internalise their cytoplasmic components into autophagic compartments to effect self-degradation, and this is known as autophagic cell death (Nixon, 2006). The observation of advanced autophagy in PD led to the hypothesis that although autophagy is a protective mechanism for cell survival, it may also be a mechanism for cell suicide. Both PCD processes have been linked to similar molecular mechanisms

and proteins. For example, p53 has been shown to act as an inducer of both apoptosis and autophagy (Thorburn, 2007), and the P13K/Akt pathway is an inhibitor of both processes (Arico et al., 2001). Furthermore, Beclin-1 which is involved in the formation of AVs, physically interacts with Bcl-2, a key regulator of apoptosis (Liang et al., 1999). These similarities suggest that autophagy and apoptosis may be more similar than was previously thought, although it must not be forgotten that the primary role of autophagy is cell protection. Nevertheless, it is clear that both processes are part of PD pathogenesis and should be further investigated.

1.5.3.   Mitochondrial Dysfunction and PD

Mitochondrial dysfunction was first implicated in the development of PD through studies on pesticides and neurotoxins (e.g. MPTP, rotenone) that disrupt complex I of the ETC on the inner mitochondrial membrane (IMM). Post mortem studies on the SNc from PD patient brain samples revealed a significant decrease in complex I activity (Schapira et al., 1998, Schapira et al., 1990; Sherer et al., 2002). Furthermore, as previously mentioned, various genes known to cause PD, such as *parkin, PINK1* and *DJ-1*, play a role in mitochondrial function.

1.5.3.1.   Structure and function of the mitochondria

Mitochondria are elongated, rod-shaped organelles consisting of the OMM, the intermembrane space (IMS), the IMM, and the mitochondrial matrix (Figure 1.8). All four respiratory chain complexes and the ATP synthase (also known as complex V) of the ETC are situated on the IMM, which is the site of oxidative phosphorylation in mitochondrial respiration. Cristae are folds formed by the IMM in order to increase the surface area, and are vital for rapid and efficient energy production (Sherwood, 2015). The mitochondrial structure facilitates efficient functional capacity of the organelle. Structural defects such as swelling of the mitochondria or dysregulation of the mitochondrial network generally leads to mitochondrial dysfunction and a decrease in the ATP levels.
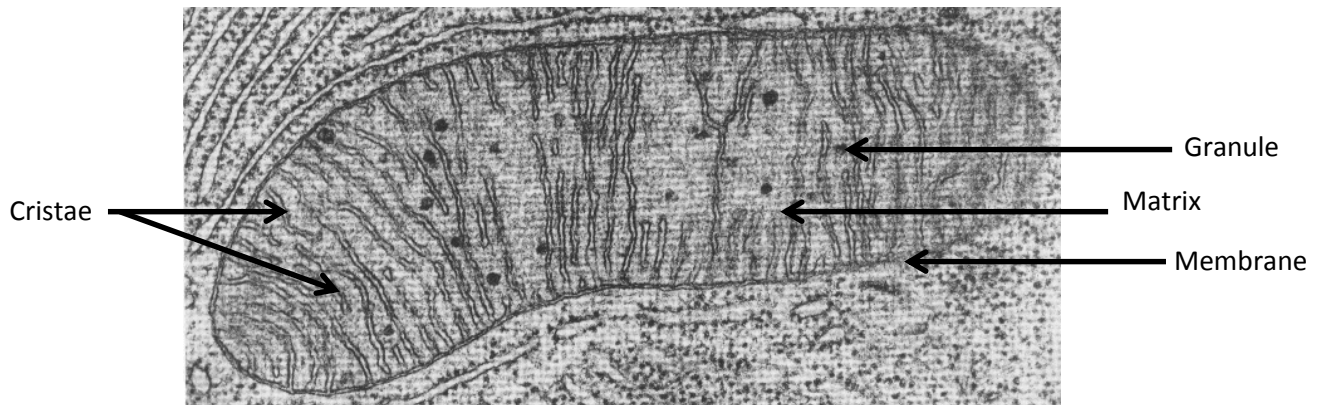
Figure 1.8. Electron micrograph of a mitochondrion. Taken from: http://www.tutorvista.com

The mitochondrion is a vital intracellular organelle found in all tissue types and it is responsible for one of the cell's key survival functions – the production of energy in the form of ATP. Mitochondria are also responsible for several other secondary functions, including regulation of cellular metabolism and respiration, signalling, cellular differentiation, cell death, control of the cell cycle and cell growth, and storage of calcium ions.

Mitochondrial respiration is defined as the series of metabolic processes by which all living cells produce energy through the oxidation of organic substances. Glycolysis is the first step of the process and occurs in the cytosol of all cells. It involves the breakdown of one molecule of glucose into two three-carbon molecules of pyruvate via a series of enzyme-controlled reactions. In glycolysis, a net yield of two ATP molecules for one molecule of glucose is produced. The pyruvate produced during glycolysis is used in the Krebs cycle (which also produces two ATP molecules) to make products needed for oxidative phosphorylation, the final step of mitochondrial respiration, which produces 34 ATP molecules per molecule of glucose (Figure 1.9). This is notably higher than the amount produced during glycolysis, signifying that glycolysis is less efficient in energy production than oxidative phosphorylation. Should oxidative phosphorylation be dysfunctional, then glycolysis assumes the role of the primary source for ATP. An example of when this occurs is in the absence of oxygen (when the cells are undergoing anaerobic respiration), oxidative phosphorylation cannot proceed, and glycolysis is then responsible for ATP production. Alternatively, if any of the five electron transport chain complexes are blocked or dysfunctional, cells will revert to glycolysis as the dominant producer of ATP.
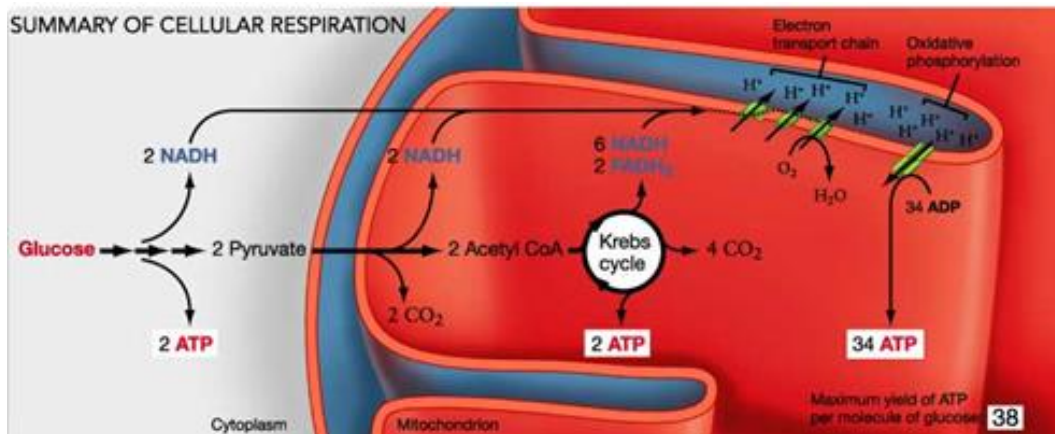
Figure 1.9. An overview of cellular respiration. For every molecule of glucose, two molecules of ATP are produced from glycolysis and the Krebs cycle, and 34 ATP molecules are produced via oxidative phosphorylation. Taken from http://www.uic.edu/.

Oxidative phosphorylation occurs on the IMM via five enzyme complexes (complex I, complex II, complex III, complex IV and ATP synthase/complex V; Figure 1.10). NADH (reduced nicotinamide adenine dinucleotide) and $FADH_2$ (reduced flavin adenine dinucleotide) act as carrier molecules, transporting hydrogen ions from the matrix to the inner membrane. NADH releases the hydrogen protons at complex I, whereas $FADH_2$ releases the protons at complex II. Once the protons are released, high energy electrons are extracted from the hydrogen. The hydrogen ions then move through the complexes and into the IMS, whilst the electrons move through the ETC via ubiquinone and cytochrome c and other specific electron carriers. When the electrons reach complex IV, they are passed to O_2, the final acceptor, and H_2O is formed. As the electrons move, energy is released which aids in the movement of more hydrogen ions into the IMS. The high concentration of hydrogen ions in the IMS then leads to a density gradient from the IMS to the matrix, forcing the hydrogen ions to move from the IMS into the matrix through the ATP synthase complex. This leads to the activation of ATP synthase, which drives the conversion of ADP and Pi into ATP (Figure 1.10).
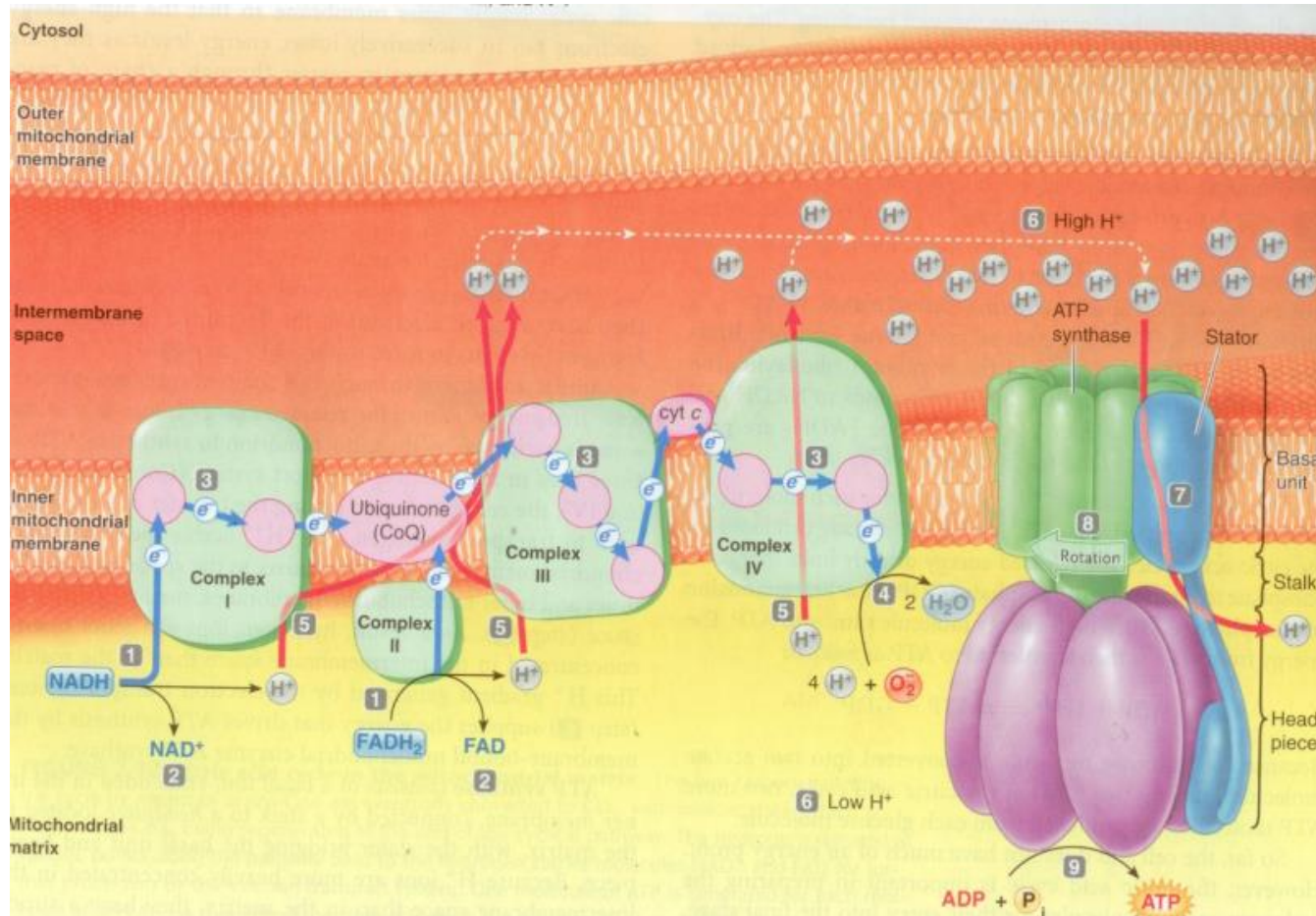
Figure 1.10. Oxidative phosphorylation at the mitochondrial inner membrane. This is shown in steps 1-9. This process involves the movement of electrons from the electron donors NADH and FADH$_2$ through a series of complexes, resulting in the movement of proton's to the IMS. This creates a high proton gradient, which in turn forces the hydrogen ions to move from the IMS into the matrix through the ATP synthase complex which drives the conversion of ADP and Pi into ATP

e$^-$, electron; NADH, reduced nicotinamide adenine dinucleotide; FADH$_2$, reduced flavin adenine dinucleotide; IMS, Intermembrane space; H$^+$, proton; ADP, adenosine diphosphate; Pi, inorganic phosphate; ATP, adenosine triphosphate. Taken from: Sherwood, 2015

The term 'mitochondrial dysfunction' can be widely used to include dysfunction in the generation of ATP, the production of ROS, involvement in apoptosis, and incorrect transport to areas in the cell (Brand and Nicholls, 2011). Mitochondria are the main producers of ROS in the cell as a by-product of respiration. ROS are part of the free radical family, which are molecules that have a shortage of electrons in their outer orbital. An example of such a molecule is oxygen, because it has two unpaired electrons in its outer orbital. ROS are scavengers, because in order to find stability they need to extract electrons from neighbouring molecules to complete their own outer orbital (Beal, 2003). This leads to oxidation of neighbouring molecules. For example, when oxygen adds an extra electron, it becomes the superoxide anion ($O_2^{\cdot-}$), which is also a free radical. When there is a complex I deficiency or any other deficiency in the respiratory chain, the amount of electrons lost to oxygen significantly increases, resulting in an increase in the levels of ROS. A cell undergoes oxidative stress when there is an imbalance between the production of ROS and the cell's ability to detoxify or neutralize the effect with antioxidants. Excessive ROS production and oxidative stress is toxic to the cell as they cause protein, lipid and DNA damage.

A second example of mitochondrial dysfunction is alterations in the mitochondrial rate of respiration. There is a constant fluctuation in the amount of energy required by tissues and cells, and the production of energy is controlled by a feedback system at the mitochondria with regulators of oxidative phosphorylation that determine either basal or maximal respiration. Basal respiration is the rate at which mitochondria function when cells only require a part of their total bioenergetic capacity. In comparison, maximal respiration is performed when the cell is in need of great amounts of energy in response to stress or an increased workload. The difference between ATP produced by oxidative phosphorylation at basal and at maximal respiration is defined as spare respiratory capacity (Desler et al., 2012). Spare respiratory capacity is able to provide cells with an extra burst of energy in response to stress, however if this is not available it will result in cell damage and death. This form of mitochondrial dysfunction whereby there is an exhaustion of spare respiratory capacity due to inconsistent respiration has been associated with cardiovascular and neurodegenerative disease (Nicholls, 2008; Yadava and Nicholls, 2007). It would therefore be appropriate to study these aspects of mitochondrial respiration in PD models, as it could further elucidate how mitochondrial dysfunction may be a cause of PD pathogenesis.

Mitochondrial membrane potential (MMP) has also been implicated as a cause of mitochondrial dysfunction and apoptosis. Membrane potential is defined as the difference in electric potential between both sides of a membrane. A voltage difference is created by the constant movement of protons and ions across the membrane. The MMP across the IMM is produced by the proton gradient formed during

oxidative phosphorylation (Gottlieb et al., 2003). As a core component of the proton motive force, the MMP is responsible for the synthesis of ATP by producing the force that pumps protons through the ATP synthase complex to generate ATP. Collapse of the MMP can compromise both the production of ATP and the integrity of the cell. If there is a loss of MMP, the permeability of the mitochondria becomes active via the mitochondrial Permeability Transition Pore (PTP). Opening of the PTP causes an inlet of solutes and water which result in swollen mitochondria. This in turn causes cytochrome c leakage and the onset of the caspase cascade and apoptosis.

It is clear that the MMP is essential for cell survival. In an intact and stable state, MMP is responsible for oxidative phosphorylation and ATP maintenance. However, a decrease in MMP results in the depolarisation of the mitochondria and can cause spontaneous cell death (Ly et al., 2003). Measurement of MMP is performed by staining the cells with the JC-1 (5,5',6,6' tetrachloro – 1,1,3,3' tetraethylbenzimidazol-carbocyanine iodide) fluorochrome. JC-1 is a lipophilic cation that is capable of entering selectively into the mitochondria and forming JC-1 aggregates upon membrane polarisation. These aggregates cause a shift in emitted light and a colour change from green to orange as the mitochondrial membrane becomes more polarised, which can be measured by means of flow cytometry.

1.5.3.2.   Mitochondria are dynamic organelles

Recent studies have shown that mitochondria are not static organelles with primary and secondary functions, but are highly dynamic, and are involved in processes such as movement, fusion, fission and mitophagy (Detmer and Chan, 2007). In most tissues, but especially in neuronal tissue, healthy mitochondria are transported towards areas with a high energy demand. In contrast, damaged or dysfunctional mitochondria move away from these areas into less demanding spaces of the cell. Movement can also promote morphological transitions in the mitochondria depending on the cell type. This is controlled by fusion and fission. Fusion and fission play major roles in maintaining the mitochondria, which is done by controlling the integrity of the mitochondria, the electrical and biochemical connectivity, the turnover of the mitochondria, and the protection of mtDNA (Berman et al., 2008).

Fusion is the merging of the double membranes of two mitochondria, resulting in a larger single organelle (Figure 1.11A). Alternatively, fission is the division of one mitochondrion into two smaller mitochondria, a healthy one and an 'impoverished one', which is tagged for degradation whilst the

healthy mitochondrion remains in the cell. Although these processes are not fully understood, fusion is controlled by the mitofusins (Mfn1 and Mfn2) and Opa1 on the OMM, whereas fission occurs via Drp1 and Fis1 (Figure 1.11A). The removal of unhealthy mitochondria in the cell is controlled by mitophagy, which is governed in part by the PINK1/parkin pathway (Section 1.7). The balance of fusion and fission is therefore vital in the maintenance of functional mitochondria and cellular requirements (Burbulla et al., 2010) and an imbalance can lead to autophagy and cellular apoptosis.

Detection of mitochondrial fusion or fission in cells is done via analysis of the mitochondrial network (Figure 1.11B). Mitochondria form tubular networks, and when they are predominantly undergoing fusion they appear joined together, resulting in a highly connected network (Legros et al., 2002). Alternatively, when the majority of the mitochondria are undergoing fission to rid the cell of damaged mitochondria, the network appears fragmented and broken. Knock down models in *Drosophila* have revealed that knock down of Drp1 and Fis1 results in elongated, connected mitochondria, whereas knock down of Opa1 and Mfn1/2 result in fragmented mitochondria (Deng et al., 2008; Ziviani et al., 2010). Conversely, overexpression of these proteins resulted in opposite effects to the knock down. The mitochondria are stained using fluorescent probes in order to observe the networks within the cells.
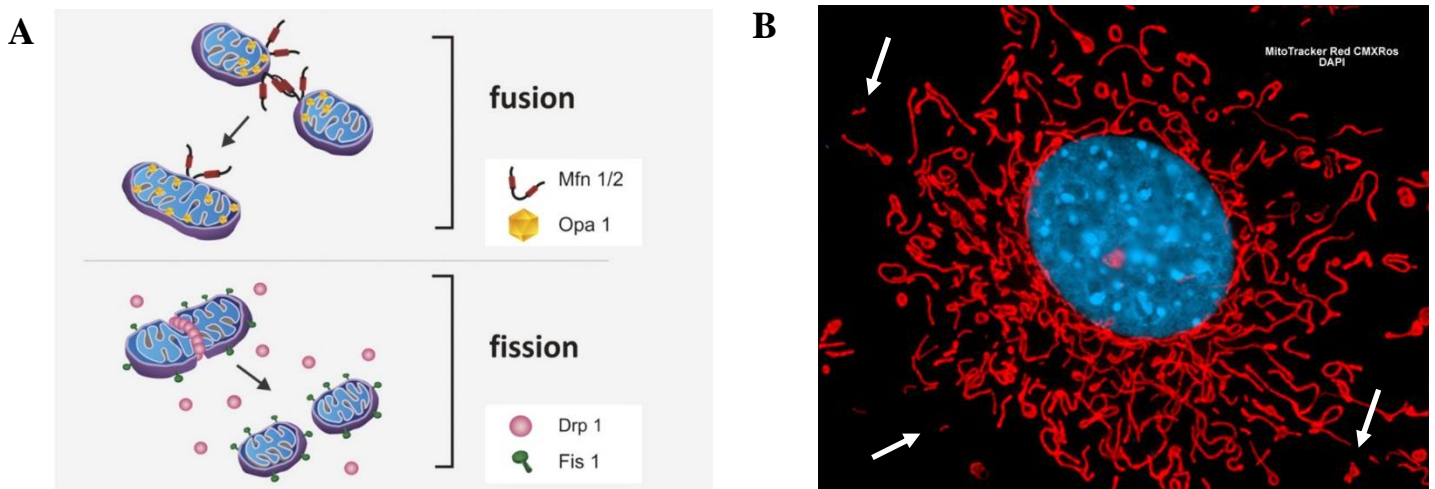
Figure 1.11. Mitochondrial fusion and fission mechanisms that form the mitochondrial network. A. Fusion is governed by the Mfn and Opa1 proteins, whereas fission occurs via Drp1 and Fis1. B. Image of the mitochondrial network stained with the red MitoTracker dye, and the nucleus stained with blue Hoechst dye. Mitochondria that have been fragmented from the network are shown by the arrows. Taken from www.mindsofmalady.com

1.6.   Treatment strategies

The current treatment for PD is through the administration of Levodopa, a dopamine precursor. Levodopa is a highly effective drug, as it can cross the BBB where it is converted into dopamine via a chemical reaction involving the enzyme aromatic L-amino acid decarboxylase (AAD), thus increasing the concentrations of dopamine in the central nervous system. Although Levodopa is a successful dopamine-replacement therapy, the long term effects of this drug on PD patients include motor fluctuations, dyskinesia, toxicity and loss of efficacy (Fahn et al., 2004).

Another treatment option for PD is deep brain stimulation (DBS) therapy. DBS is a surgical procedure, whereby electrodes are implanted into either the subthalamic nucleus or the globus pallidus within specific brain circuits, or neuronal loops, for modulation of the activity of those circuits. The electrodes are connected to an implanted pulse generator that is responsible for delivery of continuous stimulation, and the current produced then acts as either a suppressor or a driver of neuronal activity (Lozano et al., 2011). Risks of DBS include the small chance of a haemorrhage or stroke, depression and personality changes, paraesthesia's, dysarthria, motor contractions and infection. However, this treatment option is continually expanding and improving, and studies show that the clinical benefits of DBS outweigh the risks involved (Deuschl et al., 2006; Follett et al., 2010).

1.6.1.   Natural remedies

Herbal or natural remedies are fast becoming a preventative treatment or cure for diseases ranging from cardiovascular, diabetes, cancer and even the common cold (Kincheloe, 1997). It is thought that herbal medicines are less toxic than pharmaceutical agents, and the value of traditional medical systems continue to attract more media and public attention each year (Elvin-Lewis, 2001). A survey in the United States spanning seven years found a substantial increase in the use of alternative medicine therapies (Eisenberg et al., 1998). A second study observed that almost 40% of patients claimed to have used over the counter natural remedies to treat or prevent a health condition (Bennett et al., 2012), and this was reiterated in another study observing that more than one third of American adults use herbal remedies (Johnston, 2004).

The World Health Organisation estimates that 80% of the world's population use herbs as their primary method for health care needs (Winslow and Kroll, 1998). These studies have resulted in a greater focus over the past two decades on understanding these remedies and the side effects thereof, so that sufficient information and research can be obtained in order to deem these products safe for use. The use of medicinal plants in treatment of diseases has been limited by the lack of scientific data. Furthermore, research is needed to determine whether these types of products may be vital in preventing diseases that Western medicine is unable to do. The following section will focus on a detailed explanation on the natural compound curcumin, as it was investigated as a possible therapeutic agent in a cellular model of PD in the present study.

1.6.1.1.   Curcumin

Curcumin is derived from the *Curcuma longa* plant (Figure 1.12), a plant of the ginger family, and is the core component of the golden yellow curry spice turmeric. It was first described by Vogel & Pelletier in 1815, and more than 100 years later its biological characteristics and antibacterial activity were identified (Schraufstätter and Bernt, 1949). Since then, curcumin has gained considerable interest as a potential therapeutic aid, and has been shown to have anti-inflammatory, antioxidant, antimicrobial and anticarcinogenic activities (Anand et al., 2007). In addition to cell and animal models, phase I clinical trials have also shown that curcumin can be used to treat a variety of diseases including cancers, neurodegenerative diseases, cardiovascular disease, diabetes, allergy, asthma, bronchitis, inflammatory bowel disease, rheumatoid arthritis, renal ischemia, scleroderma, psoriasis and acquired immunodeficiency disease (AIDS; Aggarwal and Harikumar, 2009).

In patients with Alzheimer's disease (AD), curcumin was shown to enhance amyloid β (Aβ) uptake in macrophages (Fiala et al., 2007; Zhang et al., 2006). These results led to a 6-month clinical pilot study of curcumin in patients with AD, however no protective effect of curcumin was observed in comparison to the placebo group (Baum et al., 2008). Despite this, there were increased levels of Aβ in serum of patients who received curcumin, indicating that curcumin is able to disaggregate the Aβ-deposits in the brain. Longer studies are needed on AD patients to properly understand the effect of curcumin *in vivo*. A stage 2 18-month double-blind placebo-controlled clinical trial is currently ongoing to study the effects of curcumin on age-related cognitive decline. To date, there have been no clinical trials of curcumin exposure in PD patients. However, given its anti-inflammatory and antioxidant properties, further studies on PD are warranted.

Figure 1.12. Images representing the various forms of turmeric. A. The *Curcuma longa* plant exhibits lengthy, rectangular shaped leaves with white spike flowers. The roots are rhizomes 2-7cm in length. B. The turmeric powder comes from the roots or rhizomes of the *Curcuma longa* plant, and is commercially available as a spice used in cooking.

Anti-inflammatory

Initial animal studies found that curcumin decreases the formation of inflammatory compounds such as prostaglandins and leukotrienes (Huang et al., 1991; Kunchandy and Rao, 1990), and it was later discovered that the mechanism through which curcumin stops inflammation is by blocking JNK (Jun N-terminal kinase, Chen and Tan, 1998). JNK is responsible for the activation of various transcription factors in response to environmental stress, specifically NFκB, which plays a regulatory role in mediators of inflammation such as inflammatory cytokines (TNFα), chemokines, adhesion molecules, enzymes and kinases (Aggarwal and Harikumar, 2009). JNK also promotes cell death by activating Bcl-2. By inhibiting the activation of JNK, curcumin rescues the cell from apoptosis and tumorigenesis (Gupta et al., 2012; Pan et al., 2012). It was also found that curcumin blocks various other agents of

inflammation such as IκBα kinase and AKT, which further results in the inhibition of activation of NFκB and its gene products, ultimately providing protection against various diseases (Aggarwal et al., 2007a, Aggarwal et al., 2005; Kamat et al., 2007; Siwak et al., 2005). A complete list of the inflammatory pathways inhibited by curcumin can be found in Figure 1.13. It has been shown in these studies that curcumin is able to suppress inflammation through multiple pathways and thus provide vital protection against cellular damage.
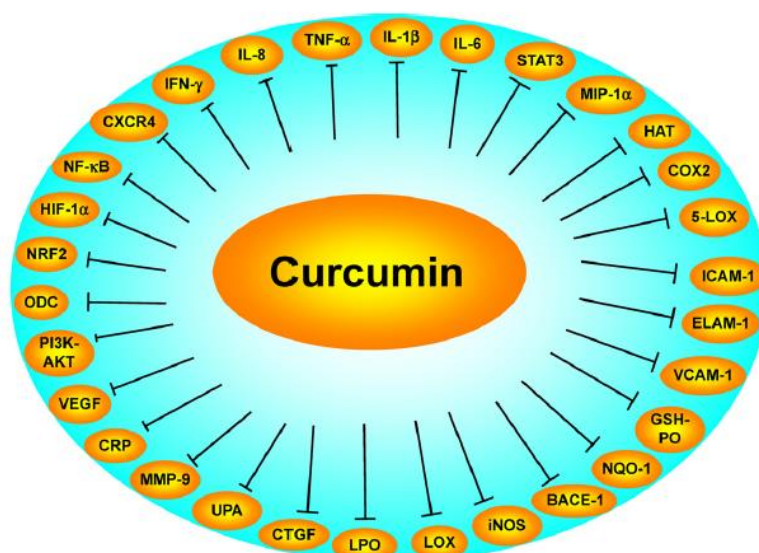
Figure 1.13. Inhibition of inflammatory pathways by curcumin. Taken from Aggarwal and Harikumar, 2009.

Antioxidant

Curcumin is largely known for its capacity as an antioxidant, through the scavenging of ROS and the inhibition of free radical generation (Manikandan et al., 2004). Furthermore, by inhibiting lipid degradation, peroxidation and cytolysis, curcumin is able to prevent oxidative cellular injury (Cohly et al., 1998). It has been suggested that this mechanism works through antiapoptotic and antioxidant properties exerted through the Bcl2-mitochondria-ROS pathway, and via the down regulation of NFκB (Chen et al., 2006; Ortiz-Ortiz et al., 2010). The human brain is highly oxidative, and consumes up to 20% of the body's oxygen. Through its antioxidant properties, curcumin would therefore be able to protect the brain against neurological disorders such as AD and PD by decreasing oxidised proteins and IL-1β. Interestingly, prevalence studies have indicated that there is a lower prevalence of neurodegenerative disorders in India, a country known for its high consumption of turmeric as a popular curry spice, compared to Westernised countries such as America. In particular, one study found a 4.4 fold reduced prevalence of AD in India compared to America (Ganguli et al., 2000). Furthermore, there

is a lower prevalence of PD in India compared to European countries (Muthane et al., 1998). Whilst this may be due to worse health care facilities and under researched areas of this developing country, it is tempting to consider that this may also be due to the high intake of turmeric and curcumin amongst this population.

To date, both animal and cell models of neurodegeneration have shown the protective effects of curcumin. In AD, curcumin reduced Aβ– induced oxidative stress in PC12 cells (Kim et al., 2001). Similarly, a MPP$^+$ model of PD in PC12 cells revealed that curcumin treatment protected the cells by inducing the anti-apoptotic protein Bcl2 and prevented dissipation of the MMP (Chen et al., 2006). A study on SH-SY5Y neuroblastoma cells affected with α-synuclein toxicity found that curcumin treatment protected the cells against this toxicity. Furthermore, it was revealed that curcumin reduced levels of intracellular ROS, and inhibited the activation of caspase 3 which ameliorated signs of apoptosis in the cells (Wang et al., 2010). Overexpression of A53T mutant α-synuclein in SH-SY5Y resulted in decreased LC3-II formation and autophagosomes, and ultimately inhibition of autophagy. Curcumin treatment to the cells reduced the levels of accumulated A53T α-synuclein and further rescued autophagy (Jiang et al., 2013).

Animal models of AD have shown that curcumin reduces the levels of oxidised proteins (Baum, 2004; Lim et al., 2001), inhibits the formation and aggregation of Aβ (Ono et al., 2004; Yang et al., 2005), and also reduces amyloid levels and plaque burden (Yang et al., 2005). Initial mouse models of PD induced by 6-OHDA (6-hydroxydopamine) and MPTP resulted in decreased levels of dopamine, which were rescued by curcumin treatment (Rajeswari, 2006; Zbarsky et al., 2005). More recently, a study by Liu and colleagues analysed the effect of curcumin on both a rotenone-induced *Drosophila* model of PD, and a rotenone-induced SH-SY5Y cellular model of PD (Liu et al., 2013). Treatment with curcumin significantly reduced dopaminergic neuronal loss and ameliorated PD-like symptoms in the *Drosophila* such as improvement in fly survival and prevention of locomotor impairment. In the PD cell model, curcumin reduced intracellular and mitochondrial ROS levels, and decreased apoptosis by inhibiting caspase 3 and caspase 9 activation (Liu et al., 2013). The previous work done on curcumin in animal and cell models have shown curcumin to play an essential role in the prevention of dopaminergic neuron loss, reduction of ROS, apoptosis and alleviation of autophagy. However the mechanism behind this drug is still unknown, and further work needs to be performed at a molecular level to determine how curcumin is able to protect cells against insult.

1.7.   The role of PINK1 in PD pathogenesis

Since *PINK1* is the focus of the present study, the following section will discuss this gene and its protein function in greater detail. *PINK1* contains 8 exons spanning 1.8kb, and encodes a 581 amino acid serine/threonine protein kinase (Figure 1.14). Valente and colleagues first discovered a homozygous G309D missense and a W437X nonsense mutation in families with autosomal recessive, early onset PD (Valente et al., 2004). *PINK1* mutations, either homozygous or compound heterozygous, are the second most common cause of autosomal recessive PD after *parkin*, and include point mutations, small insertions or deletions, genomic deletions and complex large rearrangements (Corti et al., 2011; Marongiu et al., 2007).

The PINK1 protein is comprised of a catalytic serine/threonine kinase domain as well as a mitochondrial targeting domain (Figure 1.14), resulting in its localization to the mitochondrial membrane (Gandhi et al., 2009). Studies have shown that PINK1 has autophosphorylation activity, and mutations in this protein have differential effects on its ability to phosphorylate protein substrates (Beilina et al., 2005; Silvestri et al., 2005). PINK1 is present in the cell in two forms – a cleaved, inactive protein of 55kDa, and a full-length, stable, functional protein of 65kDa. In healthy mitochondria, PINK1 translocates to the IMM via the TOMM20 machinery, where it is cleaved and rapidly degraded by the mitochondrial inner membrane rhomboid protease presenilin-associated rhomboid-like protease (Jin et al., 2010; Meissner et al., 2011) as well as other mitochondrial proteases MMP, m-AAA and ClpXP (Van Laar and Berman, 2013). Conversely, when the mitochondria are damaged or dysfunctional, the MMP is lowered, thereby inhibiting mitochondrial import of PINK1 by the TOMM machinery (Corti and Brice, 2013). This results in the accumulation of full-length PINK1 on the OMM where it plays a pivotal role with parkin in the removal of damaged mitochondria from the cell via the PINK1/parkin pathway (Becker et al., 2012; Song et al., 2013).

PINK1 is a multifunctional protein that is also required for cellular functions other than MQC, such as mitochondrial trafficking, Ca^{2+} signalling and autophagic degradation. It is fundamental in maintaining mitochondrial homeostasis and protecting the cell against stress-induced apoptosis through the regulation of the mitochondrial networks, decreasing mitochondrial oxidative stress and modulating autophagy (Van der Merwe et al., 2015). Mutations in *PINK1* have been implicated in causing mitochondrial structural defects such as alterations in mitochondrial morphology and network (Grünewald et al., 2009), as well as functional defects such as an increase in ROS production, a decrease

in the levels of ATP and a decrease in respiratory complex activity (Grünewald et al., 2009; Piccoli et al., 2008). Despite its predominant role in MQC, PINK1 has also been shown to be secondarily involved in pathways such as the UPS and autophagy, and is therefore a protein of great interest to further understand the mechanisms behind PD pathogenesis.
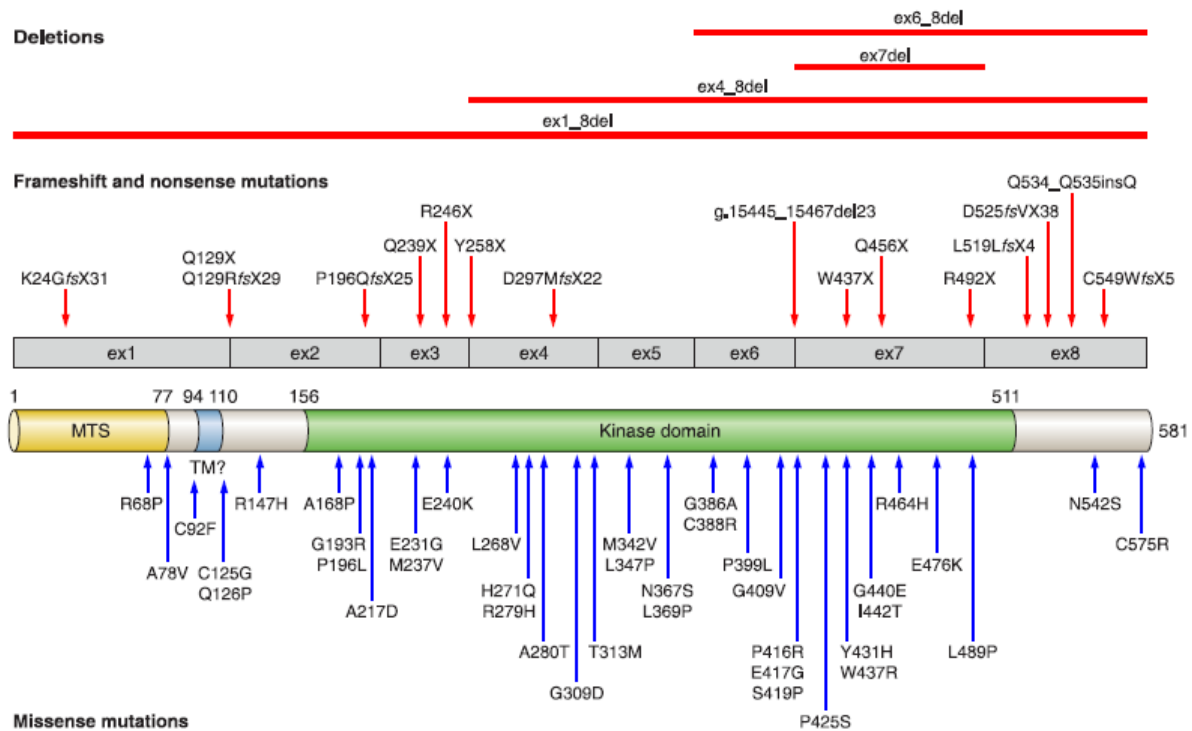
Figure 1.14. Schematic representation of *PINK1*. Deletions (red lines) and frame shift mutations (red arrows) are shown above the transcript. The protein organisations below the transcript highlight the mitochondrial targeting domain (yellow, MTS), the kinase domain (green) and the putative transmembrane region (TM, blue). Missense mutations are shown below the protein (blue arrows). Taken from Corti et al., 2011.

1.7.1. Animal models

Several animal knockout models of *PINK1,* specifically in *Drosophila*, have shown mitochondrial dysfunction, as well as muscle and dopaminergic neuron degeneration (Park et al., 2006). Results from loss-of-function *PINK1* mutant flies revealed locomotion defects in flight ability and climbing speed and abnormal muscle structure such as swollen, enlarged mitochondria with a loss of the OMM and fragmented cristae. Functionally, energy depletion was noted due to a decrease in ATP levels of mutant

flies. Studies in animal models other than *Drosophila* include mice, zebrafish and more recently murines. *PINK1*-deficiency in zebrafish revealed a developmental delay, decreased neuronal populations, and developmental retardation of dopaminergic neurons, that were rescued by PINK1 injection (Anichtchik et al., 2008; Xi et al., 2010). In comparison, knock out studies of *PINK1* in mice have interestingly shown no neuronal degeneration or PD phenotype, but rather defects in mitochondrial respiration in complexes II-IV (Gautier et al., 2008; Kitada et al., 2007), which may suggest that PINK1 functions differently in mammalian models of the disease.

Interestingly, animal knockout models of *parkin* also revealed changes in the mitochondria in comparison to the wild-type controls. A study on a *Drosophila parkin* knockout model found that mitochondrial defects were a common characteristic of pathology, and morphological differences such as irregular & dispersed myofibrillar arrangements and swollen and malformed mitochondria with disintegration of cristae were observed (Greene et al., 2003). These flies exhibited reduced lifespan, locomotor defects and male sterility. Due to the highly similar phenotypes in *parkin* and *PINK1* knockout flies, it was hypothesized that these two proteins may play similar roles in the cell, or possibly even function through a common mechanism. Studies indicate that *parkin* overexpression rescues the detrimental phenotype found in *PINK1* knock out models, whereas *PINK1* overexpression did not show any changes to the phenotype in a *parkin* knock out model (Clark et al., 2006; Park et al., 2006; Yang et al., 2006). Therefore it was determined that *parkin* and *PINK1* function through a common pathway known as the PINK1/parkin pathway, where parkin acts downstream of PINK1.

Animal models of *PINK1* mutants also reveal loss of complex I activity, decreased MMP, defective mitochondrial morphogenesis and swollen mitochondria (Clark et al., 2006; Park et al., 2006; Yang et al., 2006). This has led to the hypothesis that these phenotypic changes may be a consequence of dysfunctional fusion/ fission machinery. Initial studies in *Drosophila* showed that when *PINK1* is over-expressed, fission appears to be promoted, however when under-expressed, fusion appears to take over (Clark et al., 2006; Park et al., 2006; Yang et al., 2006). When *parkin* or *PINK1* are knocked out, elongated mitochondria were observed (similar to what can be seen when Drp1/Fis1 are knocked out and Opa1/Mfn are overexpressed), whereas when overexpressed, mitochondrial fragmentation proceeded (Figure 1.15, Ziviani et al., 2010). *PINK1* mutant flies displayed dysfunction of the dopaminergic neurons, mitochondrial aggregates and tubular structure. Either overexpression of the pro-fission protein Drp1, or under-expression of the pro-fusion protein Opa1 restored the dopamine levels and suppressed mitochondrial aggregation indicating that PINK1 may act through Drp1 to regulate fission (Deng et al., 2008; Poole et al., 2008; Yang et al., 2008). Missense mutants of *parkin* and *PINK1* exhibited a loss of mitochondrial integrity due to reduced mitochondrial fission (Poole et

al., 2008). These animal models have conclusively shown that the PINK1/parkin pathway promotes fission and inhibits fusion, either by positively regulating Mfn/Opa1 or by negatively regulating Drp1.
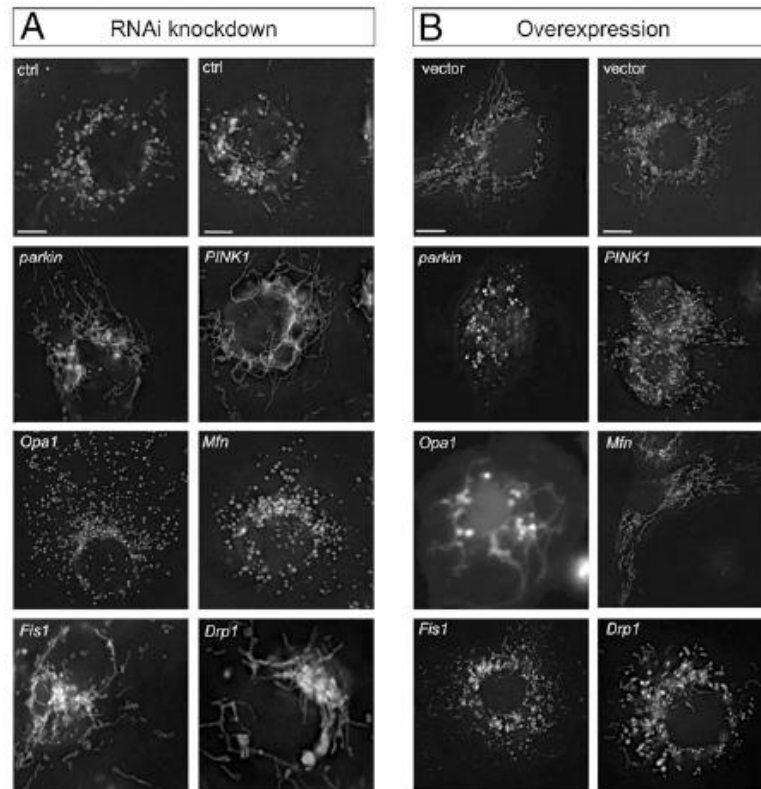
Figure 1.15. PINK1 and parkin activity either promotes mitochondrial fission or inhibits fusion in *Drosophila*. Mitochondrial network staining using Rhodamine 123 indicates that knock down of *parkin* or *PINK1* results in increased mitochondrial connectivity (similar to *Drp1/Fis1* knock down), and *parkin* or *PINK1* over expression results in network fragmentation (similar to Drp1/Fis1 over expression). Taken from Ziviani et al., 2010.

1.7.2.   Cell models and primary cultures

Several cell lines have been used to establish alternative models of PD, including HeLa, M17, SH-SY5Y, COS1, COS7, HEK293T, human fibroblasts and more recently induced pluripotent stem cells (iPSCs). An initial study investigating the PINK1/parkin interaction in mammalian cells performed RNA-interference mediated down regulation of *PINK1* and subsequent overexpression of *parkin* in a HeLa cell line, and confirmed that *parkin* and *PINK1* act in a common physiological and pathological pathway (Exner et al., 2007). Subsequent *PINK1* knock down studies in cell cultures show cells that exhibit mitochondrial dysfunction such as decreased MMP, increased ROS levels, enlarged

mitochondria with decreased number of cristae and complex I respiratory dysfunction (Dagda et al., 2009; Gegg et al., 2009; Hoepken et al., 2007; Wood-Kaczmar et al., 2008).

Interestingly, whilst *PINK1* knock down cells similarly exhibited damaged mitochondria as observed in *Drosophila* models, increased fragmentation rather than increased connectivity was exhibited in HeLa, SH-SY5Y and M17 cells (Figure 1.16, Dagda et al., 2009; Exner et al., 2007; Lutz et al., 2009; Sandebring et al., 2009). Conversely, in *parkin*-mutant fibroblasts the mitochondria appear more branched and connected compared to controls in some cases (Grünewald et al., 2010; Mortiboys et al., 2008), whereas other cases revealed increased fragmentation in patient-derived fibroblasts (Pacelli et al., 2011) or no changes (van der Merwe et al., 2014). Overexpression of *parkin* or *PINK1* in SH-SY5Y cells was able to suppress mitochondrial fragmentation induced by Drp1, thus implicating both parkin and PINK1 as pro-fusion proteins in mammalian cells (Lutz et al., 2009). These contradictory results may be due to the fact that cancer-derived cell lines and fibroblasts are actively dividing and therefore may lack the characteristics of post-mitotic neurons. It has also been suggested that cells may need an additional stressor in order for changes in the mitochondrial network to occur. Despite this drawback, studies on cell lines such as these are vital to tease out the mechanisms of genes and signalling pathways.
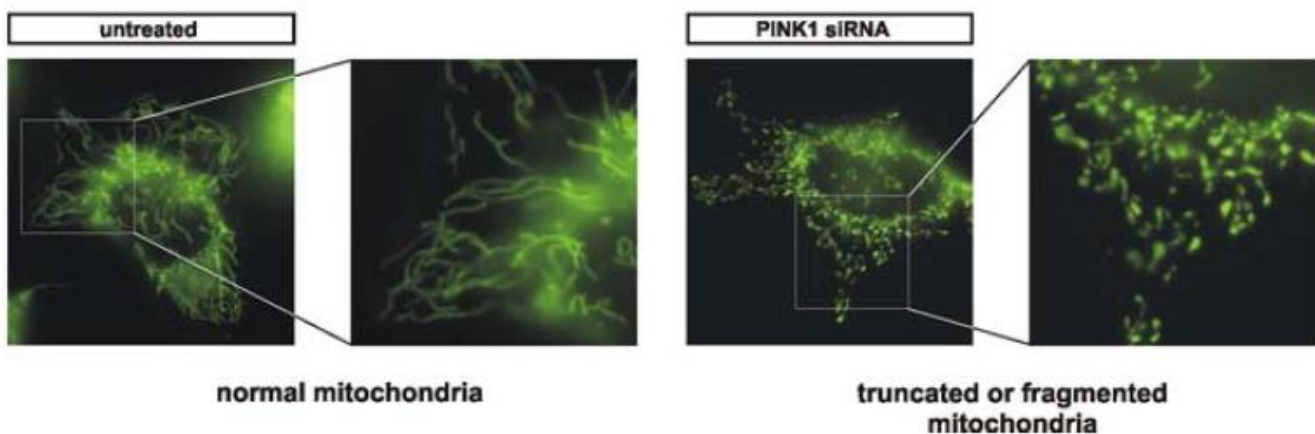
Figure 1.16. Representative examples of normal or altered (truncated or fragmented) mitochondrial morphologies in HeLa cells following down regulation of *PINK1* using siRNA. Taken from Exner et al., 2007.

A second observation in *PINK1*-deficient cell cultures is the effect of PINK1 on cellular and mitochondrial autophagy. Aggregates reminiscent of autophagosomes that appeared lysosomal in

nature were observed in *PINK1* knock down models of SH-SY5Y cells and mice neurons (Wood-Kaczmar et al., 2008). This was verified in a similar study using SH-SY5Y cells that revealed an elevated number of AVs and lysosomes in *PINK1* knock down cells that were not present in control or *PINK1* overexpressed cells (Dagda et al., 2009). This was further tested using the LC3-II marker of autophagy, which was shown to be increased when *PINK1* is under expressed (Figure 1.17). These studies suggest that a loss of PINK1 promotes autophagy in cell cultures. However it is still unknown whether autophagy is compensating for cell damage to ensure cell survival, or aiding in cell suicide, as some studies have shown that there is a decreased level of mitochondria in *PINK1* knock downs (Dagda et al., 2009), whereas other studies indicate mitochondrial elimination when *PINK1* is overexpressed (Kawajiri et al., 2010). It is clear that future studies should be conducted to determine whether an increase in LC3-II levels is indicative of increased autophagic clearance or rather inhibited lysosomal degradation.
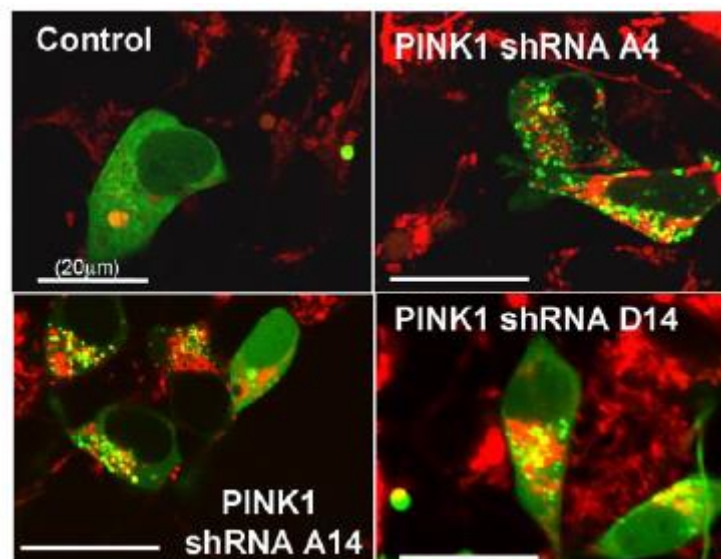
Figure 1.17. Knock down of *PINK1* increases autophagy. Confocal microscopy of MitoTracker Red-labelled mitochondria in control and three *PINK1* shRNA lines expressing LC3-II (green) indicates an increase in LC3-II in all three knock down lines compared to the control. LC3-II is colocalised with the mitochondria, indicating an increase in mitophagy. Taken from Dagda et al., 2009.

A third and increasingly popular method for understanding the mechanisms involved in the PINK1/parkin pathway is the use of iPSCs, which have the capacity to differentiate into any cell from the human body (Badger et al., 2014). In the case of PD, patient fibroblasts carrying mutations in the PD-causing genes are obtained, cultured, and differentiated using various growth factors into dopaminergic neurons. A study investigating mitochondrial dysfunction in *PINK1* mutant PD patients' iPSCs revealed an increase in ROS levels and a decrease in the production of the antioxidant glutathione

synthase (Cooper et al., 2012). Furthermore, an initial study on mutant *PINK1* iPSCs to observe the mechanism of the PINK1/parkin pathway found that when the mitochondria were depolarised, parkin recruitment to the OMM was impaired in the mutant *PINK1* iPSCs compared to control iPSCs (Seibler et al., 2011). Interestingly, observations in patient fibroblasts have differed compared to the iPSCs differentiated, indicating the importance of studies to be done in both cell cultures (Rakovic et al., 2013). Future studies should also focus on mitochondrial structure and network in iPSCs to further understand the mechanism of the PINK1/parkin pathway.

1.7.3.   Mechanism of the PINK1/parkin pathway to date

A breakthrough study by Narendra and colleagues revealed in HEK293 cells that after the addition of the mitochondrial membrane inhibitor CCCP (carbonyl cyanide 3-chlorophenylhydrazone), parkin was recruited to the OMM (Narendra et al., 2008). A second study showed that PINK1 is also recruited and accumulates at the OMM of dysfunctional mitochondria with low membrane potential and that PINK1 expression at the OMM is necessary for parkin recruitment (Narendra et al., 2010). Therefore, despite conflicting observations in animal models, cell cultures and iPSCs, the current mechanism of the PINK1/parkin pathway is thought to occur as follows:

An interaction between parkin and PINK1 is initiated by the depolarisation of mitochondria, which recruits full-length PINK1 to the OMM (Pickrell and Youle, 2015; Narendra et al., 2010). Co-immunoprecipitation experiments have determined that parkin and PINK1 are involved in a direct interaction, whereby PINK1 phosphorylates parkin and activates its E3 ligase activity at the OMM (Geisler et al., 2010; Kawajiri et al., 2010; Kim et al., 2008; Sha et al., 2009; Shiba et al., 2009; Um et al., 2009). Once phosphorylated, parkin then ubiquitinates mitochondrial substrates including fusion proteins Mfn1 and Mfn2 (Gegg et al., 2010). Mfn1 and Mfn2 are now tagged for degradation via the UPS, and once they have been removed, the balanced regulation between fusion and fission is compromised, resulting in a shift towards increased fission. This then initiates fragmentation of the mitochondrial network and therefore isolation of dysfunctional mitochondria, which are subsequently removed by mitophagy, thereby keeping the cell in a healthy state (Figure 1.18). If either *parkin* or *PINK1* is mutated or down regulated, the dysfunctional mitochondria will remain in the cytoplasm, creating an environment of oxidative stress ultimately resulting in cell death (Devireddy et al., 2015). It is thought that parkin has limited activity in the absence of PINK1, and this activity is potentiated through *PINK1* expression (Xiong et al., 2009).
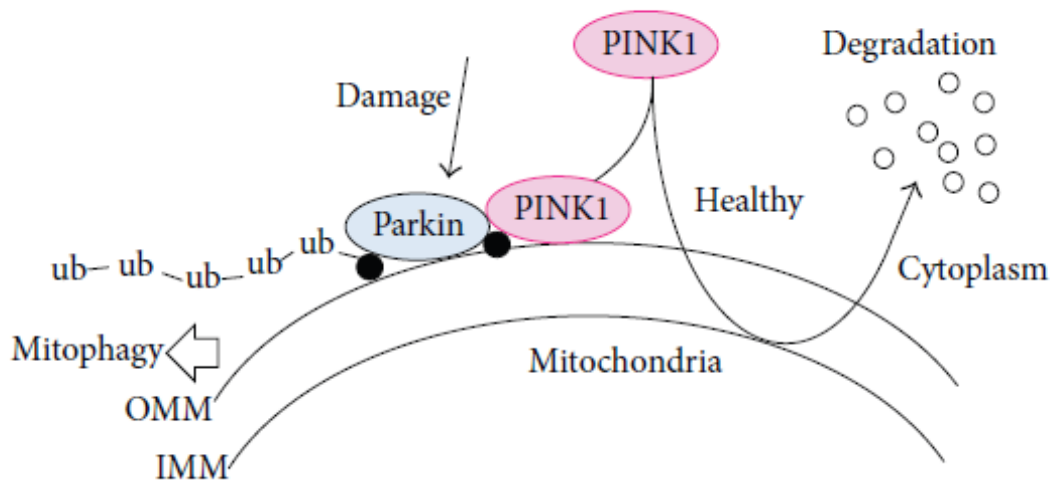
Figure 1.18. Hypothetical schematic representation of the mechanism behind the PINK1/parkin pathway. Taken from Matsuda et al., 2013.

1.8. The present study

This study involves the creation of a *PINK1* siRNA-mediated knock down model of PD in an SH-SY5Y neuroblastoma cell line in order to gain insight into PD pathogenesis. By decreasing the gene and protein expression levels of PINK1 compared to a normal wild type control and studying its physiological effects, this may provide insight into the physiological function of PINK1. Furthermore, this study investigated the potential rescue effects of curcumin, an antioxidant and anti-inflammatory compound, on the *PINK1* knock down cellular model. The mechanism and neuroprotective properties through which curcumin acts is not yet fully understood, therefore this project attempted to answer questions regarding the role of curcumin at a molecular level. In addition, in an attempt to study the effects of curcumin in patient-derived cells, South African PD patient samples were screened to identify patients with CNV in *PINK1*, and other PD-causing genes.

1.8.1.   Hypothesis

It was postulated that decreased expression of *PINK1* will result in mitochondrial functional and structural abnormalities that would include decreased cell viability, decreased MMP, decreased mitochondrial respiration and increased autophagic flux, as well as increased apoptosis and a more fragmented mitochondrial network. For some of these effects an additional stressor paraquat (known to cause mitochondrial toxicity) would be necessary for the effect to become evident or to exacerbate the defect. We hypothesised that curcumin exposure would be able to rescue all or some of these effects in a PD cellular model. Additionally, we hypothesized that copy number variation, specifically in the *PINK1* gene, would be observed in South African patients with PD.

1.8.2.   Aims & Objectives

The aim of the present study was to investigate the potentially protective effects of curcumin, in the presence or absence of paraquat, on a *PINK1* siRNA-mediated knock down cellular model of PD. The study also aimed to identify patients with copy number changes specifically in *PINK1* but also other PD-causing genes for further study.

The objectives of this study were as follows:

1. To create a PD cellular model using a *PINK1* siRNA-mediated knock down approach in SH-SY5Y neuroblastoma cells.
2. To determine the correct dosage and time of exposure for paraquat and curcumin, and establish treatment groups and an appropriate timeline for the addition of each to *PINK1* knock down cells and control cells.
3. To determine cell viability in treatment groups.
4. To measure levels of apoptosis through the detection of apoptotic markers cleaved PARP and full-length caspase 3.
5. To determine mitochondrial membrane potential in treatment groups.

6. To investigate parameters of mitochondrial respiration including basal respiration, ATP production, maximal respiration and spare respiratory capacity, as well as levels of glycolytic respiration in treatment groups.

7. To analyse mitochondrial network in treatment groups.

8. To measure levels of autophagic flux in treatment groups.

9. To screen South African PD patients for CNV mutations in *PINK1*, and other known PD-causing genes.

10. To compare results obtained from the SH-SY5Y cell line with fibroblasts obtained from patients with *PINK1* CNV mutations.

Chapter 2: Materials & Methods

2.1. Summary of methodology

SH-SY5Y neuroblastoma cells were cultured and treated with HiPerfect transfection reagent and *PINK1*/non-silencing control siRNA. Gene and protein expression of PINK1 was then tested using qRTPCR and Western blotting, to verify that knock down had been successful. Thereafter, both *PINK1* siRNA cells and control cells were subdivided into four treatment groups: i. untreated, ii. treated with 25μM paraquat for 24 hours, iii. pre-treated with 2μM curcumin for 1 hour followed by 25μM paraquat for 24 hours, and iv. treated with 2μM curcumin for 1 hour. Various parameters of mitochondrial and cellular function were measured including cell viability, apoptosis, mitochondrial respiration, mitochondrial membrane potential, mitochondrial network, and autophagic flux. This was performed to determine the effect of decreased PINK1 expression on these cells, as well as the possibly protective effect of curcumin treatment.

An objective of this study was to repeat this method in a patient-derived fibroblast model of PD. The MLPA technique was used to detect CNV in the known PD-causing genes in South African PD patients. All results were verified by qRTPCR and Sanger sequencing.

A summary of the methodology is shown in Figure 2.1.
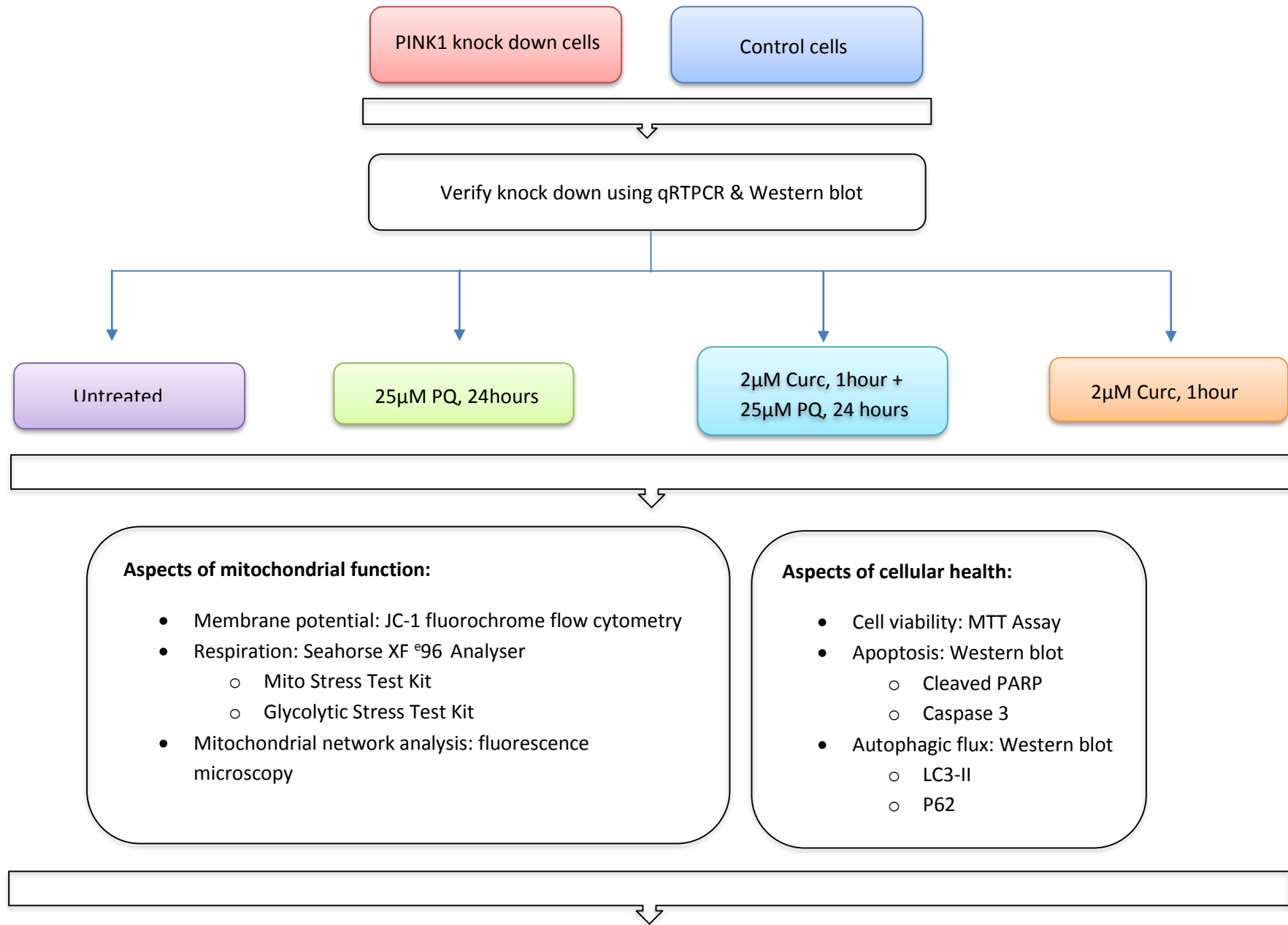
Figure 2.1. Summary of Methodology

2.2.   Creating a *PINK1* knock down cellular model of PD

The SH-SY5Y neuroblastoma cell line was ordered (European Collection of Cell Cultures, ECACC, UK) and cultured in a 1:1 ratio of Dulbecco's Modified Eagle Medium (DMEM; Lonza, Switzerland) and Ham's F12 Medium (Lonza, Switzerland). Added to the culture medium was 10% fetal bovine serum (FBS) and 1% penicillin streptomycin. Passage numbers were recorded and cells under passage 15 were used. All cell culture protocols are recorded in Appendix I. For all knock down experiments, cells were seeded into 6-well plates (CoStar, Corning Incorporated, USA) and treated with siRNA when the cells were approximately 60% confluent.

RNA interference was performed using small interfering RNA (siRNA) to determine whether the suppression of the *PINK1* gene resulted in cellular defects compared to a control. Knock down was achieved using the Flexitube siRNA kits (Qiagen, Germany). Four preselected siRNAs for *PINK1* were optimised to determine which siRNA would produce the highest decrease in PINK1 gene and protein expression. A non-silencing control siRNA with a scrambled sequence was included as a primary control for comparison. The siRNA sequences are summarised in Table 2.1. Stock siRNAs of 20μM were prepared by the addition of 250μl RNase-free H$_2$O to the siRNA, and were kept at -20°C.

Table 2.1. Sequences of the four different siRNAs used for knocking down *PINK1*

Gene	Product name	Sequence
PINK1	Hs_PINK1_2 Flexitube siRNA NM_032409	CTCCAGCGAAGCCATCTTGAA
	Hs_PINK1_3 Flexitube siRNA NM_032409	CCGGACGCTGTTCCTCGTTAT
	Hs_PINK1_4 Flexitube siRNA NM_032409	GACGCTGTTCCTCGTTATGAA
	Hs_PINK1_6 Flexitube siRNA NM_032409	ATGGGTCAGCACGTTCAGTTA

SH-SY5Y cells were cultured and seeded into 6-well plates containing 2x10^5 cells per well. For transfection, 0.6μl of the 20μM siRNA stock was added to 99.4μl serum-free medium and 12μl HiPerfect transfection reagent (Qiagen, Germany), to achieve a final concentration of 5nmol. Two controls were used to compare to the *PINK1* siRNA – i. the non-silencing control siRNA, and ii. a mock transfection control which is composed of only transfection reagent and serum-free medium, but no

siRNA. These complexes were incubated at room temperature for 15mins. During incubation, the media was removed from the cells and a new volume of 2.3ml medium was added to each well. Thereafter, the complexes were added drop-wise to the wells.

Plates were then incubated at 37°C, 5% CO_2 for 48 hours in the Forma Steri-Cycle CO_2 Incubator (Thermo Scientific, Pierce Biotechnology, USA). Previous studies using the same siRNA kit and protocol have recommended that cells be continuously treated with siRNA over a longer time period (Gegg et al., 2009; Gegg et al., 2010). This method of knock down is specific to *PINK1*, as knock down of this protein for 48 hours is insufficient to produce significant changes to the cellular phenotype. Based on this knowledge, cells were treated with the siRNA and HiPerfect transfection reagent every third day for a total of 12 days (Figure 2.2). This was also performed on the control samples.
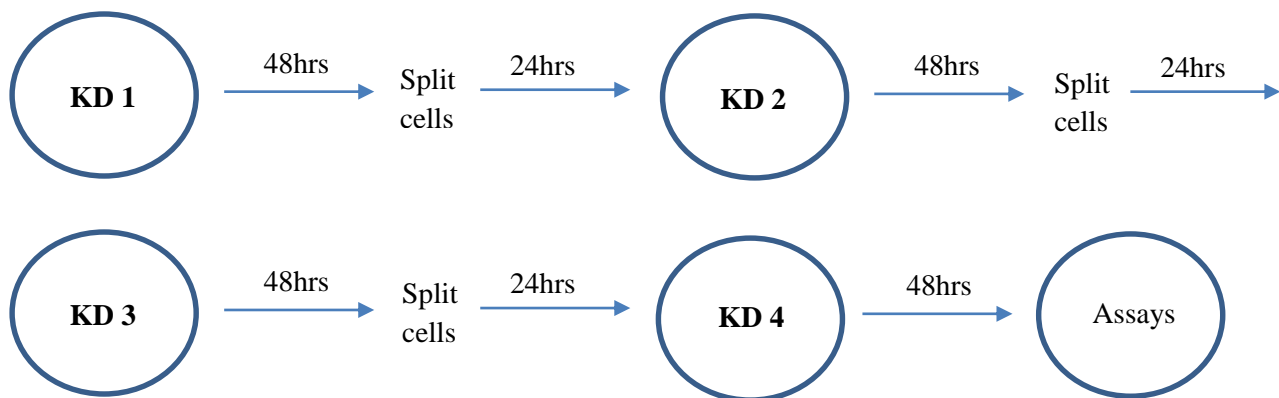
Figure 2.2. The procedure for transfecting SH-SY5Y cells with *PINK1* siRNA, control non-silencing siRNA and transfection reagent. KD, knock down.

2.2.1. Verification of efficient *PINK1* knock down by quantitative real time PCR

RNA extraction and cDNA synthesis

The RNeasy Mini kit (Qiagen, Germany) was used for isolation and purification of intracellular RNA from the SH-SY5Y cells. After the 12 day siRNA transfection period, cells were trypsinised and centrifuged (Prism Microcentrifuge, Labnet, USA) to pellet the nucleic acids. The pellet was washed and resuspended, followed by manual RNA purification according to the manufacturer's instructions.

RNA conversion into cDNA was then carried out using the Quantitect Reverse Transcription Kit (Qiagen, Germany) in a two-step process. This kit provides a convenient procedure for effective reverse transcription as well as effective genomic DNA (gDNA) elimination. The first reaction involves the removal of gDNA by the gDNA wipeout buffer, and the second step is a reverse transcription reaction prepared by the addition of reverse transcriptase (Qiagen, Germany), RT buffer (Qiagen, Germany) and RT primer mix (Qiagen, Germany). This results in high yields of cDNA template for use in subsequent qRTPCR reactions.

Quantitative Real Time PCR

qRTPCR was performed on non-silencing control cDNA, mock transfection control cDNA, and *PINK1* siRNA cDNA diluted to a concentration of 300ng/μl. Primetime Standard qPCR Assays (IDT, USA) were used specific to *PINK1* and three housekeeping genes (HKGs) – *GAPDH, B2M* and *RPL13A*. Each assay was resuspended in 1000μl TE buffer (10mM Tris, 0.1mM EDTA, pH8.0) to obtain a 10X final stock concentration. A cocktail was made up of each assay, Master Mix (Quantifast Multiplex PCR kit, Qiagen, Germany) and dH_2O for each gene. A volume of 4μl was pipetted into each well of a 384-well plate (Lasec, SA) by the epiMotion (eppendorf, Germany). Thereafter, 1μl of *PINK1* siRNA cDNA, non-silencing control cDNA and mock-transfected control cDNA was pipetted in quadruplicate to each assay in the wells.

The plate was centrifuged on the Centrifuge 5810R (eppendorf, Germany) at 1000rpm for 1min and placed in the ABI 7900HT (Applied Biosystems, USA), a fast real time PCR system, situated at the Central Analytical Facility's satellite laboratory at Tygerberg. The system was run for 1 cycle at 95°C for 10min, and 40 cycles at 95°C for 15s, and 60°C for 45s. A dissociation melting curve was included at 1 cycle at 95°C for 15s, 60°C for 15s and 90°C for 15s. Results were analysed on an Excel spreadsheet to determine the percentage knock down for the siRNA transfected cells in comparison to the non-silencing control siRNA and mock control. Standard curves were included in the initial run for each gene so as to determine the efficiency values of the assay (this value should be as close to 1 as possible). This was calculated by REST-2009© gene quantification software (http://www.gene-quantification.de/rest.html).

2.2.2. Verification of efficient PINK1 knock down by Western blot

Cell lysate extraction

Once knock down of *PINK1* had been established on a gene expression level, it was necessary to confirm that this was translated to a protein level. Cells were cultured in 6-well plates and transfected with 5nmol siRNA for the 12 day period. After knock down, 10µM CCCP (a mitochondrial uncoupler) was added to the cells for 6hours. This is standard protocol for the detection of the PINK1 protein by Western blotting, as mitochondrial depolarization causes an increase of endogenous PINK1 recruitment to the mitochondria, which can then be detected by the commercially available antibodies. Cells were then trypsinised, collected and centrifuged. Supernatant was removed and the pellet was resuspended in 1ml PBS (phosphate-buffered saline), transferred to a 1.5ml epi and re-centrifuged. Thereafter, the pellet was resuspended in 50µl cell lysis buffer (Appendix II) and kept on ice for 30min. The lysate was centrifuged (UEC13, United Scientific, USA) at 4°C for a further 10min, and the supernatant was removed and stored at -20°C for future use.

Bradford protein concentration determination

In order to calculate a standard curve of protein concentrations, 10µl of a dilution range of bovine serum albumin (BSA) standards ranging from 0 - 1000µg/µl was loaded into the wells of a luminometer plate (Nunc™, Denmark) in duplicate. A volume of 1µl of cell lysate samples was also added to the plate in duplicate. Thereafter, 200µl Bradford reagent (Sigma Aldrich, Germany) was added to each standard and lysate sample. The protein concentration of each well was determined by a Synergy HT luminometer (BioTek Instruments Inc., USA). Using the KC4™ v 3.4 software (BioTek Instruments Inc., USA), a standard curve was set up and each sample's protein concentration was calculated.

Western blot

The Mini-PROTEAN TGX Precast Gels for polyacrylamide electrophoresis were used for all Western Blots (BioRad, USA). The gels were placed in a holding apparatus and container. A 1x SDS Running Buffer was made up from 10x SDS Running Buffer (Appendix II), and poured into the container. The comb was removed from the gel and 10µl of the Precision Plus Protein Kaleidoscope (BioRad, USA) protein ladder was loaded into the first well. Samples were mixed in a 3:1 ratio with the 4X Laemmli Sample Buffer dye (BioRad, USA), and denatured for 5mins at 95°C in the GeneE Thermal Cycler

(Techne Inc., USA). Thereafter, 50µg of each lysate was loaded onto the gel, and the gel was electrophoresed for approximately 40mins at 140V.

The iBlot Gel Transfer Stacks and PVDF Membrane (Novex, Life technologies, USA) were used for transferring the gel onto a membrane. The stacks provide the necessary membrane, filter paper and sponge to perform a transfer. All elements were added to the iBlot Gel transfer device (Invitrogen, Life technologies, USA) and a roller was used to ensure no bubbles were present. The iBlot was set to voltage program P4, at 15 volts for 7mins. The membrane was then removed from the transfer apparatus and blocked with 5% fat free milk (Elite, Weigh-Less) dissolved in TBST (Tris Buffered Saline with Tween 20, Appendix II) for 90mins on a shaker to eliminate non-specific binding of the antibodies. The membrane was then washed with TBST for three cycles of 15mins each. Thereafter, the primary antibody was diluted in 5% milk at an optimal predetermined dilution (Table 2.2). GAPDH was used as a loading control for all western blots. The membrane was then incubated overnight with the antibody-milk mixture on the shaker (Labcon, USA) at 4°C.

Following the incubation period, the membrane was washed with TBST for 3X 15mins. The appropriate dilution of secondary antibody (Santa Cruz Biotechnology, USA) was then added to the membrane and placed on the orbital shaker at room temperature for 1 hour (Table 2.2). Thereafter, the membrane was washed with the same washing protocol used after the primary antibody incubation. In a dark room, the two substrate components of the SuperSignal® West Pico Chemiluminescent Substrate kit (Thermo Scientific, Pierce Biotechnology, USA), viz. the SuperSignal West Pico Luminol/Enhancer solution and the SuperSignal West Pico Stable Peroxide solution, were mixed in a 1:1 ratio. The membrane was incubated in this solution for 5mins and then placed inside an autoradiography cassette and covered with a transparent plastic sheet. Autoradiography film (Eastman Kodak Company, USA) was placed over the membrane and the cassette was closed. Exposure time varied from 10 seconds to 5mins, depending on the strength of the signal. The film was processed by the Hyperprocessor™ automatic autoradiography film processor (Amersham Pharmacia Biotech UK Ltd., UK). The size of the protein was determined when placing the film against the protein ladder on the membrane. PINK1 protein was detected at 63-65kDa, and the HKG GAPDH was detected at 37kDa (Table 2.2).

Table 2.2. Antibodies and antibody dilutions for PINK1 and GAPDH Western blot conditions.

ANTIGEN	PRIMARY Ab AND MANUFACTURER	BLOCKING BUFFER	OPTIMUM RATIO, dilution medium	SECONDARY Ab	OPTIMUM RATIO, dilution medium	PRODUCT SIZE
PINK1	CST5660S, Mouse monoclonal Ab to PINK1, 100µg/ml (Cell Signalling Technology)	5% milk	1:500, 5% milk	Goat anti-mouse	1:1000, 5% milk	63-65kDa
GAPDH	FL-335, sc-25778, Rabbit polyclonal Ab to GAPDH, 200µg/ml (Santa Cruz Biotechnology)	5% milk	1:1000, 5% milk	Goat anti-rabbit	1:7000, 5% milk	37kDa

Ab, Antibody

Quantification of Western blots

All Western blots were quantified using the Image J software (http://imagej.nih.gov/ij/). Image J is able to measure the width of the band and obtain an arbitrary unit of thickness. All blots were performed in biological and technical triplicate. *PINK1* siRNA and the mock control were normalised to the non-silencing control siRNA. Each value was then compared relative to the GAPDH value. The final value was then used for statistical analysis.

2.3.   Creation of dosage and time curves

Following the verification of PINK1 knock down at a transcriptomic and proteomic level, we aimed to determine the effect of curcumin on both control and *PINK1* knock down cells, in the presence and absence of a stressor, paraquat. In order to test this, it was essential that the correct concentration of paraquat and curcumin were added to the cells, for the correct time period. Dosage and time curves were therefore performed on the cells and an MTT (3-(4,5-dimethylthiazol-2-yl)-2,5-diphenyltetrazolium bromide) assay was used to measure the number of viable cells compared to non-viable cells.

Stocks were made up for both paraquat and curcumin. A 50mM final stock concentration was made up of 100mg Paraquat dichloride x-hydrate pestanal (Sigma Aldrich, Germany) and 7.8ml dH_2O. For curcumin, a final stock concentration of 20mM was made up by adding 10mg curcumin (Sigma Aldrich,

Germany) to 1.36ml DMSO (dimethyl sulfoxide). For the dosage curve, dilutions of paraquat were made up in DMEM for final concentrations of 10μM, 25μM, 50μM, 100 μM, 200μM and 500μM. Dilutions of curcumin were made up in DMEM for final concentrations of 1μM, 2μM, 5μM, 10μM and 20μM. These dilution ranges were adapted from previous studies utilising paraquat and curcumin on SH-SY5Y cells (Jaisin et al., 2011; Z. Liu et al., 2013; Yang and Tiffany-Castiglioni, 2008).

2.3.1. MTT Assay

SH-SY5Y cells were cultured in 48-well tissue culture plates (SPL Life Sciences, Korea) with a total of 100 000 cells seeded per well. After 24 hours, cells were then either untreated, or treated with 10μM, 25μM, 50μM, 100μM, 200μM or 500μM paraquat. All of these experiments were performed in quadruplicate on the plate. After 24 hours of treatment, an MTT assay was performed to determine the percentage of viable cells across the dilution range. An MTT assay assesses cell metabolic activity through the measurement of NADPH-dependent cellular oxidoreductase enzymes. During incubation of the cells in an MTT solution, the presence of these enzymes reduce the yellow tetrazolium MTT dye to its insoluble form formazan, which is purple. This is an indication of a living and viable cell.

A 10mg/ml solution of Thiazolyl Blue Tetrazolium Bromide (Sigma Aldrich, Germany) was made in PBS (Appendix II). The solution was covered in foil, as MTT is photosensitive, and vortexed until the powder had dissolved. Media was removed from the cells and 200μl of the MTT solution was added to each well. Cells were then incubated for 2 hours at 37^0C, 5% CO_2. After incubation, the media in each well was removed and added to microfuge tubes that were centrifuged for 2mins at 4500rpm. The supernatant was removed and pellets were resuspended in 150μl of a detergent solution made up of a 50:1 ratio of 1% Isopropanol/HCl and 0.1% Triton solution. This was then returned to the plate, which was placed in the Synergy HT plate reader spectrophotometer (Biotek, USA) and absorbance was read at 595nm using the KC4 software.

The intention for paraquat was to stress the cells so that 50% viable cells remained. Based on the readings obtained, 25μM paraquat resulted in a 50% decrease in cell viability compared to the untreated cells, and was therefore the chosen concentration of paraquat to be used in all future experiments (Results, Section 3.2). The MTT assay was repeated using cells treated with 0.5μM, 1μM, 2μM, 5μM,

10μM and 20μM dilutions of curcumin. A concentration of 2μM curcumin was selected to be used for future experiments, as this was not toxic to the cells (Section 3.2).

In order to determine the exposure time of the cells to paraquat and curcumin, cells were treated with either 25μM paraquat or 2μM curcumin in quadruplicate over different time periods including 30mins, 1hr, 2hrs, 4hrs, 8hrs, 12hrs and 24hrs. An MTT assay was then performed. Based on the cell viability results, it was decided that paraquat exposure time would be 24 hours, and curcumin exposure time would be 1 hour. Once this was determined, a protocol was established for all of the functional assays on *PINK1* siRNA cells, non-silencing control siRNA cells, and mock transfected control cells (Figure 2.3).
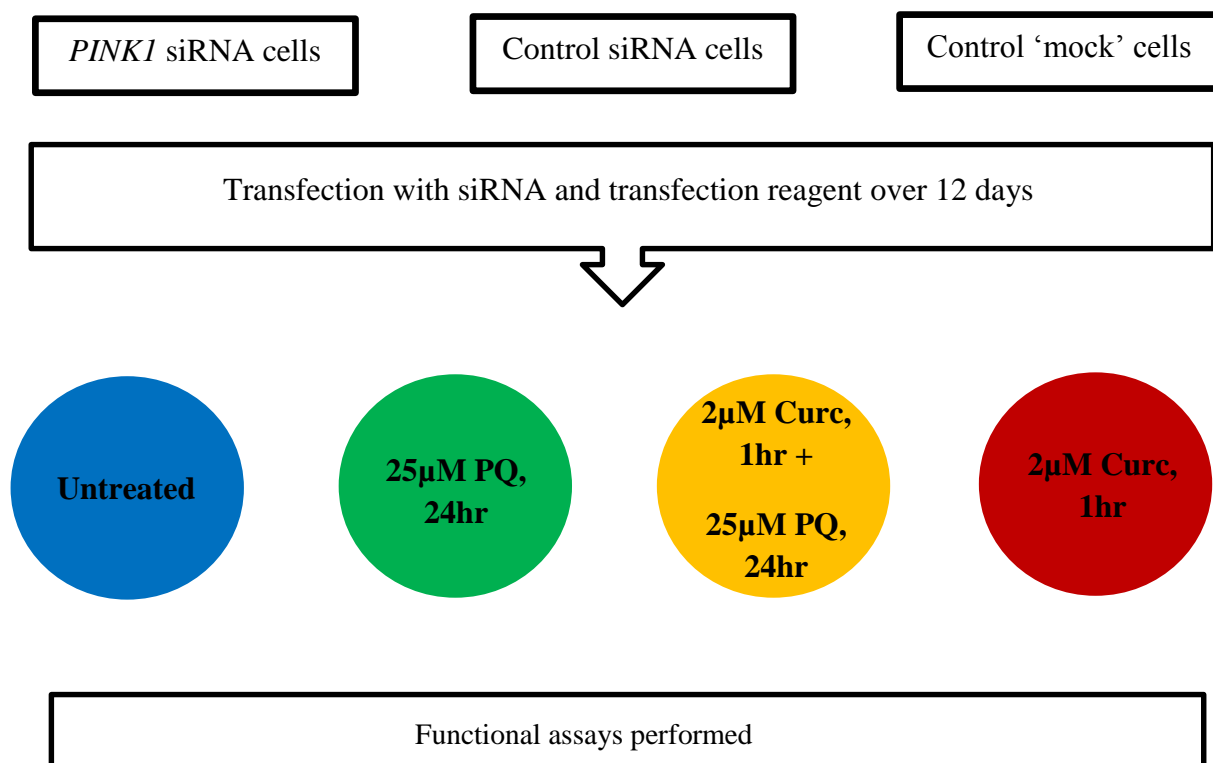
Figure 2.3. Designed protocol used for all functional assay. All three transfection groups – *PINK1* siRNA, control siRNA and control 'mock' were transfected over a 12 day period. Thereafter, cells either remained as they were (untreated, blue), were treated with 25μM paraquat (PQ) for 24 hours (green), were pre-treated with 2μM curcumin (Curc) for 1 hour and then treated with 25μM PQ for 24 hours (yellow), or were treated with 2μM Curc for 1 hour only (red).

2.4.   Cell viability

PINK1 siRNA cells, control siRNA cells, and control mock transfected cells were seeded into 48-well plates in quadruplicate. Based on the protocol in Figure 2.3, each group was then either treated with paraquat, curcumin, pre-treated with curcumin then paraquat, or remained untreated. An MTT assay was performed to determine the percentage of viable cells after each treatment. The assay was repeated for three separate runs and statistical analysis was performed (Section 2.10) to determine possible changes between each treatment group.

Results obtained from the MTT assay showed that non-silencing control siRNA and mock control cells exhibited no changes in cell viability. Based on this, and the expense of transfection reagent, it was determined that future assays would only be performed using the non-silencing control siRNA and not the mock control.

2.5.   Detection of apoptotic markers

Two proteins were used as markers for apoptosis in the treatment groups of *PINK1* siRNA and control siRNA cells – cleaved PARP and full-length caspase 3. Both proteins form part of the apoptotic cascade, and were detected through Western blot analysis (Section 2.2.2). Cell lysates were collected after each treatment condition, and their concentration was determined through Bradford protein concentration determination. A final concentration of 50μg for each lysate was loaded and run on Mini-PROTEAN TGX Precast Gels (BioRad, USA), and transferred to a membrane which was subsequently blocked in 5% milk. Primary and complementary secondary antibodies for cleaved PARP, full-length caspase 3 and GAPDH (loading control) were used (Table 2.3) and blots were quantified using Image J software. Statistical analysis was performed to determine changes in band size, and therefore changes in levels of apoptosis across treatment groups (Section 2.10)

Table 2.3. Antibodies and antibody dilutions for cleaved PARP, full-length caspase 3 and GAPDH Western blot conditions

ANTIGEN	PRIMARY Ab AND MANUFACTURER	BLOCKING BUFFER	OPTIMUM RATIO, dilution medium	SECONDARY Ab	OPTIMUM RATIO, dilution medium	PRODUCT SIZE
Cleaved PARP	CST9541S, Rabbit polyclonal Ab to cleaved PARP, 1mg/ml (Cell Signalling Technology)	5% milk	1:1000, 5% milk	Goat anti-rabbit	1:1000, 5% milk	116kDa
Caspase 3	CST9662, Rabbit polyclonal Ab to caspase 3, 1mg/ml (Cell Signalling Technology)	5% milk	1:1000, 5% milk	Goat anti-rabbit	1:1000, 5% milk	35kDa
GAPDH	FL-335, sc-25778, Rabbit polyclonal Ab to GAPDH, 200µg/ml (Santa Cruz Biotechnology)	5% milk	1:1000, 5% milk	Goat anti-rabbit	1:7000, 5% milk	37kDa

Ab, Antibody

2.6.   Measuring mitochondrial membrane potential

MMP can be measured by staining the cells with the JC-1 fluorochrome and using flow cytometric analyses. A stock concentration of 5mg/ml JC-1 and DMSO was made up (Appendix II) and stored at -20°C for future use.

2.6.1.   Staining cells with JC-1

SH-SY5Y cells were treated with either *PINK1* siRNA or control siRNA over the course of 12 days, and were then treated with one of the four treatment groups shown in Figure 2.3. The cells were then trypsinised and resuspended in 2ml DMEM. The JC-1 stock was diluted to 10µg/ml and 4µL was added to the resuspended cells. The cells were incubated at room temperature for 15mins and vortexed until the stain was properly dissolved. Cells were then centrifuged for 3mins at 1500rpm. The supernatant was discarded and the pellet resuspended in 500µl PBS.

2.6.2. Flow cytometric analysis

All flow cytometric analyses were performed on a FACSAria flow cytometer (Becton Dickinson Biosciences, USA) equipped with a 488nm Coherent Sapphire solid state laser (13-20mW), 633nm JDS Uniphase HeNe air-cooled laser (10-20mW) and 407nm Point Source Violet solid state laser (10-25mW). The FACSAria is able to sort a mixture of cells based on the fluorescent signal from each cells. Cells for this assay were sorted based on polarisation. This was done at the Central Analytical Facility at Stellenbosch University, with the help of Miss. Rozanne Adams. Samples were analysed on the flow cytometer and a minimum of 10 000 events were collected. Fluorescence intensity signal was measured using the geometric mean on the intensity histogram. JC-1 aggregates in red, indicative of healthy mitochondria and a high MMP, were measured with the PE (Phycoerythrin) fluorochrome, whereas JC-1 monomers in green, indicative of lowered MMP were measured with the FITC (Fluorescein isothiocyanate) fluorochrome. Therefore the PE/FITC ratio indicated a ratio of healthy mitochondria to depolarised mitochondria.

2.7. Measuring mitochondrial and glycolytic respiration

The XF^{e}96 Analyser (Seahorse Bioscience, USA) enables one to measure cellular metabolism and mitochondrial respiration of the cells by measuring the rate of oxygen consumed by the cells, also known as the Oxygen Consumption Rate (OCR). Furthermore, by measuring lactic acid production via protons released into the medium surrounding the cells, one can measure glycolytic respiration, by the Extracellular Acidification Rate (ECAR). The XF^{e}96 Analyser has a cartridge that enters each well of a 96-well plate. At the bottom of each cartridge are two fluorophores – one that is quenched by oxygen and therefore measures the mitochondrial component of respiration, and one that is quenched by hydrogen and measures glycolysis. A change in fluorophore emission represents a change in the levels of oxygen or hydrogen in the cells

2.7.1. The XF Cell Mito Stress Test

The XF Cell Mito Stress Test kit is designed to measure various aspects of mitochondrial respiration, including basal respiration, ATP production, maximal respiration and spare respiratory capacity. The

kit includes three drugs that are injected into the media surrounding the cells at specific time points through drug injection ports. The machine then measures and determines the response of the cells to each drug at three measurement points in real time. After three measurements of basal respiration, Oligomycin is injected into the media. Oligomycin is an ATP coupler that inhibits ATP synthesis by blocking ATP synthase (Complex V). This step enables one to determine the percentage of oxygen consumption devoted to ATP synthesis by calculating the difference in OCR before and after Oligomycin addition (Figure 2.4). The second injection is FCCP (trifluorocarbonylcyanide phenylhydrazone), an uncoupling agent that causes a drop in MMP, which results in a rapid consumption of energy and oxygen as ATP generation is halted. This enables one to determine the maximal respiration of the cells as well as the spare respiratory capacity, which is the difference between maximal OCR and basal OCR (Figure 2.4). Lastly, a combination of Rotenone and Antimycin A is injected which inhibit complex I and complex III respectively. This results in a decrease in OCR as mitochondrial respiration is shut down and an increase in ECAR as the cells switch to a glycolytic state to produce energy.
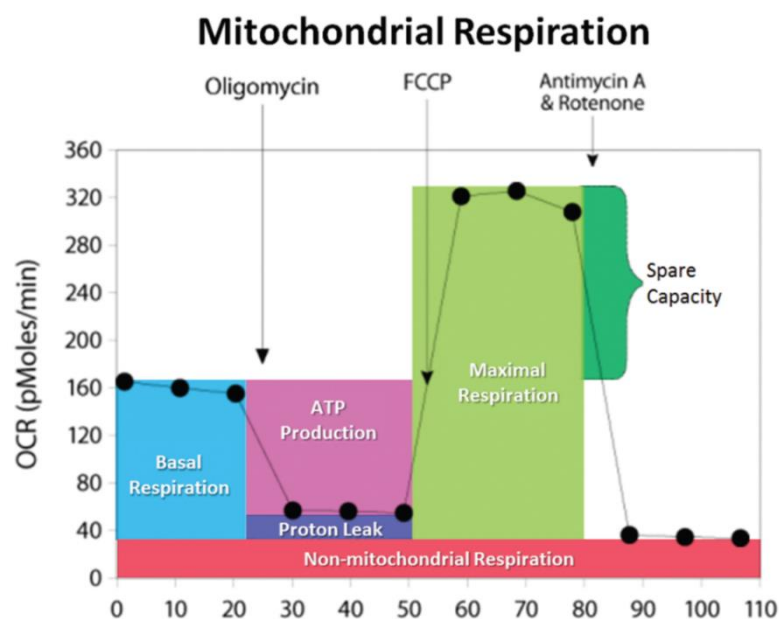
Figure 2.4. The Mito Stress Test measures the fundamental parameters of mitochondrial respiration. These include basal respiration, ATP production, maximal respiration, and spare capacity, and are measured by OCR (Oxygen Consumption Rate) in real time.

Cells underwent the knock down protocol (Section 2.2, Figure 2.2) and were then seeded into the 96-well XF Analyser Cell Culture plate (Seahorse Bioscience, USA) at a predetermined seeding density of 7500 cells per well, counted using the Scepter Handheld Cell Counter (Merck, Germany). In summary,

four rows of the plate had control siRNA cells (A-D), and four rows had *PINK1* siRNA cells (E-H). The plate was placed in the incubator overnight. Thereafter, each row was treated with one of the four treatment groups derived in Section 2.3.1. The plate setup can be seen in Figure 2.5.

Blank wells
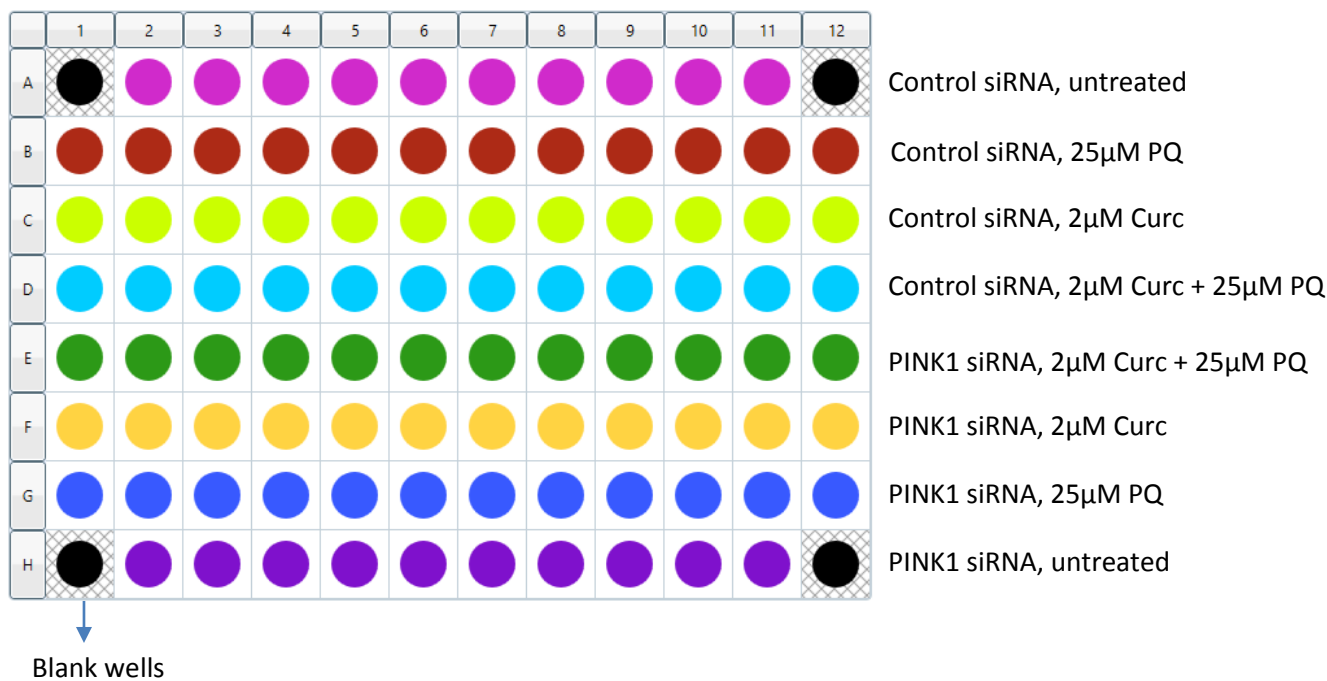
Figure 2.5. Design of the 96-well plate used for the XF Analyser Mito Stress Test. Each row of wells was treated based on the pre-determined protocol. The black corner wells were untreated and remained empty. PQ, paraquat; Curc, curcumin

Three plates are utilized during the process of mitochondrial respiratory detection - the XF Analyser Cell Culture Plate, the Utility Plate, and the Cartridge Plate (which contains the fluorophores). Whilst the cells were being treated, it was necessary to hydrate the cartridge plate overnight in order to hydrate the fluorophores and remove excess CO_2 from the plastic, as this affects the pH of the medium. A volume of 200µl XF Calibrant Media (Seahorse Bioscience, USA) was added to each well of the utility plate, and the cartridge plate was placed over the utility plate and added to the XF Seahorse incubator (37^0C, 0% CO_2) overnight.

The following day, an assay medium was made up containing 42.5ml XF Assay Medium Modified DMEM (Seahorse Bioscience, USA), 1mM Pyruvate and 25mM Glucose and pH pf 7.4. The medium

on the cells was removed and the cells were washed with 200µl of assay medium. This was removed and a further 175µl assay medium was added to the cells. The plate was then incubated in the XF Seahorse incubator for 1hour.

The stock solutions of the three drug compounds (Oligomycin, FCCP and Rotenone + Antimycin A) were made up by adding each compound to DMSO for a stock concentration of 2.5µM. The optimal final concentrations for each compound were as follows: 1µM Oligomycin, 0.5µM FCCP, 1µM Rotenone + Antimycin A. This was made up by diluting the stock solutions in assay medium. These solutions were then vortexed and 25µl was added to the cartridge plate at specific ports via a loading plate. Oligomycin was added to Port A, FCCP to Port B, and Rotenone + Antimycin A to port C. The cartridge plate was then incubated in the XF Seahorse incubator for 5mins. Thereafter, the cartridge plate and utility plate were added to the XF^{e}96 Analyser and calibrated for 20mins. The utility plate was then removed and the cell culture plate was placed over the cartridge plate and the run was initiated. Results and data were analysed on the XF^{e}96 Wave software (www.seahorsebio.com/).

2.7.2. The XF Glycolysis Stress Test

The XF Glycolysis Stress Test kit makes it possible to measure glycolysis in real time while inducing metabolic stress in order to identify key parameters of glycolytic flux in the cells: glycolysis, glycolytic capacity and glycolytic reserve. The conversion of glucose to pyruvate, and subsequently to lactate in the cytosol, results in the production and release of protons to the extracellular medium. An increase in the release of protons results in an increase in the measurable ECAR, which signifies an increase in glycolytic activity. The kit, similar to the Mito Stress Test kit, includes three drugs that are injected into the media surrounding the cells at specific time points through drug injection ports. After three measurements of ECAR in a glucose-free medium, a saturating concentration of glucose is injected to the cells (Figure 2.6), resulting in a spike of ECAR as glycolysis rates increase. Thereafter, Oligomycin is injected, which inhibits oxidative phosphorylation and therefore results in the maximal cellular glycolytic capacity. Lastly, 2-deoxy-glucose (2-DG), a glucose analogue, is injected to the cells and inhibits glycolysis (Figure 2.6).
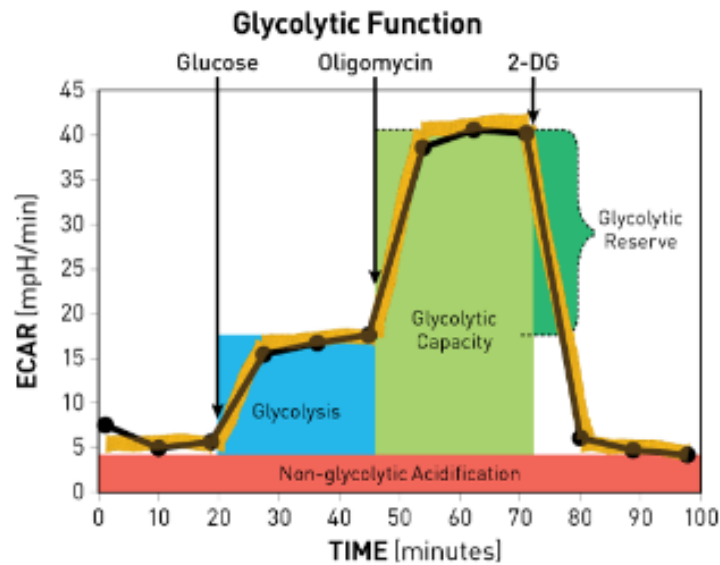
Figure 2.6. The Glycolysis Stress Test measures the fundamental parameters of glycolytic flux.
These include glycolysis, glycolytic capacity and glycolytic reserve, measured in real time by the ECAR
(extracellular acidification rate). 2-DG, 2-deoxy-glucose

Cells, the utility plate and the cartridge plate were treated and plated in the same manner as was done
in Section 2.7.1 for the Mito Stress Test (Figure 2.5). Once treated, cells were washed with 200μL
glycolysis assay medium. This was removed and a further 175μl assay medium was added to the cells.
The plate was then incubated in the XF Seahorse incubator for 1hour. Stocks were made up for the three
drug compounds of the Glycolysis Stress Test Kit – Glucose, Oligomycin and 2-DG by adding the
compound to DMSO for a stock concentration of 2.5μM. Final concentrations of 10mM Glucose, 1μM
Oligomycin and 100mM 2-DG were then made by diluting the stock solution in the glycolysis assay
medium. These solutions were added to the ports in the cartridge plate, and the same protocol for the
Mito Stress Test was followed thereafter. Results and data were analysed on the XF^{e}96 Wave software
(www.seahorsebio.com/).

2.8.   Mitochondrial network analysis

After the third knock down step (Figure 2.2), cells were seeded in 8-well chambered coverglass (Lab-
Tek, Nunc, Denmark) at a density of 10 000 cells per well, and incubated for 24 hours. Cells were then
treated with siRNA and transfection reagent for a final time, incubated for 48 hours, and treated with

the pre-determined treatment groups as shown in Figure 2.3. MitoTracker Red (Invitrogen, Life Technologies, USA) which stains for the mitochondrial network, was diluted in cell culture media to 1:1000. The Hoechst 3343 stain for the nucleus (Thermo Scientific, USA) was diluted at 1:200 in media.

After treatment, the cells were stained with both MitoTracker Red and Hoechst 33342, and then were observed on an Olympus Cell^R system attached to an IX-81 inverted fluorescence microscope equipped with an F-view-II cooled CCD camera (Soft Imaging Systems). Using a Xenon-Arc burner (Olympus Biosystems GMBH, Germany) as light source, images were excited with the 360nm, 492nm or 572nm excitation filters. Emission was collected using a UBG triple-bandpass emission filter cube. For the image frame acquisition, an Olympus Plan Apo N 60x/1.4 oil objective and the Cell^R imaging software was used. Images were processed and background-subtracted using the Cell^R software. The images were then quantified using Image J software.

Form factor (the degree of mitochondrial branching) was calculated from the measurements of mitochondrial perimeter and area. Aspect ratio, which represents the relationship of mitochondrial width and height, was determined by the ratio of the major and minor axes. The major axis is the axis that projects through the length of the mitochondrion, and the minor axis the width. The following equations were used for calculation:

Form factor = $P^2/4\pi A$ (P, perimeter of cell; A, area of cell)

Aspect ratio = Major axis/ Minor axis

Statistical analysis was performed and Bonferroni's correction for multiple comparisons was utilised. (Section 2.10).

2.9.   Autophagic flux measurement and calculation

Autophagy can be measured through the detection of autophagic proteins via Western blots. LC3-II is a protein associated with the inner and outer membrane of the autophagosome and is primarily used to

determine levels of autophagy in the cells. Furthermore, p62 is a second measure of autophagic flux, as it binds to LC3-II in the autophagosome and is rapidly degraded during autophagy. It must be noted that p62 is not only specific to autophagy, and is associated with other pathways which may affect the level of p62. Despite this, it is necessary to verify measurements of LC3-II with p62. To calculate autophagic flux, both LC3-II and p62 need to be measured after activation of basal autophagy in a starvation state, as well as after the addition of BafA1, which acts as an inhibitor of vacuolar ATPase and autophagosome-lysosome fusion. The difference in levels before and after BafA1 treatment is then defined as autophagic flux (Figure 2.7). A 20µg/ml stock solution of BafA1 was made up in ethanol (Appendix II) and stored at -20°C for future use.
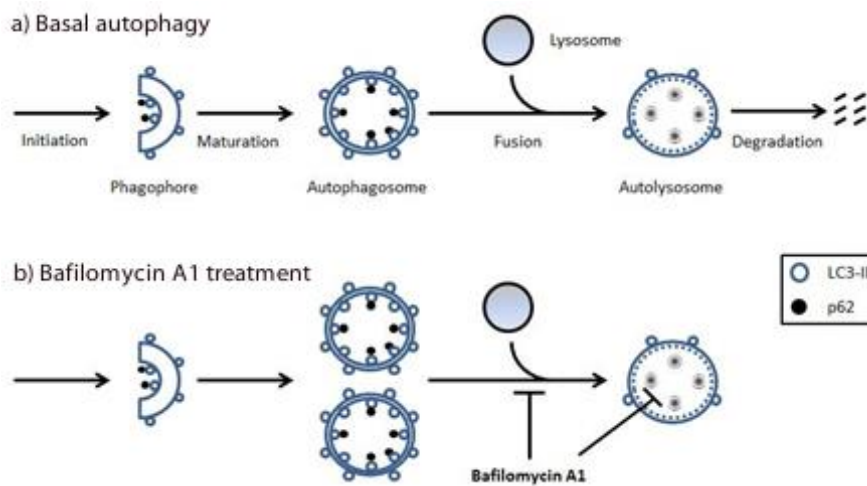
Figure 2.7. The effect of the lysosomal inhibitor Bafilomycin A1 on autophagy. Autophagic flux is calculated by the difference in LC3-II and p62 before and after the addition of bafilomycin A1. Bafilomycin A1 inhibits vacuolar-ATPase and prevents lysosomal fusion with the autophagosomes. Taken from www.vivabioscience.com

SH-SY5Y cells were seeded into 6-well plates and either *PINK1* siRNA or control siRNA was added to them. In total there were 2 groups of treated *PINK1* siRNA cells and 2 groups of control siRNA cells. After 12 days of transfection, cells were either untreated, or treated with either paraquat, curcumin or pre-treated with curcumin and then with paraquat according to the previously described protocol. Thereafter, the treatment media was aspirated and 3ml HBSS media was pipetted onto one set of *PINK1* siRNA and control siRNA cells. HBSS is a saline solution that contains 1g/L glucose and no amino acids – therefore it is capable of inducing nutrient starvation to the cells and a subsequent increase in

autophagy. Alternatively, the second set of *PINK1* siRNA and control siRNA cells were treated with a combination of HBSS and BafA1. From the stock solution, 9.7µl BafA1 was diluted in 3ml HBSS to give a final concentration of 100nM. This was added to the second group of cells, and the both groups were incubated simultaneously at 37°C for 2hours.

After incubation, the cells were lysed and protein concentration was determined through the Bradford method as described in Section 2.2.2. Both groups of samples that were treated with HBSS and HBSS+BafA1 were simultaneously run on gels and detected by Western blotting (Section 2.2.2). Antibodies for LC3-II, p62 and GAPDH (the loading control) were used at optimal concentrations (Table 2.4). It must be noted that in order to detect LC3-II, membranes were blocked in 5% BSA diluted in TBST. Primary and secondary antibodies were also diluted in 5% BSA compared to p62 and GAPDH that used 5% milk. Intensity of the bands for each protein was quantified by Image J software, and band intensities of LC3-II and p62 were each normalised to the corresponding band intensities of GAPDH. Autophagic flux was then calculated by comparing the normalised LC3-II and p62 in BafA1-treated versus untreated samples. These results were technically repeated three times, and replicated in three independent experiments. Statistical analysis was performed using GraphPad Prism software (Section 2.10).

Table 2.4. Antibodies and antibody dilutions for LC3-II, p62 and GAPDH Western blot conditions

ANTIGEN	PRIMARY Ab AND MANUFACTURER	BLOCKING BUFFER	OPTIMUM RATIO, dilution medium	SECONDARY Ab	OPTIMUM RATIO, dilution medium	PRODUCT SIZE
LC3-II	CST2775S, Rabbit monoclonal Ab to LC3-II, 1mg/ml (Cell Signalling Technology)	5% BSA	1:1000, 5% BSA	Goat anti-rabbit	1:1000, 5% BSA	16kDa
P62	AB56416, Mouse monoclonal Ab to p62, 1mg/ml (Abcam)	5% milk	1:1000, 5% milk	Goat anti-rabbit	1:1000, 5% milk	62kDa
GAPDH	FL-335, sc-25778, Rabbit polyclonal Ab to GAPDH, 200µg/ml (Santa Cruz Biotechnology)	5% milk	1:1000, 5% milk	Goat anti-rabbit	1:7000, 5% milk	37kDa

Ab, Antibody; BSA, bovine serum albumin

2.10. Statistical analysis

All statistical analyses were performed using GraphPad Prism Software V5 (www.graphpad.com/scientific-software/prism/). Column bar graphs were generated indicating the mean with standard deviation. Depending on the total number of groups being analysed, one way analysis of variance (ANOVA) and student t-tests were performed to determine the value of 'p'. All measurements of $p<0.05$ were considered statistically significant. Statistical analyses were done with the help of Miss Moleen Zunza from the Biostatistics Unit, Stellenbosch University.

2.11. Analysis of Copy Number Variation in South African PD patients

This section of work was conducted in order to detect CNV in known PD-causing genes in a cohort of South African PD patients. We specifically aimed to identify rearrangements in the *PINK1* gene, in order to obtain fibroblasts from these patients for use in a second model of PD.

2.11.1. Patient and control selection

Patients suffering from PD were recruited from the Movement Disorder clinic at Tygerberg Hospital, as well as the Parkinson's Association of South Africa. The patients were examined by a movement disorder specialist, Professor Jonathan Carr, and met the UK Parkinson's Disease Society Brain Bank Research criteria for diagnosis of PD (Gibb and Lees, 1988). Blood samples were obtained from each patient and gDNA was isolated by Dr. Sihaam Boolay (Appendix I). Furthermore, control blood samples were obtained from the Geriatric clinic at Tygerberg Hospital and the Western Province Blood Transfusion Services, and gDNA was isolated and stored at -4°C. This study was approved by the Health Research Ethics Committee at Stellenbosch University (Protocol number: 2002/C059). The approval is renewed annually. All study participants were recruited with informed written consent. For this study, a total of 210 patients from all ethnic backgrounds were analysed (Table 2.5).

Table 2.5. Clinical characteristics of 210 South African PD patients recruited for this study

	Total N = 210
AAO, mean +-SD, (range)	59.4 +- 12.3 years (20-82 years)
AAO <= 50 years	44 (20.9%)
Family history of PD	55 (26.2%)
Ethnicity	
White	75 (35.7%)
Afrikaner	56 (26.7%)
Mixed Ancestry	57 (27.1%)
Black	21 (10.0%)
Indian	1 (0.5%)

AAO, Age at onset

2.11.2. MLPA analysis

The MLPA kit (MRC Holland, Netherlands) for CNV detection in PD patients consists of two separate kits, each with a different probe mix. These probe mixes contain oligonucleotides for ligation to the exons of genes known to cause PD, as well as reference probes. More specifically, probe mix 1 is SALSA MLPA P051 (MRC Holland, Netherlands), and contains probes for exons of *PARK2, PINK1, SNCA, ATP13A2, LRRK2* and *DJ-1*. Probe mix 2, SALSA MLPA P052 (MRC Holland, Netherlands), contains probes for exons of *PARK2, UCHL1, GCH1, CAV1* and *LRRK2* (Appendix III). The MLPA kit also contains a SALSA MLPA EK1 Reagent Mix (MRC Holland, Netherlands) which includes the SALSA MLPA Buffer, Ligase-65, Ligase buffers A and B, PCR Primer mix, and SALSA polymerase.

Patient and control gDNA was diluted in dH_2O to a final concentration of 30ng/µl for each MLPA reaction. Control gDNA included samples with no known mutations in the PD genes, and 2 controls were included for each run. A negative dH_2O control was also included in the runs. Reactions for probe mixes P051 and P052 were performed at the same time, therefore two sets of the samples were run parallel to each other, one containing probe mix P051, and the other P052. A volume of 5µl of gDNA from each sample and control sample was pipetted into 0.2ml epis, and the samples were denatured in the GeneAmp® PCR system 2720 Thermal Cycler (Applied Biosystems, USA) for 5min at 95^0C and cooled to 25^0C for a further 5min. The hybridisation master mix was then prepared consisting of 0.75µl MLPA buffer and 0.75µl probe mix (either P051 or P052). A total volume of 1.5µl of the hybridisation

master mix was added to each sample and mixed well by gently pipetting up and down. Samples were placed in the thermocycler for incubation at 95^0C for 1min and then 60^0C overnight for 16 hours. Thereafter the thermocycler was paused at 54^0C.

The following day a Ligase-65 master mix was prepared containing 12.5µl dH_2O, 1.5µl Ligase buffer A, 1.5µl Ligase buffer B and 0.5µl Ligase-65 enzyme. A total volume of 16µl of the Ligase-65 master mix was added to the samples at 54^0C. Ligation of the probes to the sample DNA was then initiated by running the thermocycler for 15mins at 54^0C, followed by heat inactivation of the ligase enzyme for 5mins at 98^0C and cooling at 20^0C for 5mins. Lastly, the polymerase master mix was prepared with 3.75µl dH_2O, 1µl SALSA PCR primer mix, and 0.25µl SALSA polymerase. Samples were removed from the thermocycler after ligation and 5µl polymerase master mix was added to each epi. Samples were placed back in the thermocycler for PCR amplification for 35 cycles of 30sec 95^0C, 30sec 60^0C and 60sec 72^0C, followed by 20mins at 72^0C and cooling for 5mins at 15^0C.

Fragment separation by capillary electrophoresis was performed on the PCR products at the Central Analytical Facility of the Department of Genetics, Stellenbosch University on the ABI 3130xl ® Genetic analyser (Applied Biosystems, USA). A summary of the MLPA method is shown in Figure 2.8. The raw data was then analysed using the Coffalyser.Net software, version .131211 (http://coffalyser.software.informer.com/download/).

The results for MLPA raw data were analysed as follows:

The relative peak height (RPH) of each exon was obtained by dividing the single peak height by the sum of peak heights of all the internal control probes. A ratio was then generated by comparing each RPH to the mean value of the corresponding RPHs from a reference wild-type sample. Ratios to indicate mutations were set as follows:

- between 0.7 and 1.3 were considered to be normal (sample contains no exon rearrangements)
- between 0.3 and 0.6 indicated a heterozygous deletion
- between 1.4 and 1.6 indicated a heterozygous duplication
- Higher than or equal to 1.7 indicated a triplication

- Absence of a peak would indicate either a possible point mutation at that probe recognition site or a homozygous deletion (ratio 0.0).
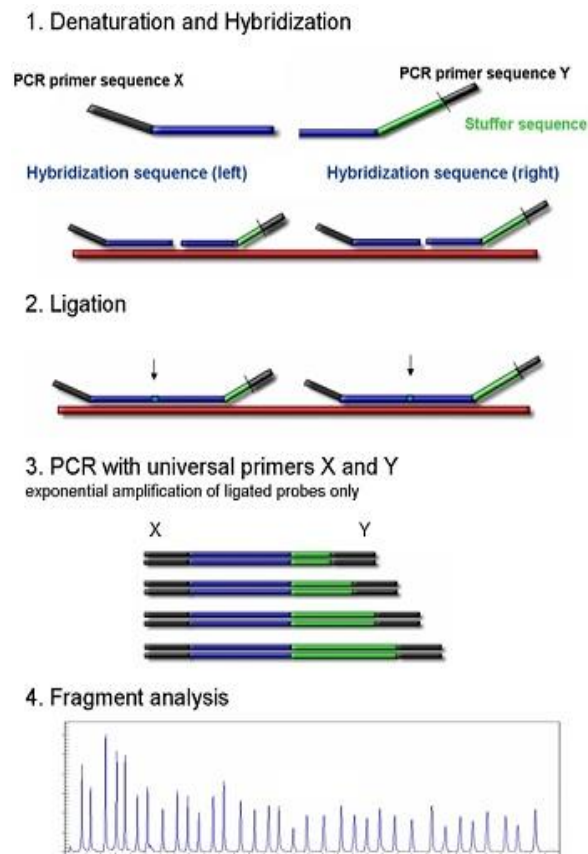
Figure 2.8. A summary of the MLPA procedure. The MLPA procedure can be divided into four major steps. 1. Denaturation of the sample DNA and hybridisation of probes to adjacent target sequences of DNA. 2. Ligation of the probes to the DNA. 3. Exponential amplification of the ligated probes during a PCR reaction. 4. Separation of the amplification products by capillary electrophoresis. Taken from www.mlpa.com.

2.11.3. Quantitative real time PCR

For verification of the MLPA results, qRTPCR was performed on the Lightcycler 96 (Roche diagnostics, Germany). Primers were available for all genes of interest as well as *β-globulin* (*HBB*), the HKG used in these experiments. All primers were diluted to 20µM, and 30ng/µl gDNA was used.

A mastermix was prepared for each reaction consisting of 7μl dH$_2$O (Roche diagnostics, Germany), 0.5μl forward primer, 0.5μl reverse primer and 10μl Lightcycler 480 SYBR Green I Master Mix (Roche diagnostics, Germany). A total volume of 18μl of the mastermix was pipetted into each well of a 96-well plate (Roche diagnostics, Germany) using the epiMotion (eppendorf, Germany) to prevent manual pipetting errors. Thereafter, 2μl of sample or control DNA was added to each well and mixed with the mastermix. All sample and control reactions were performed in triplicate. The plate was centrifuged for 1min at 1500rpm and placed in the Lightcycler 96. qRTPCR was accomplished under the following conditions: i. Preincubation at 95^{0}C for 600sec, ii. Three step amplification for 45 cycles including 95^{0}C for 10sec, 60^{0}C for 10sec followed by a touchdown to 55^{0}C after the second cycle, and 72^{0}C for 10sec, iii. Melting period of 95^{0}C for 10sec, 65^{0}C for 60s, 97^{0}C for 1sec and iv. Cooling period of 37^{0}C for 30s. Results were analysed on the Lightcycler 96 software version 1.1 (www.roche.com), which calculates relative quantification. Ct values differing by more than 1 unit per triplicate were discarded.

2.11.4. Direct Sequencing

Results from the MLPA analysis showed that sequencing was required on samples believed to be false positive due to the presence of a polymorphism in the annealing site of the probe. Primer sequences were available on request, and PCR reactions were performed on gDNA of these samples on the GeneAmp® PCR system 2720 Thermal Cycler (Applied Biosystems, USA). The PCR products were run on a 2% agarose gel to verify the presence of the exon.

A volume of 8μl of each PCR product was pipetted into a 0.2ml microcentrifuge PCR epi (Sigma-Aldrich, USA), and this was purified with 5U of both *Exonuclease I* (USN Corporation, USA) and *SAP* (Shrimp Alkaline Phosphatase; Promega, USA). The samples were mixed and spun in the Hermle Z100M microcentrifuge (Labnet, USA) and then incubated at 37°C for 15mins followed by 80°C for 10mins to deactivate the enzymes. Each product was diluted down to 30ng/μl for the sequencing reaction.

The primers used for sequencing were the same primers used during the PCR amplification diluted to 1.1μM. All automated sequencing reactions of the PCR products were performed at the Central

Analytical Facility of the Department of Genetics, Stellenbosch University using the BigDye terminator V3.1 Ready reaction kit on the ABI 3130xl ® Genetic analyser (Applied Biosystems, USA). Analysis of sequencing data was performed using the BioEdit Sequence Alignment Editor Version 7.0.5 software (Hall, 1999).

Chapter 3: Results

Page

Section A: Creation of an siRNA-mediated *PINK1* knock down cellular model of PD and the effect of curcumin exposure

3.1. Successful knock down of *PINK1* using an siRNA-mediated approach

In the present study, we attempted to knock down *PINK1* in an SH-SY5Y neuroblastoma cell line using siRNA, decreasing the expression of this gene at a transcriptional and translational level. As mentioned in Section 2.2, two different controls were used to test the expression of *PINK1* – i. non-silencing control siRNA using scrambled siRNA and ii. a mock transfected control treated only with transfection reagent. To determine the percentage knock down and cell viability levels, both control siRNA and mock control cells were used. Furthermore, the optimum PINK1 siRNA chosen for subsequent knock downs was Hs_PINK1_6_Flexitube siRNA.

Once the cells had been transfected, gene expression analysis was performed using qRTPCR and results confirmed a 75% decrease in the expression of *PINK1* mRNA normalised to the expression levels of the cells treated with non-silencing control siRNA (p=0.0018, Figure 3.1). All experiments were performed in triplicate. The mock transfected control showed similar expression to the control siRNA after normalisation (Figure 3.1).
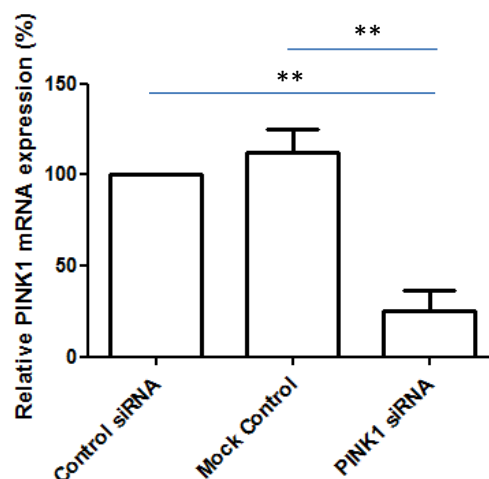
Figure 3.1. Quantitative real time PCR (qRTPCR) analysis of *PINK1* mRNA expression levels. Bar graph indicating qRTPCR of *PINK1* cDNA. *PINK1* was significantly reduced by 75% after knock down using *PINK1* siRNA (** p<0.01).

In order to detect protein expression of endogenous PINK1 *in vitro*, SH-SY5Y cells needed to be treated with CCCP prior to lysate collection. CCCP depolarises the mitochondria, resulting in a lowered membrane potential and thus recruitment of full-length PINK1 (~65kDa) to the OMM of the mitochondria. Without CCCP addition, endogenous levels of PINK1 are too low to be detected by current commercially available antibodies (Geisler et al., 2010a). Therefore control siRNA cells, mock transfected cells and *PINK1* siRNA cells were treated with 10μM CCCP for 6 hours. Results revealed a significant decrease in endogenous PINK1 expression compared to control siRNA cells (p<0.001, 54% decrease). Comparison of the mock control to the control siRNA showed no change in PINK1 protein levels (Figure 3.2A, B).
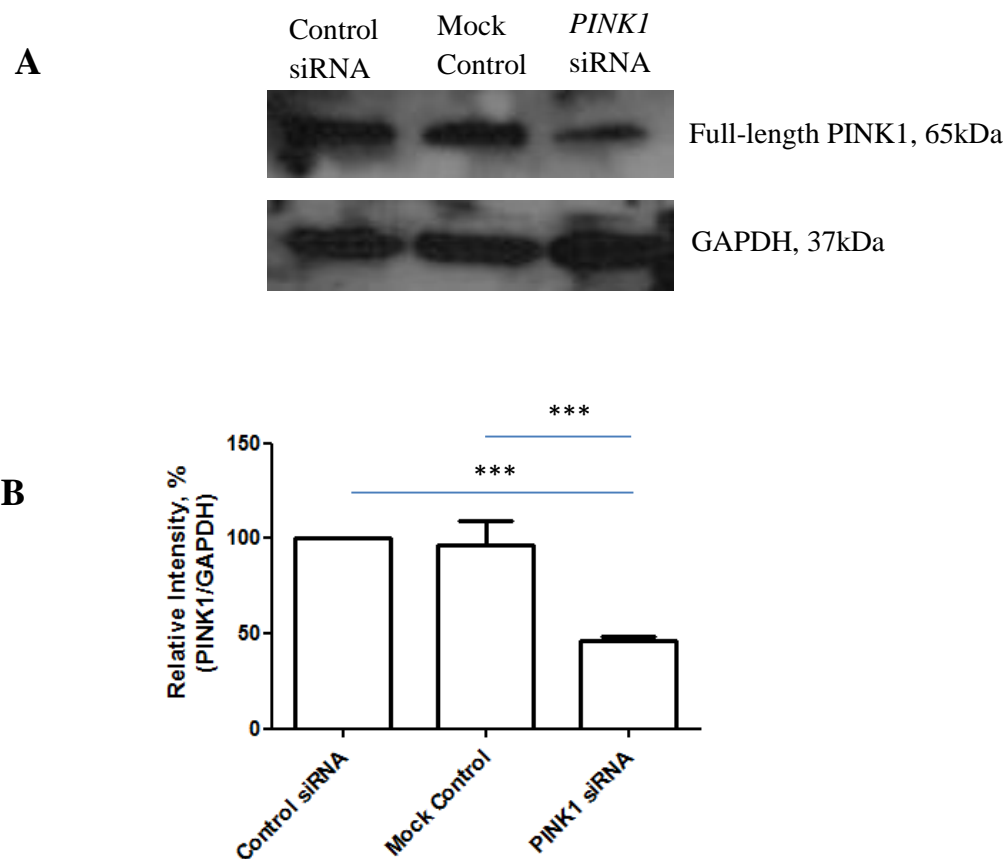
Figure 3.2. Western Blot analysis of PINK1 protein expression. A. Image indicating the detection of full-length PINK1 (65kDa, top panel) and the loading control GAPDH (37kDa, bottom panel). B. Quantification of the blots revealed significantly decreased PINK1 protein levels (by 54%) after the addition of *PINK1* siRNA compared to control siRNA (***p<0.001).

3.2.   Determining dose- and time-curves for paraquat and curcumin

Previous studies on the use of paraquat and curcumin in SH-SY5Y cells have used varying concentrations of paraquat and curcumin over different time periods (Jaisin et al., 2011; Lantto et al., 2009; Yang et al., 2010). Dosage and time curves were therefore established for both paraquat and curcumin to determine a final concentration and exposure time for each compound that would be used throughout all of the experiments. Initially, cells were seeded at densities of 50 000, 100 000, 120 000 and 140 000 in 48-well cell culture plates (SPL Life Sciences, Korea) for 24 hours to determine an optimal density as well as to ensure that the MTT protocol was optimised correctly. The MTT assay has previously been used in studies to determine optimal seeding density, the ideal concentration of the compounds, and an applicable exposure time, and was therefore an appropriate assay to use for this study (Liu et al., 2013; Li et al., 2012; Section 2.3.1).

As expected, the number of viable cells increased as the seeding density of the cells increased (Appendix IV). Based on these results, a seeding density of 100 000 cells per well was selected, as this resulted in approximately 80% confluency after 24 hours. Cells were incubated in the presence of paraquat and cell viability was measured. The optimal concentration was chosen to be 25µM, as this significantly reduced cell viability compared to untreated cells, but did not induce excessive toxicity to the cells (p<0.05, Figure 3.3A). This concentration was then used to perform a time curve where 25µM paraquat was added to the cells at various time points over 24 hours. Results revealed that optimal exposure time for 25µM paraquat is 24 hours (p=0.0145, Figure 3.3B), as this significantly reduced the cell viability.

Dose- and time-curves were also established for curcumin, and results indicated an optimal concentration of 2µM (Figure 3.4A). Concentrations over 2µM showed a significant decrease in cell viability. As the mechanism of curcumin as a treatment is being tested, the concentration used should have no toxic effect on the cells, therefore it was decided that 2µM was appropriate. The time curve with 2µM curcumin showed no significant change in cell viability over various time periods, therefore an exposure time of 1 hour was chosen as optimal as this complemented what has been done in previous studies (Figure 3.4B).
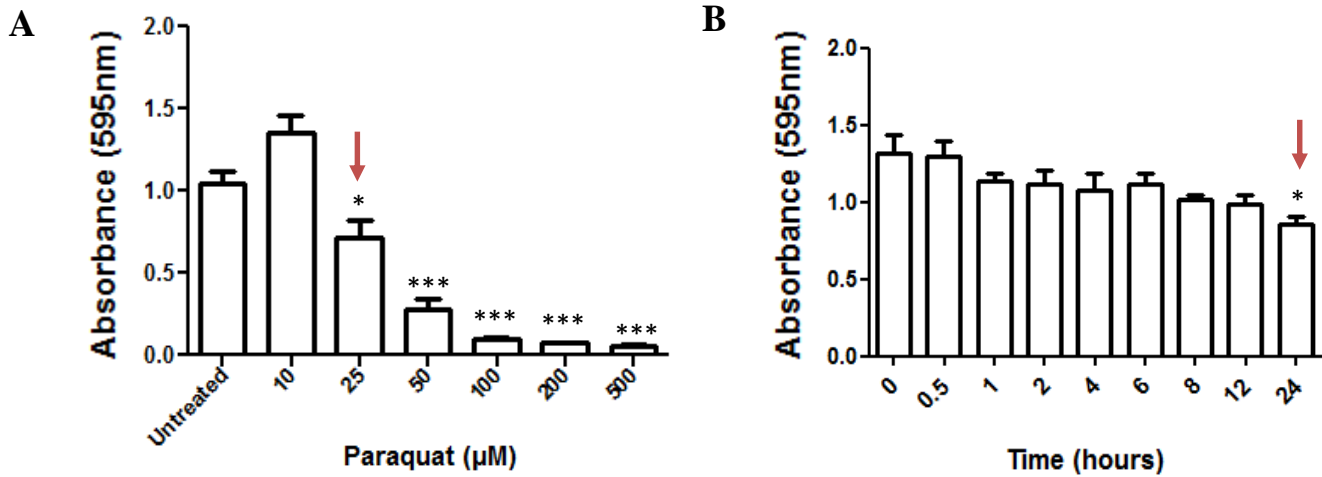
Figure 3.3. Determining a suitable concentration and time exposure of paraquat for SH-SY5Y cells. A. Dose curve indicating a significant decrease in cell viability at 25µM (*$p<0.05$). Concentrations higher than 25µM showed a highly significant decline in viability, therefore 25µM paraquat was used as an appropriate concentration for future experiments. B. Time curve indicating a significant decrease in cell viability after exposure to 25µM paraquat for 24 hours (*$p=0.0145$).
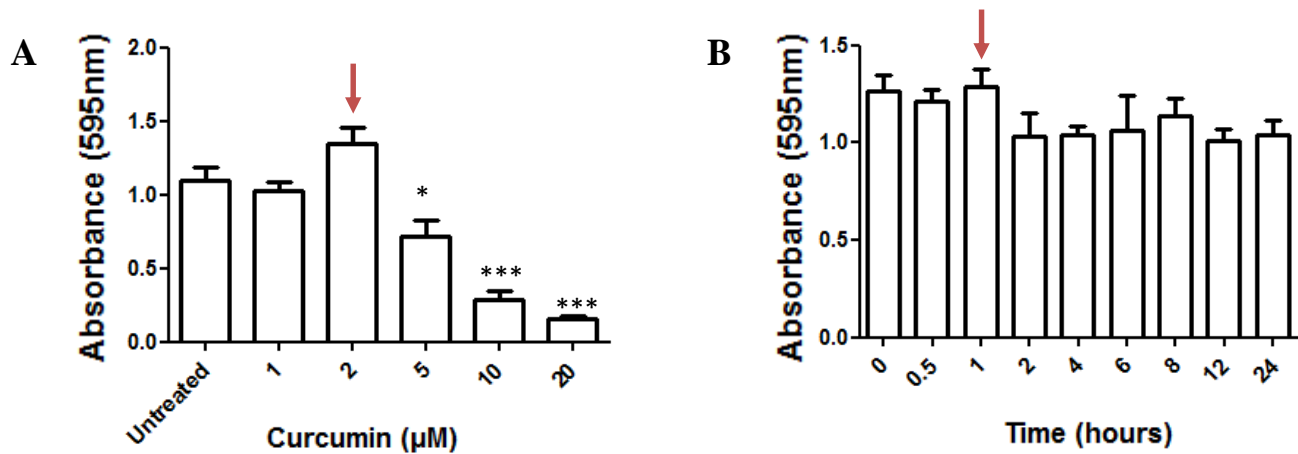
Figure 3.4. Determining a suitable concentration and time exposure of curcumin for SH-SY5Y cells. A. Dose curve indicates an optimal concentration of 2µM curcumin for future work. B. Time curve showed no significant increase or decrease in cell viability, and an optimal time of 1hour curcumin exposure was chosen.

For the remainder of the experiments, control and *PINK1* knock down cells were separated into four treatment groups, as explained in Figure 2.3:

- Untreated
- Treated with 25µM paraquat for 24 hours
- Pre-treated with 2µM curcumin for 1 hour and then treated with 25µM paraquat for 24 hours
- Treated with 2µM curcumin for 1 hour

3.3. Cell viability

Once the paraquat and curcumin exposure protocols were optimised, various parameters of cellular and mitochondrial function were measured to determine the effect of *PINK1* knock down, paraquat addition and curcumin treatment on the SH-SY5Y neuroblastoma cell line. An MTT assay was performed to measure cell viability. Results showed a significant decrease in cell viability ($p=0.0036$) in cells that had decreased PINK1 expression after normalising to the control siRNA (Figure 3.5). Mock control cells showed no difference in cell viability compared to control siRNA cells.
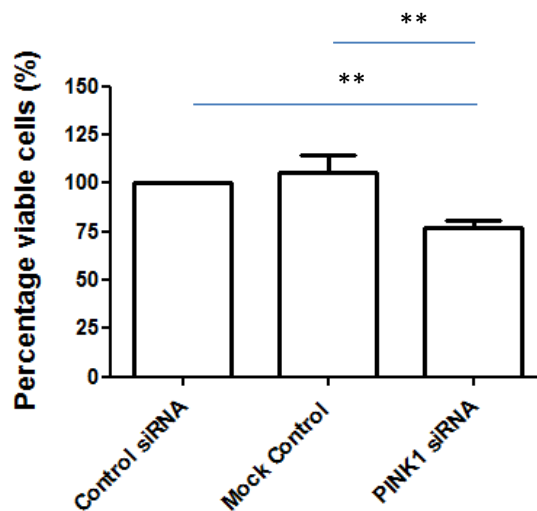
Figure 3.5. Decrease in cell viability in cells with decreased PINK1 expression. Results normalised to control siRNA indicate a significant decline in cell viability in *PINK1* knock down cells (**$p<0.01$), with a total decrease of 23%. Cell viability in *PINK1* knock down cells was also significantly decreased compared to the mock control group (**$p<0.01$).

Mock control cells, non-silencing control siRNA cells and *PINK1* siRNA cells were then separated into the four previously mentioned treatment groups, and all groups were normalised to the untreated group.

In the control siRNA, mock control and *PINK1* siRNA cells, paraquat treatment caused a significant decrease in cell viability compared to the untreated cells, as was expected (Figure 3.6A, B, C, p<0.001). In both controls, pre-treatment with curcumin prior to the addition of paraquat showed a significant improvement in the cell viability (Figure 3.6A, B, p<0.01), suggesting that curcumin may have a protective effect against paraquat. Pre-treatment with curcumin in the *PINK1* siRNA cells did not show a significant increase in cell viability (Figure 3.6C), indicating that curcumin was unable to protect the cells exposed to paraquat in a *PINK1* siRNA-mediated model of PD. The addition of curcumin alone to all three groups showed similar cell viability compared to the untreated groups (Figure 3.6A, B, C), revealing that curcumin was not toxic to the cells.

C
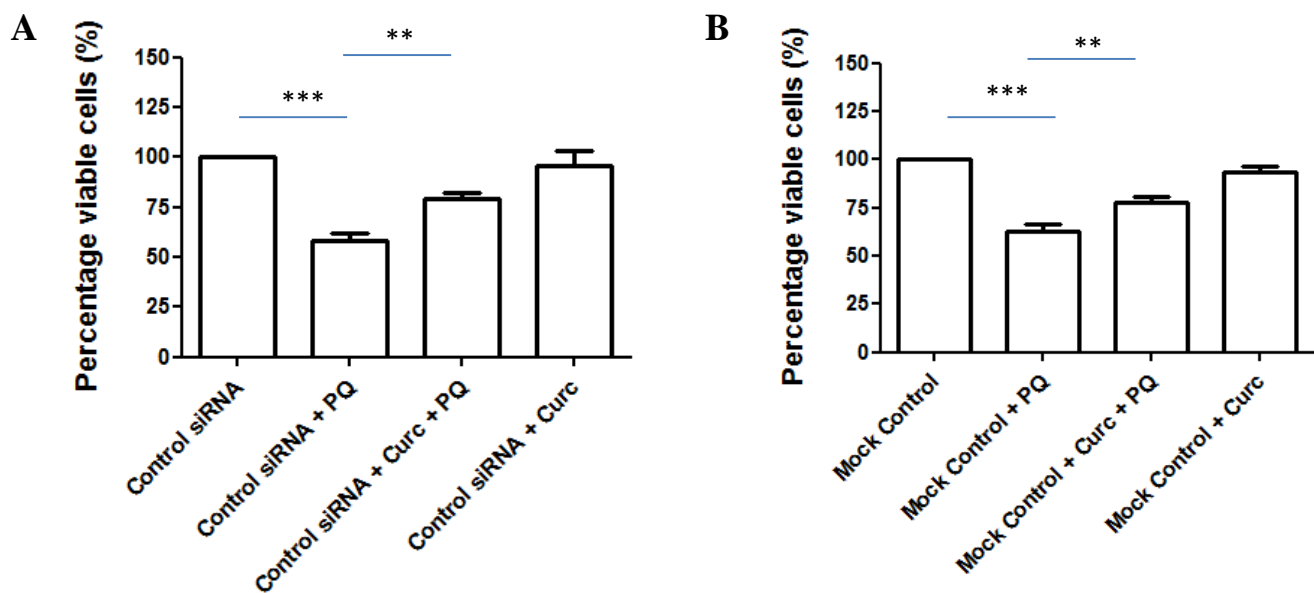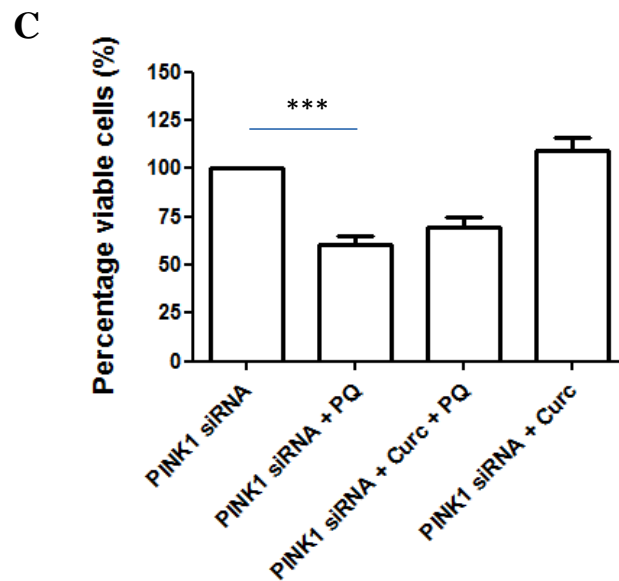
Figure 3.6. Curcumin improves cell viability in control cells. A, B. Non-silencing control cells (A) and mock control cells (B) showed a significant decrease in cell viability after paraquat treatment (***p<0.001; 58% and 62% respectively), which was rescued when pre-treated with curcumin (**p<0.01; 79% and 84% respectively). C. *PINK1* knock down cells showed a significant decrease in cell viability after paraquat treatment (***p<0.001, 60%), but no protective effect with curcumin pre-treatment was evident. PQ, paraquat; Curc, curcumin.

In summary, cell viability was decreased in a *PINK1* siRNA-mediated model of PD compared to two separate controls, suggesting that PINK1 may play a role in the maintenance of healthy cells. Furthermore, paraquat decreased cell viability, and this effect was rescued by curcumin pre-treatment in control cells, but not in the *PINK1* siRNA-treated cells. This may indicate that decreased PINK1 expression combined with paraquat treatment may damage the cells too severely, beyond a point where rescue by curcumin is possible. Curcumin-only treatment did not affect cell viability in the controls or in the *PINK1* knock down model, and was therefore not toxic to the cells.

3.4. Detection of apoptosis

Two markers from the apoptotic cascade were measured – namely cleaved PARP and full-length caspase 3 – to detect levels of apoptosis in the cells. Increased apoptosis can be shown as a combination of increased levels of cleaved PARP, and decreased levels of caspase 3. Due to the fact that the cell viability assay showed similar results for both mock control and control siRNA conditions and due to

the relatively high cost of the transfection reagent, all future experiments utilised only the non-silencing control (control siRNA), and not the mock control, as a comparative to the *PINK1* siRNA conditions.

3.4.1. Cleaved PARP

Images from the Western blots conducted on cleaved PARP and the loading control GAPDH are shown in Figure 3.7A. When quantified, it was revealed that untreated *PINK1* knock down cells had significantly higher levels of cleaved PARP protein compared to the untreated control cells (p=0.0144), indicating that there was increased apoptosis in these cells when PINK1 expression was decreased (Figure 3.7B).

Furthermore, it was revealed that paraquat treatment significantly increased levels of cleaved PARP compared to the untreated group in both *PINK1* siRNA cells (p<0.01, Figure 3.7C) and in control cells (p<0.01, Figure 3.7D). Pre-treatment with curcumin in the *PINK1* siRNA cells substantially reduced the amount of cleaved PARP compared to paraquat treatment (p<0.001, Figure 3.7C). However, in control cells curcumin pre-treatment did not significantly decrease levels of cleaved PARP compared to paraquat only cells (Figure 3.7D). In both *PINK1* siRNA and control cells, the curcumin only group significantly decreased cleaved PARP compared to untreated controls (p<0.001, Figure 3.7C, D).
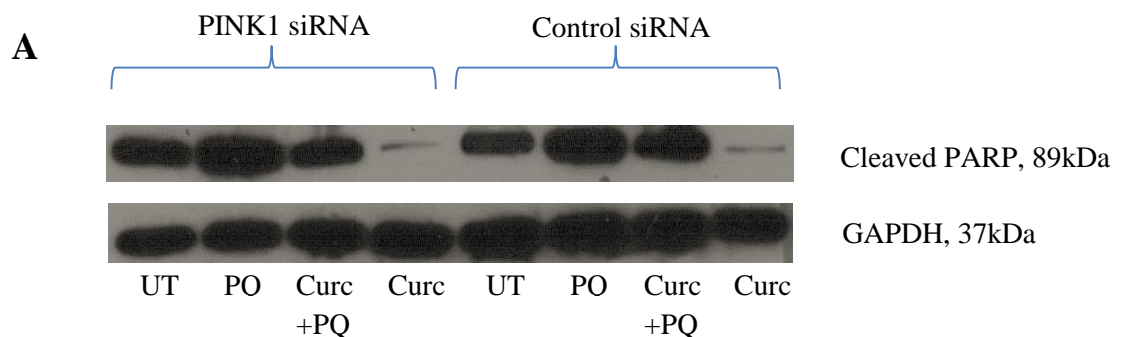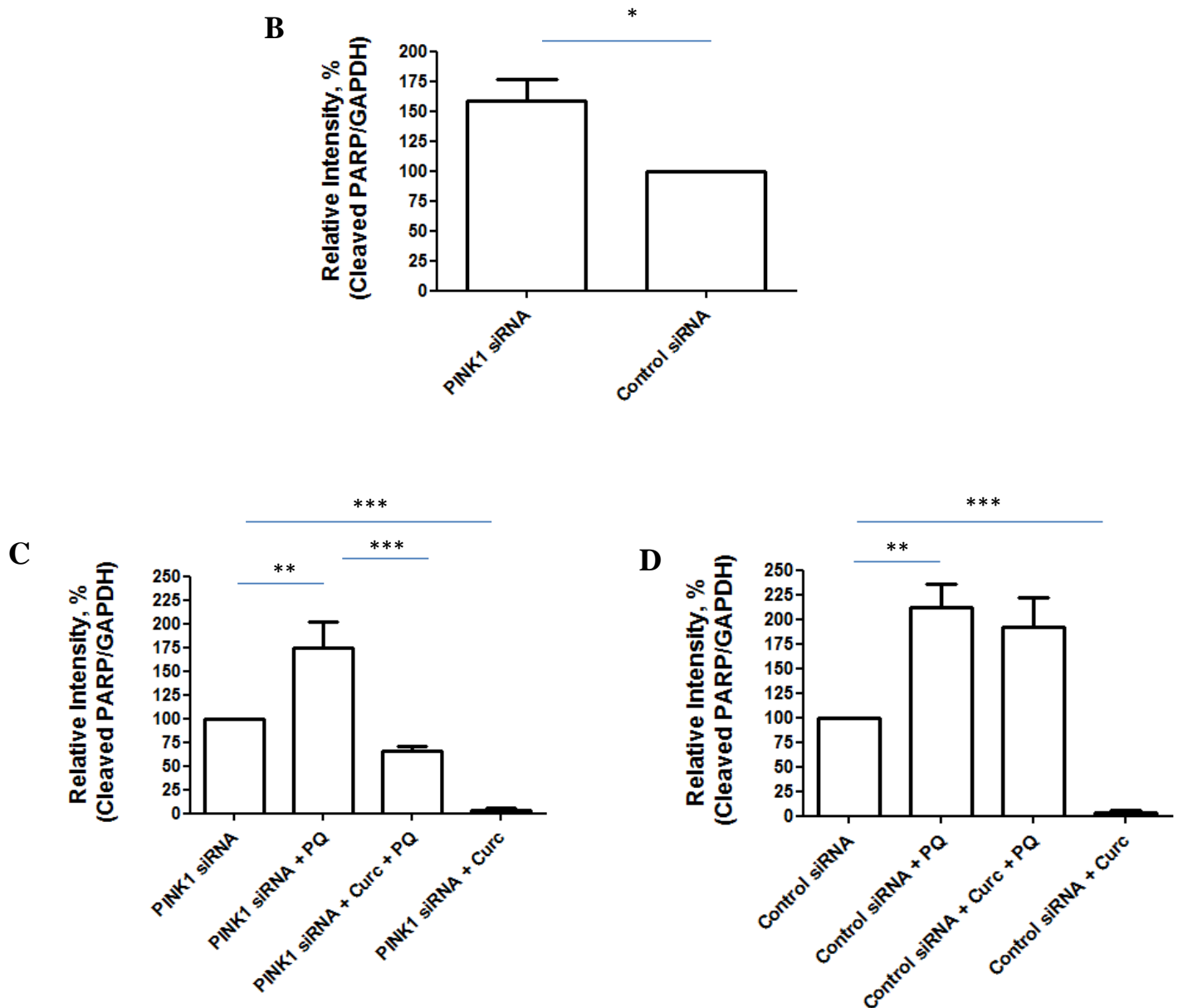
Figure 3.7. Detection of the apoptotic marker cleaved PARP in *PINK1* siRNA and control siRNA cells either untreated (UT), treated with paraquat (PQ), treated with curcumin then paraquat (Curc+PQ) or treated with curcumin alone (Curc). A. Image from the Western blots showing the detection of cleaved PARP (89kDa, top panel), and the loading control GAPDH (37kDa, bottom panel). B. *PINK1* siRNA cells had significantly increased levels of cleaved PARP compared to the control cells (*p=0.0144). C. *PINK1* siRNA cells showed significantly increased cleaved PARP after paraquat treatment compared to untreated cells (**p<0.01), and this was reduced when pre-treated with curcumin (***p<0.001). The curcumin alone group had significantly lower cleaved PARP compared to untreated cells (***p<0.001). D. Control siRNA cells showed increased cleaved PARP after paraquat treatment (**p<0.01). No changes were observed when cells were pre-treated with curcumin, but curcumin alone showed significantly reduced cleaved PARP levels compared to untreated control (***p<0.001).

3.4.2.   Full-length caspase 3

To verify the results observed from the cleaved PARP Western blots, experiments were performed using the full-length caspase 3 antibody. Caspase 3 is also a marker of apoptosis, and is processed to activated, cleaved caspase 3 when cells are undergoing apoptosis. Therefore, decreased full-length caspase 3 is associated with increased apoptosis. A representative image from the blots is shown in Figure 3.8A. When quantified, it was revealed that untreated *PINK1* siRNA cells had significantly lower levels of caspase 3 compared to untreated control cells (p=0.0169, Figure 3.8B), indicating increased apoptosis in cells with lower PINK1 expression. This result verifies the result from the cleaved PARP blots - *PINK1* siRNA cells have increased apoptosis compared to control cells, and PINK1 may play a role in the prevention of cell death.

Paraquat treatment appeared to reduce caspase 3 levels in *PINK1* siRNA and control cells, although this was not significant (Figure 3.8C, D). Pre-treatment with curcumin in both *PINK1* siRNA and control cells significantly increased caspase 3 (p<0.05, Figure 3.8C, D), verifying the results observed from the cleaved PARP blots. In *PINK1* siRNA cells, the curcumin only group revealed significantly higher levels of caspase 3 compared to the untreated cells (p<0.05, Figure 3.8C), and this was also observed in control cells (p<0.05, Figure 3.8D). The increased levels of full-length caspase 3 indicate reduced apoptosis, and therefore verify the results from the cleaved PARP blots.
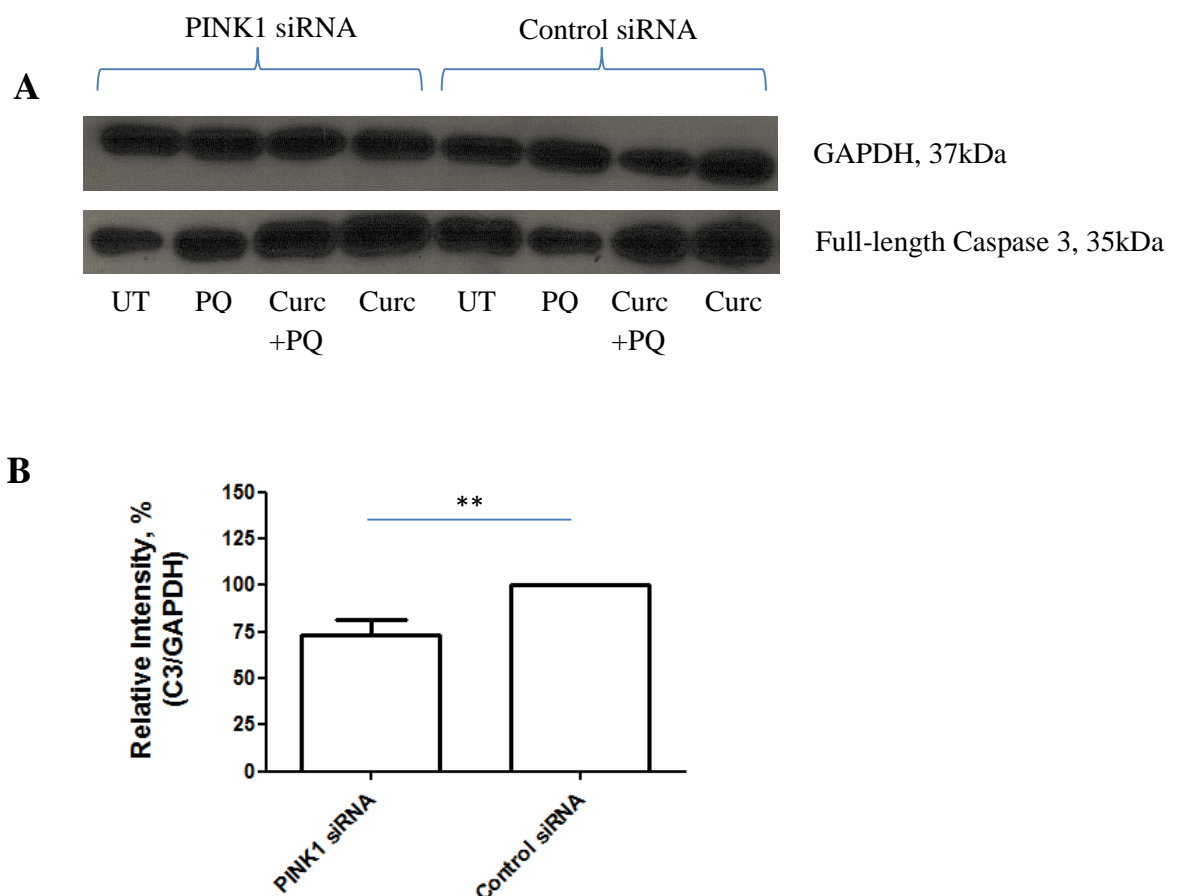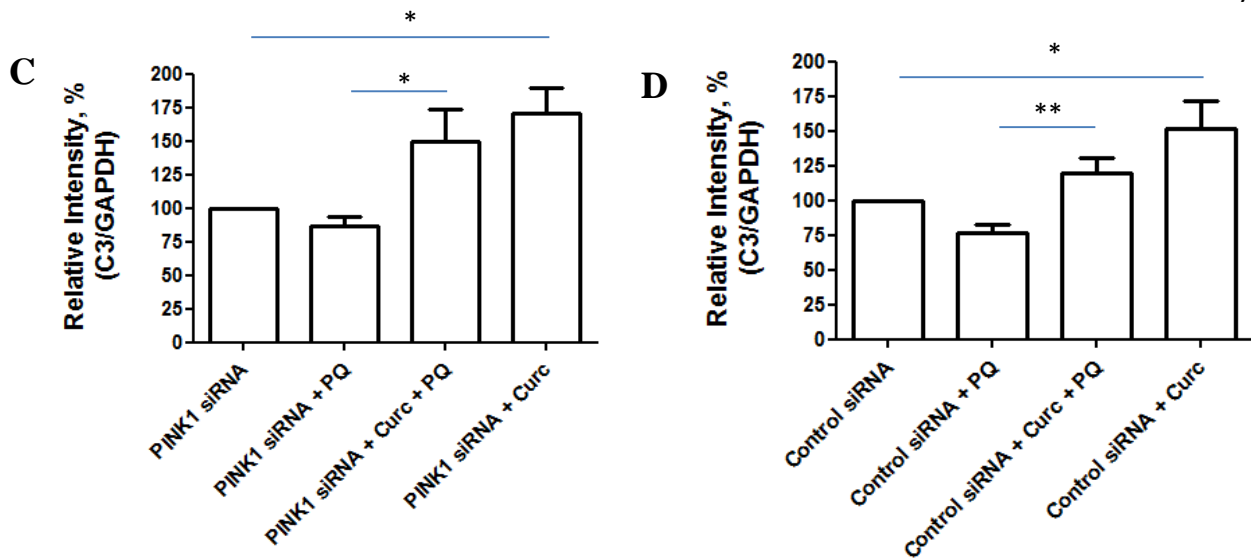
Figure 3.8. Detection of the apoptotic marker full-length caspase 3 in control siRNA and *PINK1* siRNA cells either untreated (UT), treated with paraquat (PQ), treated with curcumin then paraquat (Curc+PQ) or treated with curcumin alone (Curc). A. Image from a Western blot indicating the loading control GAPDH (37kDa, top panel), and full-length caspase 3 (35kDa, bottom panel). B. Graph representing quantitative values from the Western blots show a decrease in caspase 3 in *PINK1* siRNA cells compared to control siRNA cells (*p=0.0169), indicating an increase in apoptosis. C. In *PINK1* siRNA cells, pre-treatment with curcumin significantly increased caspase 3 levels compared to paraquat (*p<0.05), and curcumin alone significantly increased caspase 3 compared to untreated cells (*p<0.05). D. Similarly, curcumin pre-treatment increased caspase 3 compared to paraquat in control siRNA cells (p<0.01), and curcumin alone significantly increased caspase 3 compared to untreated cells (*p<0.05).

In summary, from both sets of results, it has clearly been shown that *PINK1* siRNA cells have significantly increased apoptosis compared to control cells, as shown by the increased levels of cleaved PARP and decreased levels of caspase 3. This could suggest that the PINK1 protein may play a protective role in the cell against apoptosis-driven cell death. Secondly, paraquat appeared to increase apoptosis (although not significantly in the caspase 3 blots, Figure 3.8C, D), which is to be expected, as paraquat creates an oxidative environment in the cells. Pre-treatment with curcumin reduced paraquat-induced apoptosis in both *PINK1* siRNA and control cells, and curcumin alone further decreased apoptosis compared to untreated cells.

3.5. Analysis of mitochondrial membrane potential

Based on the observations that curcumin protects the cells from the effects of paraquat treatment, the next step was to understand the mechanism of its action. It was hypothesized that curcumin may be working at a mitochondrial level due to its antioxidant properties. Therefore mitochondrial functional and structural assays were performed to test this hypothesis.

MMP is measured through the use of the JC-1 dye. JC-1 is permeable to the mitochondrial membrane, and when membrane potential is maintained, it aggregates inside the mitochondria and emits fluorescence in the PE channel. When the MMP is lost and cells are depolarised, JC-1 remains in the cytoplasm in its monomeric form, and emits fluorescence through the FITC channel. Therefore changes in MMP can then be determined by calculating the ratio of PE/FITC mean intensity values. The lower the value, the more depolarised the MMP.

Results from the flow cytometric analysis with JC-1 revealed that as per our hypothesis, the PE/FITC ratio (and therefore the MMP) in *PINK1* siRNA cells was significantly decreased compared to control cells (p=0.008, Figure 3.9A). This would suggest that when PINK1 expression is decreased, mitochondrial dysfunction will occur. The addition of paraquat to both *PINK1* siRNA and control cells significantly reduced the PE: FITC ratio (p<0.05, Figure 3.9B, C), and pre-treatment with curcumin resulted in increased PE: FITC ratio compared to paraquat treated cells (p<0.05, Figure 3.9B, C). There was no significant changes between curcumin only treatment and untreated groups in both *PINK1* siRNA and control cells (Figure 3.9B, C).

B

C
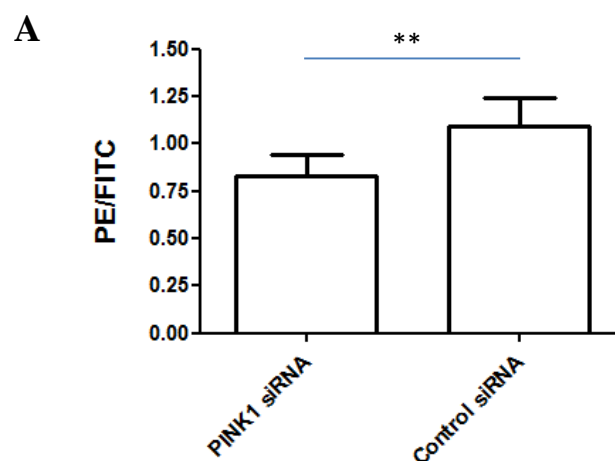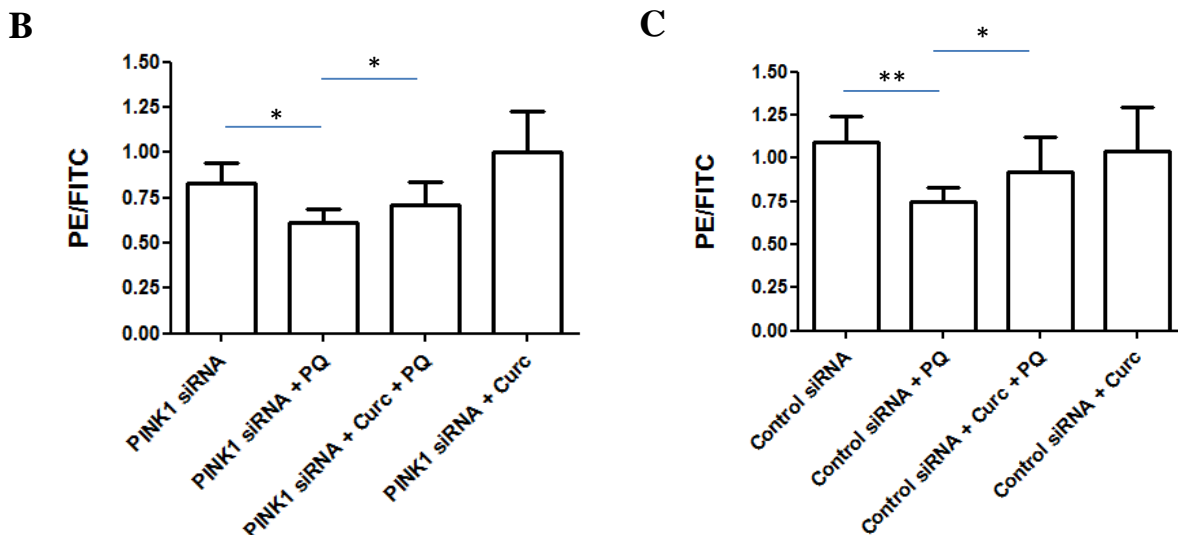
Figure 3.9. Mitochondrial membrane potential shown by a ratio of PE/FITC values. A. *PINK1* siRNA cells had a significantly lower ratio compared to control cells (***p=0.0008). B, C. *PINK1* siRNA (B) and control (C) cells both showed significantly decreased ratios after the addition of paraquat (**p<0.01, *p<0.05), and these were significantly increased when pre-treated with curcumin (*p<0.05). No significant differences were found after curcumin treatment alone compared to the untreated group. PQ, paraquat; Curc, curcumin

3.6.   Analysis of mitochondrial respiration and glycolysis

Mitochondrial respiration was measured in *PINK1* siRNA cells and compared to the non-silencing control siRNA cells. The effect of paraquat and curcumin treatment on mitochondrial respiration was also analysed. By using the Seahorse XF Analyser, it is possible to detect the rates of oxygen consumption for respiration (OCR, oxygen consumption rate) and proton release for glycolysis (ECAR, extracellular acidification rate) in the media surrounding the cells, thus determining the bioenergetic status of the cell. The results obtained represent an average of 11 replicates per measurement (N=11).

3.6.1.   OCR – The Mitochondrial Stress Test

OCR, an indication of mitochondrial respiration, was measured under four conditions:

i.   Basal respiration

ii.   Addition of Oligomycin, a complex V inhibitor, resulting in suspended ATP synthesis and allowing for the calculation of overall ATP production (difference in OCR between basal respiration and respiration after Oligomycin addition)

iii.   Addition of an uncoupler FCCP, which results in maximal respiration and allows for the calculation of spare respiratory capacity (difference in OCR between maximal and basal respiration)

iv.   Addition of complex I inhibitor Rotenone and complex III inhibitor Antimycin A, which arrests respiration

The point-to-point OCR data is presented in Figure 3.10A for non-silencing control siRNA cells (red line) and *PINK1* siRNA cells (purple line) at basal levels, and after the addition of Oligomycin, FCCP and Rotenone + Antimycin A. Quantification before and after the addition of the drug compounds revealed that *PINK1* siRNA cells had significantly decreased OCR at basal respiration (Figure 3.10B, $p<0.001$), decreased ATP production ($p=0.002$, Figure 3.10C) decreased maximal respiration (Figure 3.10D, $p=0.0015$) and reduced spare respiratory capacity (Figure 3.10E, $p=0.0154$). In summary, these results reveal that in the absence of PINK1, all aspects of mitochondrial respiration are negatively affected.

A
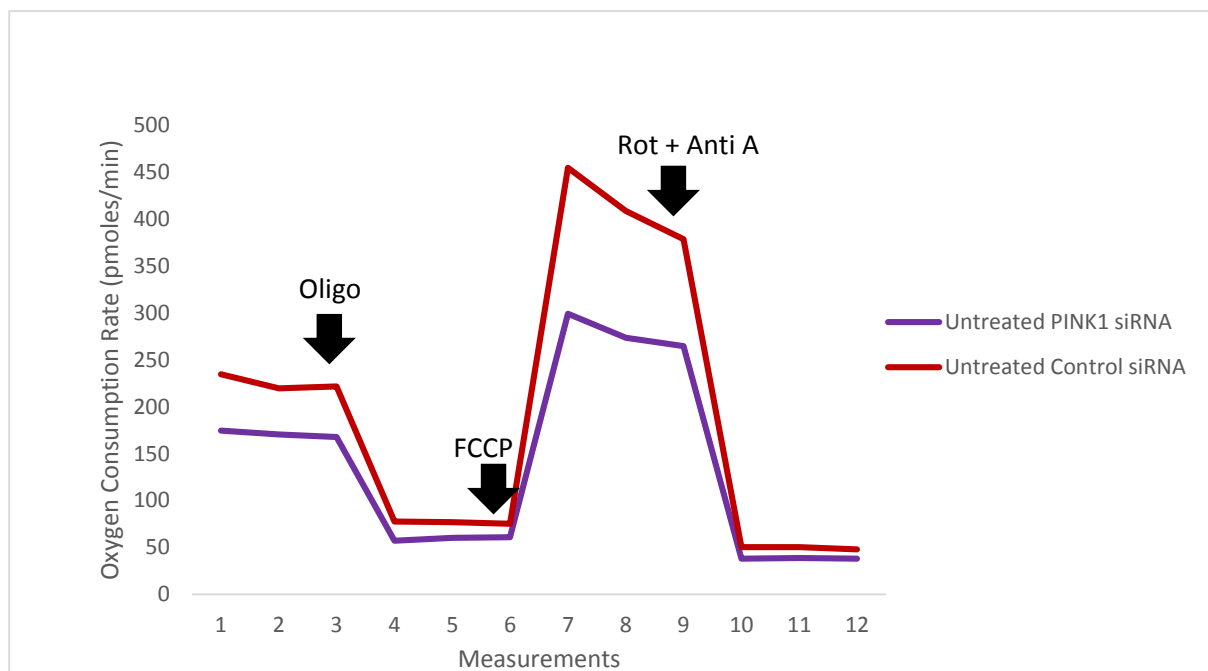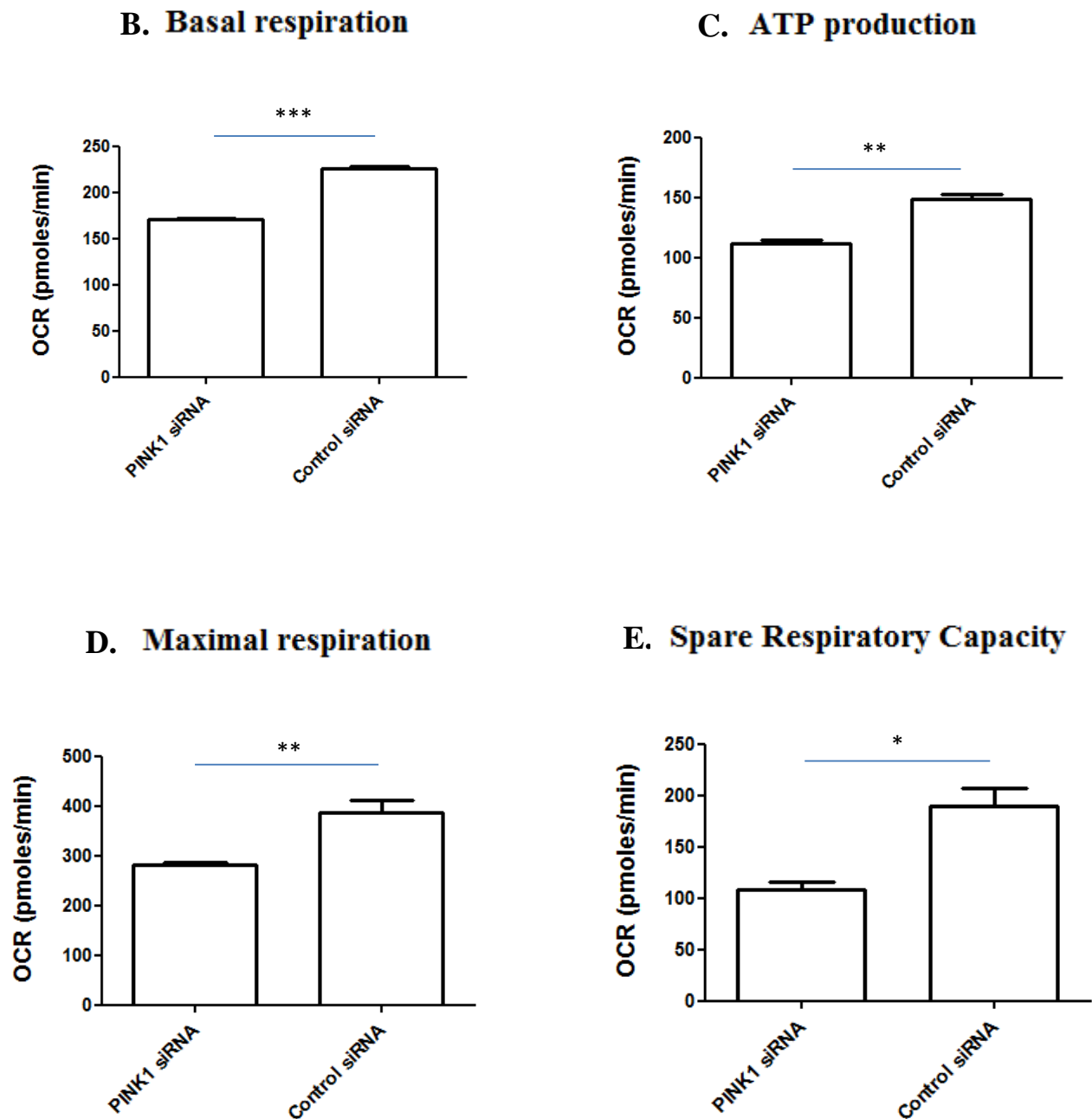
Figure 3.10. *PINK1* siRNA cells exhibit decreased mitochondrial respiration in comparison to control siRNA cells. A. Point-to-point line graph of *PINK1* siRNA cells (purple line) and control siRNA cells (red line) after the addition of Oligomycin (Oligo), FCCP and Rotenone + Antimycin A (Rot + Anti A). Each measurement represents 9min 12sec interval. *PINK1* siRNA cells showed significantly decreased oxygen consumption rate (OCR) across all conditions. B. Basal respiration, ***$p < 0.0001$, C. ATP production, **$p = 0.002$, D. Maximal respiration, **$p = 0.0015$, E. Spare respiratory capacity,*$p = 0.0154$. N=11.

Next, *PINK1* siRNA and control cells were then either left untreated, or treated with paraquat, curcumin or pre-treated with curcumin followed by paraquat exposure, according to the pre-determined protocol (Figure 2.3). The overall mitochondrial respiration results for both the *PINK1* siRNA and control cells can be seen in Figure 3.11A and B respectively.
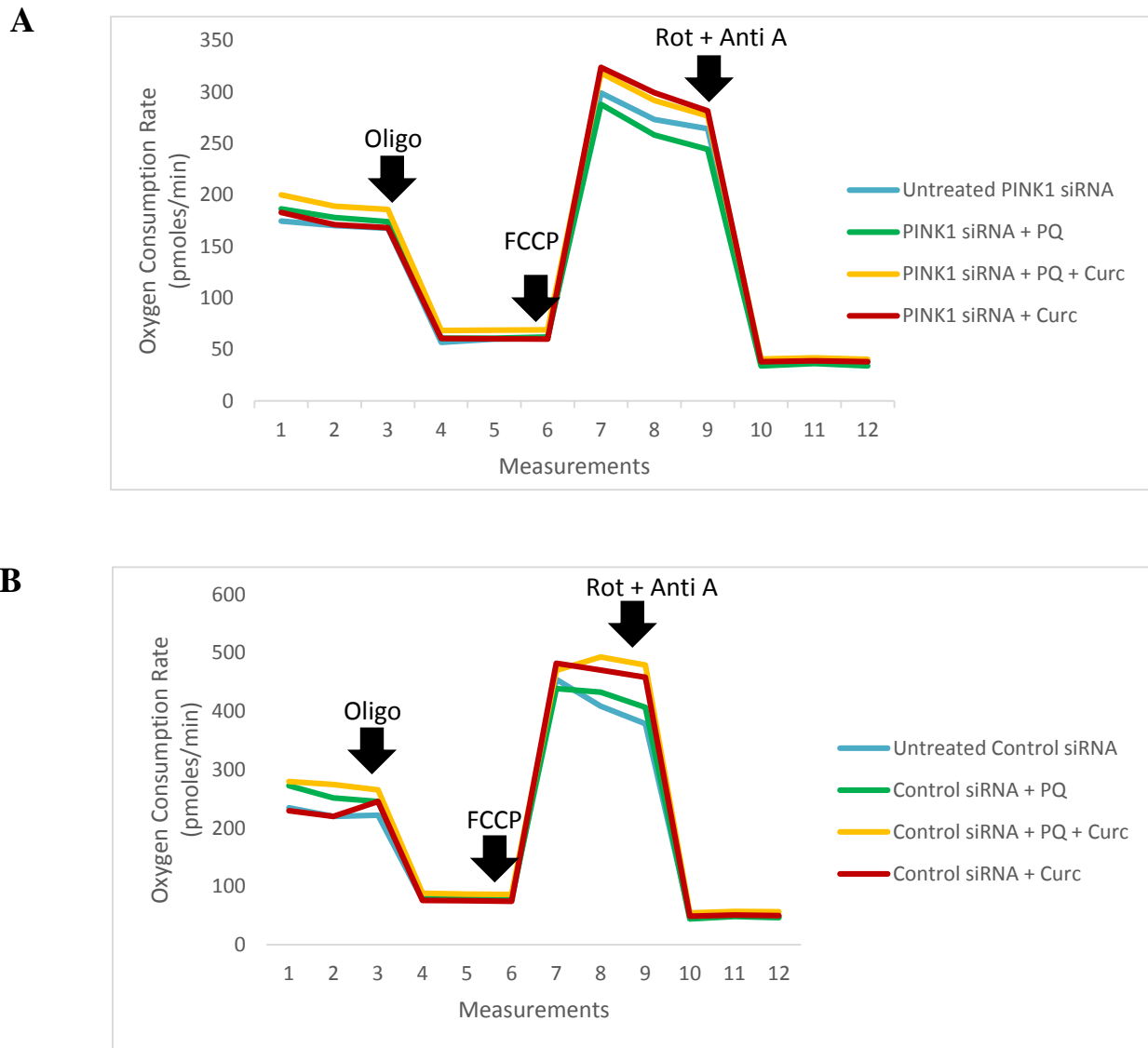
Figure 3.11. Point-by-point line graphs indicating oxygen consumption rate (OCR) in each treatment group in *PINK1* siRNA cells (A) and control cells (B) after the addition of drug compounds. Each measurement represents 9min 12sec interval. N=11. Oligo, Oligomycin; Rot, rotenone; Anti A, Antimycin A; PQ, paraquat; Curc, curcumin

Basal respiration

No significant changes were observed in OCR in *PINK1* siRNA cells at basal respiration (Figure 3.12A). Paraquat treatment in control cells interestingly resulted in a significant increase at a basal level ($p<0.001$, Figure 3.12B), and this was further increased when cells were pre-treated with curcumin ($p<0.001$, Figure 3.12B). The curcumin alone group had no significant effect on OCR at a basal level in control cells (Figure 3.12B), although it appeared to keep the OCR at the same level as the untreated cells. These results are difficult to interpret, and it has been suggested that often readings at a basal level can be inaccurate (personal communication, Dr. Francois van Der Westhuizen, North West University, South Africa).

ATP production

In both *PINK1* siRNA and control cells, there were no significant changes in OCR across all treatment groups, indicating no changes in ATP production (Figure 3.12C, D).

Maximal respiration

In *PINK1* siRNA and control cells, paraquat treatment had no effect on OCR after the addition of the mitochondrial uncoupler FCCP (Figure 3.12E, F). Pre-treatment with curcumin prior to paraquat treatment significantly increased OCR compared to the paraquat-only group in *PINK1* siRNA cells ($p<0.01$, Figure 3.12E) and in control cells ($p<0.05$, Figure 3.12F). Furthermore, curcumin only treatment significantly increased OCR compared to the untreated group in both *PINK1* siRNA cells ($p<0.05$, Figure 3.12E) and in control cells ($p<0.001$, Figure 3.12F). These results suggest a possible rescue effect of curcumin on stressed, depolarised mitochondria.

Spare respiratory capacity

No changes were observed across all treatment groups in *PINK1* siRNA cells (Figure 3.12G). In control cells, pre-treatment with curcumin significantly increased OCR, and therefore spare capacity, compared to the paraquat treatment group ($p<0.05$, Figure 3.12H). No other changes were observed in control cells.

Basal respiration
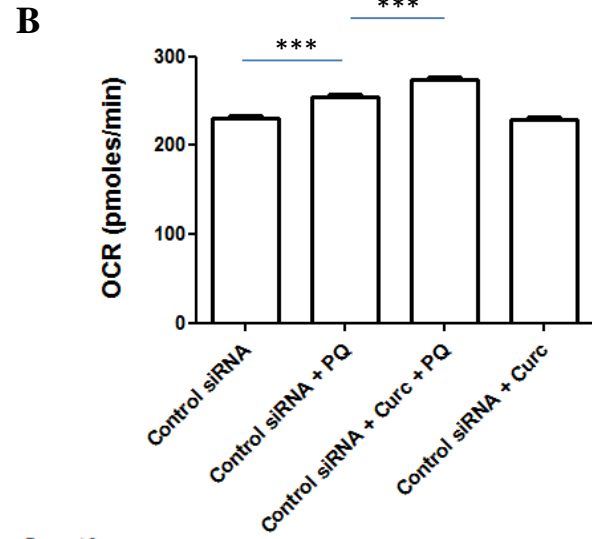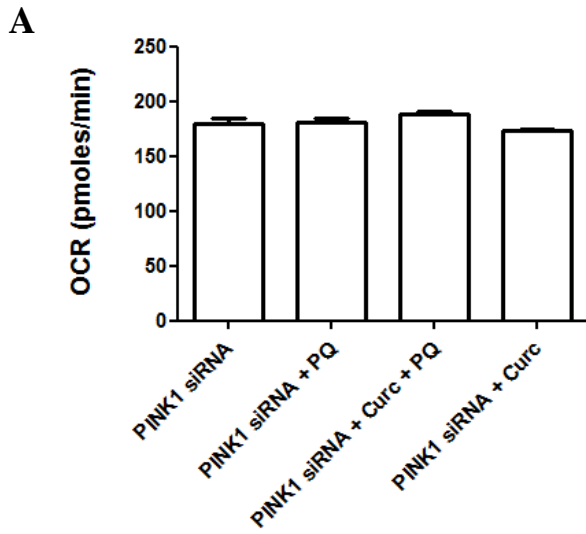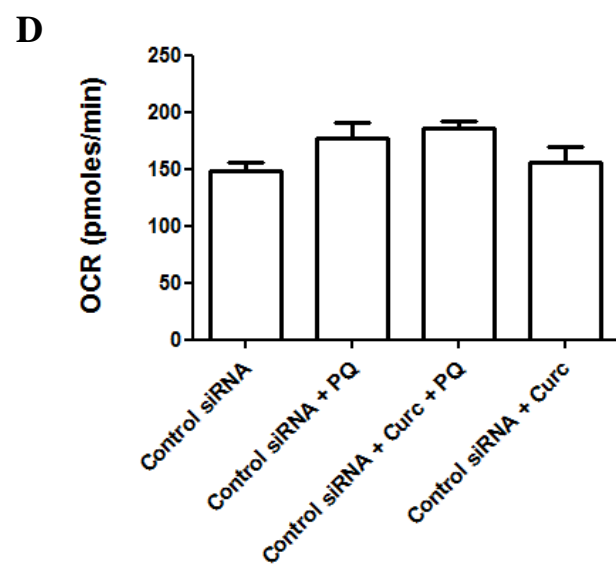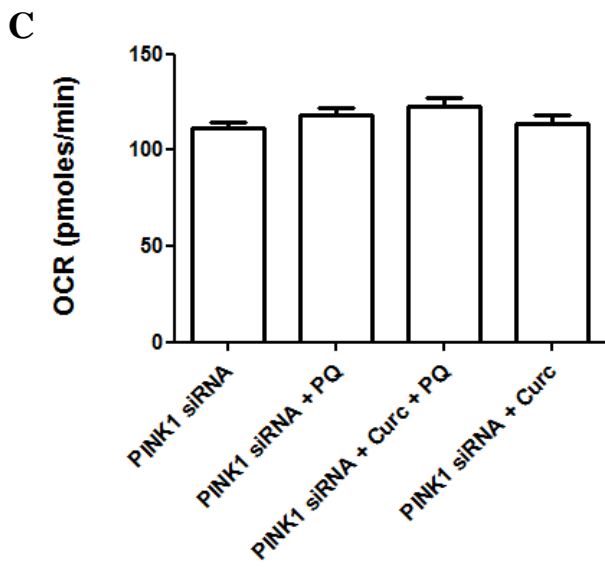
ATP production

Maximal respiration
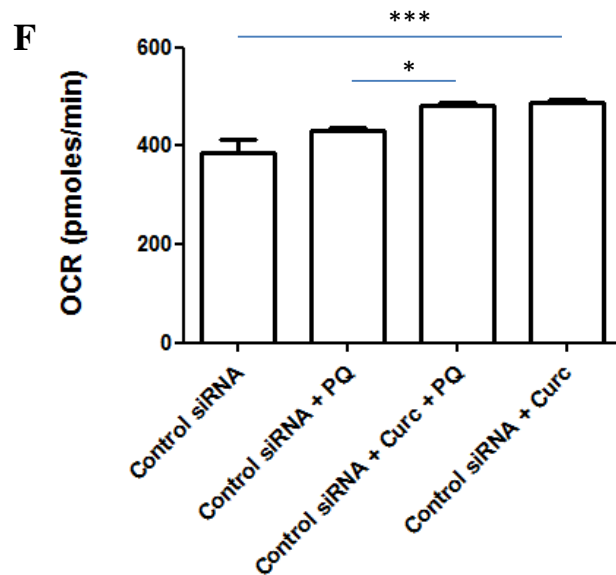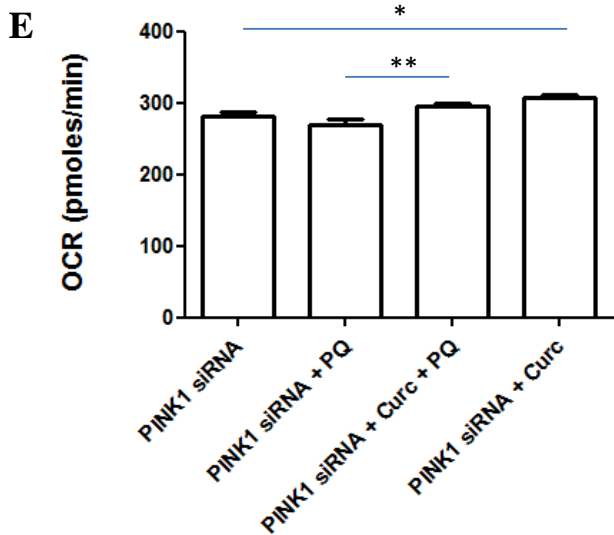
Spare Respiratory Capacity
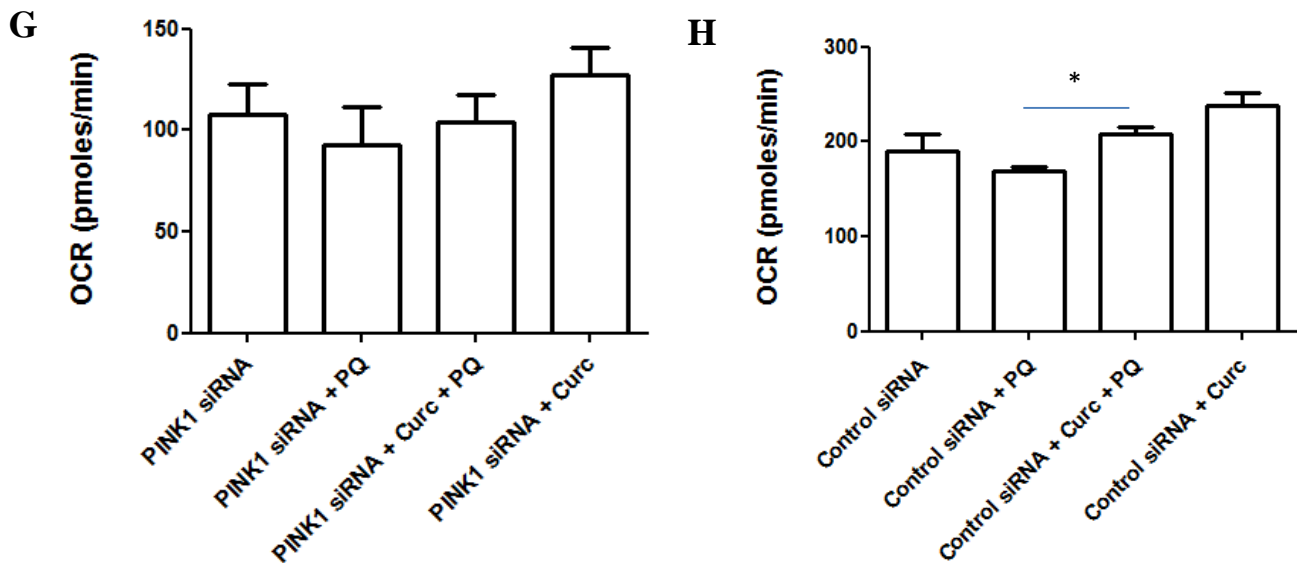
Figure 3.12. Basal respiration, ATP production, maximal respiration and spare respiratory capacity in *PINK1* siRNA and control cells. A. No changes were observed in basal respiration in *PINK1* siRNA cells. B. In control siRNA cells, OCR was significantly higher in the paraquat-group compared to the untreated group (***$p<0.001$). The paraquat-curcumin group significantly increased OCR compared to the paraquat group (***$p<0.001$). C, D. No changes were observed in ATP production in *PINK1* siRNA cells (C) or control cells (D). E, F. Pre-treatment with curcumin significantly increased OCR compared to paraquat treatment in *PINK1* siRNA (E, **$p<0.01$) and control (F, *$p<0.05$) cells. Curcumin alone increased OCR compared to the untreated group in *PINK1* siRNA (E, *$p<0.05$) and control (F, $p<0.001$) cells. G. No changes in spare respiratory capacity were observed in *PINK1* siRNA cells. H. Pre-treatment with curcumin significantly increased spare respiratory capacity in control cells compared to the paraquat treated cells (*$p<0.05$). OCR, oxygen consumption rate; PQ, paraquat; Curc, curcumin

In summary, the above results on aspects of mitochondrial respiration show that:

a) Decreased PINK1 expression, using an siRNA model, has a negative effect on basal respiration, ATP production, maximal respiration and spare respiratory capacity.

b) Paraquat does not affect mitochondrial respiration at this concentration of 25µM.

c) Pre-treatment with curcumin prior to paraquat is able to increase basal respiration, maximal respiration and spare respiratory capacity compared to paraquat treatment in control cells, and also increases maximal respiration in *PINK1* siRNA cells. These results suggest that when cells are under a certain level of stress, curcumin is able to rescue mitochondrial respiration. Despite this, pre-treatment with curcumin prior to the addition of paraquat was not able to rescue basal respiration, ATP production and spare respiratory capacity in *PINK1* siRNA cells. This could suggest that curcumin can only rescue cells on a mitochondrial level when PINK1 is present and functional in these cells.

d) Treatment with curcumin alone significantly increases maximal respiration in both control and *PINK1* siRNA cells compared to the untreated groups, which suggests a particular function of curcumin in the mitochondria when they have been depolarised.

3.6.2.   ECAR – The Glycolysis Stress Test

ATP is primarily produced via mitochondrial respiration and the oxidative phosphorylation pathway. However, glycolysis can become the primary producer of ATP when oxidative phosphorylation is damaged or inhibited. It is therefore important to investigate key parameters of glycolytic function in order to understand critical information regarding cellular energy demands. The Glycolysis Stress Test Kit (Seahorse Bioscience, USA) enables one to determine the rate of glycolysis, the glycolytic capacity, and the glycolytic reserve in cells while inducing metabolic stress.

ECAR detects lactic acid production by measuring the rate that free protons are released from the cells, in other words, when the protons 'acidify' the medium. ECAR was measured under the following conditions:

i.   Basal, non-glycolytic acidification measured in glucose-free medium.

ii.   Addition of a saturating concentration of glucose, to determine glycolysis rates (difference between ECAR before and after glucose addition).

iii.   Addition of the ATP synthase inhibitor Oligomycin to measure the glycolytic capacity of the cells (difference between ECAR at basal levels and after the addition of Oligomycin). Glycolytic reserve can also be determined by subtracting the rates of glycolysis from the rates of glycolytic capacity.

iv.   Addition of a saturating concentration of 2-DG, a glucose analogue which inhibits glycolysis by its actions on hexokinase.

The point-by-point graph for control cells (red line) compared to *PINK1* siRNA cells (purple line) is shown in Figure 3.13A. After quantification, it was revealed that the ECAR under basal conditions in a glucose-free medium was significantly lower in *PINK1* siRNA cells compared to control cells (Figure 3.13B, $p<0.001$). *PINK1* siRNA cells also exhibited significantly lower glycolytic capacity compared to control cells (Figure 3.13C, $p=0.0445$). These results would indicate that in the absence of *PINK1*, when oxidative phosphorylation is restricted, cells are unable to produce sufficient levels of ATP due to inhibition of basal lactic acid production and glycolytic capacity. The ECAR rates for glycolysis and glycolytic reserve showed no significance between the cells ($p>0.05$; Appendix V).

A
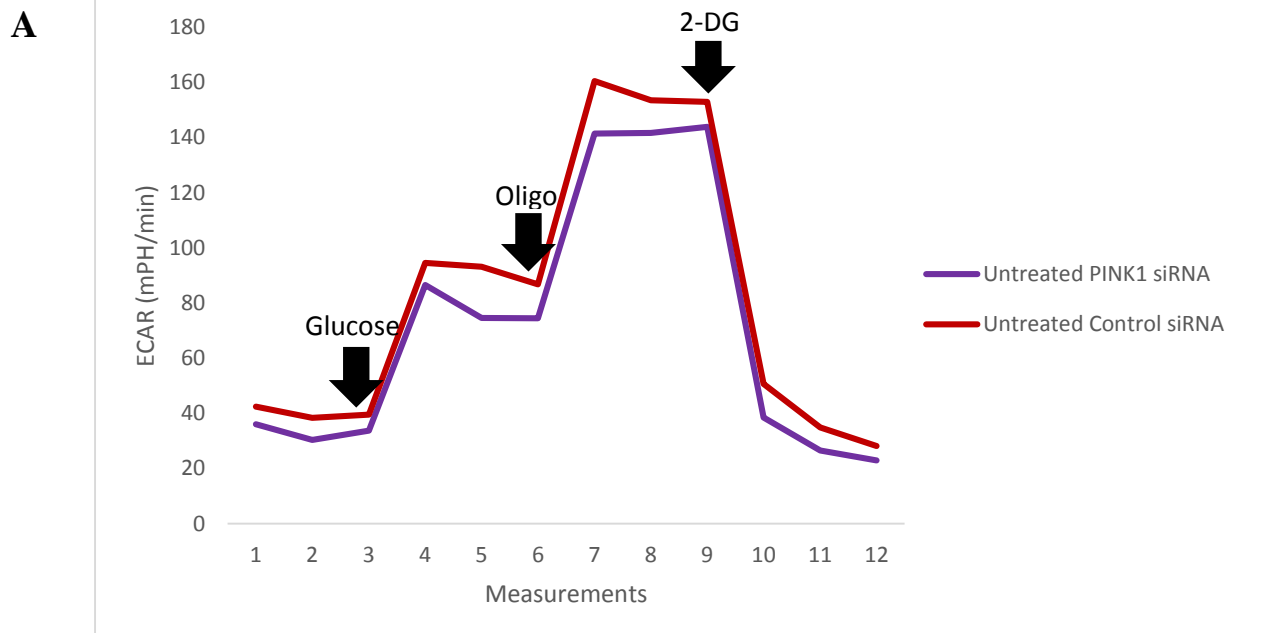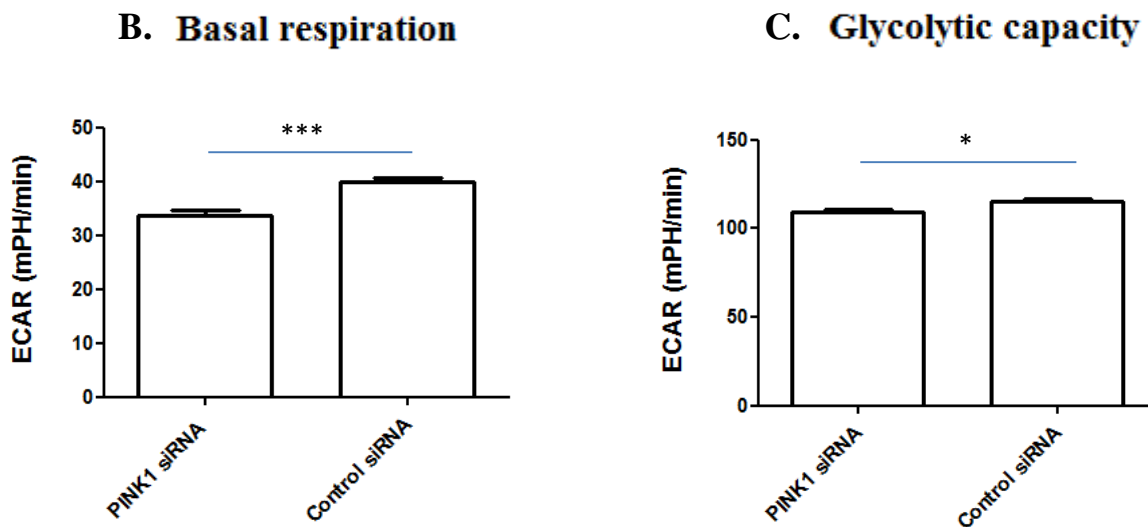
Figure 3.13. Reduced ECAR observed in *PINK1* siRNA cells at basal levels and glycolytic capacity. A. *PINK1* siRNA cells (purple line) compared to control siRNA cells (red line) after the addition of Glucose, Oligomycin (Oligo) and 2-DG (2-deoxy-D-glucose). Each measurement represents 9min 12sec interval. B, C. *PINK1* siRNA cells show significantly decreased ECAR compared to control cells at basal levels (B, ***$p<0.001$) and for glycolytic capacity (C, *$p=0.0445$). N=11.

ECAR measurements for *PINK1* siRNA and control cells following the treatment protocol (Figure 2.3) are shown in Figure 3.14A and B respectively. Quantification of these results revealed no significant differences between each treatment group in glycolysis rates, glycolytic capacity and glycolytic reserve in *PINK1* siRNA and control cells (Appendix V). At a basal level, paraquat treatment significantly decreased ECAR in *PINK1* siRNA cells compared to untreated cells ($p<0.001$), as did curcumin alone (Figure 3.14C, $p<0.05$). Pre-treatment of the cells with curcumin prior to the addition of paraquat resulted in a significantly higher ECAR compared to the paraquat-only group (Figure 3.14C, $p<0.001$). There were no significant changes in control cells at a basal level (Figure 3.14D).
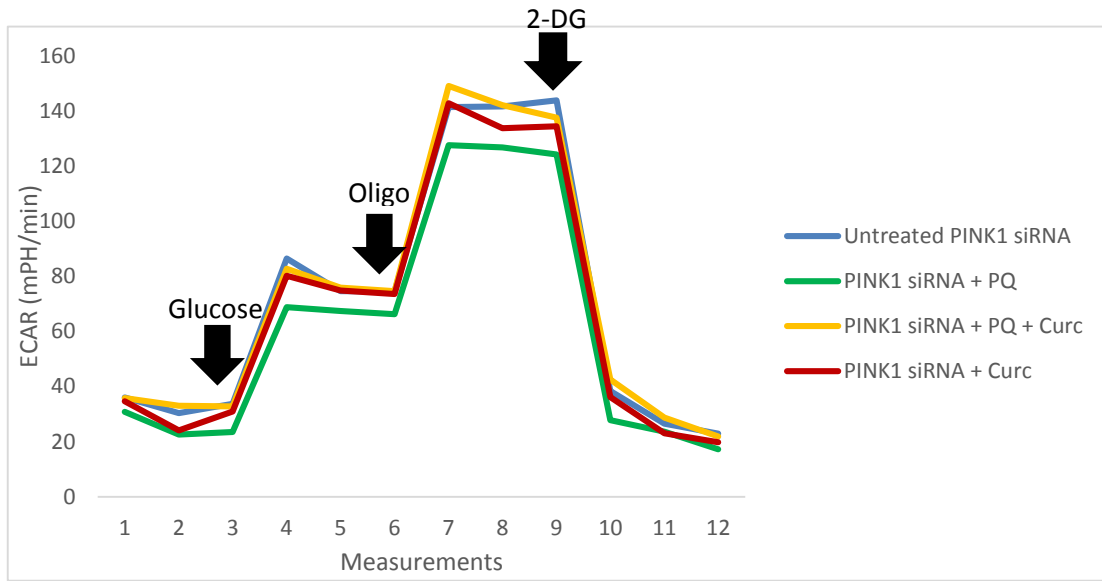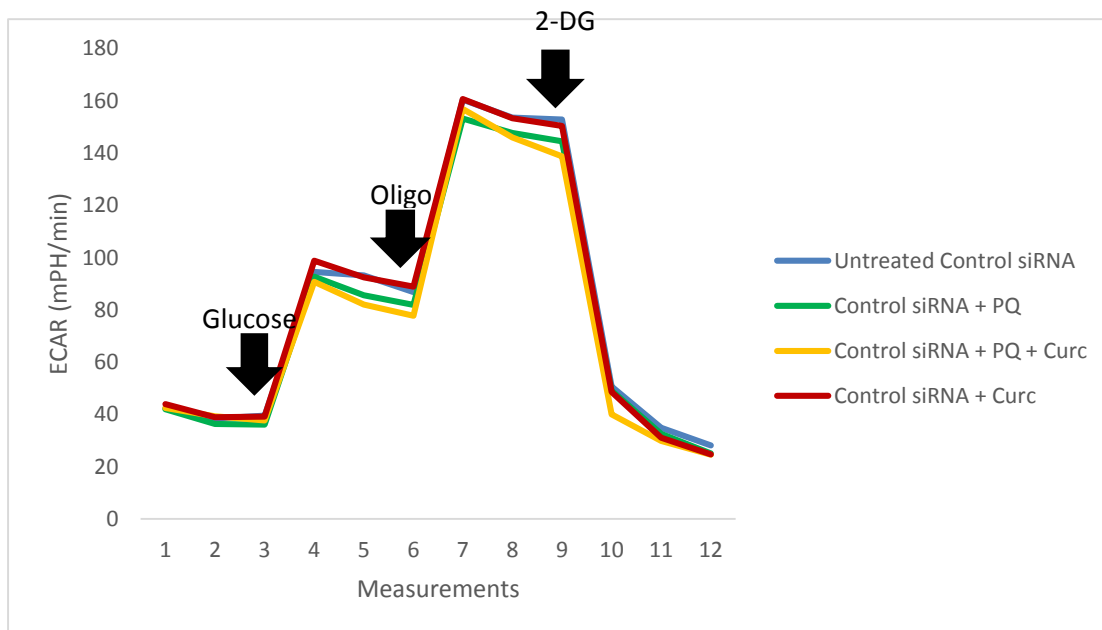
Basal respiration
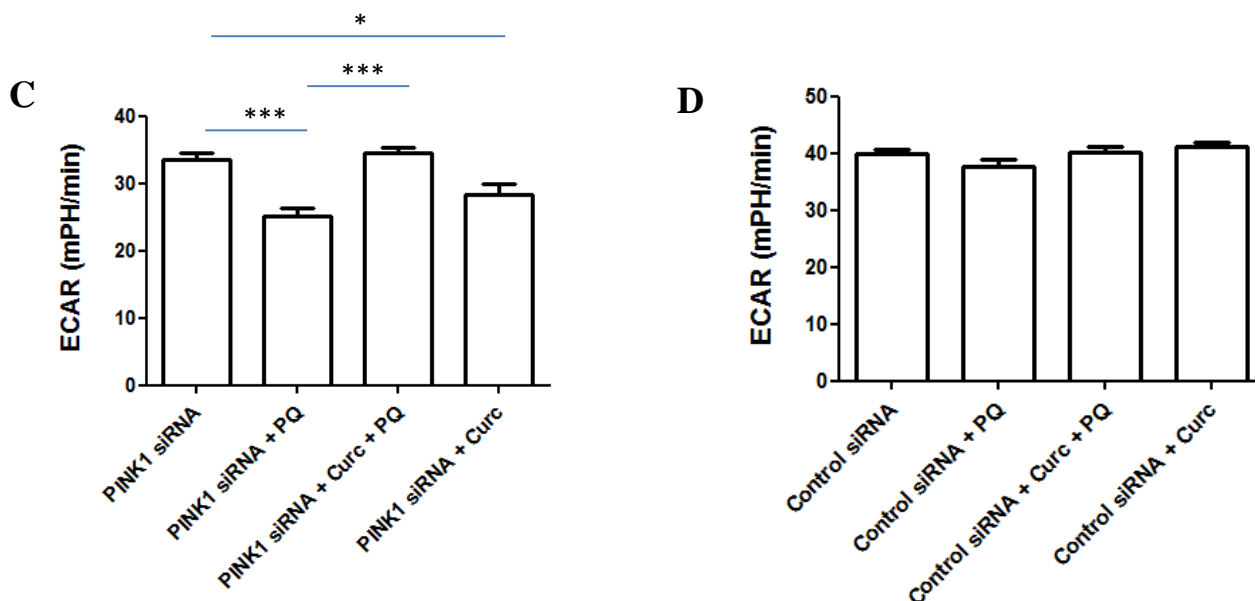
Figure 3.14. Reduced ECAR observed at basal levels in *PINK1* siRNA cells after paraquat treatment. A, B. Point-by-point graphs for ECAR in *PINK1* siRNA cells (A) and control cells (B) after the addition of Glucose, Oligomycin (Oligo) and 2-DG. Each measurement represents 9min 12sec interval. C. In *PINK1* siRNA cells, ECAR was significantly decreased after the addition of paraquat (***p<0.001), and this was rescued by pre-treatment with curcumin (***p<0.001). Curcumin treatment alone resulted in decreased ECAR compared to untreated cells (*p<0.05). D. No significant difference in ECAR across all treatment groups in control cells. N=11.

In summary, treatment with paraquat, curcumin, or both, does not appear to have an effect on aspects of glycolysis. However, decreased PINK1 expression results in decreased basal acidification rates after paraquat-only and curcumin-only treatment, and this is rescued by curcumin pre-treatment. This may suggest that curcumin can activate cellular acidification only under highly stressful conditions – such as a combination of decreased PINK1 expression and paraquat treatment.

Together, the results from mitochondrial respiration and glycolytic analysis have provided detail into the role of curcumin at a cellular level. As a known antioxidant, curcumin is able to increase mitochondrial respiration and ATP production in control cells, and this effect appears to be more pronounced when the cells are stressed by paraquat. Curcumin was unable to elevate basal respiration

in *PINK1* siRNA cells which could suggest that PINK1 expression may be necessary for curcumin to function efficiently. However, despite this, curcumin increased respiration in stressed control and *PINK1* siRNA cells when the mitochondria were depolarized (after the addition of FCCP). Furthermore, in a glucose-free medium, curcumin increased the rate of extracellular acidification in stressed *PINK1* siRNA cells. These results could collectively suggest that the greater the stress on the cells (i.e. addition of paraquat/ FCCP/ glucose-free medium), the greater the effect that curcumin may have.

3.7. Mitochondrial network analysis

As mentioned in the methodology, SH-SY5Y cells were visualized using Hoechst 33342 and MitoTracker Red to indicate nuclear architecture and mitochondrial morphology respectively (Section 2.8). Quantification of these images through Image J software allowed for the calculation of both form factor (the degree of branching) and aspect ratio (measurement of mitochondrial length) as specified in Section 2.8. The higher the form factor, the less fragmented the mitochondrial network. The number of replicates used in these experiments (N) was 3.

3.7.1. Form Factor

The images obtained for each treatment group in *PINK1* siRNA and control cells are shown in Figure 3.15, A-H. White arrows highlight areas of increased fusion, and yellow arrows increased fragmentation. Quantification of the images, calculation of form factor, and subsequent statistical analysis indicated that although there was a trend of increased form factor, (and therefore increased fusion), and the cells appeared more fused in *PINK1* siRNA cells (white arrow, Figure 3.15A) compared to control cells (yellow arrow, Figure 3.15B), this was not significant (Figure 3.15I). In both *PINK1* siRNA and control cells, paraquat treatment resulted in significantly decreased form factor compared to untreated cells (Figure 3.15J, K, $p<0.05$), suggesting that paraquat treatment caused increased mitochondrial network fragmentation. Curcumin pre-treatment prior to paraquat treatment appeared to increase form factor compared to paraquat treated cells. This was not statistically significant in *PINK1* knock down cells (Figure 3.15J), but it was significant in control cells (Figure 3.15K, $p<0.05$). Curcumin treatment alone in *PINK1* siRNA cells had a lower form factor compared to the untreated cells, but this was not significant (Figure 3.15J). Curcumin alone in control cells appeared to increase form factor more than untreated cells, but this was not significant (Figure 3.15K).

A. *PINK1* siRNA
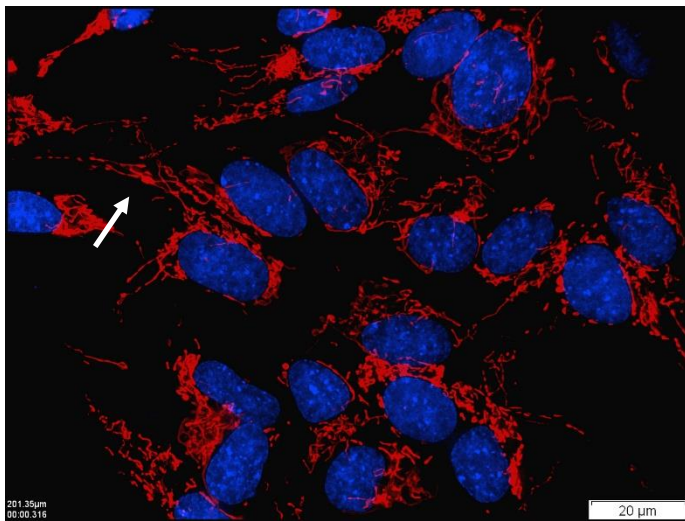
B. Control siRNA
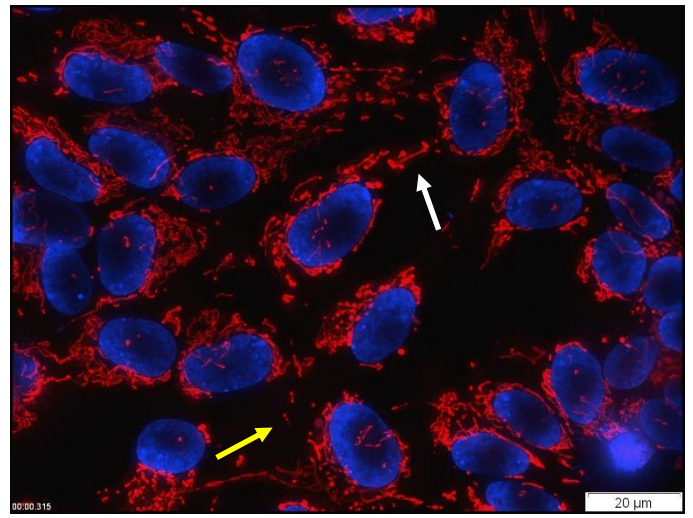
C. *PINK1* siRNA + PQ
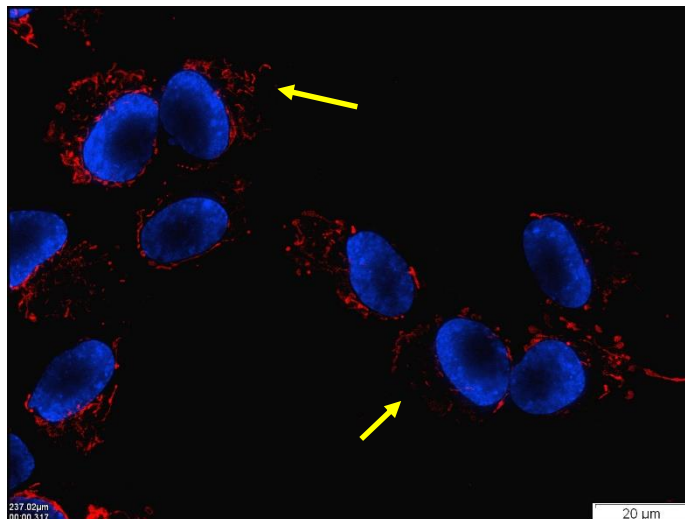
D. Control siRNA + PQ
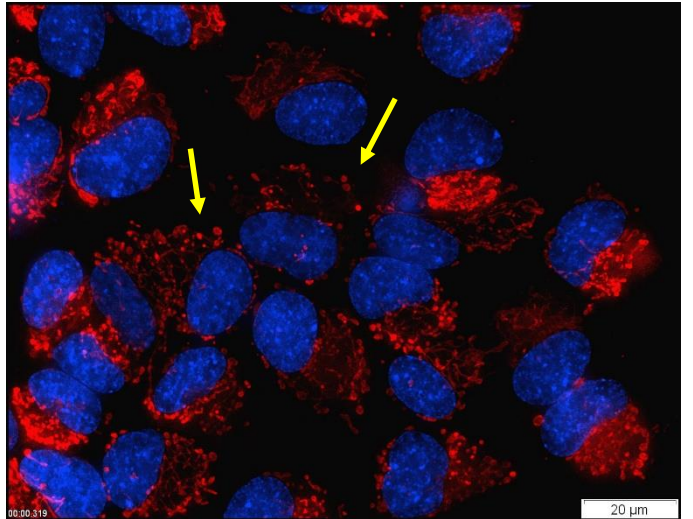
E. *PINK1* siRNA + Curc + PQ
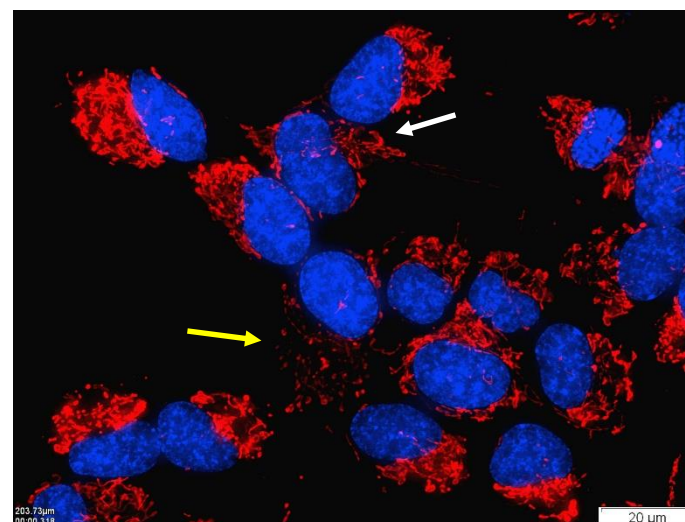
F. Control siRNA + Curc + PQ
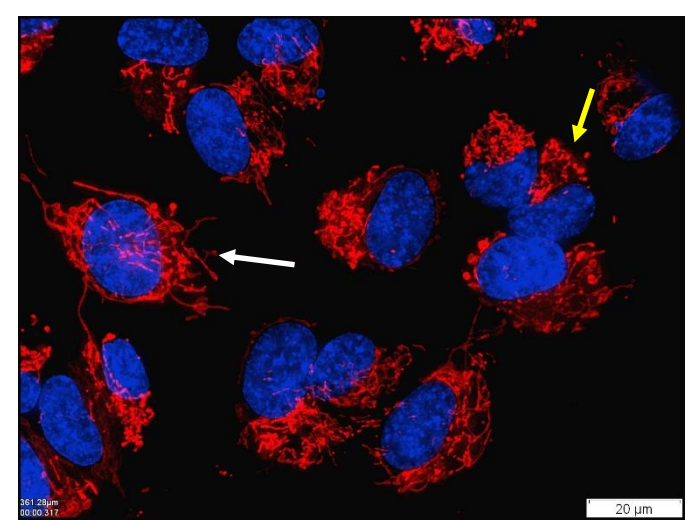
G. *PINK1* siRNA + Curc

H. Control siRNA + Curc

I

J

K
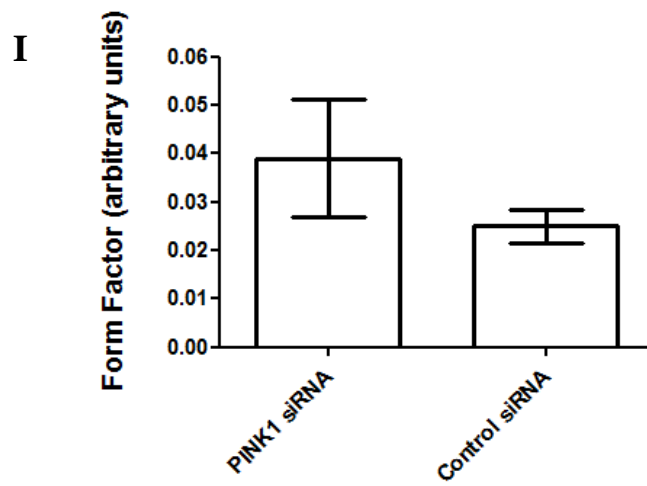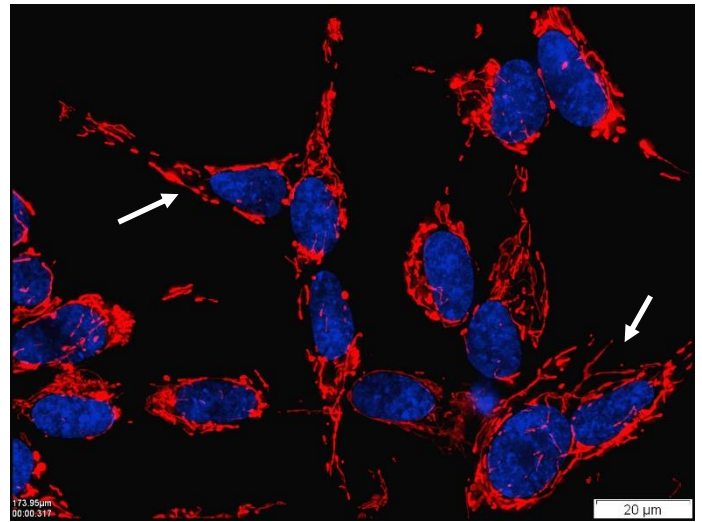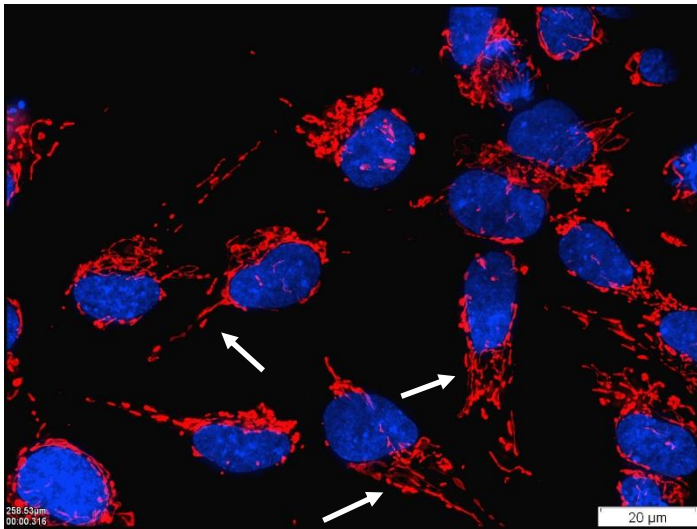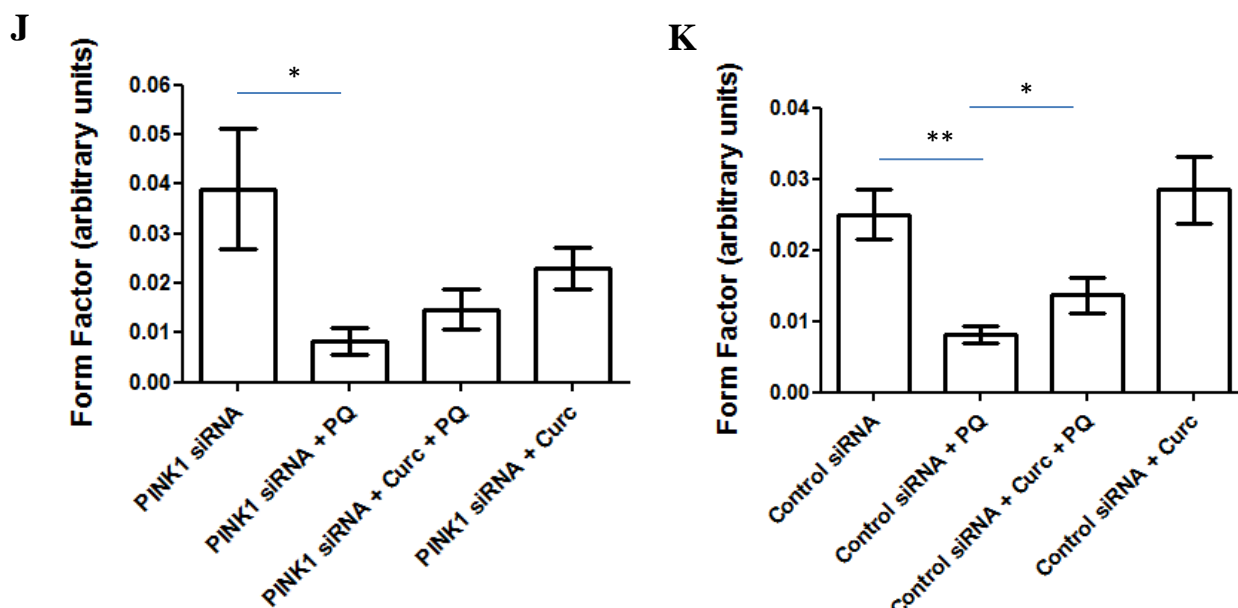
Figure 3.15. Fluorescence microscopy images of SH-SY5Y neuroblastoma cells stained for the nucleus (blue; Hoechst) and the mitochondrial network (red, MitoTracker), and quantification and calculation of form factor in these cells. A-H. Micrographs from all treatment groups. The white arrows represent areas of increased fusion, whereas the yellow arrows indicate areas of increased fragmentation. I. *PINK1* siRNA and control cells did not show significant changes in form factor. J. Paraquat treatment significantly reduced form factor compared to the untreated group in *PINK1* siRNA cells (*$p<0.05$). K. Paraquat treatment significantly reduced form factor in control cells (**$p<0.01$), and this was rescued by curcumin pre-treatment (*$p<0.05$). N=3. PQ, paraquat; Curc, curcumin

3.7.2. Aspect ratio

Aspect ratio is defined as the measurement of the ratio between the major and minor axis of the ellipse equivalent to the mitochondria, and is an indication of mitochondrial length. The higher the aspect ratio, the longer the mitochondrial length. *PINK1* siRNA cells had a significantly increased aspect ratio compared to control cells (Figure 3.16A, $p=0.0091$). In *PINK1* siRNA and control siRNA cells, paraquat treatment alone significantly decreased the aspect ratio compared to the untreated groups (Figure 3.16B, C, $p<0.001$). Pre-treatment with curcumin did not affect the aspect ratio in comparison with the paraquat only group in both *PINK1* knock down and control cells (Figure 3.16B, C). In *PINK1* siRNA cells, curcumin treatment alone significantly reduced the aspect ratio compared to the untreated

group (Figure 3.16B, p<0.001). However, in the control cells curcumin treatment alone significantly increased the aspect ratio compared to the untreated group (Figure 3.16C, p<0.05).
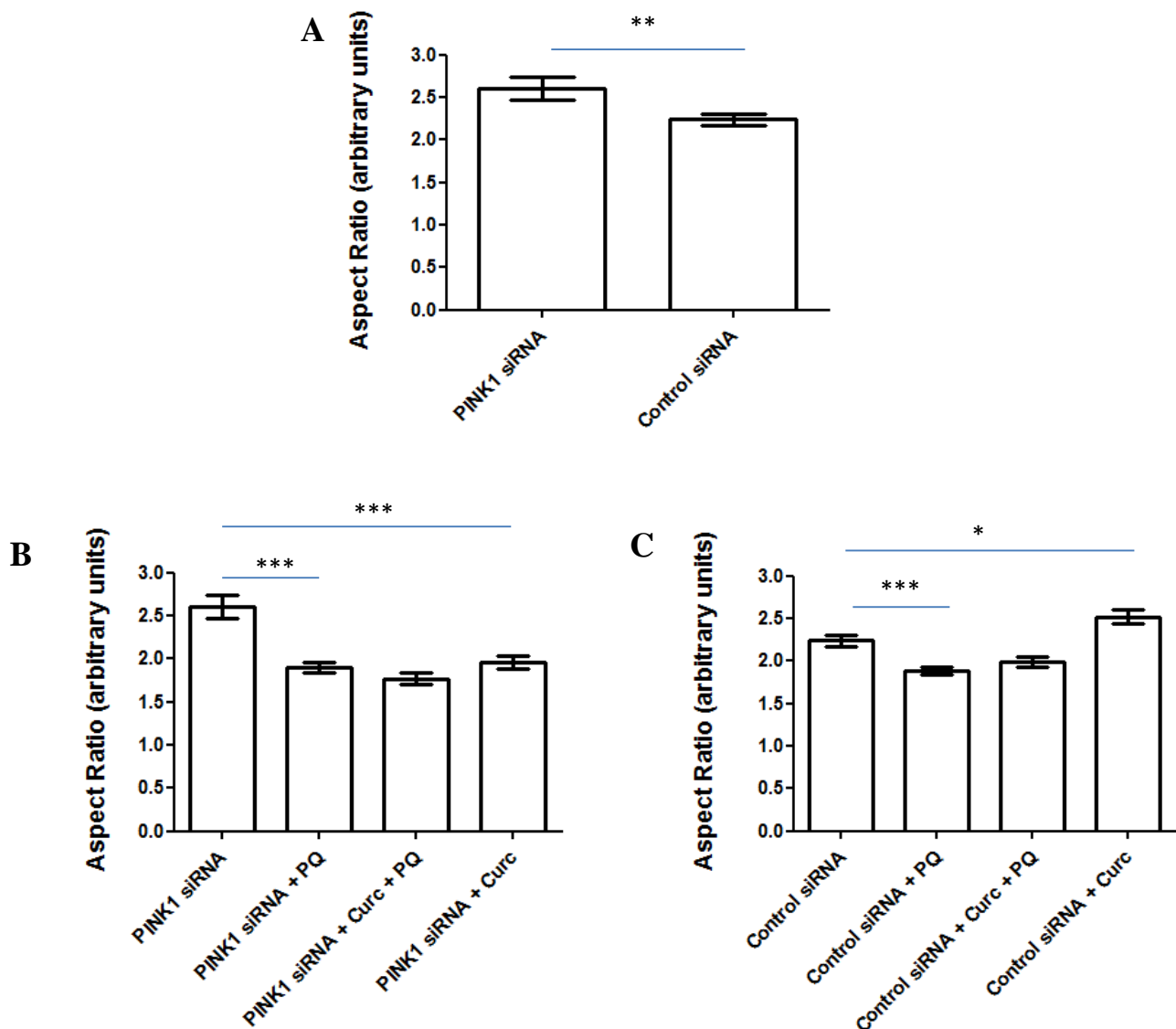
Figure 3.16. Quantification and calculation of aspect ratio in SH-SY5Y neuroblastoma cells. A. *PINK1* siRNA cells had a significantly increased aspect ratio compared to control cells (**p=0.0091). B. Paraquat-only and curcumin-only groups had significantly reduced aspect ratio compared to the untreated group in *PINK1* siRNA cells (***p<0.001). C. Paraquat-only group had significantly reduced aspect ratio compared to the untreated group in control cells (***p<0.001), and the curcumin-only group was significantly increased compared to the untreated group (*p<0.05). PQ, paraquat; Curc, curcumin

In summary, whilst there were no changes in the degree of branching in *PINK1* siRNA cells compared to control cells, the aspect ratio was significantly increased. The aspect ratio measures the mitochondrial length, so if the *PINK1* siRNA cells had longer mitochondria, this might have an effect on ATP production and oxidative stress levels. Paraquat-treated cells were more fragmented, and had lower aspect ratios, and were therefore shorter in length. Curcumin treatment resulted in significantly increased aspect ratio in control cells, and significantly decreased aspect ratio in *PINK1* siRNA cells. These results indicate that curcumin may have an effect on the mitochondrial length, and that this effect may differ in the presence or absence of PINK1.

3.8.   Autophagic flux

As previously described in the Materials and Methods, Section 2.9, autophagic flux is measured by assessing the difference in the levels of two markers of autophagy (LC3-II and p62), in the presence or absence of BafA1, an inhibitor of autophagosomal and lysosomal fusion. If LC3-II and p62 is increased after BafA1 treatment, there is an accumulation of autophagosomes, which is indicative of an increase in autophagic flux and the rate of clearance via autophagy is increased. If LC3-II is decreased after BafA1 treatment, then autophagic flux is decreased and there is a slower rate of autophagy and clearance of damaged organelles and proteins from the cell. Western blots were performed using both LC3-II and p62 antibodies in the presence and absence of BafA1. Differences in intensities were calculated, and normalised to the loading control GAPDH. The blot images are shown in Figure 3.17, A and B.

-BafA1   **+BafA1**

A PINK1 siRNA   Control siRNA   **B**   PINK1 siRNA   Control siRNA

p62, 62kDa

GAPDH, 37kDa

LC3-I, 14kDa
LC3-II, 16kDa

UT   PQ   Curc Curc   UT   PQ   Curc Curc   UT   PQ   Curc Curc   UT   PQ   PQ + Curc
           +PQ   +PQ   +PQ   Curc
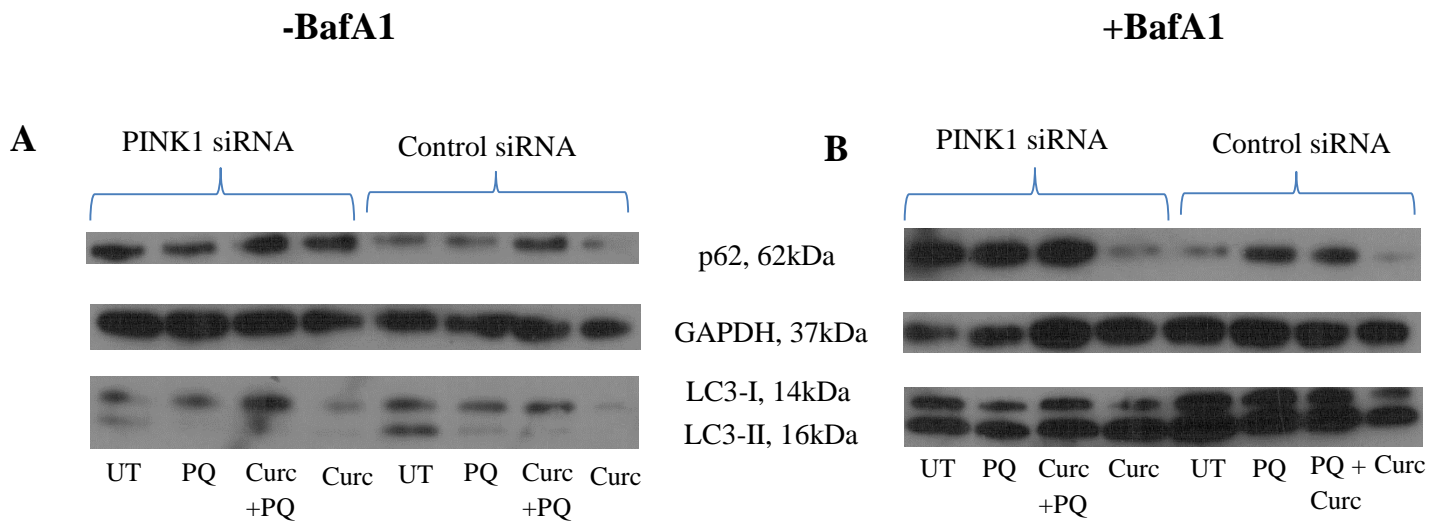
Figure 3.17. Western blot images detecting markers for autophagy p62 (62kDa, top panel) and LC3-II (16kDa, bottom panel), and the loading control GAPDH (37kDa, middle panel). A. Samples were not treated with BafA1 (-BafA1). B. Samples were treated with 100nM BafA1 for 2 hours (+BafA1). UT, untreated; PQ, paraquat; Curc, curcumin; BafA1, Bafilomycin A1

3.8.1.   Detection of LC3-II

Blots were quantified, and the difference between before (-BafA1) and after (+BafA1) treatment was calculated and normalised to the loading control GAPDH. Results comparing *PINK1* siRNA cells to control cells showed that LC3-II levels were significantly increased in *PINK1* siRNA cells (Figure 3.18A, $p < 0.05$).

Paraquat treatment in *PINK1* siRNA and control cells did not result in changes in LC3-II levels (Figure 3.18B, C). The concentration of paraquat added to the cells may be too low for there to be an effect on autophagic flux. Curcumin pre-treatment had no effect on the *PINK1* siRNA cells (Figure 3.18B), but significantly increased autophagic flux compared to the paraquat-only group in the control cells (Figure 3.18C, $p < 0.01$). Curcumin treatment alone also significantly increased LC3-II compared to the untreated group in control cells (Figure 3.18C, $p < 0.001$). These results could suggest that curcumin can only successfully induce autophagy in the presence of PINK1. Furthermore, this could indicate an

induction of autophagy when cells are treated with curcumin, and will be discussed in greater detail in the Discussion section.
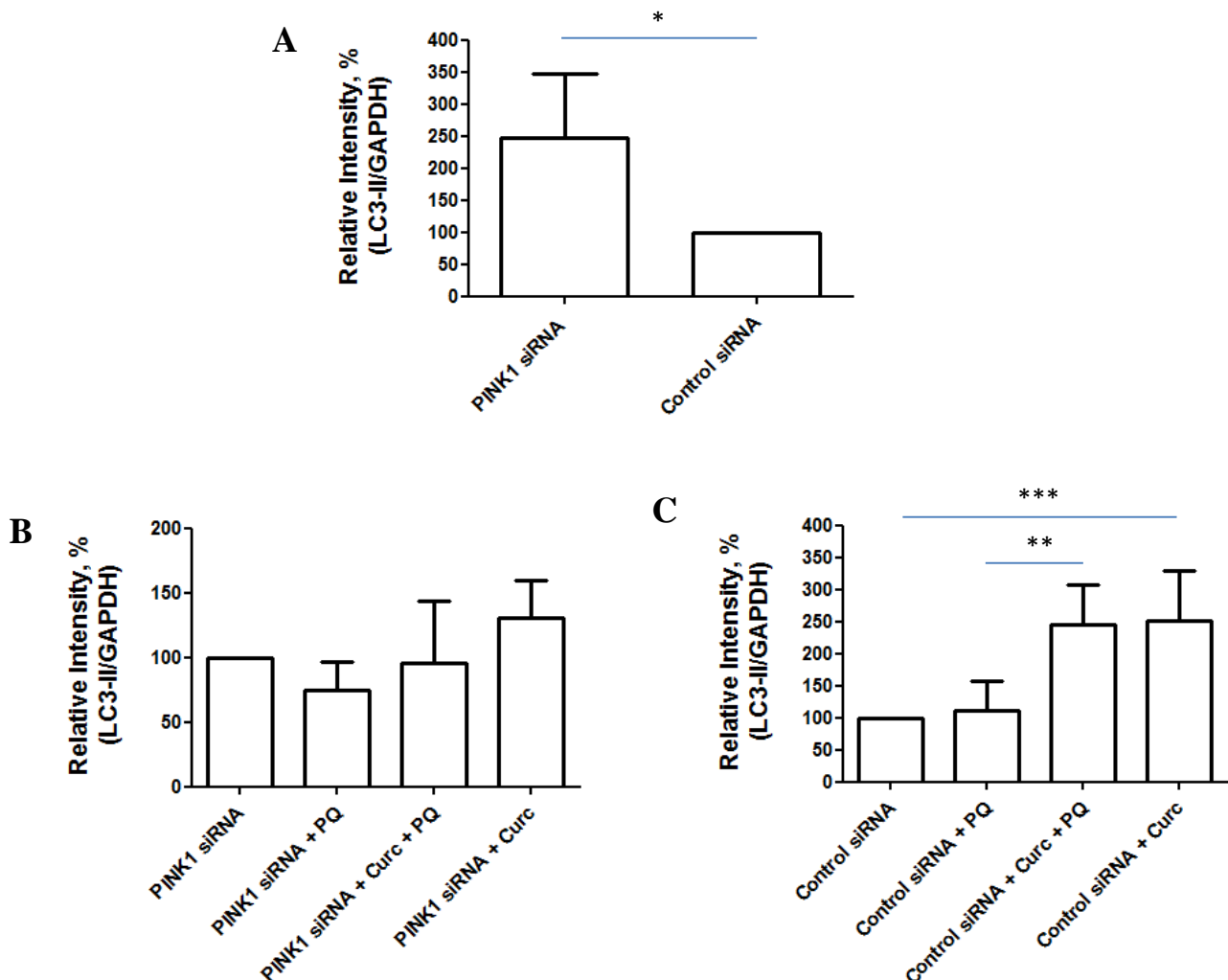
Figure 3.18. Quantification of LC3-II Western blots. Blots were quantified, and the difference between before (-BafA1) and after (+BafA1) treatment was calculated and normalised to the loading control GAPDH. A. Normalised results show LC3-II, and therefore autophagic flux, is significantly increased in *PINK1* siRNA cells compared to control cells (*p=0.0152). B. No significant differences in autophagic flux were observed across treatment groups in *PINK1* siRNA cells. C. In control cells, pre-treatment with curcumin prior to paraquat significantly increased LC3-II levels compared to the paraquat-only treated group (**p<0.01). Also, curcumin treatment alone resulted in significantly increased LC3-II levels compared to the untreated group (***p<0.001). PQ, paraquat; Curc, curcumin

3.8.2. Detection of p62

Results from the p62 blots showed a significantly increased level of p62 in the *PINK1* siRNA cells compared to the control cells (Figure 3.19A, p<0.01). This result indicates that autophagic flux was increased in *PINK1* siRNA cells, and confirms the result shown from the LC3-II blots. In *PINK1* siRNA cells, there was a trend decrease in p62 levels after curcumin pre-treatment, although this was not significant (Figure 3.19B). In control cells, there was also no significance across treatment groups (Figure 3.19C).
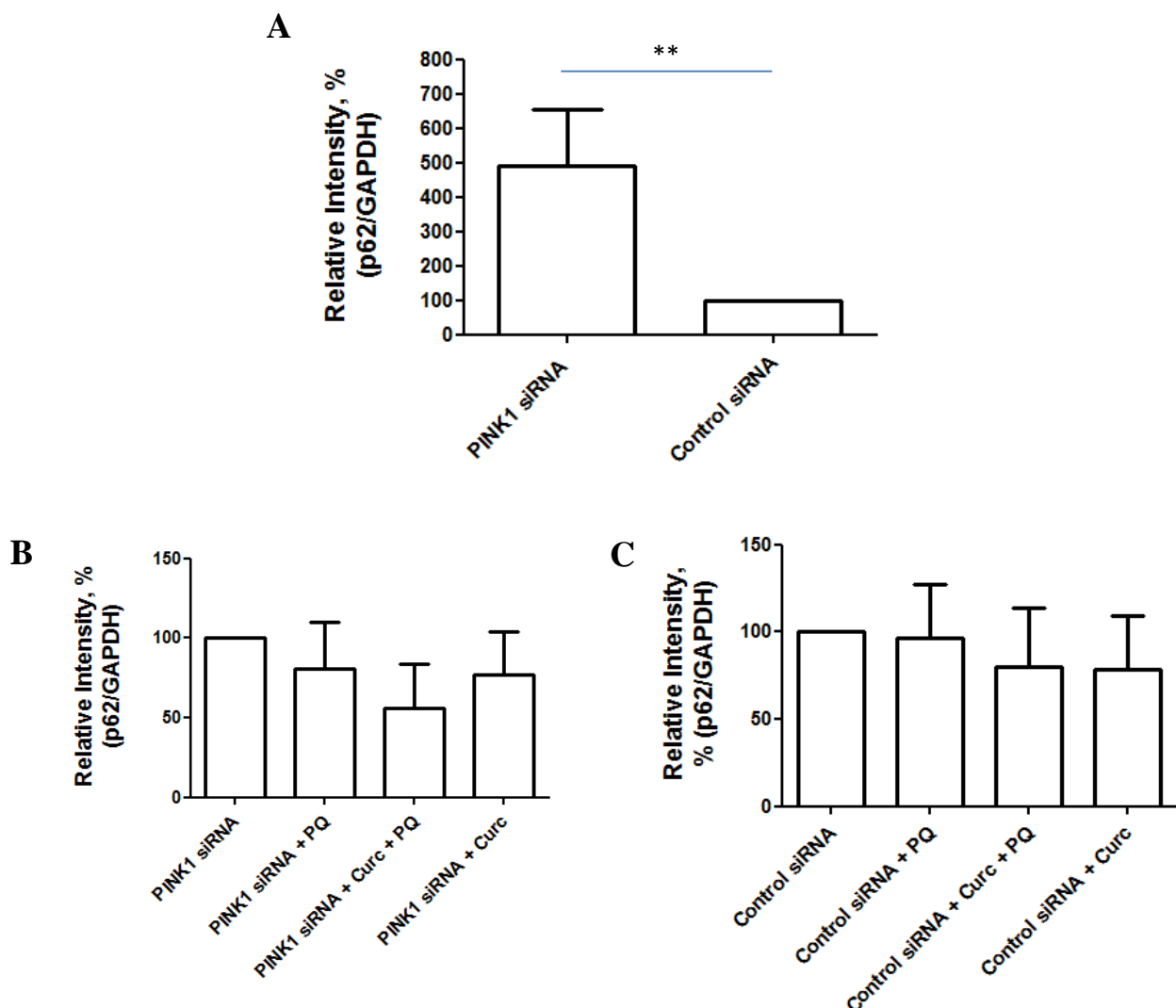
Figure 3.19. Quantification of p62 Western blots. Blots were quantified, and the difference between before (-BafA1) and after (+BafA1) treatment was calculated and normalised to the loading control GAPDH. A. Normalised results show p62, and therefore autophagic flux, is significantly increased in *PINK1* siRNA cells compared to control cells (**p=0.002). B, C. There were no significant changes in the levels of p62 across all treatment groups in *PINK1* siRNA cells (B) or in control cells (C). PQ, paraquat; Curc, curcumin

It is thought that p62 may be a less reliable as a marker for autophagy than LC3-II, as it is not solely functional at the autophagy process. It may be interesting to identify the other pathways in which p62 is active. Based on this observation, we believe that LC3-II is a more definitive marker for autophagic flux. In summary, we observed an increased autophagic flux in *PINK1* siRNA cells compared to control cells. This may be a compensatory mechanism through which clearance of the accumulated damaged proteins and mitochondria is increased. Interestingly, curcumin treatment also resulted in an increase in autophagic flux in control cells, possibly to prevent cell death and maintain a healthy cellular environment.

Section B: Copy number variation study on genomic DNA from PD patients

3.9. Analysis of copy number variation in PD patients

Given the interesting findings observed in the first part of this study, the second part of the study focused on identifying South African PD patients with CNV changes in the *PINK1* gene, as comparison of our findings in a siRNA model to that of a patient-derived cellular model would be an important and necessary next step. CNV includes rearrangements such as deletions, duplications or triplications that potentially lead to null mutations. Patients were screened using the MLPA technique and all putative CNV were verified using qRTPCR.

In a previous study, 229 South African PD patients were analysed for exonic rearrangements using the MLPA technique (Haylett et al., 2012; Keyser et al., 2009). No *PINK1* CNV changes were found in any of these patients. In the present study, an additional 210 PD patients from different South African ethnic groups, including White, Afrikaner, Black, Mixed Ancestry and Indian, were recruited. This section will focus on the mutations found from the MLPA analysis and whether or not these mutations were false positives (which was determined by qRTPCR verification).

3.9.1. Mutations observed after MLPA technique

Two MLPA kits were used, P051 and P052 (For a full list of the probes for each exon in both kits, refer to Appendix III, taken from www.mlpa.com). Initial analysis showed a large number of individuals with putative CNV mutations in *PINK1* exons 1, 4, 5 and 8, *DJ-1* exons 1, 3 and 7, *PARK2* exons 4, 5, 9 and 11, and *SNCA* exon 5. However, after verification of these mutations by either repeating the MLPA analysis or performing qRTPCR to determine whether these mutations were true or false positives, it was found that the original putative mutations observed were no longer present – revealing that the MLPA method produced a number of false positive results. One true heterozygous *PARK2* exon 4 deletion was confirmed in patient 96.69. Where possible, samples with known CNV changes (detected in previous studies; Keyser et al., 2009) were included in the qRTPCR verification experiments as positive controls. An example of the results from a qRTPCR run on *SNCA* exon 5 is shown in Figure 3.20. Due to the observation that the false positives continuously occurred in the same exons, it was hypothesized that there are SNPs at these probe positions affecting the binding of the probes, thus leading to false positive results (Section 3.9.2).
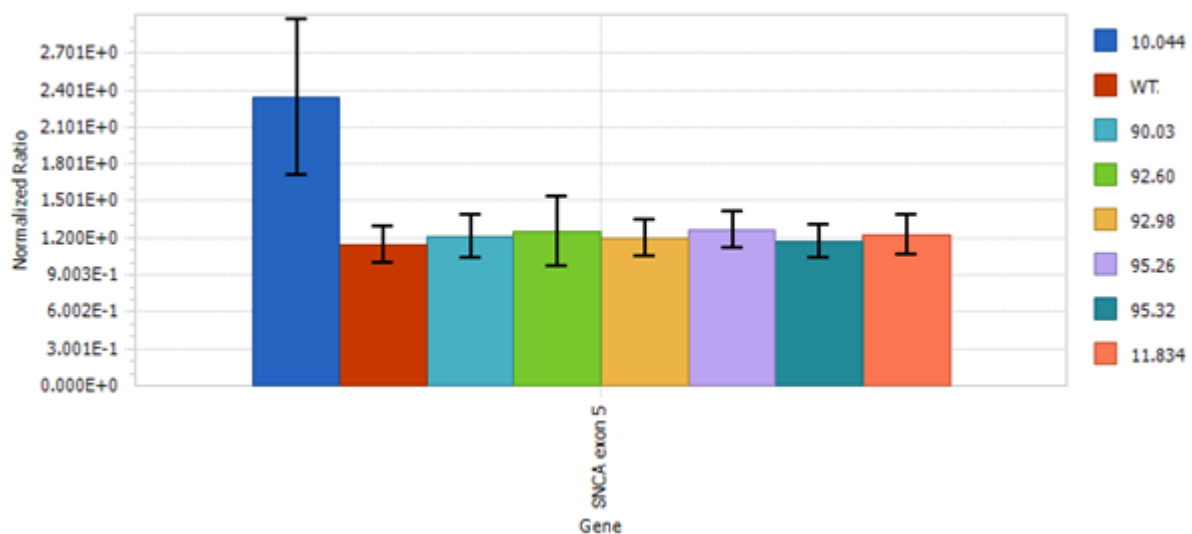
Figure 3.20. Verification of false positives in *SNCA* exon 5 using qRTPCR. Results from qRTPCR indicated that all patients with a query *SNCA* exon 5 mutation did not harbour the mutation (90.03, 92.60, 92.98, 95.26, 95.32, 11.834). The wild type control (WT, red) had the same ratio compared to all patients. The positive control sample, 10.044 (dark blue), is known to harbour a *SNCA* exon 5 triplication. qRTPCR, quantitative real time PCR

The heterozygous deletion in *PARK2* exon 4 was observed in patient 96.69 in both P051 (Figure 3.21A, ratio = 0.55) and P052 (Figure 3.21B, ratio = 0.41) probe mixes. This result was verified using qRTPCR (Figure 3.21C). Positive controls included a PD patient homozygous for a *PARK2* exon 4 deletion (patient 56.45, dark blue), and a control heterozygous for *PARK2* exon 4 deletion (patient 67.23, red). As shown in Figure 3.21C, patient 96.69 (light blue) revealed relative expression of *PARK2* exon 4 similar to that of the heterozygous control 67.23, thus confirming the presence of a heterozygous deletion in *PARK2* exon 4 in patient 96.69. Sanger sequencing was performed in all 12 *PARK2* exons to determine the presence of a possible point mutation, but no pathogenic polymorphisms were found.

C
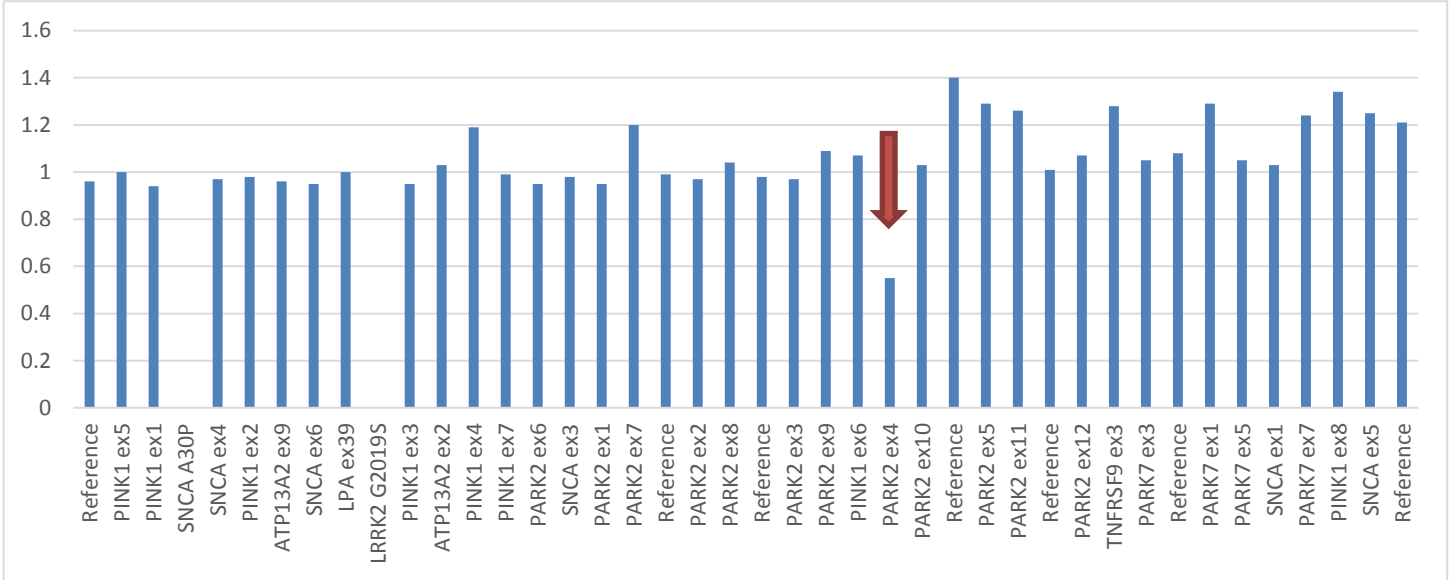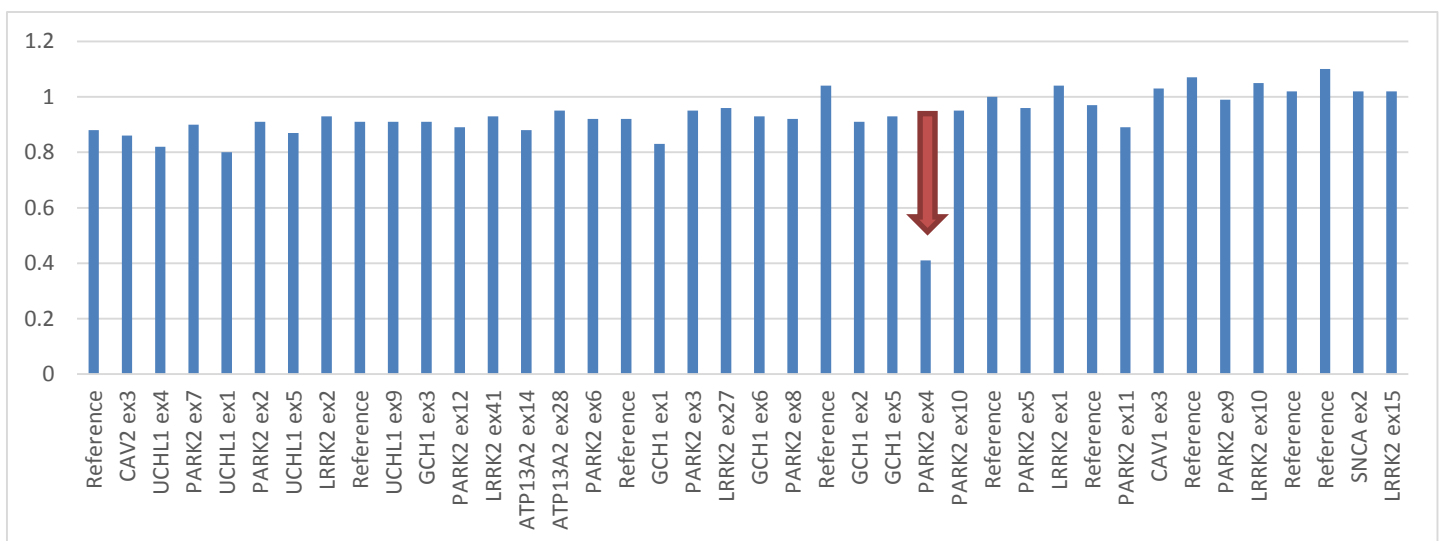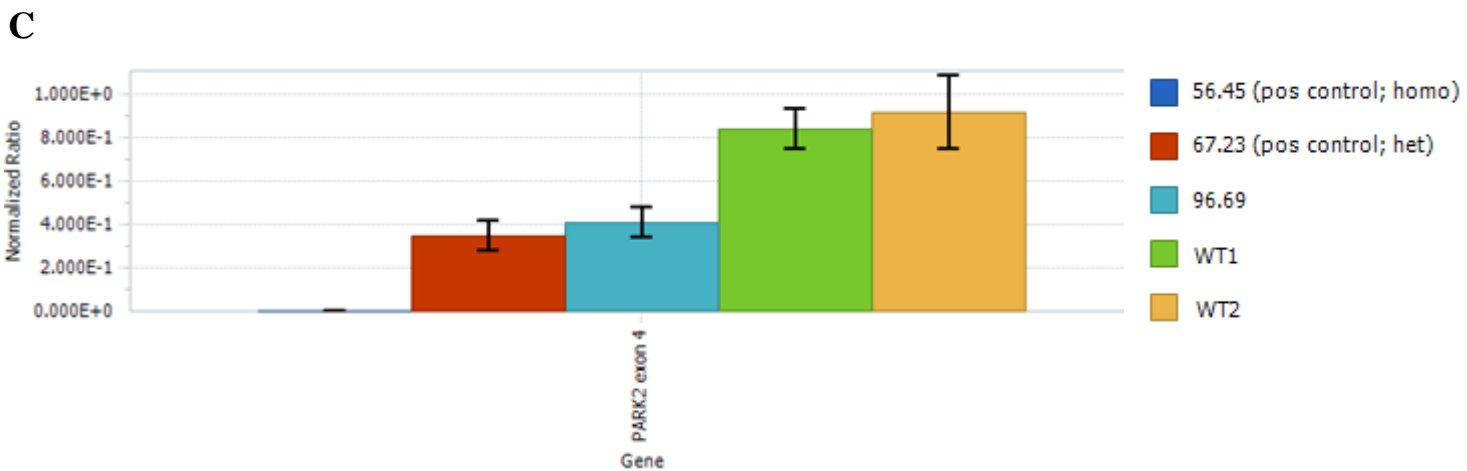
Figure 3.21. MLPA results from patient 96.69 indicate a heterozygous deletion of *PARK2* exon 4. A, B. Graphs indicating the ratio values of all exons in Mix 1 P051 (A) and Mix 2 P052 (B), with an arrow showing the deletion (ratio value < 0.6) for *PARK2* exon 4 in both mixes. C. Real time PCR verified that the mutation for patient 96.69 (light blue) was present in 1 allele, similar to that of a heterozygous control 67.23 (red). Pos, positive; homo, homozygous; het, heterozygous

3.9.2. Sequencing based on common false positives

A large number of putative mutations in particular exons across every MLPA run and various samples led us to the hypothesis that the patients may harbour non-pathogenic SNPs at the site of the primers for these specific exons. These frequent occurrences are summarised in Table 3.1, and include *PARK2* exons 4, 5, 9 and 11, *SNCA* exon 5 and *PINK1* exon 1. The ethnic breakdown was also indicated, as we believed that the unique ethnic background in our cohort (particularly in black and mixed ancestry patients) may have caused these results. Interestingly, the majority of *PARK2* exon 5 putative mutations did occur in mixed ancestry and black individuals, and the remainder appeared spread across all ethnic groups except Indian.

Table 3.1. Table indicating the number of patients associated with putative mutations in several exons, as well as the percentage ethnic breakdown

Exon	Mix	Number of patients with putative mutation		Ethnic group (%)				
		Deletion	Duplication	W	Af	MA	B	I
PARK2 ex5	P051	13	-	0	0	69.2	30.7	0
SNCA ex5	P051	2	9	36.4	36.4	0	27.2	0
PINK1 ex1	P051	2	3	40	40	0	20	0
PARK2 ex4	P052	4	9	46.1	15.4	30.8	7.7	0
PARK2 ex9	P052	-	5	40	0	40	20	0
PARK2 ex11	P052	1	4	60	0	20	20	0

W, White; Af, Afrikaner; MA, Mixed Ancestry; B, Black; I, Indian

Sequencing performed on select patient samples indicated that there were no polymorphisms observed in *SNCA* exon 5, *PINK1* exon 1 and *PARK2* exon 4, 9 and 11. It was however found that patients with a *PARK2* exon 5 deletion in P051 had a common polymorphism A574C in the annealing site of the MLPA P051 probe for *PARK2* exon 5, resulting in an M192L amino acid change (Figure 3.22). This would explain why the exon was not able to be amplified in these patients.
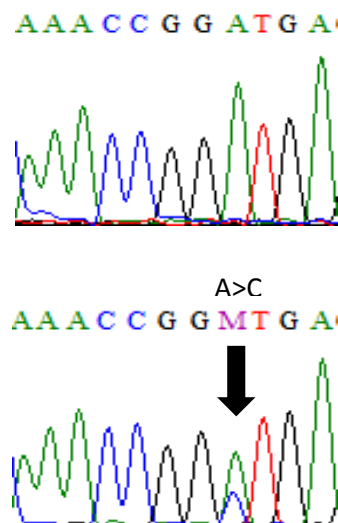
Figure 3.22. Chromatogram illustrating the M192L polymorphism in *PARK2* exon 5 that caused false positive results in the MLPA analysis.

In summary, analysis using MLPA did not reveal any *PINK1* CNV mutations in a total of 210 South African PD patients. A number of false positive mutations were identified that were not verified on repeated MLPA runs or qRTPCR. A common polymorphism M192L *PARK2* exon 5 was identified in a number of patients resulting in false positive deletions in kit P051. One patient was shown to harbour a heterozygous deletion in *PARK2* exon 4.

Chapter 4: Discussion

Page

In the present study, we aimed to create a cellular model of PD by decreasing the expression of the PD-causing gene *PINK1*. In doing so, this would enable us to study the role of PINK1 in the cell, as well as the effect of curcumin on this model. PINK1 was successfully knocked down using siRNA, and this was validated at both gene and protein expression levels. In summary, decreased PINK1 expression resulted in a number of cellular and mitochondrial alterations which included:

- Decreased MMP
- Decreased mitochondrial respiration and ATP production
- Decreased glycolytic capacity
- Increased apoptosis
- Increased autophagic flux
- Decreased cell viability

These results indicate the vital role of PINK1 in the upkeep of a healthy cellular environment, as well as in the maintenance of functional mitochondria. In the event of a mutation resulting in decreased PINK1 protein function, there is an accumulation of damaged mitochondria, which may ultimately result in neuronal cell death.

When studying the effect of curcumin on this model of PD, we attempted to answer a number of questions. These include, does curcumin protect these cells from cell death? Does curcumin play a role in mitochondrial maintenance? What is the particular mechanism behind the action of curcumin? How will curcumin act in the presence and absence of an additional stressor? Our results show that in general, paraquat or curcumin treatment on their own had the same effect on control or *PINK1* siRNA cells (Table 4.1). However, marked differences between the control and *PINK1* siRNA cells were observed with curcumin pre-treatment followed by paraquat exposure. These findings can be summarized as follows:

- Curcumin rescued the MMP in both control and *PINK1* siRNA cells after paraquat treatment
- Curcumin increased maximal respiration in both control and *PINK1* siRNA cells
- Curcumin increased spare respiratory capacity only in control cells with paraquat treatment

- Curcumin resulted in a less fragmented mitochondrial network only in control cells with paraquat treatment
- Curcumin resulted in decreased apoptosis in both control and *PINK1* siRNA cells
- Curcumin resulted in increased autophagic flux in control cells with paraquat treatment
- Curcumin increased the number of viable cells in culture, but this was only seen in control cells and not *PINK1* siRNA cells, and only with paraquat treatment

Therefore, in summary, our findings show that curcumin is able to 'rescue' many of the damaging effects of paraquat but some of these protective effects were seen only in the healthy cells and not in the *PINK1* knock down cells.

Table 4.1. Summary of the results observed in paraquat- and curcumin-treated control and *PINK1* siRNA cells.

	Control cells			*PINK1* siRNA cells		
	Paraquat (compared to untreated)	Curcumin + Paraquat (compared to paraquat)	Curcumin (compared to untreated)	Paraquat (compared to untreated)	Curcumin + Paraquat (compared to paraquat)	Curcumin (compared to untreated)
Mitochondrial membrane potential	Decrease	Increase	No change	Decrease	Increase	No change
Mitochondrial Respiration – Basal	Increase	Increase	No change	No change	No change	No change
Maximal	No change	Increase	Increase	No change	Increase	Increase
ATP production	No change	No change	No change	No change	No change	No change
Spare respiratory capacity	No change	Increase	No change	No change	No change	No change
Glycolysis test – Basal	No change	No change	No change	Decrease	Increase	Decrease
Glycolysis	No change	No change	No change	No change	No change	No change
Glycolytic capacity	No change	No change	No change	No change	No change	No change
Glycolytic reserve	No change	No change	No change	No change	No change	No change
Mitochondrial network - form factor	Decrease	Increase	No change	Decrease	No change	No change
Mitochondrial network - aspect ratio	Decrease	No change	Increase	Decrease	No change	Decrease
Apoptosis (as measured by cleaved PARP)	Increase	No change	Decrease	Increase	Decrease	Decrease
Apoptosis (as measured by Caspase 3)	No change	Decrease	Decrease	No change	Decrease	Decrease
Autophagic flux – LC3-II	No change	Increase	Increase	No change	No change	No change
Autophagic flux - p62	No change	No change	No change	No change	No change	No change
Cell viability	Decrease	Increase	No change	Decrease	No change	No change

4.1. Effects observed in a *PINK1* siRNA model of PD

Approximately 11 years ago, Valente and colleagues discovered that mutations in *PINK1* were a cause of hereditary early onset PD (Valente et al., 2004). Since then, numerous studies have been performed to further our understanding of PINK1, and to date it has been established as a core protein (either directly or indirectly) in the machinery that protects the cells from death – the UPS, MQC and autophagy. When *PINK1* is mutated, resulting in either an absent or a misfolded, dysfunctional protein, these processes are drastically affected and severe consequences ensue.

Previous studies analysing mitochondrial function in SH-SY5Y cells after siRNA-mediated knock down of *PINK1* revealed similar results to our study. MMP was found to be reduced when PINK1 was absent, resulting in depolarised mitochondria, a subsequent drop in proton movement and decreased ATP production (Exner et al., 2007; Gautier et al., 2008; Grünewald et al., 2009; Vives-Bauza et al., 2010; Wood-Kaczmar et al., 2008). In terms of mitochondrial respiration, whilst our results indicated decreased mitochondrial respiration across all measurements (basal respiration, ATP production, maximal respiration, spare respiratory capacity), other studies have presented conflicting data. A study on iPSCs derived from individuals carrying *PINK1* mutations observed increased basal respiration in *PINK1* mutant cells (Cooper et al., 2012), and a second study in patient-derived fibroblasts with *PINK1* mutations observed no defects across all areas of mitochondrial respiration (Siuda et al., 2014). They hypothesized that there may be a compensatory mechanism preventing dysfunctional respiration. The reason for these contrasting results may be the different cell types used, or possibly technical differences with different XF Analysers. To date, very few studies have analysed OCR in a PINK1-deficient model of PD, and it is clear that mitochondrial respiration needs to be studied to a greater extent in order to further our understanding of the role of PINK1.

After decreasing the expression of PINK1 in SH-SY5Y cells, we observed decreased cell viability and increased apoptosis, which has also been found in previous studies using a similar approach and confirmed in other cell lines including M17, HeLa and PC12 cells, and animal models of PD (Deng et al., 2005; Gegg et al., 2009; Geisler et al., 2010b; Poole et al., 2008; Sandebring et al., 2009; Sha et al., 2009; Wood-Kaczmar et al., 2008). It is thought that the damage to the mitochondria results in increased cell death. The present study also observed elevated autophagic flux in the PINK1-deficient cells. Based on this finding, we hypothesized that when the cells become damaged and start to die, levels of

autophagy might increase in an attempt to rid the cell of the dysfunctional proteins/ mitochondria, thus acting as a compensatory mechanism.

In agreement with this hypothesis, Dagda and colleagues observed an increase in the number of AVs, increased LC3-II levels and autophagic flux in PINK1-deficient SH-SY5Y cells (Dagda et al., 2009). Various ultrastructural studies have shown increased lysosomal content in *PINK1* knock down cells (Marongiu et al., 2007; Wood-Kaczmar et al., 2008), and these results were also found to occur in *Drosophila*, which observed increased basal autophagy in *PINK1* mutant flies (Liu and Lu, 2010). This suggests that autophagy may be upregulated in an attempt to protect the cell against damage caused by the absence of PINK1. Interestingly, levels of parkin have been shown to be increased in some *PINK1* knock down cell lines, and may also be involved in this compensatory mechanism (Cherra et al., 2010; Chu, 2010). It may be possible that when PINK1 expression is reduced and the amount of dysfunctional mitochondria increases, parkin initiates the autophagic response in an attempt to clear the mitochondria and reduce cell death.

In contrast, other studies have found decreased levels of autophagy in the absence of PINK1. Gegg and colleagues used a similar 12-day knock down approach to our study, and revealed a reduced autophagic flux in their model (Gegg et al., 2010). Another study that reduced *PINK1* expression in SH-SY5Y cells also revealed decreased autophagy, and this was increased when *PINK1* was overexpressed (Michiorri et al., 2010). The different observations in PINK1-deficient cells may be due to different experimental settings and knock down protocols. Nevertheless, it is still essential that the role of PINK1 and parkin in autophagy be further studied using various models and experimental designs. Autophagy is a highly complex process, and it could be that current methods of detecting it are not accurate enough. Once it has been established how PINK1 regulates autophagy, it could result in a better understanding of other functions of PINK1, such as its role in fission and fusion regulation.

4.2. The role of curcumin in cell viability and apoptosis

This study investigated the effect of curcumin in our cellular model of PD, and to our knowledge this was a novel aspect of our research that has not yet been studied to date. Furthermore, we tested the effect of curcumin in the presence and absence of a stressor. A particularly interesting result was observed when curcumin pre-treatment protected the PINK1-deficient and control cells exposed to paraquat from apoptosis (Table 4.1).

Various *in vivo* and *in vitro* models of PD have also shown that curcumin protects neurons and other cells from cell death. In a 6-OHDA rat model, Zbarsky and colleagues revealed that curcumin treatment protected neurons in the SNc from apoptosis, and this led to improved striatal dopamine levels (Zbarsky et al., 2005). A cellular model of 6-OHDA in MES23.5 cells also found that curcumin reduced cytotoxicity and restored cell viability (Wang et al., 2009). Curcumin prevented MPTP-induced injuries to dopaminergic neurons in an MPTP mouse model of PD (Pan et al., 2012), and similar effects were observed in cellular models. In PC12 cells, curcumin prevented cytochrome c release and PARP activation (Raza et al., 2008), protected MPP^+-induced cytotoxicity and apoptosis (Chen et al., 2006), and reduced A53T α-synuclein-induced cell death (Jiang et al., 2013; Wang et al., 2010). Furthermore, curcumin reduced rotenone-induced cell death in SH-SY5Y cells, and alleviated PD-like symptoms in *Drosophila* (Z. Liu et al., 2013).

To date, there have been several pathways that curcumin has been implicated in that protect cells from damage and death. Curcumin has various molecular targets including growth and transcription factors and their receptors, cytokines, enzymes and genes that regulate apoptosis (Aggarwal et al., 2007b). This causes downstream effects on pathways such as the JNK pathway. JNK is a member of the mitogen-activated protein kinase (MAPK) family, and is activated by environmental stress and apoptotic agents. When upregulated, JNK causes increased cell death by translocating Bax to the mitochondria, resulting in the release of cytochrome c. The JNK pathway has been associated with dopaminergic neuronal degeneration, and it has been suggested that inhibitors of this pathway may slow the progression of PD (Mythri and Bharath, 2012). Activation of this pathway occurs via the phosphorylation of JNK1, JNK2 and c-Jun. Pan and colleagues revealed that curcumin inhibited this phosphorylation in an MPTP mouse model of PD, thus diminishing the effects of apoptosis (Pan et al., 2012). Other studies have suggested that JNK may not be a direct target of curcumin, but rather that curcumin interferes with regulators upstream of MAPK, which in turn leads to the unresponsiveness of the JNK cascade (Chen and Tan, 1998; Mythri and Bharath, 2012; Yu et al., 2010).

Pan and colleagues also investigated the effect of curcumin on the Bcl-2/Bax heterodimer, which is the active component for cell death protection (Rezende et al., 2008; Zhang et al., 2004). When Bcl-2 is phosphorylated, it becomes inactive, allowing for the pro-apoptotic protein Bax to be released from the dimer complex (Biswas et al., 2007). Once freed, Bax forms pores on the OMM, resulting in increased mitochondrial membrane permeability and the release of cytochrome c, which promotes apoptosis through the activation of the caspase cascade. By preventing the phosphorylation of Bcl-2, the release

of Bax and induction of apoptosis could also be prevented. In an MPTP-induced mouse model of PD, curcumin was able to attenuate the phosphorylation of Bcl-2 proteins, strengthen the interaction between Bcl-2 and Bax, and prevent Bax translocation to the cytosol (Pan et al., 2012). Other studies have also observed that curcumin was able to induce the overexpression of Bcl-2 proteins, whilst decreasing the levels of Bax in cellular models of PD (Chen et al., 2006; Chen and Tan, 1998). Interestingly, JNK is involved in the regulation of the activation of Bcl-2 family members, further highlighting a role for curcumin in this pathway. Importantly, curcumin's role in preventing apoptosis potentially has significant implications for its use as a neuroprotective agent in the treatment of neurodegenerative disorders.

4.3. Curcumin's role in maintaining healthy mitochondria

When determining the effect of curcumin on mitochondrial function in PINK1-deficient cells, two major findings were observed: i. curcumin increased maximal respiration after paraquat treatment, and ii. curcumin increased MMP in these cells (Table 4.1). The maximum respiratory rate reflects an unstable state in the cells where the addition of a mitochondrial uncoupler stimulates increased respiration. Maximal respiration is indicative of the maximum activity of electron transport and substrate oxidation that is achievable by the cells, and a decrease in maximal respiration is a strong indicator of mitochondrial dysfunction (Brand and Nicholls, 2011). Therefore the observation that curcumin increases the maximal respiratory rate, as well as the MMP, suggests that it plays a role in protection of mitochondrial function in paraquat-induced and PINK1-deficient cells. To our knowledge, this is the second study that has assessed the effect of curcumin on OCR using the XF Analyser, the first of which found that curcumin reversed metabolic defects in breast epithelial cells (Vaughan et al., 2013).

Various studies on different diseases affected by mitochondrial damage have been conducted to determine the effect of curcumin on mitochondrial function. Mythri and colleagues used peroxynitrite (PN), a free radical that mediates complex I injury, to damage mouse brain mitochondria *in vivo* and *in vitro*. When these cells were pre-treated with curcumin, they were protected against PN damage and the decreased MMP, complex I injury and decreased glutathione antioxidant levels were all attenuated (Mythri et al., 2010, Mythri et al., 2007). Furthermore, curcumin increased the activity of all five complexes of the ETC and subsequently decreased mitochondrial dysfunction in rats with renal oxidant damage (Molina-Jijón et al., 2011) and in aluminium-treated rats (Sood et al., 2011). Rats treated with

curcumin prior to reperfusion injury also portrayed increased mitochondrial respiratory capacity and attenuated reperfusion injury damage (González-Salazar et al., 2011).

Studies have shown curcumin to act as a strong antioxidant, capable of reducing the levels of oxidative stress and ROS, and increasing the MMP (Chen et al., 2006; Harish et al., 2010; Zhao et al., 2011). The effects of curcumin on the mitochondria have also been observed in models of PD. Wang and colleagues over-expressed α-synuclein in SH-SY5Y cells which resulted in elevated ROS levels, cytotoxicity and apoptosis. The addition of curcumin protected the cells from these defects (Wang et al., 2010). A second study demonstrated that curcumin prevented damage in a rotenone-induced SH-SY5Y model by reducing levels of ROS (Z. Liu et al., 2013). Our study confirms the role of curcumin in prevention of mitochondrial damage by increasing mitochondrial respiration, and stabilising MMP. Once the mitochondria are protected and functional, this leads to cellular health and reduced cell death.

4.4. Curcumin's role in autophagy

Curcumin treatment resulted in significantly increased autophagic flux in control cells treated with paraquat, but this was not observed in PINK1-deficient cells (Table 4.1). Therefore curcumin plays a role in autophagic induction when cells are under stress (i.e. after the addition of paraquat), but not to the same extent when PINK1 expression is decreased in the cells. This could indicate that the extent of the damage caused to both the mitochondria and the general health of the cell without sufficient levels of PINK1 is too severe to be rescued by curcumin. On the other hand, this could also suggest that curcumin is only able to induce autophagy in the presence of PINK1. To our knowledge, this is the first study to look at the effect of curcumin on autophagy in a *PINK1* knock down cell line. Therefore the action of curcumin on PINK1 will need to be studied further and in greater depth in the future. Other functional assays including the analysis of mitophagy or ROS levels should be performed, and this also needs to be studied in an *in vivo PINK1* knock out model of PD.

Analysis of autophagic flux is currently the gold standard for measuring autophagy. (Nelson and Shacka, 2013). Over the past few years, there has been much debate surrounding the role of autophagy in cells. Whilst some researchers firmly believe that autophagy plays a vital role in cell survival by removing dysfunctional proteins and organelles, others suggest that autophagy is a key promotor of non-apoptotic programmed cell death, by engulfing the cytoplasm. Cell damage and cell death can therefore either result from autophagy being too active, or too inactive (Nelson and Shacka, 2013).

Interestingly, curcumin appears to induce autophagy in most studies, but depending on the cell type and disease it can either cause autophagic cell death or cell survival.

Curcumin was initially thought to have anticarcinogenic properties when it induced cell death in malignant cells, but not healthy cells (Karunagaran et al., 2005). Over the past decade, studies have shown that curcumin induces cell death through the induction of autophagy, and this has been observed in hepatocellular carcinoma cells (Qian et al., 2011), colon cancer cells (Basile et al., 2013; Lee et al., 2011), malignant glioma cells (Zhuang et al., 2012), leukaemia cells (Jia et al., 2009; Wu et al., 2011) and oesophageal cancer cells (O'Sullivan-Coyne et al., 2009). Despite this evidence, curcumin-induced autophagy appears to only enhance cell death in certain tumour types, whilst mediating chemotherapeutic resistance in others (Wilken et al., 2011). A study performed on colon cancer stem cells revealed that curcumin induced proliferation and autophagic survival, permitting long term persistence of colorectal cancer (Kantara et al., 2014).

The predominant consensus suggests that autophagy triggers cell survival in neurodegenerative disorders rather than autophagic cell death. Maintenance of proper autophagic function is critical to providing neuroprotection to non-dividing neuronal cells, as increased autophagic flux results in an increased rate of clearance of damaging cellular materials and thus the regulation of a healthy cellular environment (Harris and Rubinsztein, 2012; Nelson and Shacka, 2013). In our study, we observed increased autophagic flux in curcumin-treated paraquat-induced cells, suggesting that autophagy resulted in cell survival rather than cell death. Very few studies have been conducted on the effect of curcumin on autophagy in PD. Jiang and colleagues overexpressed mutant A53T α-synuclein in SH-SY5Y cells which resulted in impaired autophagy (Jiang et al., 2013). Curcumin treatment reduced A53T accumulation, recovered autophagy, and also resulted in downregulation of the mTOR (mammalian target of rapamycin)/ p70S6K (p70 ribosomal protein S6 kinase) pathway. A study on APP/PS1 double transgenic AD mice also showed that curcumin decreased mTOR expression, thus enhancing autophagy and resulting in increased clearance of Aβ (Wang et al., 2014). mTOR is a protein kinase that acts as a key regulator of autophagy. When active, mTOR inhibits autophagy, but when inactivated by rapamycin or nutrient starvation, autophagy is induced. Therefore by inhibiting the mTOR pathway, curcumin allows for induction of autophagy.

A summary of the results from this section is depicted in Figure 4.1. Paraquat exposure to cells with either healthy PINK1 protein (control) or absent/ mutant PINK1 (*PINK1* siRNA) had a negative effect,

and resulted in mitochondrial dysfunction and cell death. Pre-treatment with curcumin, however, resulted in a rescue effect on these cells, as shown in Figure 4.1.
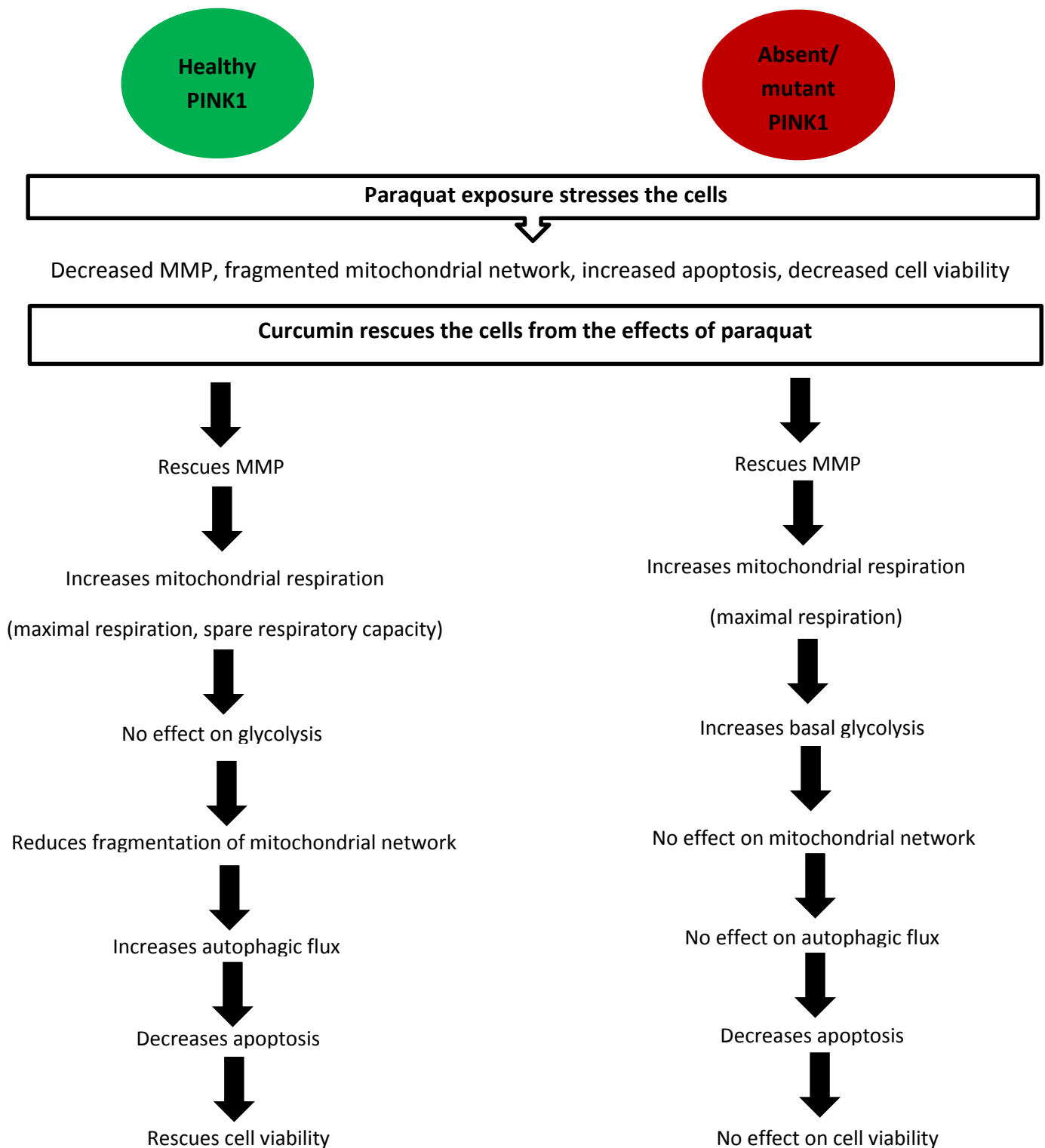
Figure 4.1. Diagram highlighting the rescue effect of curcumin from paraquat in cells with either healthy or absent/ mutant PINK1

4.5. No *PINK1* CNV mutations detected in South African PD patients

The aim of this section of the study was to detect CNV primarily in *PINK1*, and secondarily in other PD-causing genes *parkin*, *SNCA, LRRK2* and *DJ-1*, in a cohort of South African PD patients. Once detected, we could then have obtained patient's fibroblasts, and compared the effects in these to that observed in our PINK1-deficient SH-SY5Y cell model. Furthermore, we could have tested the effects of curcumin on these fibroblasts. Fibroblasts have been known to serve as a useful primary PD cell model as they are readily available and obtainable from a skin biopsy, express most of the PD genes at relatively high levels, and they reflect cumulative cellular damage according to the age of the patient (Auburger et al., 2012). Unfortunately, we were unable to detect CNV in *PINK1* in our patient cohort, and were therefore unable to repeat the study on patient-derived fibroblasts with *PINK1* mutations. Furthermore, no CNV was detected in *SNCA, LRRK2* or *DJ-1*. The only mutation found in our cohort of 210 patients screened in this study was a heterozygous deletion of *parkin* exon 4 in a white male patient with an AAO of 49 and no family history of PD. No other CNV or point mutations in *parkin* were found in this patient.

Heterozygous mutations in *parkin* have played a controversial role in recessive genes, and it is still unknown whether they are pathogenic in themselves (Corti et al., 2011). Kay and colleagues screened over 2000 patients with PD, as well as age-matched controls (Kay et al., 2010). Interestingly, a total of 0.95% of control subjects carried a heterozygous CNV mutation in *parkin*, compared to 0.86% of patients. This indicates that there is no compelling evidence for association of heterozygous *parkin* mutations with PD. Conversely, it has been reported in several studies that individuals who are heterozygous carriers of mutations in *parkin* can also present with PD (Bonifati et al., 2005; Hedrich et al., 2004; West et al., 2002). It is thought that heterozygous mutations are not sufficient to cause PD, but are rather associated with a higher risk of developing the disease and may play a role in a threshold effect for parkinsonism (Klein et al., 2007).

The mutation frequency of *PINK1* mutation carriers varies from 0-15% worldwide, depending on the population, making this gene the second most frequent cause of autosomal recessive EOPD - after *parkin* (Corti et al., 2011; Deas et al., 2009; Nuytemans et al., 2010). The majority of *PINK1* mutations are point mutations and small insertions/deletions, whilst larger deletions and complex rearrangements are rare (Cazeneuve et al., 2009; Marongiu et al., 2007). To our knowledge, CNV in *PINK1* using the MLPA kit has been reported in two studies focussed specifically at early onset cases – one heterozygous

deletion of exon 1 was observed in a Brazilian cohort (Moura et al., 2012) and a compound heterozygous deletion of exon 2 + deletion of exon 2, 3 and 4, was found in an Iranian cohort (Darvish et al., 2013). In both studies, the CNV in *PINK1* was only observed in one patient. This highlights the rarity of exonic or genomic rearrangements in *PINK1* in certain populations.

In comparison to *PINK1*, *parkin* mutations are far more frequent, and are responsible for 10-20% of EOPD cases worldwide (Corti et al., 2011). *Parkin* mutations have been found in numerous families with different ethnic backgrounds, including individuals with African ancestry (Haylett et al., 2012; Hedrich et al., 2004; Lücking et al., 2000; Periquet et al., 2003). In a previous study, Haylett and colleagues aimed to assess the genetic contribution of *parkin* mutations (both point mutations and exon rearrangements) in a group of 229 South African PD patients. Seven patients (3.1%) had homozygous or compound heterozygous mutations in *parkin*, and seven patients had heterozygous sequence variants (Haylett et al., 2012), concluding that mutations in the *parkin* gene are not a major contributor to PD in the South African population. The results from the present study confirm that the known PD-causing genes are only a rare cause of PD in South African patients. A study on Zambian PD patients found one heterozygous *parkin* mutation in a cohort of 39 patients (Yonova-Doing et al., 2012). Together, these studies highlight a concerning situation relating to the genetic cause of PD in African individuals. It is clear that in comparison to other populations, mutations in the known PD-causing genes are less frequent in African populations, and this may be due to the hypothesis that there are still unknown genetic causes of PD, and these may be specific to the African population.

Currently, genetic characterization of the African population remains limited, although recently the African Genome Variation Project (AGVP) was set up to assess genetic diversity in Africa by the WGS of 320 individuals (Gurdasani et al., 2015). High levels of genetic diversity are observed in African populations, and studying these populations in greater detail could lead to the discovery of genetic determinants that may contribute to the global understanding of disease (Ramsay et al., 2011).

4.6. Study limitations

Patient-derived dopaminergic neurons would be an ideal cell type in which to study the pathogenesis of PD. Unfortunately, the individual would need to be deceased before these cells can be obtained, and brain cells post mortem may have an altered phenotype and gene expression profile compared to when

the cells were still active. Therefore, an alternative method for studying PD is to create a disease model that can replicate dopaminergic neurons as best as possible. The SH-SY5Y cell line used in this study is commonly used as a cellular model for PD (Xie et al., 2010). Advantages of using this cell type include ease of access, culturing ability, and capacity to under or over express genes. Whilst SH-SY5Y cells do possess many characteristics of dopaminergic neurons, they are not derived from patients with PD, and were therefore a limitation of this study. As mentioned above, we would ideally have repeated this work in *PINK1*-mutant fibroblasts, but this was not available to us. From fibroblasts, one could then have created iPSC dopaminergic neurons, which are advantageous in that they are patient-derived neuronal cells. However, one must be cautious when regarding this cell type, as the characteristics of an iPSC-derived neuron may not mirror those of patient neurons.

Experimental limitations of this study included the protein expression level of PINK1 after siRNA treatment. Whilst a decrease in protein expression of 54% was sufficient to induce mitochondrial and cellular dysfunction, this does not accurately portray the effect seen in PINK1-associated PD, where 100% of the protein is truncated or absent. Therefore, a 100% decrease in PINK1 protein expression would have been preferable, but this was not possible with the methodology used in this study. Secondly, each experiment was performed in triplicate, and was also biologically replicated three times (n=3). Whilst this is considered a standard protocol, some of the results presented with large error bars after statistical analysis. It is thought that the statistical power of these results could have been increased if 'n' was greater than 3.

This study determined one optimal concentration for paraquat and curcumin to be used in all functional assays. However, in order to better understand the effect of paraquat and curcumin, a dosage curve of varying concentrations can also be performed for each assay. One could then observe whether a higher/ lower concentration had a better/ worse effect on the cells compared to other doses. Furthermore, we could have included other treatment groups such as paraquat and curcumin combined, or post-treatment with curcumin (rather than only pre-treatment). Other studies have found that pre-treatment with curcumin before a stressor produces the best results (Mythri et al., 2010), and that was the reason for the chosen protocol in this study. Additionally, future experiments should verify the results from the MTT assay with an independent assay, such as the WST-1 or ATP assay.

For Western blot detection of protein markers for apoptosis and autophagy, two markers were used for each process. For apoptosis, we initially aimed to use cleaved caspase 3 as a marker to verify the results

found from cleaved PARP. Cleaved caspase 3 is a reliable and frequently used marker of apoptosis. However we were unable to detect the protein in our lysates with the available antibodies, and therefore chose to use full-length caspase 3. Whilst these results verified the majority of the observations from cleaved PARP, other markers available for apoptosis such as cleaved and full-length caspase 8 and 9 could also have been utilised in our study. As previously mentioned, the use of p62 as a marker of autophagy can often be regarded as unreliable, therefore other autophagy-specific markers such as Atg proteins or Beclin-1 should be studied and utilised in future experiments. In addition, the measurement of autophagic flux by Western blotting is in itself a limitation. Western blotting is able to measure a 'rate', and is also a difficult method to assess small changes in LC3-II and p62 protein levels accurately (Loos et al., 2014). New techniques need to be established whereby flux can be measured in a highly sensitive, robust and well-quantifiable manner.

Lastly, the polymorphisms observed in *PARK2* exon 5 were only observed in Mixed Ancestry and Black individuals (Table 3.1), and led to false positive CNV findings. Therefore, manufacturers of MLPA kits need to take into account these ethnic-specific polymorphisms for the design of more appropriate probes.

4.7. Future work

As previously mentioned, we found no patients with CNV in the *PINK1* gene, and were therefore unable to obtain fibroblasts (Section 3.10). In order to verify these results in a patient-derived cell model of PD, we will contact either researchers or cell banks that may have access to *PINK1* mutant fibroblasts. Whilst studying cells with *PINK1* CNV is ideal, these mutations are extremely rare, and fibroblasts with *PINK1* point mutations may be another option. Once obtained, the various functional assays used in this study should be performed to determine the effect of *PINK1* mutations in these cells. Additional assays should also be executed, such as measurement of mitophagy and the levels of ROS and antioxidants.

Furthermore, we will aim to establish a protocol for culturing iPSCs from the fibroblasts. One option is that this will be performed in collaboration with researchers from the University of Cape Town in South Africa, as this methodology has been successfully set up in fibroblasts from patients with spinocerebellar ataxia (Watson et al., 2015). In addition, it would also be ideal to repeat this study in an

animal model of PD. Once established, we would have three models of PINK1-deficient PD – fibroblasts, iPSCs, and an animal model. Using this multi-tiered approach, one could study the effects of curcumin in each system, compare the results, and create a better understanding of its mode of action. Subsequent to those studies, a clinical trial could be launched for curcumin in South African patients suffering from PD.

Accumulating various models in which to study PD is advantageous in that it enables one to study the effects of other compounds of interest. For example, resveratrol is an antioxidant enriched in grapes, and has beneficiary effects similar to that of curcumin (Bereswill et al., 2010; Sharma et al., 2007). Several studies performed on the effect of resveratrol in PD have found that it attenuates oxidative stress and exerted neuroprotection in rat models of the disease (Jin et al., 2008; Wu et al., 2011). Future work could focus on the effect of this compound and other natural, non-toxic antioxidants on our models of PD.

4.8. Concluding remarks

In conclusion, this study has shown that down regulation of PINK1 results in mitochondrial dysfunction and neuronal cell death. Mitochondria are active players in apoptosis via the intrinsic mitochondrial death pathway, and understanding the effects of curcumin on the mitochondria in models of PD may be key to develop this drug as a therapeutic option in patients with PD and related neurodegenerative disorders. Whilst pharmacological and surgical interventions are available, the current options exhibit distinct side effects with long term treatment. There is a great need to develop new treatments with i. less side effects and ii. that can simultaneously target the multiple pathways associated with this disorder.

The greatest challenge facing researchers that have studied curcumin is that it is an enigma – how can one single molecule possess such diverse activities? In this study, we aimed to create a better understanding of the function of curcumin, and to determine whether it may be a potential therapeutic agent for patients suffering from PD. We have shown that curcumin reduced apoptosis and improved mitochondrial respiration and MMP in our model of PD. Curcumin did not increase autophagic flux in our model, but rather in control cells stressed by paraquat, speculating a possible role for curcumin in the PINK1/parkin pathway and mitophagy.

Future studies on the effect of curcumin on PD are vital, as this compound may be an ideal neuroprotective agent. Curcumin is known to have a variety of beneficial properties including antioxidant and anti-inflammatory, which could lead to its ability to promote cell survival in neurodegenerative diseases such as PD and AD. In addition, curcumin is advantageous as it has low toxicity, and is already commercially available from pharmacies in the form of a concentrated capsule or as a component of the curry spice turmeric. Further work on clinical applications of curcumin in patients suffering from PD and other diseases may reveal that this compound is a key element for the development of therapeutic modalities aimed at preventing or halting neuronal cell death.

Appendix I: Laboratory protocols:

1. Culturing SH-SY5Y neuroblastoma cells

Flasks were labelled correctly and the work bench was prepared and cleaned with ethanol to ensure no contamination. Medium for SH-SY5Y cells was made up of a 1:1 ratio of DMEM: Ham's F12, and treated with 10% FBS and 1% penicillin streptomycin. A volume of 1ml media was added to frozen stocks of cells, and this was placed in a 15ml Flacon tube and centrifuged for 3mins at 4500rpm. The supernatant was discarded and the pellet was resuspended in 2ml media. A volume of 4ml media was added to a 25cm² CellBIND flask (Corning, USA), and the resuspended cell solution was then pipetted directly into the flask. Flasks were incubated at 37°C, 5% CO_2 until 80-90% confluency.

1.1. Trypsinising the cells

Once confluent, cells were trypsinised and relocated to either a larger 75cm² flask, or a tissue culture plate specific to the experiment. Media was pipetted out of the flask, and cells were washed with 5ml PBS. Once removed, 5ml trypsin was added to the cells and the flask was incubated at 37°C until they no longer adhered to the flask surface. Thereafter, 4ml media was pipetted into the flask and mixed with the cells and the trypsin. This was then pipetted out of the flask and into a 15ml Falcon tube, which was centrifuged for 3min at 4500rpm. The supernatant was discarded and the pellet was resuspended in media, the volume of which was also dependent on which flask/ plate the cells would be seeded into.

1.2. Freezing down procedure

Freezing media was made up using 3.2ml media and 0.8ml DMSO. Once trypsinised and resuspended in 3ml media, a total volume of 1ml of resuspended cells was mixed with a volume of 1ml freezing media. Thereafter, two volumes of 1ml of the cell suspension + freezing media combination was aliquoted into 2X 2ml sterile cryotubes. The 2ml cryotubes were placed in the -80°C freezer for a minimum of 4hrs. The tubes were then carried in liquid nitrogen to the liquid nitrogen storage containers and placed in the boxes. One vial was thawed, put into a 25cm² flask containing 5ml culture medium and incubated for three days as a control to check for viability and exclude contamination (Freshney, 2010).

2. Genomic DNA isolation from blood samples

Four 5ml blood samples in EDTA tubes were aliquoted into 2 sterile 50ml tubes. These were then filled to the 45ml mark with cold cell lysis buffer. Each tube was well shaken and left on ice for 10mins. The tubes were shaken again, after which cells were pelleted by spinning at 3000rpm for 10mins. The supernatant was poured off and the wash step was repeated. Thereafter a volume of 900µl sodium acetate (3M solution) and 100µl of 10% sodium dodecyl sulfate (SDS) was added to each pellet. The pellet was resuspended in this solution and 100µl of proteinase K was added to each tube. The mixture was incubated at 37°C overnight.

The following day, 2ml dH_2O and 500µl 3M Na-acetate was added to each tube, after which the solution was mixed. A volume of 2,5ml of phenol-chloroform was added to each tube and the mixture shaken on a shaking platform at room temperature. The mixture was then transferred to a 10ml glass Corex tube and spun at 7000rpm for 12mins at a temperature of between 4 °C and 10 °C. The supernatant was then transferred to a clean Corex tube without disturbing the interphase. Thereafter, 2,5ml octonal-chloroform was added to each tube. The tubes were sealed tightly and slowly mixed by inversion until the mixture turned milky. The tubes were then centrifuged without lids at 7000 rpm for 10mins in a Sorval centrifuge at a temperature of between 4°C and 10 °C. The supernatant was poured into a 12ml plastic tube, and 5-7ml ethanol was slowly added. The tube was closed and mixed until the DNA precipitated.

The DNA was transferred to a 1,5ml Eppendorf tube, which was filled with 70% ethanol and centrifuged at 14000rpm for 3mins. The supernatant was poured off and the wash was repeated. The pellet was then dried at room temperature for 30mins, after which 500µl of a 1x Tris-EDTA solution was added to each tube. The tubes were incubated overnight at 37°C. Thereafter, the solutions were mixed for three days on a rotating wheel at 30rpm. The concentration of the DNA solution was read by the Nanodrop and the sample was diluted to a concentration of 0.1-0.2µg/µl. All gDNA isolations were performed by Miss Ina Le Roux and Dr. Sihaam Boolay.

Appendix II: Solutions for various techniques used in the present study:

2.1. Cell lysates

Passive lysis buffer

50mM Hepes

100mM NaCl

10mM EDTA

1% Triton X-100

4mM NaPPi

2mM Na_3VO_4

H_2O

pH 7.5

Cell lysis buffer

5ml passive lysis buffer

100µl 50mM PMSF

¼ protease inhibitor tablet (Roche diagnostics, Germany).

2.2. Western blots

10x SDS Running Buffer

30g Tris base

144g Glycine

100ml 10% SDS

ddH$_2$O to a final volume of 1L

- 1x SDS Running Buffer

Dilute 100ml 10x SDS Running Buffer in 900ml distilled water

5% Milk for membrane blocking

10g milk powder

200ml TBST

Mixed together and placed on magnetic stirrer until powder dissolved

TBST

8g NaCl

20ml 1M Tris-HCl (pH 7.6)

1ml Tween 20

pH 7.6

ddH$_2$O to a final volume of 1L

2.3. Confocal microscopy

4% paraformaldehyde

8g paraformaldehyde

200ml PBS

Dissolve paraformaldehyde in PBS by adding 1M NaOH and heating it to 50°C for 30mins with constant stirring. Adjust final pH to 7.4-7.6.

<u>Mounting media</u>

12g Mowiol 4-88

30g Glycerol

30ml ddH$_2$O

Add 60ml of a 0.2M Tris stock solution (pH 8.5) and stir overnight at room temperature. Dissolve remaining Mowiol by heating to 50˚C with constant stirring. Centrifuge at 5000g for 15 min. Aliquot and store supernatant at -20˚C.

<10mg anti-fading agent

A small quantity of anti-fading agent (n-propylgallate) was dissolved in 1ml mounting media at 50°C for 1 hour. This was centrifuged at 5000g for 2min and stored in the dark at 4°C for up to three weeks.

2.4. Solutions for functional assays

<u>5mg/ml MTT stock solution</u>

10mg Thiazolyl blue tetrazolium bromide

2ml PBS

<u>5mg/ml JC-1 stock solution</u>

5mg Tetraethyl benzimidazolyl carbocyanine iodide

1ml DMSO

<u>20µg/ml Bafilomycin A1 stock solution</u>

100µg Bafilomycin A1

5ml ethanol

Appendix III: MLPA probes and reagents list

3.1.   Mix P051 probe list (Taken from www.MLPA.com)

Length (nt)	SALSA MLPA probe	reference	PARK7	ATP13A2	PINK1	SNCA	PARK2	LRRK2
64-70-76-82	Q-fragments: DNA quantity; only visible with less than 100 ng sample DNA							
88-92-96	D-fragments: Low signal of 88 or 96 nt fragment indicates incomplete denaturation							
100	X-fragment: Specific for the X chromosome							
105	Y-fragment: Specific for the Y chromosome							
130	Reference probe 00797-L00463	5q31						
136 * ¬	**TNFRSF9** probe 20271-L27994		Upstream					
143 *	**PINK1** probe 20270-L27992				Exon 5			
148 ¥ «	**PINK1** probe 03691-L27542				Exon 1			
154 ¥ §	**SNCA** probe 02166-L27543					A30P Mut		
160 *	Reference probe 09787-L10202	15q21						
166 ¥	**SNCA** probe 02168-L27544					Exon 4		
172 ¥ «	**PINK1** probe 03692-L27545				Exon 2			
178 ¥ «	**ATP13A2** probe 11715-L27546			Exon 9				
184 ¥	**SNCA** probe 02169-L28011					Exon 6		
190 *	Reference probe 08067-L19457	9p13						
196 ¥ §	**LRRK2** probe 04575-L27549							G2019S Mut
202 * Ж	**PARK2** probe 20272-SP0951-L27900						Exon 4	
209 ¥ «	**PINK1** probe 12067-L28012				Exon 3			
215 ¥ «	**ATP13A2** probe 11716-L28013			Exon 2				
222 *	Reference probe 06746-L27899	8q12						
229	**PINK1** probe 03698-L03154				Exon 7			
237 ¥	**PARK2** probe 20225-L24881						Exon 1	
245 *	**PARK7** probe 20273-L27643		Exon 6					
253 ¥	**SNCA** probe 04616-L27552					Exon 3		
260 *	Reference probe 16433-L27655	18q21						
265 ¥ ¬	**LPA** probe 20224-L27548						Downstream	
272 *	**PARK7** probe 20274-L27644		Exon 2					
279 *	**SNCA** probe 20255-L03103					Exon 2		
287 ¥	**PARK2** probe 02174-L27554						Exon 2	
294 *	Reference probe 18776-L27898	3p22						
302 ¥	**PARK2** probe 02180-L27553						Exon 8	
310 *	**PINK1** probe 20276-L27646				Exon 6			
319 *	**PARK7** probe 20277-L27647		Exon 4					
325 ¥	**PARK2** probe 02181-L27555						Exon 9	
335 *	Reference probe 18737-L27897	2q36						
343 *	**PARK2** probe 20278-L27648						Exon 6	
350 *	**PARK7** probe 20279-L27649		Exon 1					
359 ¥	**PARK2** probe 02182-L27556						Exon 10	
370 ¥	**PARK7** probe 20254-L27588		Exon 5					
377 ¥	**PARK2** probe 02183-L27896						Exon 11	
384 *	Reference probe 18677-L24031	11p14						
395 ¥	**PARK2** probe 02184-L27585						Exon 12	
405 * «	**PINK1** probe 20280-L27650				Exon 4			
413 ¥	**PARK7** probe 20101-L27586		Exon 3					
423 *	**PARK2** probe 20281-L27651						Exon 5	
429 ¥ «	**PARK7** probe 03690-L27587		Exon 1					
437 *	Reference probe 10731-L11313	6p12						
452 ¥	**SNCA** probe 04096-L27589					Exon 1		
459 ¥	**PARK7** probe 02189-L27590		Exon 7					
469 ¥ «	**PINK1** probe 03697-L27591				Exon 8			
477 *	**PARK2** probe 20282-L27652						Exon 3	
486 ¥	**SNCA** probe 03689-L27592					Exon 5		
494 *	**PARK2** probe 20283-L27895						Exon 7	
500 *	Reference probe 19555-L27674	2p13						

3.2. Mix P052 probe list (Taken from www.MLPA.com)

Length (nt)	SALSA MLPA probe	Chromosomal position						
		reference	ATP13A2	UCHL1	PARK2	CAV1/2	LRRK2	GCH1
64-70-76-82	Q-fragments: DNA quantity; only visible with less than 100 ng sample DNA							
88-92-96	D-fragments: Low signal of 88 or 96 nt fragment indicates incomplete denaturation							
100	X-fragment: Specific for the X chromosome							
105	Y-fragment: Specific for the Y chromosome							
130 ¥	Reference probe 00797-L19287	5q31						
136 Ø	**PACRG** probe 03204-L02565				6q26			
142 * «	**UCHL1** probe 20285-L27662			Exon 6				
148 ¥	**PARK2** probe 20257-L27598				Exon 5			
154 *	Reference probe 14199-L27215	2q12						
161 ¥	**PARK2** probe 03366-L27599				Exon 7			
166 ¥ «	**UCHL1** probe 03679-L27600			Exon 1				
172 ¥ §	**LRRK2** probe 04574-L27601						G2019S	
177 «	**UCHL1** probe 03681-L03096			Exon 5				
183 *	Reference probe 09496-L28060	11q24						
190 ¥	**LRRK2** probe 20256-L23585						Exon 41	
196 *	**PARK2** probe 20286-L27663				Exon 8			
203 ¥	**UCHL1** probe 02937-L27602			Exon 9				
209 ¥	**GCH1** probe 04405-L27930							Exon 3
217 ¥	**PARK2** probe 06135-L27603				Exon 12			
224 *	Reference probe 06746-L28025	8q12						
230 ¥ «	**ATP13A2** probe 11717-L27610		Exon 14					
238 *	**UCHL1** probe 20287-L27664			Exon 8				
244 ¥	**PARK2** probe 03365-L27611				Exon 6			
254 * Ж «	**UCHL1** probe 20288-SP0953-L28061			Exon 4				
261 ¥	**GCH1** probe 04618-L28062							Exon 1
265 *	Reference probe 16225-L18478	16q12						
274 ¥	**PARK2** probe 05654-L28095				Exon 3			
281 ¥	**LRRK2** probe 04281-L27614						Exon 27	
286 *	**PARK2** probe 20289-L27933				Exon 9			
294 * «	**UCHL1** probe 20290-L27667			Exon 3				
303 * Ж	**PARK2** probe 20291-SP0954-L27668				Exon 2			
310 *	Reference probe 18380-L25673	10q22						
319 ¥	**GCH1** probe 03683-L27615							Exon 2
328 ¥	**GCH1** probe 03685-L27616							Exon 5
334 ¥	**LRRK2** probe 04283-L27617						Exon 49	
343 ¥	**PARK2** probe 19810-L27618				Exon 4			
350 ¥	**PARK2** probe 03369-L27619				Exon 10			
359 *	Reference probe 10727-L26803	6p12						
369 *	**GCH1** probe 15131-L27620							Exon 4
379 ¥	**LRRK2** probe 04278-L27621						Exon 1	
388 *	**GCH1** probe 20292-L27669							Exon 6
395 ¥	**PARK2** probe 04614-L27622				Exon 11			
405 ¥	**CAV1** probe 03359-L27627					Exon 3		
415 *	Reference probe 12747-L27779	9q34						
422 * «	**UCHL1** probe 20293-L27670			Exon 2				
429 ¥	**LRRK2** probe 04279-L27624						Exon 10	
443 * «	**UCHL1** probe 20294-L27671			Exon 7				
448 * «	**ATP13A2** probe 20295-L27934		Exon 27					
460 *	Reference probe 16287-L25505	20q11						
466 ¥	**LRRK2** probe 04280-L28024						Exon 15	
477 ¥ «	**CAV2** probe 04091-L27626					Exon 3		
486 *	**LRRK2** probe 20296-L27936						Exon 2	
494 *	Reference probe 19137-L26747	21q22						
500 *	Reference probe 19555-L27674	2p13						

Appendix IV: Determination of optimal cell seeding density for MTT Assay
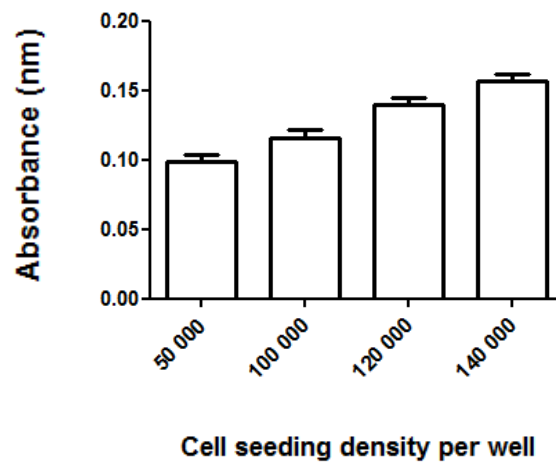
Based on the confluency of the cells after 24 hours, it was decided to seed cells at 100 000 cells per well for future cell viability work.

Appendix V: Analysis of glycolysis resulted in no significance for the following results:

5.1. Measurements of ECAR to determine levels of glycolysis and glycolytic reserve in *PINK1* siRNA and Control siRNA cells were not significant
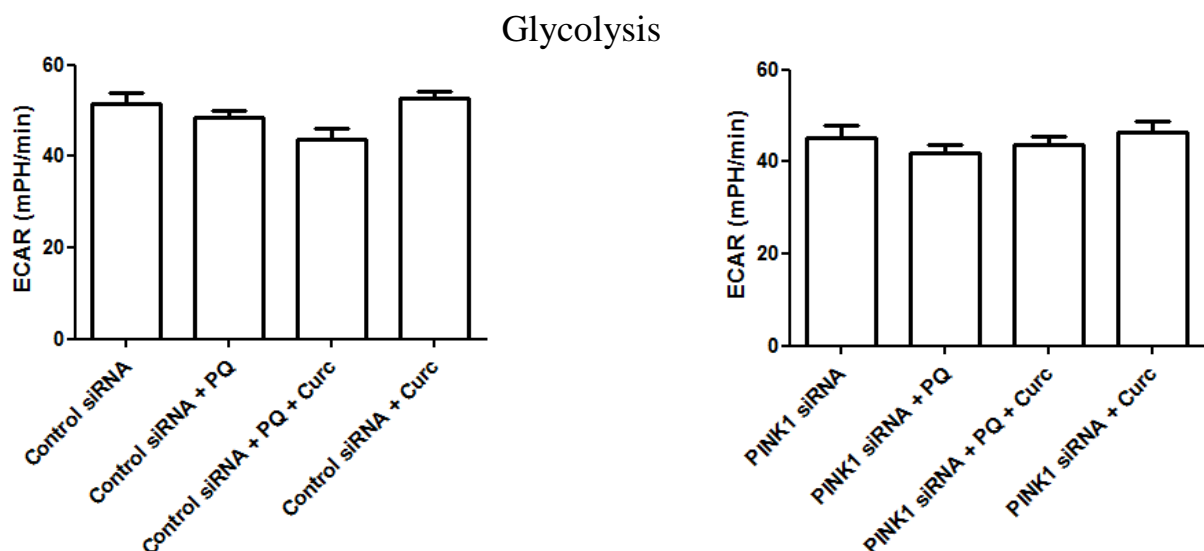
Glycolytic capacity
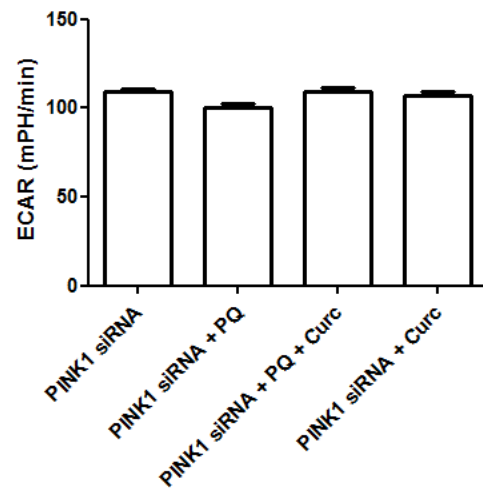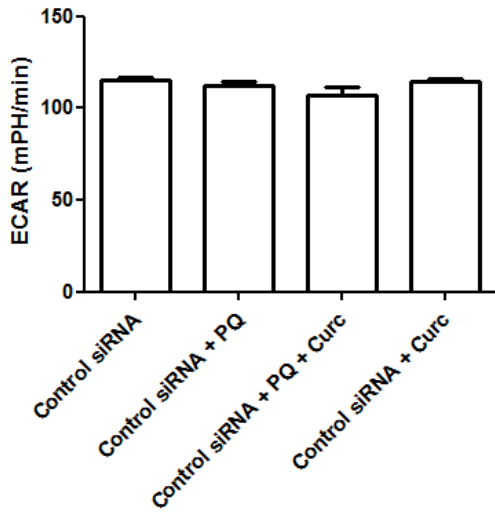
Glycolytic Reserve
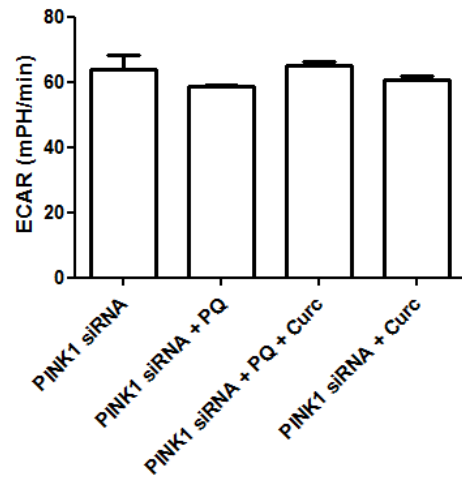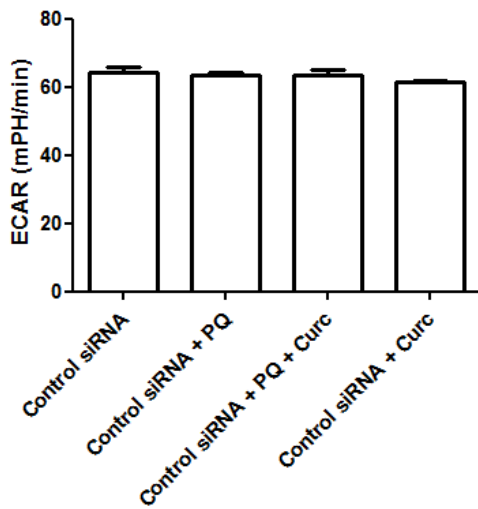
5.2. No significant changes were observed across treatment groups in both control and *PINK1* siRNA cells for glycolysis, glycolytic capacity, or glycolytic reserve.

References

Electronic

Coffalyser.Net: http://coffalyser.software.informer.com/download

GraphPad Prism: http://.graphpad.com/scientific-software/prism

Image J: http://imagej.nih.gov/ij

Lightcycler 96: http://roche.com

REST: http://gene-quantification.de/rest.html

XF^e96 Wave: http://seahorsebio.com

Journals & Books

Aggarwal, B.B., Harikumar, K.B., 2009. Potential therapeutic effects of curcumin, the anti-inflammatory agent, against neurodegenerative, cardiovascular, pulmonary, metabolic, autoimmune and neoplastic diseases. Int. J. Biochem. Cell Biol., Directed Issue: Epigenetics and Disease 41, 40–59. doi:10.1016/j.biocel.2008.06.010

Aggarwal, B.B., Sethi, G., Baladandayuthapani, V., Krishnan, S., Shishodia, S., 2007a. Targeting cell signaling pathways for drug discovery: an old lock needs a new key. J. Cell. Biochem. 102, 580–592. doi:10.1002/jcb.21500

Aggarwal, B.B., Shishodia, S., Takada, Y., Banerjee, S., Newman, R.A., Bueso-Ramos, C.E., Price, J.E., 2005. Curcumin Suppresses the Paclitaxel-Induced Nuclear Factor-κB Pathway in Breast Cancer Cells and Inhibits Lung Metastasis of Human Breast Cancer in Nude Mice. Clin. Cancer Res. 11, 7490–7498. doi:10.1158/1078-0432.CCR-05-1192

Aggarwal, B.B., Sundaram, C., Malani, N., Ichikawa, H., 2007b. Curcumin: the Indian solid gold. Adv. Exp. Med. Biol. 595, 1–75. doi:10.1007/978-0-387-46401-5_1

Alam, M., Schmidt, W.J., 2002. Rotenone destroys dopaminergic neurons and induces parkinsonian symptoms in rats. Behav. Brain Res. 136, 317–324. doi:10.1016/S0166-4328(02)00180-8

Alkan, C., Coe, B.P., Eichler, E.E., 2011. Genome structural variation discovery and genotyping. Nat. Rev. Genet. 12, 363–376. doi:10.1038/nrg2958

Anand, P., Kunnumakkara, A.B., Newman, R.A., Aggarwal, B.B., 2007. Bioavailability of Curcumin: Problems and Promises. Mol. Pharm. 4, 807–818. doi:10.1021/mp700113r

Anichtchik, O., Diekmann, H., Fleming, A., Roach, A., Goldsmith, P., Rubinsztein, D.C., 2008. Loss of PINK1 Function Affects Development and Results in Neurodegeneration in Zebrafish. J. Neurosci. 28, 8199–8207. doi:10.1523/JNEUROSCI.0979-08.2008

Arico, S., Petiot, A., Bauvy, C., Dubbelhuis, P.F., Meijer, A.J., Codogno, P., Ogier-Denis, E., 2001. The Tumor Suppressor PTEN Positively Regulates Macroautophagy by Inhibiting the Phosphatidylinositol 3-Kinase/Protein Kinase B Pathway. J. Biol. Chem. 276, 35243–35246. doi:10.1074/jbc.C100319200

Auburger, G., Klinkenberg, M., Drost, J., Marcus, K., Morales-Gordo, B., Kunz, W.S., Brandt, U., Broccoli, V., Reichmann, H., Gispert, S., Jendrach, M., 2012. Primary skin fibroblasts as a model of Parkinson's disease. Mol. Neurobiol. 46, 20–27. doi:10.1007/s12035-012-8245-1

Badger, J.L., Cordero-Llana, O., Hartfield, E.M., Wade-Martins, R., 2014. Parkinson's disease in a dish – Using stem cells as a molecular tool. Neuropharmacology, The Synaptic Basis of Neurodegenerative Disorders 23rd Neuropharmacology Conference 76, Part A, 88–96. doi:10.1016/j.neuropharm.2013.08.035

Barth, S., Glick, D., Macleod, K.F., 2010. Autophagy: assays and artifacts. J. Pathol. 221, 117–124. doi:10.1002/path.2694

Basile, V., Belluti, S., Ferrari, E., Gozzoli, C., Ganassi, S., Quaglino, D., Saladini, M., Imbriano, C., 2013. bis-Dehydroxy-Curcumin Triggers Mitochondrial-Associated Cell Death in Human Colon Cancer Cells through ER-Stress Induced Autophagy. PLoS ONE 8, e53664. doi:10.1371/journal.pone.0053664

Baum, L., Lam, C.W.K., Cheung, S.K.-K., Kwok, T., Lui, V., Tsoh, J., Lam, L., Leung, V., Hui, E., Ng, C., Woo, J., Chiu, H.F.K., Goggins, W.B., Zee, B.C.-Y., Cheng, K.F., Fong, C.Y.S., Wong, A., Mok, H., Chow, M.S.S., Ho, P.C., Ip, S.P., Ho, C.S., Yu, X.W., Lai, C.Y.L., Chan, M.-H., Szeto, S., Chan, I.H.S., Mok, V., 2008. Six-month randomized, placebo-controlled, double-blind, pilot clinical trial of curcumin in patients with Alzheimer disease. J. Clin. Psychopharmacol. 28, 110–113. doi:10.1097/jcp.0b013e318160862c

Beal, M.F., 2003. Mitochondria, Oxidative Damage, and Inflammation in Parkinson's Disease. Ann. N. Y. Acad. Sci. 991, 120–131. doi:10.1111/j.1749-6632.2003.tb07470.x

Becker, D., Richter, J., Tocilescu, M.A., Przedborski, S., Voos, W., 2012. Pink1 kinase and its membrane potential (Deltaψ)-dependent cleavage product both localize to outer mitochondrial membrane by unique targeting mode. J. Biol. Chem. 287, 22969–22987. doi:10.1074/jbc.M112.365700

Beilina, A., Brug, M.V.D., Ahmad, R., Kesavapany, S., Miller, D.W., Petsko, G.A., Cookson, M.R., 2005. Mutations in PTEN-induced putative kinase 1 associated with recessive parkinsonism have differential effects on protein stability. Proc. Natl. Acad. Sci. U. S. A. 102, 5703–5708. doi:10.1073/pnas.0500617102

Bereswill, S., Muñoz, M., Fischer, A., Plickert, R., Haag, L.-M., Otto, B., Kühl, A.A., Loddenkemper, C., Göbel, U.B., Heimesaat, M.M., 2010. Anti-Inflammatory Effects of Resveratrol, Curcumin and Simvastatin in Acute Small Intestinal Inflammation. PLoS ONE 5, e15099. doi:10.1371/journal.pone.0015099

Berman, S.B., Pineda, F.J., Hardwick, J.M., 2008. Mitochondrial fission and fusion dynamics: the long and short of it. Cell Death Differ. 15, 1147–1152. doi:10.1038/cdd.2008.57

Biswas, S.C., Shi, Y., Sproul, A., Greene, L.A., 2007. Pro-apoptotic Bim induction in response to nerve growth factor deprivation requires simultaneous activation of three different death signaling pathways. J. Biol. Chem. 282, 29368–29374. doi:10.1074/jbc.M702634200

Bonifati, V., 2014. Genetics of Parkinson's disease – state of the art, 2013. Parkinsonism Relat. Disord., Proceedings of XX World Congress on Parkinson's Disease and Related Disorders 20, Supplement 1, S23–S28. doi:10.1016/S1353-8020(13)70009-9

Bonifati, V., Rohé, C.F., Breedveld, G.J., Fabrizio, E., Mari, M.D., Tassorelli, C., Tavella, A., Marconi, R., Nicholl, D.J., Chien, H.F., Fincati, E., Abbruzzese, G., Marini, P., Gaetano, A.D., Horstink, M.W., Maat-Kievit, J.A., Sampaio, C., Antonini, A., Stocchi, F., Montagna, P., Toni, V., Guidi, M., Libera, A.D., Tinazzi, M., Pandis, F.D., Fabbrini, G., Goldwurm, S., Klein, A. de, Barbosa, E., Lopiano, L., Martignoni, E., Lamberti, P., Vanacore, N., Meco, G., Oostra, B.A., Network, T.I.P.G., 2005. Early-onset parkinsonism associated with PINK1 mutations Frequency, genotypes, and phenotypes. Neurology 65, 87–95. doi:10.1212/01.wnl.0000167546.39375.82

Braak, H., Tredici, K.D., Rüb, U., de Vos, R.A.I., Jansen Steur, E.N.H., Braak, E., 2003. Staging of brain pathology related to sporadic Parkinson's disease. Neurobiol. Aging 24, 197–211. doi:10.1016/S0197-4580(02)00065-9

Brand, M.D., Nicholls, D.G., 2011. Assessing mitochondrial dysfunction in cells. Biochem. J. 435, 297–312. doi:10.1042/BJ20110162

Burbulla, L.F., Krebiehl, G., Krüger, R., 2010. Balance is the challenge – The impact of mitochondrial dynamics in Parkinson's disease. Eur. J. Clin. Invest. 40, 1048–1060. doi:10.1111/j.1365-2362.2010.02354.x

Cazeneuve, C., Sân, C., Ibrahim, S.A., Mukhtar, M.M., Kheir, M.M., LeGuern, E., Brice, A., Salih, M.A., 2009. A new complex homozygous large rearrangement of the PINK1 gene in a Sudanese family with early onset Parkinson's disease. neurogenetics 10, 265–270. doi:10.1007/s10048-009-0174-4

Chartier-Harlin, M.-C., Dachsel, J.C., Vilariño-Güell, C., Lincoln, S.J., Leprêtre, F., Hulihan, M.M., Kachergus, J., Milnerwood, A.J., Tapia, L., Song, M.-S., Le Rhun, E., Mutez, E., Larvor, L., Duflot, A., Vanbesien-Mailliot, C., Kreisler, A., Ross, O.A., Nishioka, K., Soto-Ortolaza, A.I., Cobb, S.A., Melrose, H.L., Behrouz, B., Keeling, B.H., Bacon, J.A., Hentati, E., Williams, L., Yanagiya, A., Sonenberg, N., Lockhart, P.J., Zubair, A.C., Uitti, R.J., Aasly, J.O., Krygowska-Wajs, A., Opala, G., Wszolek, Z.K., Frigerio, R., Maraganore, D.M., Gosal, D., Lynch, T., Hutchinson, M., Bentivoglio, A.R., Valente, E.M., Nichols, W.C., Pankratz, N., Foroud, T., Gibson, R.A., Hentati, F., Dickson, D.W., Destée, A., Farrer, M.J., 2011. Translation Initiator EIF4G1 Mutations in Familial Parkinson Disease. Am. J. Hum. Genet. 89, 398–406. doi:10.1016/j.ajhg.2011.08.009

Chaudhuri, K.R., Healy, D.G., Schapira, A.H.V., National Institute for Clinical Excellence, 2006. Non-motor symptoms of Parkinson's disease: diagnosis and management. Lancet Neurol. 5, 235–245. doi:10.1016/S1474-4422(06)70373-8

Chen, J., Tang, X.Q., Zhi, J.L., Cui, Y., Yu, H.M., Tang, E.H., Sun, S.N., Feng, J.Q., Chen, P.X., 2006. Curcumin protects PC12 cells against 1-methyl-4-phenylpyridinium ion-induced apoptosis by bcl-2-mitochondria-ROS-iNOS pathway. Apoptosis 11, 943–953. doi:10.1007/s10495-006-6715-5

Chen, Y.-R., Tan, T.-H., 1998. Inhibition of the c-Jun N-terminal kinase (JNK) signaling pathway by curcumin. Oncogene 17, 173–178. doi:10.1038/sj.onc.1201941

Cherra, S.J., Dagda, R.K., Chu, C.T., 2010. Review: autophagy and neurodegeneration: survival at a cost? Neuropathol. Appl. Neurobiol. 36, 125–132. doi:10.1111/j.1365-2990.2010.01062.x

Chu, C.T., 2010. A pivotal role for PINK1 and autophagy in mitochondrial quality control: implications for Parkinson disease. Hum. Mol. Genet. 19, R28–R37. doi:10.1093/hmg/ddq143

Chu, C.T., Zhu, J., Dagda, R.K., 2007. Beclin 1-Independent Pathway of Damage-Induced Mitophagy and Autophagic Stress: Implications for Neurodegeneration and Cell Death. Autophagy 3, 663–666. doi:10.4161/auto.4625

Ciechanover, A., Brundin, P., 2003. The Ubiquitin Proteasome System in Neurodegenerative Diseases: Sometimes the Chicken, Sometimes the Egg. Neuron 40, 427–446. doi:10.1016/S0896-6273(03)00606-8

Clark, I.E., Dodson, M.W., Jiang, C., Cao, J.H., Huh, J.R., Seol, J.H., Yoo, S.J., Hay, B.A., Guo, M., 2006. Drosophila pink1 is required for mitochondrial function and interacts genetically with parkin. Nature 441, 1162–1166. doi:10.1038/nature04779

Cohly, H.H.P., Taylor, A., Angel, M.F., Salahudeen, A.K., 1998. Effect of Turmeric, Turmerin and Curcumin on H2O2-Induced Renal Epithelial (LLC-PK1) Cell Injury. Free Radic. Biol. Med. 24, 49–54. doi:10.1016/S0891-5849(97)00140-8

Cooper, O., Seo, H., Andrabi, S., Guardia-Laguarta, C., Graziotto, J., Sundberg, M., McLean, J.R., Carrillo-Reid, L., Xie, Z., Osborn, T., Hargus, G., Deleidi, M., Lawson, T., Bogetofte, H., Perez-Torres, E., Clark, L., Moskowitz, C., Mazzulli, J., Chen, L., Volpicelli-Daley, L., Romero, N., Jiang, H., Uitti, R.J., Huang, Z., Opala, G., Scarffe, L.A., Dawson, V.L., Klein, C., Feng, J., Ross, O.A., Trojanowski, J.Q., Lee, V.M.-Y., Marder, K., Surmeier, D.J., Wszolek, Z.K., Przedborski, S., Krainc, D., Dawson, T.M., Isacson, O., 2012. Pharmacological Rescue of Mitochondrial Deficits in iPSC-Derived Neural Cells from Patients with Familial Parkinson's Disease. Sci. Transl. Med. 4, 141ra90–141ra90. doi:10.1126/scitranslmed.3003985

Corti, O., Brice, A., 2013. Mitochondrial quality control turns out to be the principal suspect in parkin and PINK1-related autosomal recessive Parkinson's disease. Curr. Opin. Neurobiol., Neurogenetics 23, 100–108. doi:10.1016/j.conb.2012.11.002

Corti, O., Lesage, S., Brice, A., 2011. What Genetics Tells us About the Causes and Mechanisms of Parkinson's Disease. Physiol. Rev. 91, 1161–1218. doi:10.1152/physrev.00022.2010

Costello, S., Cockburn, M., Bronstein, J., Zhang, X., Ritz, B., 2009. Parkinson's Disease and Residential Exposure to Maneb and Paraquat From Agricultural Applications in the Central Valley of California. Am. J. Epidemiol. 169, 919–926. doi:10.1093/aje/kwp006

Dagda, R.K., Cherra, S.J., Kulich, S.M., Tandon, A., Park, D., Chu, C.T., 2009. Loss of PINK1 Function Promotes Mitophagy through Effects on Oxidative Stress and Mitochondrial Fission. J. Biol. Chem. 284, 13843–13855. doi:10.1074/jbc.M808515200

Dagda, R.K., Zhu, J., Kulich, S.M., Chu, C.T., 2008. Mitochondrially localized ERK2 regulates mitophagy and autophagic cell stress. Autophagy 4, 770–782. doi:10.4161/auto.6458

Darvish, H., Movafagh, A., Omrani, M.D., Firouzabadi, S.G., Azargashb, E., Jamshidi, J., Khaligh, A., Haghnejad, L., Naeini, N.S., Talebi, A., Heidari-Rostami, H.R., Noorollahi-Moghaddam, H., Karkheiran, S., Shahidi, G.-A., Paknejad, S.M.H., Ashrafian, H., Abdi, S., Kayyal, M., Akbari, M., Pedram, N., Emamalizadeh, B., 2013. Detection of copy number changes in genes associated with Parkinson's disease in Iranian patients. Neurosci. Lett. 551, 75–78. doi:10.1016/j.neulet.2013.07.013

Deas, E., Plun-Favreau, H., Wood, N.W., 2009. PINK1 function in health and disease. EMBO Mol. Med. 1, 152–165. doi:10.1002/emmm.200900024

Dehay, B., Bové, J., Rodríguez-Muela, N., Perier, C., Recasens, A., Boya, P., Vila, M., 2010. Pathogenic Lysosomal Depletion in Parkinson's Disease. J. Neurosci. 30, 12535–12544. doi:10.1523/JNEUROSCI.1920-10.2010

Deng, H., Dodson, M.W., Huang, H., Guo, M., 2008. The Parkinson's disease genes pink1 and parkin promote mitochondrial fission and/or inhibit fusion in Drosophila. Proc. Natl. Acad. Sci. 105, 14503–14508. doi:10.1073/pnas.0803998105

Deng, H., Jankovic, J., Guo, Y., Xie, W., Le, W., 2005. Small interfering RNA targeting the PINK1 induces apoptosis in dopaminergic cells SH-SY5Y. Biochem. Biophys. Res. Commun. 337, 1133–1138. doi:10.1016/j.bbrc.2005.09.178

Desler, C., Hansen, T.L., Frederiksen, J.B., Marcker, M.L., Singh, K.K., Juel Rasmussen, L., 2012. Is There a Link between Mitochondrial Reserve Respiratory Capacity and Aging? J. Aging Res. 2012, e192503. doi:10.1155/2012/192503

Detmer, S.A., Chan, D.C., 2007. Functions and dysfunctions of mitochondrial dynamics. Nat. Rev. Mol. Cell Biol. 8, 870–879. doi:10.1038/nrm2275

Deuschl, G., Schade-Brittinger, C., Krack, P., Volkmann, J., Schäfer, H., Bötzel, K., Daniels, C., Deutschländer, A., Dillmann, U., Eisner, W., Gruber, D., Hamel, W., Herzog, J., Hilker, R., Klebe, S., Kloß, M., Koy, J., Krause, M., Kupsch, A., Lorenz, D., Lorenzl, S., Mehdorn, H.M., Moringlane, J.R., Oertel, W., Pinsker, M.O., Reichmann, H., Reuß, A., Schneider, G.-H., Schnitzler, A., Steude, U., Sturm, V., Timmermann, L., Tronnier, V., Trottenberg, T., Wojtecki, L., Wolf, E., Poewe, W., Voges, J., 2006. A Randomized Trial of Deep-Brain Stimulation for Parkinson's Disease. N. Engl. J. Med. 355, 896–908. doi:10.1056/NEJMoa060281

Devireddy, S., Liu, A., Lampe, T., Hollenbeck, P.J., 2015. The Organization of Mitochondrial Quality Control and Life Cycle in the Nervous System In Vivo in the Absence of PINK1. J. Neurosci. 35, 9391–9401. doi:10.1523/JNEUROSCI.1198-15.2015

DPMSA, P.N.B.M.F., FMedSci, M.J.B.M.Ms.F.F., FRCP, P.S.M.P., 2012. Clinical Pharmacology, 11e, 11 edition. ed. Churchill Livingstone, Edinburgh.

Eeden, S.K.V.D., Tanner, C.M., Bernstein, A.L., Fross, R.D., Leimpeter, A., Bloch, D.A., Nelson, L.M., 2003. Incidence of Parkinson's Disease: Variation by Age, Gender, and Race/Ethnicity. Am. J. Epidemiol. 157, 1015–1022. doi:10.1093/aje/kwg068

Eisenberg DM, Davis RB, Ettner SL, et al, 1998. Trends in alternative medicine use in the united states, 1990-1997: Results of a follow-up national survey. JAMA 280, 1569–1575. doi:10.1001/jama.280.18.1569

Elvin-Lewis, M., 2001. Should we be concerned about herbal remedies. J. Ethnopharmacol. 75, 141–164. doi:10.1016/S0378-8741(00)00394-9

Exner, N., Treske, B., Paquet, D., Holmström, K., Schiesling, C., Gispert, S., Carballo-Carbajal, I., Berg, D., Hoepken, H.-H., Gasser, T., Krüger, R., Winklhofer, K.F., Vogel, F., Reichert, A.S., Auburger, G., Kahle, P.J., Schmid, B., Haass, C., 2007a. Loss-of-function of human PINK1 results in mitochondrial pathology and can be rescued by parkin. J. Neurosci. Off. J. Soc. Neurosci. 27, 12413–12418. doi:10.1523/JNEUROSCI.0719-07.2007

Exner, N., Treske, B., Paquet, D., Holmström, K., Schiesling, C., Gispert, S., Carballo-Carbajal, I., Berg, D., Hoepken, H.-H., Gasser, T., Krüger, R., Winklhofer, K.F., Vogel, F., Reichert, A.S., Auburger, G., Kahle, P.J., Schmid, B., Haass, C., 2007b. Loss-of-Function of Human PINK1 Results in Mitochondrial Pathology and Can Be Rescued by Parkin. J. Neurosci. 27, 12413–12418. doi:10.1523/JNEUROSCI.0719-07.2007

Fahn, S., Oakes, D., Shoulson, I., Kieburtz, K., Rudolph, A., Lang, A., Olanow, C.W., Tanner, C., Marek, K., Parkinson Study Group, 2004. Levodopa and the progression of Parkinson's disease. N. Engl. J. Med. 351, 2498–2508. doi:10.1056/NEJMoa033447

Feuk, L., Carson, A.R., Scherer, S.W., 2006. Structural variation in the human genome. Nat. Rev. Genet. 7, 85–97. doi:10.1038/nrg1767

Fiala, M., Liu, P.T., Espinosa-Jeffrey, A., Rosenthal, M.J., Bernard, G., Ringman, J.M., Sayre, J., Zhang, L., Zaghi, J., Dejbakhsh, S., Chiang, B., Hui, J., Mahanian, M., Baghaee, A., Hong, P., Cashman, J., 2007. Innate immunity and transcription of MGAT-III and Toll-like receptors in Alzheimer's disease patients are improved by bisdemethoxycurcumin. Proc. Natl. Acad. Sci. U. S. A. 104, 12849–12854. doi:10.1073/pnas.0701267104

Follett, K.A., Weaver, F.M., Stern, M., Hur, K., Harris, C.L., Luo, P., Marks, W.J., Rothlind, J., Sagher, O., Moy, C., Pahwa, R., Burchiel, K., Hogarth, P., Lai, E.C., Duda, J.E., Holloway, K., Samii, A., Horn, S., Bronstein, J.M., Stoner, G., Starr, P.A., Simpson, R., Baltuch, G., De Salles, A., Huang, G.D., Reda, D.J., 2010. Pallidal versus Subthalamic Deep-Brain Stimulation for Parkinson's Disease. N. Engl. J. Med. 362, 2077–2091. doi:10.1056/NEJMoa0907083

Fukushima, T., Tanaka, K., Lim, H., Moriyama, M., 2002. Mechanism of cytotoxicity of paraquat. Environ. Health Prev. Med. 7, 89–94. doi:10.1265/ehpm.2002.89

Fukushima, T., Tawara, T., Lsobe, A., Hojo, N., Shiwaku, K., Yamane, Y., 1995. Radical formation site of cerebral complex I and Parkinson's disease. J. Neurosci. Res. 42, 385–390. doi:10.1002/jnr.490420313

Gandhi, S., Wood-Kaczmar, A., Yao, Z., Plun-Favreau, H., Deas, E., Klupsch, K., Downward, J., Latchman, D.S., Tabrizi, S.J., Wood, N.W., Duchen, M.R., Abramov, A.Y., 2009. PINK1-Associated Parkinson's Disease Is Caused by Neuronal Vulnerability to Calcium-Induced Cell Death. Mol. Cell 33, 627–638. doi:10.1016/j.molcel.2009.02.013

Ganguli M, Chandra V, Kamboh M, et al, 2000. Apolipoprotein e polymorphism and alzheimer disease: The indo-us cross-national dementia study. Arch. Neurol. 57, 824–830. doi:10.1001/archneur.57.6.824

Gao, J., Liu, R., Zhao, E., Huang, X., Nalls, M.A., Singleton, A.B., Chen, H., 2015. Head injury, potential interaction with genes, and risk for Parkinson's disease. Parkinsonism Relat. Disord. 21, 292–296. doi:10.1016/j.parkreldis.2014.12.033

Gautier, C.A., Kitada, T., Shen, J., 2008. Loss of PINK1 causes mitochondrial functional defects and increased sensitivity to oxidative stress. Proc. Natl. Acad. Sci. 105, 11364–11369. doi:10.1073/pnas.0802076105

Gegg, M.E., Cooper, J.M., Chau, K.-Y., Rojo, M., Schapira, A.H.V., Taanman, J.-W., 2010. Mitofusin 1 and mitofusin 2 are ubiquitinated in a PINK1/parkin-dependent manner upon induction of mitophagy. Hum. Mol. Genet. 19, 4861–4870. doi:10.1093/hmg/ddq419

Gegg, M.E., Cooper, J.M., Chau, K.-Y., Rojo, M., Schapira, A.H.V., Taanman, J.-W., 2010. Mitofusin 1 and mitofusin 2 are ubiquitinated in a PINK1/parkin-dependent manner upon induction of mitophagy. Hum. Mol. Genet. 19, 4861–4870. doi:10.1093/hmg/ddq419

Gegg, M.E., Cooper, J.M., Schapira, A.H.V., Taanman, J.-W., 2009. Silencing of PINK1 Expression Affects Mitochondrial DNA and Oxidative Phosphorylation in DOPAMINERGIC Cells. PLoS ONE 4, e4756. doi:10.1371/journal.pone.0004756

Geisler, S., Holmström, K.M., Skujat, D., Fiesel, F.C., Rothfuss, O.C., Kahle, P.J., Springer, W., 2010a. PINK1/Parkin-mediated mitophagy is dependent on VDAC1 and p62/SQSTM1. Nat. Cell Biol. 12, 119–131. doi:10.1038/ncb2012

Geisler, S., Holmström, K.M., Treis, A., Skujat, D., Weber, S.S., Fiesel, F.C., Kahle, P.J., Springer, W., 2010b. The PINK1/Parkin-mediated mitophagy is compromised by PD-associated mutations. Autophagy 6, 871–878.

Gibb, W.R., Lees, A.J., 1988. The relevance of the Lewy body to the pathogenesis of idiopathic Parkinson's disease. J. Neurol. Neurosurg. Psychiatry 51, 745–752. doi:10.1136/jnnp.51.6.745

Goldman, S.M., 2014. Environmental Toxins and Parkinson's Disease. Annu. Rev. Pharmacol. Toxicol. 54, 141–164. doi:10.1146/annurev-pharmtox-011613-135937

González-Salazar, A., Molina-Jijón, E., Correa, F., Zarco-Márquez, G., Calderón-Oliver, M., Tapia, E., Zazueta, C., Pedraza-Chaverri, J., 2011. Curcumin Protects from Cardiac Reperfusion Damage by Attenuation of Oxidant Stress and Mitochondrial Dysfunction. Cardiovasc. Toxicol. 11, 357–364. doi:10.1007/s12012-011-9128-9

Gottlieb, E., Armour, S.M., Harris, M.H., Thompson, C.B., 2003. Mitochondrial membrane potential regulates matrix configuration and cytochrome c release during apoptosis. Cell Death Differ. 10, 709–717. doi:10.1038/sj.cdd.4401231

Greene, J.C., Whitworth, A.J., Kuo, I., Andrews, L.A., Feany, M.B., Pallanck, L.J., 2003. Mitochondrial pathology and apoptotic muscle degeneration in Drosophila parkin mutants. Proc. Natl. Acad. Sci. 100, 4078–4083. doi:10.1073/pnas.0737556100

Grünewald, A., Gegg, M.E., Taanman, J.-W., King, R.H., Kock, N., Klein, C., Schapira, A.H.V., 2009. Differential effects of PINK1 nonsense and missense mutations on mitochondrial function and morphology. Exp. Neurol., Brain Stimulation in Psychiatry 219, 266–273. doi:10.1016/j.expneurol.2009.05.027

Grünewald, A., Voges, L., Rakovic, A., Kasten, M., Vandebona, H., Hemmelmann, C., Lohmann, K., Orolicki, S., Ramirez, A., Schapira, A.H.V., Pramstaller, P.P., Sue, C.M., Klein, C., 2010. Mutant Parkin Impairs Mitochondrial Function and Morphology in Human Fibroblasts. PLoS ONE 5, e12962. doi:10.1371/journal.pone.0012962

Gurdasani, D., Carstensen, T., Tekola-Ayele, F., Pagani, L., Tachmazidou, I., Hatzikotoulas, K., Karthikeyan, S., Iles, L., Pollard, M.O., Choudhury, A., Ritchie, G.R.S., Xue, Y., Asimit, J., Nsubuga, R.N., Young, E.H., Pomilla, C., Kivinen, K., Rockett, K., Kamali, A., Doumatey, A.P., Asiki, G., Seeley, J., Sisay-Joof, F., Jallow, M., Tollman, S., Mekonnen, E., Ekong, R., Oljira, T., Bradman, N., Bojang, K., Ramsay, M., Adeyemo, A., Bekele, E., Motala, A., Norris, S.A., Pirie, F., Kaleebu, P., Kwiatkowski, D., Tyler-Smith, C., Rotimi, C., Zeggini, E., Sandhu, M.S., 2015. The African Genome Variation Project shapes medical genetics in Africa. Nature 517, 327–332. doi:10.1038/nature13997

Hara, T., Nakamura, K., Matsui, M., Yamamoto, A., Nakahara, Y., Suzuki-Migishima, R., Yokoyama, M., Mishima, K., Saito, I., Okano, H., Mizushima, N., 2006. Suppression of basal autophagy in neural cells causes neurodegenerative disease in mice. Nature 441, 885–889. doi:10.1038/nature04724

Harish, G., Venkateshappa, C., Mythri, R.B., Dubey, S.K., Mishra, K., Singh, N., Vali, S., Bharath, M.M.S., 2010. Bioconjugates of curcumin display improved protection against glutathione depletion mediated oxidative stress in a dopaminergic neuronal cell line: Implications for Parkinson's disease. Bioorg. Med. Chem. 18, 2631–2638. doi:10.1016/j.bmc.2010.02.029

Harris, H., Rubinsztein, D.C., 2012. Control of autophagy as a therapy for neurodegenerative disease. Nat. Rev. Neurol. 8, 108–117. doi:10.1038/nrneurol.2011.200

Haylett, W.L., Keyser, R.J., du Plessis, M.C., van der Merwe, C., Blanckenberg, J., Lombard, D., Carr, J., Bardien, S., 2012. Mutations in the parkin gene are a minor cause of Parkinson's disease in the South African population. Parkinsonism Relat. Disord. 18, 89–92. doi:10.1016/j.parkreldis.2011.09.022

Hedrich, K., Eskelson, C., Wilmot, B., Marder, K., Harris, J., Garrels, J., Meija-Santana, H., Vieregge, P., Jacobs, H., Bressman, S.B., Lang, A.E., Kann, M., Abbruzzese, G., Martinelli, P., Schwinger, E., Ozelius, L.J., Pramstaller, P.P., Klein, C., Kramer, P., 2004. Distribution, type, and origin of Parkin mutations: Review and case studies. Mov. Disord. 19, 1146–1157. doi:10.1002/mds.20234

Hertzman, C., Wiens, M., Bowering, D., Snow, B., Calne, D., 1990. Parkinson's disease: A case-control study of occupational and environmental risk factors. Am. J. Ind. Med. 17, 349–355. doi:10.1002/ajim.4700170307

Hoepken, H.-H., Gispert, S., Morales, B., Wingerter, O., Del Turco, D., Mülsch, A., Nussbaum, R.L., Müller, K., Dröse, S., Brandt, U., Deller, T., Wirth, B., Kudin, A.P., Kunz, W.S., Auburger, G., 2007. Mitochondrial dysfunction, peroxidation damage and changes in glutathione metabolism in PARK6. Neurobiol. Dis. 25, 401–411. doi:10.1016/j.nbd.2006.10.007

Hr, X., Ls, H., Gy, L., 2010. SH-SY5Y human neuroblastoma cell line: in vitro cell model of dopaminergic neurons in Parkinson's disease. Chin. Med. J. (Engl.) 123, 1086–1092.

Huang, M.-T., Lysz, T., Ferraro, T., Abidi, T.F., Laskin, J.D., Conney, A.H., 1991. Inhibitory Effects of Curcumin on in Vitro Lipoxygenase and Cyclooxygenase Activities in Mouse Epidermis. Cancer Res. 51, 813–819.

Huang X, Chen P, Kaufer DI, Tröster AI, Poole C, 2006. Apolipoprotein e and dementia in parkinson disease: A meta-analysis. Arch. Neurol. 63, 189–193. doi:10.1001/archneur.63.2.189

Ibáñez, P., Bonnet, A.-M., Débarges, B., Lohmann, E., Tison, F., Agid, Y., Dürr, A., Brice, A., Pollak, P., 2004. Causal relation between α-synuclein locus duplication as a cause of familial Parkinson's disease. The Lancet 364, 1169–1171. doi:10.1016/S0140-6736(04)17104-3

Imai, Y., Soda, M., Murakami, T., Shoji, M., Abe, K., Takahashi, R., 2003. A Product of the Human Gene Adjacent to parkin Is a Component of Lewy Bodies and Suppresses Pael Receptor-induced Cell Death. J. Biol. Chem. 278, 51901–51910. doi:10.1074/jbc.M309655200

Imai, Y., Soda, M., Takahashi, R., 2000. Parkin Suppresses Unfolded Protein Stress-induced Cell Death through Its E3 Ubiquitin-protein Ligase Activity. J. Biol. Chem. 275, 35661–35664. doi:10.1074/jbc.C000447200

Jafari, S., Etminan, M., Aminzadeh, F., Samii, A., 2013. Head injury and risk of Parkinson disease: A systematic review and meta-analysis. Mov. Disord. 28, 1222–1229. doi:10.1002/mds.25458

Jaisin, Y., Thampithak, A., Meesarapee, B., Ratanachamnong, P., Suksamrarn, A., Phivthong-ngam, L., Phumala-Morales, N., Chongthammakun, S., Govitrapong, P., Sanvarinda, Y., 2011. Curcumin I protects the dopaminergic cell line SH-SY5Y from 6-hydroxydopamine-induced neurotoxicity through attenuation of p53-mediated apoptosis. Neurosci. Lett. 489, 192–196. doi:10.1016/j.neulet.2010.12.014

Jiang, T.-F., Zhang, Y.-J., Zhou, H.-Y., Wang, H.-M., Tian, L.-P., Liu, J., Ding, J.-Q., Chen, S.-D., 2013. Curcumin ameliorates the neurodegenerative pathology in A53T α-synuclein cell model of Parkinson's disease through the downregulation of mTOR/p70S6K signaling and the recovery of macroautophagy. J. Neuroimmune Pharmacol. Off. J. Soc. NeuroImmune Pharmacol. 8, 356–369. doi:10.1007/s11481-012-9431-7

Jia, Y.-L., Li, J., Qin, Z.-H., Liang, Z.-Q., 2009. Autophagic and apoptotic mechanisms of curcumin-induced death in K562 cells. J. Asian Nat. Prod. Res. 11, 918–928. doi:10.1080/10286020903264077

Jin, F., Wu, Q., Lu, Y.-F., Gong, Q.-H., Shi, J.-S., 2008. Neuroprotective effect of resveratrol on 6-OHDA-induced Parkinson's disease in rats. Eur. J. Pharmacol. 600, 78–82. doi:10.1016/j.ejphar.2008.10.005

Jin, S.M., Lazarou, M., Wang, C., Kane, L.A., Narendra, D.P., Youle, R.J., 2010. Mitochondrial membrane potential regulates PINK1 import and proteolytic destabilization by PARL. J. Cell Biol. 191, 933–942. doi:10.1083/jcb.201008084

Johnston, R.D., 2004. The Politics of Healing: Histories of Alternative Medicine in Twentieth-Century North America. Routledge.

Kamat, A.M., Sethi, G., Aggarwal, B.B., 2007. Curcumin potentiates the apoptotic effects of chemotherapeutic agents and cytokines through down-regulation of nuclear factor-κB and nuclear factor-κB–regulated gene products in IFN-α–sensitive and IFN-α–resistant human bladder cancer cells. Mol. Cancer Ther. 6, 1022–1030. doi:10.1158/1535-7163.MCT-06-0545

Kamel, F., Tanner, C.M., Umbach, D.M., Hoppin, J.A., Alavanja, M.C.R., Blair, A., Comyns, K., Goldman, S.M., Korell, M., Langston, J.W., Ross, G.W., Sandler, D.P., 2007. Pesticide Exposure and Self-reported Parkinson's Disease in the Agricultural Health Study. Am. J. Epidemiol. 165, 364–374. doi:10.1093/aje/kwk024

Kantara, C., O'Connell, M., Sarkar, S., Moya, S., Ullrich, R., Singh, P., 2014. Curcumin Promotes Autophagic Survival of a Subset of Colon Cancer Stem Cells, Which Are Ablated by DCLK1-siRNA. Cancer Res. 74, 2487–2498. doi:10.1158/0008-5472.CAN-13-3536

Karunagaran, D., Rashmi, R., Kumar, T.R.S., 2005. Induction of apoptosis by curcumin and its implications for cancer therapy. Curr. Cancer Drug Targets 5, 117–129.

Kawajiri, S., Saiki, S., Sato, S., Sato, F., Hatano, T., Eguchi, H., Hattori, N., 2010. PINK1 is recruited to mitochondria with parkin and associates with LC3 in mitophagy. FEBS Lett. 584, 1073–1079. doi:10.1016/j.febslet.2010.02.016

Kay, D.M., Stevens, C.F., Hamza, T.H., Montimurro, J.S., Zabetian, C.P., Factor, S.A., Samii, A., Griffith, A., Roberts, J.W., Molho, E.S., Higgins, D.S., Gancher, S., Moses, L., Zareparsi, S., Poorkaj, P., Bird, T., Nutt, J., Schellenberg, G.D., Payami, H., 2010. A comprehensive analysis of deletions, multiplications, and copy number variations in PARK2. Neurology 75, 1189–1194. doi:10.1212/WNL.0b013e3181f4d832

Keyser, R.J., Lombard, D., Veikondis, R., Carr, J., Bardien, S., 2009. Analysis of exon dosage using MLPA in South African Parkinson's disease patients. neurogenetics 11, 305–312. doi:10.1007/s10048-009-0229-6

Kim, M.-S., Kang, H.-J., Moon, A., 2001. Inhibition of Invasion and Induction of apoptosis by curcumin in H-ras-Transformed MCF10A human breast epithelial cells. Arch. Pharm. Res. 24, 349–354. doi:10.1007/BF02975105

Kim, Y., Park, J., Kim, S., Song, S., Kwon, S.-K., Lee, S.-H., Kitada, T., Kim, J.-M., Chung, J., 2008. PINK1 controls mitochondrial localization of Parkin through direct phosphorylation. Biochem. Biophys. Res. Commun. 377, 975–980. doi:10.1016/j.bbrc.2008.10.104

Kincheloe, L., n.d. Herbal medicines can reduce costs in HMO. [WWW Document].

Kitada, T., Pisani, A., Porter, D.R., Yamaguchi, H., Tscherter, A., Martella, G., Bonsi, P., Zhang, C., Pothos, E.N., Shen, J., 2007. Impaired dopamine release and synaptic plasticity in the striatum of PINK1-deficient mice. Proc. Natl. Acad. Sci. 104, 11441–11446. doi:10.1073/pnas.0702717104

Klein, C., Lohmann-Hedrich, K., Rogaeva, E., Schlossmacher, M.G., Lang, A.E., 2007. Deciphering the role of heterozygous mutations in genes associated with parkinsonism. Lancet Neurol. 6, 652–662. doi:10.1016/S1474-4422(07)70174-6

Ko, H.S., Coelln, R. von, Sriram, S.R., Kim, S.W., Chung, K.K.K., Pletnikova, O., Troncoso, J., Johnson, B., Saffary, R., Goh, E.L., Song, H., Park, B.-J., Kim, M.J., Kim, S., Dawson, V.L., Dawson, T.M., 2005. Accumulation of the Authentic Parkin Substrate Aminoacyl-tRNA Synthetase Cofactor, p38/JTV-1, Leads to Catecholaminergic Cell Death. J. Neurosci. 25, 7968–7978. doi:10.1523/JNEUROSCI.2172-05.2005

Ko, H.S., Kim, S.W., Sriram, S.R., Dawson, V.L., Dawson, T.M., 2006. Identification of Far Upstream Element-binding Protein-1 as an Authentic Parkin Substrate. J. Biol. Chem. 281, 16193–16196. doi:10.1074/jbc.C600041200

Komatsu, M., Waguri, S., Chiba, T., Murata, S., Iwata, J., Tanida, I., Ueno, T., Koike, M., Uchiyama, Y., Kominami, E., Tanaka, K., 2006. Loss of autophagy in the central nervous system causes neurodegeneration in mice. Nature 441, 880–884. doi:10.1038/nature04723

Krüger, R., Müller, T., Riess, O., 2000. Involvement of α-synuclein in Parkinson's disease and other neurodegenerative disorders. J. Neural Transm. 107, 31–40. doi:10.1007/s007020050002

Kunchandy, E., Rao, M.N.A., 1990. Oxygen radical scavenging activity of curcumin. Int. J. Pharm. 58, 237–240. doi:10.1016/0378-5173(90)90201-E

Kuroda, Y., Mitsui, T., Kunishige, M., Shono, M., Akaike, M., Azuma, H., Matsumoto, T., 2006. Parkin enhances mitochondrial biogenesis in proliferating cells. Hum. Mol. Genet. 15, 883–895. doi:10.1093/hmg/ddl006

Langston, J.W., 1985. The Case of the Tainted Heroin. The Sciences 25, 34–42. doi:10.1002/j.2326-1951.1985.tb02766.x

Lantto, T.A., Colucci, M., Závadová, V., Hiltunen, R., Raasmaja, A., 2009. Cytotoxicity of curcumin, resveratrol and plant extracts from basil, juniper, laurel and parsley in SH-SY5Y and CV1-P cells. Food Chem. 117, 405–411. doi:10.1016/j.foodchem.2009.04.018

Larry Baum, A.N., 2004. Curcumin interaction with copper and iron suggests one possible mechanism of action in Alzheimer's disease animal models. J. Alzheimer39s Dis. JAD 6, 367–77; discussion 443–9.

Lee, Y.J., Kim, N.-Y., Suh, Y.-A., Lee, C., 2011. Involvement of ROS in Curcumin-induced Autophagic Cell Death. Korean J. Physiol. Pharmacol. 15, 1. doi:10.4196/kjpp.2011.15.1.1

Legros, F., Lombès, A., Frachon, P., Rojo, M., 2002. Mitochondrial Fusion in Human Cells Is Efficient, Requires the Inner Membrane Potential, and Is Mediated by Mitofusins. Mol. Biol. Cell 13, 4343–4354. doi:10.1091/mbc.E02-06-0330

Lehman, N.L., 2009. The ubiquitin proteasome system in neuropathology. Acta Neuropathol. (Berl.) 118, 329–347. doi:10.1007/s00401-009-0560-x

Lesage, S., Condroyer, C., Klebe, S., Lohmann, E., Durif, F., Damier, P., Tison, F., Anheim, M., Honoré, A., Viallet, F., Bonnet, A.-M., Ouvrard-Hernandez, A.-M., Vidailhet, M., Durr, A., Brice, A., 2012. EIF4G1 in familial Parkinson's disease: pathogenic mutations or rare benign variants? Neurobiol. Aging 33, 2233.e1–2233.e5. doi:10.1016/j.neurobiolaging.2012.05.006

Liang, X.H., Jackson, S., Seaman, M., Brown, K., Kempkes, B., Hibshoosh, H., Levine, B., 1999. Induction of autophagy and inhibition of tumorigenesis by beclin 1. Nature 402, 672–676. doi:10.1038/45257

Lim, G.P., Chu, T., Yang, F., Beech, W., Frautschy, S.A., Cole, G.M., 2001. The Curry Spice Curcumin Reduces Oxidative Damage and Amyloid Pathology in an Alzheimer Transgenic Mouse. J. Neurosci. 21, 8370–8377.

Liou, H.H., Tsai, M.C., Chen, C.J., Jeng, J.S., Chang, Y.C., Chen, S.Y., Chen, R.C., 1997. Environmental risk factors and Parkinson's disease A case-control study in Taiwan. Neurology 48, 1583–1588. doi:10.1212/WNL.48.6.1583

Liu, S., Lu, B., 2010. Reduction of Protein Translation and Activation of Autophagy Protect against PINK1 Pathogenesis in Drosophila melanogaster. PLoS Genet 6, e1001237. doi:10.1371/journal.pgen.1001237

Liu, T.-Y., Tan, Z.-J., Jiang, L., Gu, J.-F., Wu, X.-S., Cao, Y., Li, M.-L., Wu, K.-J., Liu, Y.-B., 2013. Curcumin induces apoptosis in gallbladder carcinoma cell line GBC-SD cells. Cancer Cell Int. 13, 64. doi:10.1186/1475-2867-13-64

Liu, Z., Li, T., Yang, D., Smith, W.W., 2013. Curcumin protects against rotenone-induced neurotoxicity in cell and drosophila models of Parkinson's disease. Adv. Park. Dis. 02, 18. doi:10.4236/apd.2013.21004

Li, Y., Zhang, J., Ma, D., Zhang, L., Si, M., Yin, H., Li, J., 2012. Curcumin inhibits proliferation and invasion of osteosarcoma cells through inactivation of Notch-1 signaling. FEBS J. 279, 2247–2259. doi:10.1111/j.1742-4658.2012.08607.x

Loos, B., Toit, A. du, Hofmeyr, J.-H.S., 2014. Defining and measuring autophagosome flux—concept and reality. Autophagy 10, 2087–2096. doi:10.4161/15548627.2014.973338

Lozano, A.M., Giacobbe, P., Hamani, C., Rizvi, S.J., Kennedy, S.H., Kolivakis, T.T., Debonnel, G., Sadikot, A.F., Lam, R.W., Howard, A.K., Ilcewicz-Klimek, M., Honey, C.R., Mayberg, H.S., 2011. A multicenter pilot study of subcallosal cingulate area deep brain stimulation for treatment-resistant depression. J. Neurosurg. 116, 315–322. doi:10.3171/2011.10.JNS102122

Lücking, C.B., Dürr, A., Bonifati, V., Vaughan, J., De Michele, G., Gasser, T., Harhangi, B.S., Meco, G., Denèfle, P., Wood, N.W., Agid, Y., Nicholl, D., Breteler, M.M.B., Oostra, B.A., De Mari, M., Marconi, R., Filla, A., Bonnet, A.-M., Broussolle, E., Pollak, P., Rascol, O., Rosier, M., Arnould, A., Brice, A., 2000. Association between Early-Onset Parkinson's Disease and Mutations in the Parkin Gene. N. Engl. J. Med. 342, 1560–1567. doi:10.1056/NEJM200005253422103

Luk, K.C., Lee, V.M.-Y., 2014. Modeling Lewy pathology propagation in Parkinson's disease. Parkinsonism Relat. Disord., Proceedings of XX World Congress on Parkinson's Disease and Related Disorders 20, Supplement 1, S85–S87. doi:10.1016/S1353-8020(13)70022-1

Lutz, A.K., Exner, N., Fett, M.E., Schlehe, J.S., Kloos, K., Lammermann, K., Brunner, B., Kurz-Drexler, A., Vogel, F., Reichert, A.S., Bouman, L., Vogt-Weisenhorn, D., Wurst, W., Tatzelt, J., Haass, C., Winklhofer, K.F., 2009. Loss of Parkin or PINK1 Function Increases Drp1-dependent Mitochondrial Fragmentation. J. Biol. Chem. 284, 22938–22951. doi:10.1074/jbc.M109.035774

Ly, J.D., Grubb, D.R., Lawen, A., 2003. The mitochondrial membrane potential (Δψm) in apoptosis; an update. Apoptosis 8, 115–128. doi:10.1023/A:1022945107762

Macleod, A.D., Taylor, K.S.M., Counsell, C.E., 2014. Mortality in Parkinson's disease: A systematic review and meta-analysis. Mov. Disord. 29, 1615–1622. doi:10.1002/mds.25898

Mader, B.J., Pivtoraiko, V.N., Flippo, H.M., Klocke, B.J., Roth, K.A., Mangieri, L.R., Shacka, J.J., 2012. Rotenone Inhibits Autophagic Flux Prior to Inducing Cell Death. ACS Chem. Neurosci. 3, 1063–1072. doi:10.1021/cn300145z

Manikandan, P., Sumitra, M., Aishwarya, S., Manohar, B.M., Lokanadam, B., Puvanakrishnan, R., 2004. Curcumin modulates free radical quenching in myocardial ischaemia in rats. Int. J. Biochem. Cell Biol. 36, 1967–1980. doi:10.1016/j.biocel.2004.01.030

Marongiu, R., Brancati, F., Antonini, A., Ialongo, T., Ceccarini, C., Scarciolla, O., Capalbo, A., Benti, R., Pezzoli, G., Dallapiccola, B., Goldwurm, S., Valente, E.M., 2007. Whole gene deletion and splicing mutations expand the PINK1 genotypic spectrum. Hum. Mutat. 28, 98–98. doi:10.1002/humu.9472

McCormack, A.L., Thiruchelvam, M., Manning-Bog, A.B., Thiffault, C., Langston, J.W., Cory-Slechta, D.A., Di Monte, D.A., 2002. Environmental Risk Factors and Parkinson's Disease: Selective Degeneration of Nigral Dopaminergic Neurons Caused by the Herbicide Paraquat. Neurobiol. Dis. 10, 119–127. doi:10.1006/nbdi.2002.0507

Meissner, C., Lorenz, H., Weihofen, A., Selkoe, D.J., Lemberg, M.K., 2011. The mitochondrial intramembrane protease PARL cleaves human Pink1 to regulate Pink1 trafficking. J. Neurochem. 117, 856–867. doi:10.1111/j.1471-4159.2011.07253.x

Michiorri, S., Gelmetti, V., Giarda, E., Lombardi, F., Romano, F., Marongiu, R., Nerini-Molteni, S., Sale, P., Vago, R., Arena, G., Torosantucci, L., Cassina, L., Russo, M.A., Dallapiccola, B., Valente, E.M., Casari, G., 2010. The Parkinson-associated protein PINK1 interacts with Beclin1 and promotes autophagy. Cell Death Differ. 17, 962–974. doi:10.1038/cdd.2009.200

Miller, W.C., DeLong, M.R., 1987. Altered Tonic Activity of Neurons in the Globus Pallidus and Subthalamic Nucleus in the Primate MPTP Model of Parkinsonism, in: Carpenter, M.B., Jayaraman, A. (Eds.), The Basal Ganglia II, Advances in Behavioral Biology. Springer US, pp. 415–427.

Mizushima, N., 2007. Autophagy: process and function. Genes Dev. 21, 2861–2873. doi:10.1101/gad.1599207

Mohammadi-Bardbori, A., Ghazi-Khansari, M., 2008. Alternative electron acceptors: Proposed mechanism of paraquat mitochondrial toxicity. Environ. Toxicol. Pharmacol. 26, 1–5. doi:10.1016/j.etap.2008.02.009

Molina-Jijón, E., Tapia, E., Zazueta, C., El Hafidi, M., Zatarain-Barrón, Z.L., Hernández-Pando, R., Medina-Campos, O.N., Zarco-Márquez, G., Torres, I., Pedraza-Chaverri, J., 2011. Curcumin prevents Cr(VI)-induced renal oxidant damage by a mitochondrial pathway. Free Radic. Biol. Med. 51, 1543–1557. doi:10.1016/j.freeradbiomed.2011.07.018

Moore, D.J., Dawson, V.L., Dawson, T.M., 2003. Role for the ubiquitin-proteasome system in Parkinson's disease and other neurodegenerative brain amyloidoses. NeuroMolecular Med. 4, 95–108. doi:10.1385/NMM:4:1-2:95

Mortiboys, H., Thomas, K.J., Koopman, W.J.H., Klaffke, S., Abou-Sleiman, P., Olpin, S., Wood, N.W., Willems, P.H.G.M., Smeitink, J.A.M., Cookson, M.R., Bandmann, O., 2008. Mitochondrial function and morphology are impaired in parkin-mutant fibroblasts. Ann. Neurol. 64, 555–565. doi:10.1002/ana.21492

Moura, K.C.V., Junior, M., Campos, R., de Rosso, A.L., Zuma, C., Nicaretta, D.H., Pereira, J., Santos, O., Silva, D.J., Santos-Rebouças, C., Barros, N., Pimentel, M., Gonçrcia M., alves, 2012. Exon Dosage Variations in Brazilian Patients with Parkinson's Disease: Analysis of *SNCA*, *PARKIN*, *PINK1* and *DJ-1* Genes. Dis. Markers 32, 173–178. doi:10.3233/DMA-2011-0873

Muthane, U., Yasha, T.C., Shankar, S.K., 1998. Low numbers and no loss of melanized nigral neurons with increasing age in normal human brains from India. Ann. Neurol. 43, 283–287. doi:10.1002/ana.410430304

Mythri, R.B., Bharath, M.M.S., 2012. Curcumin: a potential neuroprotective agent in Parkinson's disease. Curr. Pharm. Des. 18, 91–99.

Mythri, R.B., Harish, G., Dubey, S.K., Misra, K., Bharath, M.M.S., 2010. Glutamoyl diester of the dietary polyphenol curcumin offers improved protection against peroxynitrite-mediated nitrosative stress and damage of brain mitochondria in vitro: implications for Parkinson's disease. Mol. Cell. Biochem. 347, 135–143. doi:10.1007/s11010-010-0621-4

Mythri, R.B., Jagatha, B., Pradhan, N., Andersen, J., Bharath, M.M.S., 2007. Mitochondrial Complex I Inhibition in Parkinson's Disease: How Can Curcumin Protect Mitochondria? Antioxid. Redox Signal. 9, 399–408. doi:10.1089/ars.2006.1479

Narendra, D.P., Jin, S.M., Tanaka, A., Suen, D.-F., Gautier, C.A., Shen, J., Cookson, M.R., Youle, R.J., 2010. PINK1 Is Selectively Stabilized on Impaired Mitochondria to Activate Parkin. PLoS Biol 8, e1000298. doi:10.1371/journal.pbio.1000298

Narendra, D., Tanaka, A., Suen, D.-F., Youle, R.J., 2008. Parkin is recruited selectively to impaired mitochondria and promotes their autophagy. J. Cell Biol. 183, 795–803. doi:10.1083/jcb.200809125

Nelson, M.P., Shacka, J.J., 2013. Autophagy Modulation in Disease Therapy: Where Do We Stand? Curr. Pathobiol. Rep. 1, 239–245. doi:10.1007/s40139-013-0032-9

Nicholls, D.G., 2008. Oxidative Stress and Energy Crises in Neuronal Dysfunction. Ann. N. Y. Acad. Sci. 1147, 53–60. doi:10.1196/annals.1427.002

Nichols, N., Bras, J.M., Hernandez, D.G., Jansen, I.E., Lesage, S., Lubbe, S., Singleton, A.B., 2015. EIF4G1 mutations do not cause Parkinson's disease. Neurobiol. Aging 36, 2444.e1–2444.e4. doi:10.1016/j.neurobiolaging.2015.04.017

Nixon, R.A., 2006. Autophagy in neurodegenerative disease: friend, foe or turncoat? Trends Neurosci. 29, 528–535. doi:10.1016/j.tins.2006.07.003

Nuytemans, K., Theuns, J., Cruts, M., Van Broeckhoven, C., 2010. Genetic etiology of Parkinson disease associated with mutations in the SNCA, PARK2, PINK1, PARK7, and LRRK2 genes: a mutation update. Hum. Mutat. 31, 763–780. doi:10.1002/humu.21277

Olanow, C.W., McNaught, K.S.P., 2006. Ubiquitin–proteasome system and Parkinson's disease. Mov. Disord. 21, 1806–1823. doi:10.1002/mds.21013

Ono, K., Hasegawa, K., Naiki, H., Yamada, M., 2004. Curcumin has potent anti-amyloidogenic effects for Alzheimer's β-amyloid fibrils in vitro. J. Neurosci. Res. 75, 742–750. doi:10.1002/jnr.20025

Ortiz-Ortiz, M.A., Morán, J.M., Ruiz-Mesa, L.M., Niso-Santano, M., Bravo-SanPedro, J.M., Gómez-Sánchez, R., González-Polo, R.A., Fuentes, J.M., 2010. Curcumin exposure induces expression of the Parkinson's disease-associated leucine-rich repeat kinase 2 (LRRK2) in rat mesencephalic cells. Neurosci. Lett. 468, 120–124. doi:10.1016/j.neulet.2009.10.081

O'Sullivan-Coyne, G., O'Sullivan, G.C., O'Donovan, T.R., Piwocka, K., McKenna, S.L., 2009. Curcumin induces apoptosis-independent death in oesophageal cancer cells. Br. J. Cancer 101, 1585–1595. doi:10.1038/sj.bjc.6605308

Ozelius, L.J., Senthil, G., Saunders-Pullman, R., Ohmann, E., Deligtisch, A., Tagliati, M., Hunt, A.L., Klein, C., Henick, B., Hailpern, S.M., Lipton, R.B., Soto-Valencia, J., Risch, N., Bressman, S.B., 2006. LRRK2 G2019S as a Cause of Parkinson's Disease in Ashkenazi Jews. N. Engl. J. Med. 354, 424–425. doi:10.1056/NEJMc055509

Pacelli, C., De Rasmo, D., Signorile, A., Grattagliano, I., di Tullio, G., D'Orazio, A., Nico, B., Comi, G.P., Ronchi, D., Ferranini, E., Pirolo, D., Seibel, P., Schubert, S., Gaballo, A., Villani, G., Cocco, T., 2011. Mitochondrial defect and PGC-1α dysfunction in parkin-associated familial Parkinson's disease. Biochim. Biophys. Acta BBA - Mol. Basis Dis., Translating nuclear receptors from health to disease 1812, 1041–1053. doi:10.1016/j.bbadis.2010.12.022

Paisán-Ruíz, C., Lang, A.E., Kawarai, T., Sato, C., Salehi-Rad, S., Fisman, G.K., Al-Khairallah, T., George-Hyslop, P.S., Singleton, A., Rogaeva, E., 2005. LRRK2 gene in Parkinson disease Mutation analysis and case control association study. Neurology 65, 696–700. doi:10.1212/01.WNL.0000167552.79769.b3

Pan, Y., Wang, Y., Cai, L., Cai, Y., Hu, J., Yu, C., Li, J., Feng, Z., Yang, S., Li, X., Liang, G., 2012. Inhibition of high glucose-induced inflammatory response and macrophage infiltration by a novel curcumin derivative prevents renal injury in diabetic rats. Br. J. Pharmacol. 166, 1169–1182. doi:10.1111/j.1476-5381.2012.01854.x

Parkinson, J., 2002. An essay on the shaking palsy. 1817. J. Neuropsychiatry Clin. Neurosci. 14, 223–236; discussion 222.

Park, J., Lee, S.B., Lee, S., Kim, Y., Song, S., Kim, S., Bae, E., Kim, J., Shong, M., Kim, J.-M., Chung, J., 2006. Mitochondrial dysfunction in Drosophila PINK1 mutants is complemented by parkin. Nature 441, 1157–1161. doi:10.1038/nature04788

P, A., S, V., F, J.-A., Mt, H., Pp, M., J, M., A, M.-P., M, R., Ec, H., Y, A., 1997. Apoptosis and autophagy in nigral neurons of patients with Parkinson's disease. Histol. Histopathol. 12, 25–31.

Periquet, M., Latouche, M., Lohmann, E., Rawal, N., De Michele, G., Ricard, S., Teive, H., Fraix, V., Vidailhet, M., Nicholl, D., Barone, P., Wood, N.W., Raskin, S., Deleuze, J.-F., Agid, Y., Dürr, A., Brice, A., French Parkinson's Disease Genetics Study Group, European Consortium on Genetic Susceptibility in Parkinson's Disease, 2003. Parkin mutations are frequent in patients with isolated early-onset parkinsonism. Brain J. Neurol. 126, 1271–1278.

Piccoli, C., Sardanelli, A., Scrima, R., Ripoli, M., Quarato, G., D'Aprile, A., Bellomo, F., Scacco, S., Michele, G.D., Filla, A., Iuso, A., Boffoli, D., Capitanio, N., Papa, S., 2008. Mitochondrial Respiratory Dysfunction in Familiar Parkinsonism Associated with PINK1 Mutation. Neurochem. Res. 33, 2565–2574. doi:10.1007/s11064-008-9729-2

Pickrell, A.M., Youle, R.J., 2015. The Roles of PINK1, Parkin, and Mitochondrial Fidelity in Parkinson's Disease. Neuron 85, 257–273. doi:10.1016/j.neuron.2014.12.007

Polymeropoulos, M.H., Lavedan, C., Leroy, E., Ide, S.E., Dehejia, A., Dutra, A., Pike, B., Root, H., Rubenstein, J., Boyer, R., Stenroos, E.S., Chandrasekharappa, S., Athanassiadou, A., Papapetropoulos, T., Johnson, W.G., Lazzarini, A.M., Duvoisin, R.C., Iorio, G.D., Golbe, L.I.,

Nussbaum, R.L., 1997. Mutation in the α-Synuclein Gene Identified in Families with Parkinson's Disease. Science 276, 2045–2047. doi:10.1126/science.276.5321.2045

Poole, A.C., Thomas, R.E., Andrews, L.A., McBride, H.M., Whitworth, A.J., Pallanck, L.J., 2008. The PINK1/Parkin pathway regulates mitochondrial morphology. Proc. Natl. Acad. Sci. U. S. A. 105, 1638–1643. doi:10.1073/pnas.0709336105

Pringsheim, T., Jette, N., Frolkis, A., Steeves, T.D.L., 2014. The prevalence of Parkinson's disease: A systematic review and meta-analysis. Mov. Disord. 29, 1583–1590. doi:10.1002/mds.25945

Priyadarshi, A., Khuder, S.A., Schaub, E.A., Priyadarshi, S.S., 2001. Environmental Risk Factors and Parkinson's Disease: A Metaanalysis. Environ. Res. 86, 122–127. doi:10.1006/enrs.2001.4264

Puissant, A., Fenouille, N., Auberger, P., 2012. When autophagy meets cancer through p62/SQSTM1. Am. J. Cancer Res. 2, 397–413.

Qian, H., Yang, Y., Wang, X., 2011. Curcumin enhanced adriamycin-induced human liver-derived Hepatoma G2 cell death through activation of mitochondria-mediated apoptosis and autophagy. Eur. J. Pharm. Sci. Off. J. Eur. Fed. Pharm. Sci. 43, 125–131. doi:10.1016/j.ejps.2011.04.002

Rajeswari, A., 2006. Curcumin protects mouse brain from oxidative stress caused by 1-methyl-4-phenyl-1,2,3,6-tetrahydropyridine. Eur. Rev. Med. Pharmacol. Sci. 10, 157–161.

Rakovic, A., Shurkewitsch, K., Seibler, P., Grünewald, A., Zanon, A., Hagenah, J., Krainc, D., Klein, C., 2013. Phosphatase and Tensin Homolog (PTEN)-induced Putative Kinase 1 (PINK1)-dependent Ubiquitination of Endogenous Parkin Attenuates Mitophagy STUDY IN HUMAN PRIMARY FIBROBLASTS AND INDUCED PLURIPOTENT STEM CELL-DERIVED NEURONS. J. Biol. Chem. 288, 2223–2237. doi:10.1074/jbc.M112.391680

Ramsay, M., Tiemessen, C.T., Choudhury, A., Soodyall, H., 2011. Africa: The Next Frontier for Human Disease Gene Discovery? Hum. Mol. Genet. ddr401. doi:10.1093/hmg/ddr401

Raza, H., John, A., Brown, E.M., Benedict, S., Kambal, A., 2008. Alterations in mitochondrial respiratory functions, redox metabolism and apoptosis by oxidant 4-hydroxynonenal and antioxidants curcumin and melatonin in PC12 cells. Toxicol. Appl. Pharmacol. 226, 161–168. doi:10.1016/j.taap.2007.09.002

Rezende, A.C.S., Vieira, A.S., Rogério, F., Rezende, L.F., Boschero, A.C., Negro, A., Langone, F., 2008. Effects of systemic administration of ciliary neurotrophic factor on Bax and Bcl-2 proteins in the lumbar spinal cord of neonatal rats after sciatic nerve transection. Braz. J. Med. Biol. Res. Rev. Bras. Pesqui. Médicas E Biológicas Soc. Bras. Biofísica Al 41, 1024–1028.

Sandebring, A., Thomas, K.J., Beilina, A., van der Brug, M., Cleland, M.M., Ahmad, R., Miller, D.W., Zambrano, I., Cowburn, R.F., Behbahani, H., Cedazo-Mínguez, A., Cookson, M.R., 2009. Mitochondrial Alterations in PINK1 Deficient Cells Are Influenced by Calcineurin-Dependent Dephosphorylation of Dynamin-Related Protein 1. PLoS ONE 4, e5701. doi:10.1371/journal.pone.0005701

Schapira, A.H.V., Cooper, J.M., Dexter, D., Clark, J.B., Jenner, P., Marsden, C.D., 1990. Mitochondrial Complex I Deficiency in Parkinson's Disease. J. Neurochem. 54, 823–827. doi:10.1111/j.1471-4159.1990.tb02325.x

Schapira, A.H.V., Gu, M., Taanman, J.-W., Tabrizi, S.J., Seaton, T., Cleeter, M., Cooper, J.M., 1998. Mitochondria in the etiology and pathogenesis of parkinson's disease. Ann. Neurol. 44, S89–S98. doi:10.1002/ana.410440714

Schraufstätter, E., Bernt, H., 1949. Antibacterial Action of Curcumin and Related Compounds. Nature 164, 456–457. doi:10.1038/164456a0

Scott, R.C., Juhász, G., Neufeld, T.P., 2007. Direct Induction of Autophagy by Atg1 Inhibits Cell Growth and Induces Apoptotic Cell Death. Curr. Biol. 17, 1–11. doi:10.1016/j.cub.2006.10.053

Seibler, P., Graziotto, J., Jeong, H., Simunovic, F., Klein, C., Krainc, D., 2011. Mitochondrial Parkin Recruitment Is Impaired in Neurons Derived from Mutant PINK1 Induced Pluripotent Stem Cells. J. Neurosci. 31, 5970–5976. doi:10.1523/JNEUROSCI.4441-10.2011

Sha, D., Chin, L.-S., Li, L., 2009. Phosphorylation of parkin by Parkinson disease-linked kinase PINK1 activates parkin E3 ligase function and NF-κB signaling. Hum. Mol. Genet. ddp501. doi:10.1093/hmg/ddp501

Sharma, S., Chopra, K., Kulkarni, S.K., Agrewala, J.N., 2007. Resveratrol and curcumin suppress immune response through CD28/CTLA-4 and CD80 co-stimulatory pathway. Clin. Exp. Immunol. 147, 155–163. doi:10.1111/j.1365-2249.2006.03257.x

Sherer, T.B., Betarbet, R., Greenamyre, J.T., 2002. Environment, Mitochondria, and Parkinson's Disease. The Neuroscientist 8, 192–197. doi:10.1177/1073858402008003004

Sherer, T.B., Betarbet, R., Testa, C.M., Seo, B.B., Richardson, J.R., Kim, J.H., Miller, G.W., Yagi, T., Matsuno-Yagi, A., Greenamyre, J.T., 2003. Mechanism of Toxicity in Rotenone Models of Parkinson's Disease. J. Neurosci. 23, 10756–10764.

Sherwood, L., 2015. Human Physiology: From Cells to Systems. Cengage Learning.

Shiba, K., Arai, T., Sato, S., Kubo, S., Ohba, Y., Mizuno, Y., Hattori, N., 2009. Parkin stabilizes PINK1 through direct interaction. Biochem. Biophys. Res. Commun. 383, 331–335. doi:10.1016/j.bbrc.2009.04.006

Silvestri, L., Caputo, V., Bellacchio, E., Atorino, L., Dallapiccola, B., Valente, E.M., Casari, G., 2005. Mitochondrial import and enzymatic activity of PINK1 mutants associated to recessive parkinsonism. Hum. Mol. Genet. 14, 3477–3492. doi:10.1093/hmg/ddi377

Singleton, A.B., Farrer, M., Johnson, J., Singleton, A., Hague, S., Kachergus, J., Hulihan, M., Peuralinna, T., Dutra, A., Nussbaum, R., Lincoln, S., Crawley, A., Hanson, M., Maraganore, D., Adler, C., Cookson, M.R., Muenter, M., Baptista, M., Miller, D., Blancato, J., Hardy, J., Gwinn-Hardy, K., 2003. α-Synuclein Locus Triplication Causes Parkinson's Disease. Science 302, 841–841. doi:10.1126/science.1090278

Siuda, J., Jasinska-Myga, B., Boczarska-Jedynak, M., Opala, G., Fiesel, F.C., Moussaud-Lamodière, E.L., Scarffe, L.A., Dawson, V.L., Ross, O.A., Springer, W., Dawson, T.M., Wszolek, Z.K., 2014. Early-onset Parkinson's disease due to PINK1 p.Q456X mutation – Clinical and functional study. Parkinsonism Relat. Disord. 20, 1274–1278. doi:10.1016/j.parkreldis.2014.08.019

Siwak, D.R., Shishodia, S., Aggarwal, B.B., Kurzrock, R., 2005. Curcumin-induced antiproliferative and proapoptotic effects in melanoma cells are associated with suppression of IκB kinase and nuclear factor κB activity and are independent of the B-Raf/mitogen-activated/extracellular signal-regulated protein kinase pathway and the Akt pathway. Cancer 104, 879–890. doi:10.1002/cncr.21216

Snyder, H., Mensah, K., Theisler, C., Lee, J., Matouschek, A., Wolozin, B., 2003. Aggregated and Monomeric α-Synuclein Bind to the S6' Proteasomal Protein and Inhibit Proteasomal Function. J. Biol. Chem. 278, 11753–11759. doi:10.1074/jbc.M208641200

Song, S., Jang, S., Park, J., Bang, S., Choi, S., Kwon, K.-Y., Zhuang, X., Kim, E., Chung, J., 2013. Characterization of PINK1 (PTEN-induced putative kinase 1) mutations associated with Parkinson disease in mammalian cells and Drosophila. J. Biol. Chem. 288, 5660–5672. doi:10.1074/jbc.M112.430801

Sood, P.K., Nahar, U., Nehru, B., 2011. Curcumin Attenuates Aluminum-Induced Oxidative Stress and Mitochondrial Dysfunction in Rat Brain. Neurotox. Res. 20, 351–361. doi:10.1007/s12640-011-9249-8

Spillantini, M.G., Schmidt, M.L., Lee, V.M.-Y., Trojanowski, J.Q., Jakes, R., Goedert, M., 1997. α-Synuclein in Lewy bodies. Nature 388, 839–840. doi:10.1038/42166

St. P. McNaught, K., Belizaire, R., Isacson, O., Jenner, P., Olanow, C.W., 2003. Altered Proteasomal Function in Sporadic Parkinson's Disease. Exp. Neurol. 179, 38–46. doi:10.1006/exnr.2002.8050

Sul, J.-W., Park, M.-Y., Shin, J., Kim, Y.-R., Yoo, S.-E., Kong, Y.-Y., Kwon, K.-S., Lee, Y.H., Kim, E., 2013. Accumulation of the parkin substrate, FAF1, plays a key role in the dopaminergic neurodegeneration. Hum. Mol. Genet. ddt006. doi:10.1093/hmg/ddt006

Takahashi, R., Imai, Y., 2003. Pael receptor, endoplasmic reticulum stress, and Parkinson's disease. J. Neurol. 250, iii25–iii29. doi:10.1007/s00415-003-1305-8

Tan, C.-C., Yu, J.-T., Tan, M.-S., Jiang, T., Zhu, X.-C., Tan, L., 2014. Autophagy in aging and neurodegenerative diseases: implications for pathogenesis and therapy. Neurobiol. Aging 35, 941–957. doi:10.1016/j.neurobiolaging.2013.11.019

Tanner, C.M., Kamel, F., Ross, G.W., Hoppin, J.A., Goldman, S.M., Korell, M., Marras, C., Bhudhikanok, G.S., Kasten, M., Chade, A.R., Comyns, K., Richards, M.B., Meng, C., Priestley, B., Fernandez, H.H., Cambi, F., Umbach, D.M., Blair, A., Sandler, D.P., Langston, J.W., 2011. Rotenone, Paraquat, and Parkinson's Disease. Environ. Health Perspect. 119, 866–872. doi:10.1289/ehp.1002839

Taylor, J.P., Hardy, J., Fischbeck, K.H., 2002. Toxic Proteins in Neurodegenerative Disease. Science 296, 1991–1995. doi:10.1126/science.1067122

Thorburn, A., 2007. Apoptosis and autophagy: regulatory connections between two supposedly different processes. Apoptosis 13, 1–9. doi:10.1007/s10495-007-0154-9

Toft, M., Ross, O.A., 2010. Copy number variation in Parkinson's disease. Genome Med 2, 1–4. doi:10.1186/gm183

Trinh, J., Farrer, M., 2013. Advances in the genetics of Parkinson disease. Nat. Rev. Neurol. 9, 445+.

Tu, P., Galvin, J.E., Baba, M., Giasson, B., Tomita, T., Leight, S., Nakajo, S., Iwatsubo, T., Trojanowski, J.Q., Lee, V.M.-Y., 1998. Glial cytoplasmic inclusions in white matter oligodendrocytes of multiple system atrophy brains contain insoluble α-synuclein. Ann. Neurol. 44, 415–422. doi:10.1002/ana.410440324

Um, J.W., Stichel-Gunkel, C., Lübbert, H., Lee, G., Chung, K.C., 2009. Molecular interaction between parkin and PINK1 in mammalian neuronal cells. Mol. Cell. Neurosci. 40, 421–432. doi:10.1016/j.mcn.2008.12.010

Valente, E.M., Abou-Sleiman, P.M., Caputo, V., Muqit, M.M.K., Harvey, K., Gispert, S., Ali, Z., Turco, D.D., Bentivoglio, A.R., Healy, D.G., Albanese, A., Nussbaum, R., González-Maldonado, R., Deller, T., Salvi, S., Cortelli, P., Gilks, W.P., Latchman, D.S., Harvey, R.J., Dallapiccola, B., Auburger, G., Wood, N.W., 2004. Hereditary Early-Onset Parkinson's Disease Caused by Mutations in PINK1. Science 304, 1158–1160. doi:10.1126/science.1096284

van der Mark, M., Brouwer, M., Kromhout, H., Nijssen, P., Huss, A., Vermeulen, R., 2011. Is Pesticide Use Related to Parkinson Disease? Some Clues to Heterogeneity in Study Results. Environ. Health Perspect. 120, 340–347. doi:10.1289/ehp.1103881

Van der Merwe, C., Christoffel, A., Loos, B., Bardien, S., Dashti, Z.J., 2015. Evidence for a common biological pathway linking three Parkinson's Disease causing genes.

van der Merwe, C., Loos, B., Swart, C., Kinnear, C., Henning, F., van der Merwe, L., Pillay, K., Muller, N., Zaharie, D., Engelbrecht, L., Carr, J., Bardien, S., 2014. Mitochondrial impairment observed in fibroblasts from South African Parkinson's disease patients with parkin mutations. Biochem. Biophys. Res. Commun. 447, 334–340. doi:10.1016/j.bbrc.2014.03.151

Van Laar, V.S., Berman, S.B., 2013. The interplay of neuronal mitochondrial dynamics and bioenergetics: Implications for Parkinson's disease. Neurobiol. Dis., Mitochondrial dynamics and quality control in neuropsychiatric diseases 51, 43–55. doi:10.1016/j.nbd.2012.05.015

Vaughan, R.A., Garcia-Smith, R., Dorsey, J., Griffith, J.K., Bisoffi, M., Trujillo, K.A., 2013. Tumor necrosis factor alpha induces Warburg-like metabolism and is reversed by anti-inflammatory curcumin in breast epithelial cells. Int. J. Cancer 133, 2504–2510. doi:10.1002/ijc.28264

Vilariño-Güell, C., Wider, C., Ross, O.A., Dachsel, J.C., Kachergus, J.M., Lincoln, S.J., Soto-Ortolaza, A.I., Cobb, S.A., Wilhoite, G.J., Bacon, J.A., Behrouz, B., Melrose, H.L., Hentati, E., Puschmann, A., Evans, D.M., Conibear, E., Wasserman, W.W., Aasly, J.O., Burkhard, P.R., Djaldetti, R., Ghika, J., Hentati, F., Krygowska-Wajs, A., Lynch, T., Melamed, E., Rajput, A., Rajput, A.H., Solida, A., Wu, R.-M., Uitti, R.J., Wszolek, Z.K., Vingerhoets, F., Farrer, M.J., 2011. VPS35 Mutations in Parkinson Disease. Am. J. Hum. Genet. 89, 162–167. doi:10.1016/j.ajhg.2011.06.001

Vives-Bauza, C., Zhou, C., Huang, Y., Cui, M., Vries, R.L.A. de, Kim, J., May, J., Tocilescu, M.A., Liu, W., Ko, H.S., Magrané, J., Moore, D.J., Dawson, V.L., Grailhe, R., Dawson, T.M., Li, C., Tieu, K., Przedborski, S., Snyder, S.H., 2010. PINK1-Dependent Recruitment of Parkin to Mitochondria in Mitophagy. Proc. Natl. Acad. Sci. U. S. A. 107, 378–383.

Wang, C., Zhang, X., Teng, Z., Zhang, T., Li, Y., 2014. Downregulation of PI3K/Akt/mTOR signaling pathway in curcumin-induced autophagy in APP/PS1 double transgenic mice. Eur. J. Pharmacol. 740, 312–320. doi:10.1016/j.ejphar.2014.06.051

Wang, J., Du, X.-X., Jiang, H., Xie, J.-X., 2009. Curcumin attenuates 6-hydroxydopamine-induced cytotoxicity by anti-oxidation and nuclear factor-kappa B modulation in MES23.5 cells. Biochem. Pharmacol. 78, 178–183. doi:10.1016/j.bcp.2009.03.031

Wang, M.S., Boddapati, S., Emadi, S., Sierks, M.R., 2010. Curcumin reduces α-synuclein induced cytotoxicity in Parkinson's disease cell model. BMC Neurosci. 11, 57. doi:10.1186/1471-2202-11-57

Watson, L.M., Wong, M.M.K., Becker, E.B.E., 2015. Induced pluripotent stem cell technology for modelling and therapy of cerebellar ataxia. Open Biol. 5, 150056. doi:10.1098/rsob.150056

West, A., Periquet, M., Lincoln, S., Lücking, C.B., Nicholl, D., Bonifati, V., Rawal, N., Gasser, T., Lohmann, E., Deleuze, J.-F., Maraganore, D., Levey, A., Wood, N., Dürr, A., Hardy, J., Brice, A., Farrer, M., 2002. Complex relationship between Parkin mutations and Parkinson disease. Am. J. Med. Genet. 114, 584–591. doi:10.1002/ajmg.10525

Wilken, R., Veena, M.S., Wang, M.B., Srivatsan, E.S., 2011. Curcumin: A review of anti-cancer properties and therapeutic activity in head and neck squamous cell carcinoma. Mol. Cancer 10, 12. doi:10.1186/1476-4598-10-12

Winslow L, Kroll DJ, 1998. HErbs as medicines. Arch. Intern. Med. 158, 2192–2199. doi:10.1001/archinte.158.20.2192

Wirdefeldt, K., Adami, H.-O., Cole, P., Trichopoulos, D., Mandel, J., 2011. Epidemiology and etiology of Parkinson's disease: a review of the evidence. Eur. J. Epidemiol. 26, 1–58. doi:10.1007/s10654-011-9581-6

Wood-Kaczmar, A., Gandhi, S., Yao, Z., Abramov, A.S.Y., Miljan, E.A., Keen, G., Stanyer, L., Hargreaves, I., Klupsch, K., Deas, E., Downward, J., Mansfield, L., Jat, P., Taylor, J., Heales, S., Duchen, M.R., Latchman, D., Tabrizi, S.J., Wood, N.W., 2008. PINK1 Is Necessary for Long Term Survival and Mitochondrial Function in Human Dopaminergic Neurons. PLoS ONE 3, e2455. doi:10.1371/journal.pone.0002455

Wrangel, C. von, Schwabe, K., John, N., Krauss, J.K., Alam, M., 2015. The rotenone-induced rat model of Parkinson's disease: Behavioral and electrophysiological findings. Behav. Brain Res. 279, 52–61. doi:10.1016/j.bbr.2014.11.002

Wu, F., Xu, H.-D., Guan, J.-J., Hou, Y.-S., Gu, J.-H., Zhen, X.-C., Qin, Z.-H., 2015. Rotenone impairs autophagic flux and lysosomal functions in Parkinson's disease. Neuroscience 284, 900–911. doi:10.1016/j.neuroscience.2014.11.004

Wu, J.-C., Lai, C.-S., Badmaev, V., Nagabhushanam, K., Ho, C.-T., Pan, M.-H., 2011. Tetrahydrocurcumin, a major metabolite of curcumin, induced autophagic cell death through coordinative modulation of PI3K/Akt-mTOR and MAPK signaling pathways in human leukemia HL-60 cells. Mol. Nutr. Food Res. 55, 1646–1654. doi:10.1002/mnfr.201100454

Wu, Y., Li, X., Zhu, J.X., Xie, W., Le, W., Fan, Z., Jankovic, J., Pan, T., 2011. Resveratrol-Activated AMPK/SIRT1/Autophagy in Cellular Models of Parkinson's Disease. Neurosignals 19, 163–174. doi:10.1159/000328516

Xilouri, M., Brekk, O.R., Landeck, N., Pitychoutis, P.M., Papasilekas, T., Papadopoulou-Daifoti, Z., Kirik, D., Stefanis, L., 2013. Boosting chaperone-mediated autophagy in vivo mitigates α-synuclein-induced neurodegeneration. Brain 136, 2130–2146. doi:10.1093/brain/awt131

Xiong, H., Wang, D., Chen, L., Choo, Y.S., Ma, H., Tang, C., Xia, K., Jiang, W., Ronai, Z., Zhuang, X., Zhang, Z., 2009. Parkin, PINK1, and DJ-1 form a ubiquitin E3 ligase complex promoting unfolded protein degradation. J. Clin. Invest. 119, 650–660. doi:10.1172/JCI37617

Xi, Y., Ryan, J., Noble, S., Yu, M., Yilbas, A.E., Ekker, M., 2010. Impaired dopaminergic neuron development and locomotor function in zebrafish with loss of pink1 function. Eur. J. Neurosci. 31, 623–633. doi:10.1111/j.1460-9568.2010.07091.x

Yadava, N., Nicholls, D.G., 2007. Spare Respiratory Capacity Rather Than Oxidative Stress Regulates Glutamate Excitotoxicity after Partial Respiratory Inhibition of Mitochondrial Complex I with Rotenone. J. Neurosci. 27, 7310–7317. doi:10.1523/JNEUROSCI.0212-07.2007

Yamin, G., Glaser, C.B., Uversky, V.N., Fink, A.L., 2003. Certain Metals Trigger Fibrillation of Methionine-oxidized α-Synuclein. J. Biol. Chem. 278, 27630–27635. doi:10.1074/jbc.M303302200

Yang, F., Lim, G.P., Begum, A.N., Ubeda, O.J., Simmons, M.R., Ambegaokar, S.S., Chen, P.P., Kayed, R., Glabe, C.G., Frautschy, S.A., Cole, G.M., 2005. Curcumin Inhibits Formation of Amyloid β Oligomers and Fibrils, Binds Plaques, and Reduces Amyloid in Vivo. J. Biol. Chem. 280, 5892–5901. doi:10.1074/jbc.M404751200

Yang, W., Tiffany-Castiglioni, E., 2008. Paraquat-induced apoptosis in human neuroblastoma SH-SY5Y cells: involvement of p53 and mitochondria. J. Toxicol. Environ. Health A 71, 289–299. doi:10.1080/15287390701738467

Yang, W., Tiffany-Castiglioni, E., Lee, M.-Y., Son, I.-H., 2010. Paraquat induces cyclooxygenase-2 (COX-2) implicated toxicity in human neuroblastoma SH-SY5Y cells. Toxicol. Lett. 199, 239–246. doi:10.1016/j.toxlet.2010.09.005

Yang, Y., Gehrke, S., Imai, Y., Huang, Z., Ouyang, Y., Wang, J.-W., Yang, L., Beal, M.F., Vogel, H., Lu, B., 2006. Mitochondrial pathology and muscle and dopaminergic neuron degeneration caused by inactivation of Drosophila Pink1 is rescued by Parkin. Proc. Natl. Acad. Sci. U. S. A. 103, 10793–10798. doi:10.1073/pnas.0602493103

Yang, Y., Ouyang, Y., Yang, L., Beal, M.F., McQuibban, A., Vogel, H., Lu, B., 2008. Pink1 regulates mitochondrial dynamics through interaction with the fission/fusion machinery. Proc. Natl. Acad. Sci. 105, 7070–7075. doi:10.1073/pnas.0711845105

Yonova-Doing, E., Atadzhanov, M., Quadri, M., Kelly, P., Shawa, N., Musonda, S.T.S., Simons, E.J., Breedveld, G.J., Oostra, B.A., Bonifati, V., 2012. Analysis of LRRK2, SNCA, Parkin, PINK1, and DJ-1 in Zambian patients with Parkinson's disease. Parkinsonism Relat. Disord. 18, 567–571. doi:10.1016/j.parkreldis.2012.02.018

Yu, S., Zheng, W., Xin, N., Chi, Z.-H., Wang, N.-Q., Nie, Y.-X., Feng, W.-Y., Wang, Z.-Y., 2010. Curcumin prevents dopaminergic neuronal death through inhibition of the c-Jun N-terminal kinase pathway. Rejuvenation Res. 13, 55–64. doi:10.1089/rej.2009.0908

Zbarsky, V., Datla, K.P., Parkar, S., Rai, D.K., Aruoma, O.I., Dexter, D.T., 2005. Neuroprotective properties of the natural phenolic antioxidants curcumin and naringenin but not quercetin and fisetin in a 6-OHDA model of Parkinson's disease. Free Radic. Res. 39, 1119–1125. doi:10.1080/10715760500233113

Zhang, L., Fiala, M., Cashman, J., Sayre, J., Espinosa, A., Mahanian, M., Zaghi, J., Badmaev, V., Graves, M.C., Bernard, G., Rosenthal, M., 2006. Curcuminoids enhance amyloid-β uptake by macrophages of Alzheimer's disease patients. J. Alzheimers Dis. 10, 1–7.

Zhang, X., Chen, S., Huang, K., Le, W., 2013. Why should autophagic flux be assessed? Acta Pharmacol. Sin. 34, 595–599. doi:10.1038/aps.2012.184

Zhang, X., Li, L., Chen, S., Yang, D., Wang, Y., Zhang, X., Wang, Z., Le, W., 2011. Rapamycin treatment augments motor neuron degeneration in SOD1G93A mouse model of amyotrophic lateral sclerosis. Autophagy 7, 412–425. doi:10.4161/auto.7.4.14541

Zhang, Z., Lapolla, S.M., Annis, M.G., Truscott, M., Roberts, G.J., Miao, Y., Shao, Y., Tan, C., Peng, J., Johnson, A.E., Zhang, X.C., Andrews, D.W., Lin, J., 2004. Bcl-2 homodimerization involves two distinct binding surfaces, a topographic arrangement that provides an effective mechanism for Bcl-2 to capture activated Bax. J. Biol. Chem. 279, 43920–43928. doi:10.1074/jbc.M406412200

Zhao, X.-C., Zhang, L., Yu, H.-X., Sun, Z., Lin, X.-F., Tan, C., Lu, R.-R., 2011. Curcumin protects mouse neuroblastoma Neuro-2A cells against hydrogen-peroxide-induced oxidative stress. Food Chem. 129, 387–394. doi:10.1016/j.foodchem.2011.04.089

Zhuang, W., Long, L., Zheng, B., Ji, W., Yang, N., Zhang, Q., Liang, Z., 2012. Curcumin promotes differentiation of glioma-initiating cells by inducing autophagy. Cancer Sci. 103, 684–690. doi:10.1111/j.1349-7006.2011.02198.x

Zhu, J., Horbinski, C., Guo, F., Watkins, S., Uchiyama, Y., Chu, C.T., 2007. Regulation of Autophagy by Extracellular Signal-Regulated Protein Kinases During 1-Methyl-4-Phenylpyridinium-Induced Cell Death. Am. J. Pathol. 170, 75–86. doi:10.2353/ajpath.2007.060524

Zimprich, A., Benet-Pagès, A., Struhal, W., Graf, E., Eck, S.H., Offman, M.N., Haubenberger, D., Spielberger, S., Schulte, E.C., Lichtner, P., Rossle, S.C., Klopp, N., Wolf, E., Seppi, K., Pirker, W., Presslauer, S., Mollenhauer, B., Katzenschlager, R., Foki, T., Hotzy, C., Reinthaler, E., Harutyunyan, A., Kralovics, R., Peters, A., Zimprich, F., Brücke, T., Poewe, W., Auff, E., Trenkwalder, C., Rost, B., Ransmayr, G., Winkelmann, J., Meitinger, T., Strom, T.M., 2011. A Mutation in VPS35, Encoding a Subunit of the Retromer Complex, Causes Late-Onset Parkinson Disease. Am. J. Hum. Genet. 89, 168–175. doi:10.1016/j.ajhg.2011.06.008

Ziviani, E., Tao, R.N., Whitworth, A.J., 2010. Drosophila Parkin requires PINK1 for mitochondrial translocation and ubiquitinates Mitofusin. Proc. Natl. Acad. Sci. 107, 5018–5023. doi:10.1073/pnas.0913485107